Characterising the Effect of Dietary Fat Composition on Cardiac and Hepatic Function and Metabolism

Nikola Srnic

Trinity College
University of Oxford

A thesis submitted for the degree of
Doctor of Philosophy in Cardiovascular Science

Hillary 2025

Declaration

This thesis is entirely my own work. Work completed by anyone else or at different institutions is clearly stated. Professor Leanne Hodson, Professor Lisa Heather, Dr. David Dearlove, and Dr. Kieran Smith provided supervision. Funding was provided by the British Heart Foundation. No part of this thesis has been submitted for any degree at this or any other university; however, some of this thesis has been previously published and presented:

Chapter 1: Parts of this chapter have been previously published in invited review manuscripts:

Srnic N, Westcott F, Caney E, Hodson L. Dietary fat quantity and composition influences hepatic lipid metabolism and metabolic disease risk in humans. *Dis Model Mech* 1 January 2025; 18 (1): dmm050878 doi: 10.1242/dmm.050878. Epub 2025 Jan 29; and in

Heather LC, Gopal K, **Srnic N**, Ussher JR. Redefining Diabetic Cardiomyopathy: Perturbations in Substrate Metabolism at the Heart of Its Pathology. *Diabetes*. 2024 May 1;73(5):659-670. doi: 10.2337/dbi23-0019.

Chapter 3: Findings presented in this chapter have been published: **Srnic N**, Dearlove D, Johnson E, MacLeod C, Krupa A, McGonnell A, Frazer-Morris C, O'Rourke P, Parry S, Hodson L. Greater oxidation of dietary linoleate compared with palmitate in humans following an acute high-carbohydrate diet. Clin Nutr. 2024 Oct;43(10):2305-2315. doi: 10.1016/j.clnu.2024.08.028. 2024 Aug 24. PMID: 39226718.

Recruitment and sample collection for 10 out of the 20 participants were completed by Dr. Siôn Parry and Dr. David Dearlove; lipid extractions for 10 plasma samples were complete by Paige O'Rourke. The remaining participant recruitment, sample collection, processing and analysis, and data analysis were completed by myself.

Chapter 4: Recruitment and sample collection for 3 of 28 participants was completed by Dr. Siôn Parry, insulin kinetic modelling was performed by Dr. Kieran Smith, MRI/S scan acquisitions were performed by radiographers at the Oxford Centre for Clinical Magnetic Resonance Research, and the code to analyse spectroscopy data was created by Associate Prof. Ladislav Valkovic, Associate Prof. Chris Rodgers, and Dr. Ferenc Mozes. All remaining participant recruitment, sample collection, processing and analysis, and data analysis were completed by myself.

Publications

1. **Srnic N***, Westcott F*, Caney E, Hodson L. Dietary fat quantity and composition influences hepatic lipid metabolism and metabolic disease risk in humans. *Dis Model Mech* 1 January 2025; 18 (1): dmm050878. (*joint authorship)

2. **Srnic N**, Dearlove DJ, Johnson E, … Hodson L. Greater oxidation of dietary linoleate compared with palmitate in humans following an acute high-carbohydrate diet. *Clinical Nutrition* 2024 Oct;43(10):2305-2315.

3. Heather LC, Gopal K, **Srnic N**, Ussher JR. Redefining Diabetic Cardiomyopathy: Perturbations in Substrate Metabolism at the Heart of Its Pathology. *Diabetes*. 2024 May 1;73(5):659-670.

Presentations & Prizes

1. Poster presentation: "Unsaturated compared with saturated fatty acids improve *in vivo* human cardiac energetics, systolic, and diastolic function and are associated with upregulated fatty acid oxidation in human cardiomyocytes" at the Society for Heart and Vascular Metabolism in Bordeaux, France, June 2025. *Awarded best poster presentation prize*

2. Poster presentation: "Unsaturated compared with saturated fatty acids improve *in vivo* human cardiac energetics and diastolic function and are associated with upregulated fatty acid oxidation in human cardiomyocytes" at the International Society for Heart Research World Congress in Nara, Japan, May 2025.

3. Poster presentation: "Elevated cardiometabolic disease risk in males compared with females is not explained by differences in fasting and postprandial insulin secretion and clearance" at the Society for Endocrinology, British Endocrinology Society in Harrogate, United Kingdom, March 2025. *Awarded commendation prize*

4. Oral presentation: "Cardiovascular disease risk factors are adversely altered by an isocaloric high fat diet enriched with saturated compared with polyunsaturated fat in healthy humans" at the International Congress of Lipids and Atherosclerosis in Seoul, South Korea, September 2024. *Awarded best oral presentation prize*

5. Poster presentation: "A high fat diet enriched with saturated compared with polyunsaturated fat has a more detrimental effect on the hepato-cardiac axis in healthy humans" at the Society for Heart and Vascular Metabolism in St. Louis, USA, September 2024.

6. Oral presentation during the late-breaking basic and translational science session: "An isocaloric high fat diet enriched with saturated compared with polyunsaturated fat has a more detrimental effect on clinical cardiometabolic risk factors in healthy humans" at the European Society for Cardiology Congress in London, United Kingdom, August 2024.

Following this presentation at the European Society for Cardiology, I was interviewed for and the presented work was shared by The Times: "*Daily croissant can take a toll on your heart in under a month*", Sept. 2024, The Telegraph: "*Just three weeks of eating badly found to raise heart disease risk*", & The British Hearth Foundation: "*Research reveals hidden dangers of high saturated fat diet*", Sept. 2024.

7. Oral presentation: "A saturated compared with polyunsaturated fat enriched high fat diet has a more detrimental effect on the hepato-cardiac axis in healthy humans" at the Medical Sciences Doctoral Training Centre Annual Symposium in Oxford, United Kingdom, July 2024. *Awarded best oral presentation prize*

8. Oral presentation: "Dietary fat composition influences cardiometabolic disease risk factors in metabolically healthy humans" at the National BHF Students Research Day in Bristol, United Kingdom, April 2024.

9. Oral presentation: "A high fat isocaloric diet enriched with saturated fat compared with polyunsaturated fat increases cardiometabolic disease risk factors in metabolically healthy humans" at The Physiological Society: Dietary Manipulations for Health and in the Prevention and Management of Disease in Manchester, United Kingdom, March 2024.

10. Oral and poster presentation: "An acute upregulation of hepatic de novo lipogenesis does not attenuate the partitioning of polyunsaturated fatty acids into oxidation pathways" at the Society for Endocrinology, British Endocrinology Society in Glasgow, United Kingdom, November 2023. *Awarded best poster presentation prize*

11. Oral presentation: "Liver Handling of Dietary Fatty Acids: Effect of Metabolic State" at The Physiological Society: Early Career Life Sciences Symposium in Manchester, United Kingdom, November 2023. *Awarded best oral presentation prize*

12. Poster presentation: "Investigating the mechanisms underlying the differential handling of saturated and polyunsaturated fatty acids in human cardiomyocytes" at the Department of Physiology, Anatomy, and Genetics Graduate Student's Research Day, University of Oxford, Oxford, United Kingdom, October 2023. *Awarded best poster presentation prize*

13. Poster presentation: "Investigating the mechanisms underlying the differential handling of saturated and polyunsaturated fatty acids in human cardiomyocytes" at the 50th anniversary meeting of British Society for Cardiovascular Research, Oxford, United Kingdom, August 2023.

Acknowledgements

This work would not have been possible without the contributions of several individuals. First, thank you to Prof. Lisa Heather and Prof. Leanne Hodson for their support, patience, and encouragement throughout my DPhil. Their extensive knowledge, positive attitudes, and excitement for science have fostered in me a passion for research that I will take into the future. I'd also like to thank Dr. David Dearlove and Dr. Kieran Smith for their support, thoughtful discussions, and reassurance through this process. Thank you to Elspeth and Amy for maintaining and running the lab, teaching and training me, and troubleshooting any issue in the lab.

I am very appreciative for all the individuals who volunteered their time to participate in these studies, this work would not have been possible without their generosity and commitment. I want to extend my gratitude towards Diana, Sarah, and Michelle for their friendship and excellent nursing support during study days; and to the radiographers at OCMR for their help in performing the MR scans and enjoyable company. Thank you to Fredrik, Jeremy, Harsha, Tom, Hamish, and Jiawen for providing medical cover. I'd also like to thank the Oxford Biobank for helping with recruitment, the British Heart Foundation for funding this research, and the broader OCDEM and CMRG community for their support.

There are several friends at and away from the lab who have contributed to the positive memories associated with this DPhil. Thank you to Felix, Kaitlyn, Emily, Aaron, Ríona, Marcos, Adam, and Mary, and to Isabelle, Sabrina, Jen, and AnneMichaela for all the fun and laughter.

Finally, I would like to thank my parents, Vesna and Djordje Srnic, for their support at each step of this journey.

Abstract

Dietary macronutrient composition may modulate cardiometabolic disease (CMD) risk, as consuming a diet enriched in saturated fat (SFA), compared with unsaturated fat, leads to greater intrahepatic triglyceride (IHTG) accumulation, despite similar weight gain. However, it is difficult to differentiate the effects of weight gain from dietary fat composition on CMD risk as most studies have been conducted with overfeeding interventions. Therefore, the aim of this thesis was to investigate if, during weight-neutral conditions, dietary SFAs, compared with polyunsaturated FAs (PUFAs), undergo differential handling and induce divergent effects on hepatic and cardiac metabolism and function.

Participants free from diagnosed-metabolic disease consumed a mixed test meal with [U^{13}C]palmitate or [U^{13}C]linoleate after following a 3-day high-carbohydrate diet, which upregulated markers of hepatic *de novo* lipogenesis by ~65% (p<0.05). Despite shifting hepatic metabolism towards esterification and away from oxidation, appearance of ^{13}C in expired CO_2, a marker of whole-body dietary FA oxidation, was ~46% (p<0.01) greater following [U^{13}C]linoleate compared with [U^{13}C]palmitate consumption.

Participants free-from diagnosed metabolic disease underwent an MRI/S scan and postprandial study day with stable-isotope tracers before and after consuming an isocaloric SFA- or PUFA-enriched high-fat diet (HFD) for up to 24 days. There were minimal changes in body weight. However, consuming a PUFA-enriched HFD reduced IHTG content by ~19% (p<0.05) and induced beneficial changes in blood pressures, markers of whole-body dietary FA oxidation, cardiac PCr/ATP (pre: 1.52±0.13; post: 1.78±0.40; p<0.05), cardiac function, and insulin-kinetics. Consuming a SFA-enriched HFD tended to increase IHTG content BY ~17% (p=0.09), and adversely altered markers of cardiac function, whole-body dietary FA oxidation, and insulin resistance.

To further probe if FA composition, independent of FA quantity, impacts the heart, human inducible pluripotent stem cell-derived cardiomyocytes (hiPSC-CMs) were cultured in a 400μmol/L SFA- or PUFA-enriched FA mixture to model the human HFD from Chapter 4. PUFA-enriched lipid mix treated hiPSC-CMs did not reduce media FA uptake and upregulated FA metabolism pathways (p_{adj}<0.05), while SFA-enriched lipid mix treated hiPSC-CMs reduced FA uptake by ~67% (p<0.01) and upregulated ribosomal biogenesis (p_{adj}<0.05).

Taken together, these findings suggest dietary FAs undergo differential intracellular metabolism, dietary FA composition impacts CMD risk independent of body weight, and dietary FAs may directly modulate human cardiomyocyte metabolism and function.

Table of Contents

List of Abbreviations

3OHB	3-β-hydroxybutyrate
AA	Arachidonic acid
ACC	Acetyl-CoA carboxylase
ACSL	Acyl-CoA synthetase
AD	Aortic distensibility
ALA	α-Linoleic acid
AMARES	Advanced method for accurate, robust and efficient spectral tracking
AMP	Adenosine monophosphate
AMPK	AMP-activated protein kinase
ANOVA	Analysis of variance
ANCOVA	Analysis of covariance
ApoB	Apolipoprotein B
ARNTL	Aryl hydrocarbon receptor nuclear translocation-like protein
ATM	Ataxia telangiectasia mutated
ATF	Activating transcription factor
ATGL	Adipocyte triglyceride lipase
ATP	Adenosine triphosphate
AUC	Area under the curve
BHT	Butylated hydroxytoluene
BMI	Body mass index
BCA	Bicinchoninic acid
BSA	Bovine serum albumin
CD36	Cluster of differentiation 36
cDNA	Complementary deoxyribonucleic acid
CE	Cholesterol ester
CHD	Coronary heart disease
CHO	Carbohydrate
ChREBP	Carbohydrate response element binding protein
CMD	Cardiometabolic disease
CO	Cardiac output
CPT1	Carnitine palmitoyl transferase 1
CPT2	Carnitine palmitoyl transferase 2
CRU	Clinical research unit
CVD	Cardiovascular disease
D	Deuterium
DAG	Diacylglycerol
DEXA	Dual energy x-ray absorptiometry
DGAT	Diacylglycerol transferase
DHA	Docosahexaenoic acid
DMEM	Dulbecco’s modified eagle medium

DNL	*De novo* lipogenesis
DNMT3α	DNA methyltransferase 3α
ECG	Electrocardiogram
EDTA	Ethylenediaminetetraacetic acid
EF	Ejection Fraction
ELVOL6	Elongated fatty acid elongase 6
EPA	Eicosapentaenoic acid
ER	Endoplasmic reticulum
EDV	End-diastolic volume
ESV	End-systolic volume
ETV	ETS translocation variant
F	Female
FA	Fatty acid
FABP	Fatty acid binding protein
FAME	Fatty acid methyl ester
FAS	Fatty acid synthase
FAT	Fatty acid translocase
FC	Fold change
FDR	False discovery rate
FPG	Fasting plasma glucose
GC	Gas chromatography
GCKR	Glucokinase regulatory protein
GCMS	Gas chromatography-mass spectrometry
GLP1	Glucagon-like peptide-1
GLUT	Glucose transporter
GO	Gene ontology
GPAT	Glycerol-3-phosphate acyltransferase
GSEA	Gene set enrichment analysis
^{1}H	Proton
HDL	High-density lipoprotein
HFD	High-fat diet
HFLC	High-fat low-carbohydrate
HFrEF	Heart failure with a reduced ejection fraction
HFpEF	Heart failure with a preserved ejection fraction
HIF1α	Hypoxia-inducible factor-1α
hiPSC-CM	Human inducible pluripotent stem cell derived cardiomyocyte
HLA	Horizontal long axis
HOMA-IR	Homeostatic model assessment for insulin resistance
HSL	Hormone sensitive lipase
ICR	Insulin clearance rate
IDL	Intermediate-density lipoprotein
IFN	Interferon
IHTG	Intrahepatic triglyceride

IRMS	Isotope-ratio mass spectrometry
ISR	Insulin secretion rate
KD	Ketogenic diet
LA	Linoleic acid
LCFA	Long-chain fatty acid
LDH	Lactate dehydrogenase
LDL	Low-density lipoprotein
LDL-R	Low-density lipoprotein receptor
LFHC	Low-fat high-carbohydrate
LPL	Lipoprotein lipase
LV	Left ventricle
LVH	Left ventricular hypertrophy
M	Male
M/z	Mass-charge ratio
MASH	Metabolic dysfunction-associated steatohepatitis
MASLD	Metabolic dysfunction-associated steatotic liver disease
MBOAT7	Membrane-bound O-acyltransferase domain-containing protein 7
MEF2c	Myocyte enhancer factor 2c
Mol%	Molar percent
MRI/S	Magnetic resonance imaging/spectroscopy
MSigDB	Molecular signatures database
MUFA	Monounsaturated fatty acid
NAFLD	Non-alcoholic fatty liver disease
NASH	Non-alcoholic steatohepatitis
NFκB2	Nuclear factor-κB subunit 2
NEFA	Non-esterified fatty acid
NSD	No significant difference
OA	Oleic acid
OCDEM	Oxford Centre for Diabetes, Endocrinology, and Metabolism
OCMR	Oxford Centre for Clinical Magnetic Resonance Imaging
Paleo	Paleolithic
PBS	Phosphate buffered saline
PCA	Principle component analysis
PCr	Phosphocreatine
PKB	Protein kinase B
PL	Phospholipid
PMSF	Phenylmethylsulphonyl fluoride
PNPLA3	Patatin-like phospholipase domain containing protein 3
PPARα	Peroxisome proliferator-activated receptor-α
PUFA	Polyunsaturated fatty acid
PVA	Polyvinyl alcohol
qPCR	Quantitative polymerase chain reaction

R_a	Rate of appearance
RCT	Randomised control trial
RNA	Ribonucleic acid
ROS	Reactive oxygen species
RPMI	Roswell Park Memorial Institute
RQ	Respiratory quotient
RV	Right ventricle
SA	Short axis
SCD	Stearoyl-CoA desaturase
S_f	Svedberg floatation rate
SFA	Saturated fatty acid
SLAP	Standard light Antarctic precipitation
SNP	Single nucleotide polymorphism
SPE	Solid phase extraction
SREBP1c	Sterol regulatory element binding protein 1c
SSFP	Steady state free precession
STEAM	Stimulated echo acquisition mode
SV	Stroke volume
T2D	Type 2 diabetes
TCA	The citric acid cycle
TDI	Tissue doppler imaging
TE	Total energy
TF	Transcription factor
TG	Triglyceride
TM6SF2	Transmembrane 6 superfamily member 2
TMM	Trimmed mean of M-values
TRL	Triglyceride-rich lipoprotein
TTR	Tracer-tracee ratio
VHL	Von Hippel-Lindau tumour suppressor
VLA	Vertical long axis
VLDL	Very-low density lipoprotein
VPDB	Vienna-PeeDee belemnite standard
VSMOW	Vienna standard mean ocean water

List of Tables

Chapter 1

Chapter 3

Chapter 4

Chapter 5

Appendix 1

Appendix 3

List of Figures

Chapter 1

Chapter 2

Chapter 3

Chapter 4

Appendix 2

Appendix 3

Chapter 1

General Introduction

1.1 Overview

Obesity is a chronic condition associated with an increased risk of developing cardiometabolic disease (CMD), collectively this includes, but is not limited to, metabolic dysfunction-associated steatotic liver disease (MASLD), cardiovascular disease (CVD), dyslipidaemia, metabolic syndrome, hypertension, insulin resistance, and type 2 diabetes (T2D) (1-4). Individuals defined as overweight or obese have a body mass index (BMI) 25-29.9 kg/m^2 or >30 kg/m^2, respectively, where the increased body weight typically results from abnormal or excess adiposity (5). Current evidence suggests the development of obesity is multifactorial and results from complex interactions between modifiable and non-modifiable lifestyle, genetic, environmental, and social risk factors (2). An individual's diet is one modifiable lifestyle risk factor associated with obesity, where consuming calories in excess of an individual's metabolic requirements may increase adiposity and BMI, and therefore, may impact CMD risk (6-8). However, the macronutrient composition of an individual's diet may modulate metabolic health, with effects that may be independent of changes in body weight and adiposity. Luukkonen *et al.* reported that individuals who consumed a diet enriched in saturated fat (SFA), compared with those who consumed a diet enriched in unsaturated fat or carbohydrates, had greater fat accumulation within the liver (known as intrahepatic triglyceride (IHTG), a hallmark of MASLD) despite similar weight gain (9). Further, these divergent, weight-independent effects of dietary SFA, compared with unsaturated FAs, on metabolic health may be due to differences in intracellular and systemic handling (9). However, as most studies investigating the effects of dietary FA composition on CMD risk have been conducted under overfeeding conditions (9-11), it is difficult to differentiate the effects of weight gain from dietary macronutrient composition. Therefore, to characterise the effect of dietary FA composition on CMD risk, in this thesis I investigated the effects of dietary SFA, compared with polyunsaturated FA (PUFAs) on hepatic and cardiac metabolism and function in weight-

neutral conditions. I focused on long-chain FA (LCFA), with fatty-acyl chains between 14 and 20 carbons, as they are the predominant FAs in the diet and plasma-TG, and metabolised slightly differently from short, medium, and very-long chain FA (12); discussions surrounding FAs are assumed to mean LCFA unless otherwise stated.

1.2 Cellular Lipid Metabolism

In the plasma, FAs circulate as albumin bound non-esterified FA (NEFA) or in protein-lipid particles termed lipoproteins. FAs are classified by the number of carbons in the hydrocarbon tail, and the number, location (i.e. n-6, n-3), and orientation (*cis* vs. *trans*) of double bonds. The most abundant FAs in the human plasma-TG are listed in Table 1.1 (13).

Table 1.1. Fatty Acid Abundance in Plasma-TG in Humans

Fatty Acid	Structure	Class	Abundance (mol%)
Oleate	18:1n-9	MUFA	~37.7
Palmitate	16:0	SFA	~29.5
Linoleate	18:2n-6	PUFA	~15.0
Palmitoleate	16:1n-7	MUFA	~5.1
Stearate	18:0	SFA	~4.5
Myristate	14:0	SFA	~3.3
α-Linoleate	18:3n-3	PUFA	~0.9
Arachidonate	20:4n-6	PUFA	~0.8

Abbreviations: MUFA, monounsaturated fatty acid; PUFA, polyunsaturated fatty acid; SFA, saturated fatty acid; TG, triglyceride. Data adapted from (13)

Most FAs enter cells through transporters, such as fatty acid translocase/cluster of differentiation 36 (FAT/CD36) and FA binding protein (FABP), or receptor-mediated endocytosis of lipoproteins, a minority of FAs enter cells through simple diffusion (14-17). Alternatively, certain cells can synthesise FAs from non-lipid precursors through *de novo* lipogenesis (DNL) (6). Upon entering a cell or following synthesis, FAs are rapidly activated by long-chain fatty acyl-CoA synthetases (ACSL) into fatty acyl-CoAs, and partitioned into

metabolic, biosynthetic, signaling, or structural pathways (18). The primary metabolic pathways for FAs include *i)* oxidation, to generate adenosine triphosphate (ATP), *ii)* esterification, to form primarily, but not exclusively, TG, and, *iii)* secretion pathways, where FA enter the plasma as NEFAs or as TG in very-low density lipoproteins (VLDL) or chylomicrons.

1.2.1 FA Oxidation

In many tissues, FAs are used to generate ATP. This is achieved predominantly, but not exclusively by, mitochondrial β-oxidation, which requires FAs to be transported into the mitochondrial matrix by the carnitine shuttle (Fig. 1.1) (19). In the matrix, fatty acyl-CoAs are broken down into acetyl-CoA, NADH, and $FADH_2$, which are subsequently oxidised by the citric acid (TCA) cycle and electron transport chain to produce ATP, CO_2, and water. In hepatocyte mitochondria, FA-derived acetyl-CoA can be partitioned into ketogenesis. This pathway partially oxidises FAs to form ketone bodies, such as 3-β-hydroxybutyrate (3OHB), which are secreted into the plasma as fuel sources for tissues (20).

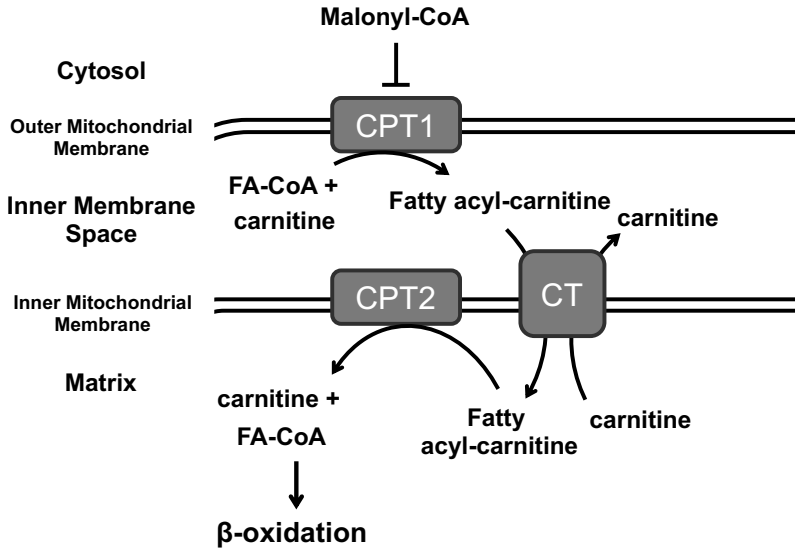

Figure 1.1. Mitochondrial fatty acid import and oxidation. Carnitine palmitoyl transferase 1 (CPT1) combines a fatty acyl-CoA with carnitine to form a fatty acyl-carnitine, this is transported into the matrix by carnitine translocase (CT) in exchange for a carnitine (21). In the matrix, carnitine palmitoyl transferase 2 (CPT2), catalyses the reverse reaction of CPT1 to reform the fatty acyl-CoA.

1.2.2 FA Esterification

Within cells, FAs are esterified and stored as TG in lipid droplets (22). While most FAs are esterified into TG, either by the GPAT or MAG pathway (Fig. 1.2), FAs can also be esterified with cholesterol, forming cholesterol-esters (CE), or partitioned into lipid synthesis pathways to form phospholipids (PL), sphingolipids, or ceramides (23, 24). FAs that have accumulated in excess of immediate requirements for oxidation or secretion are stored as TG within lipid droplets until needed (22).

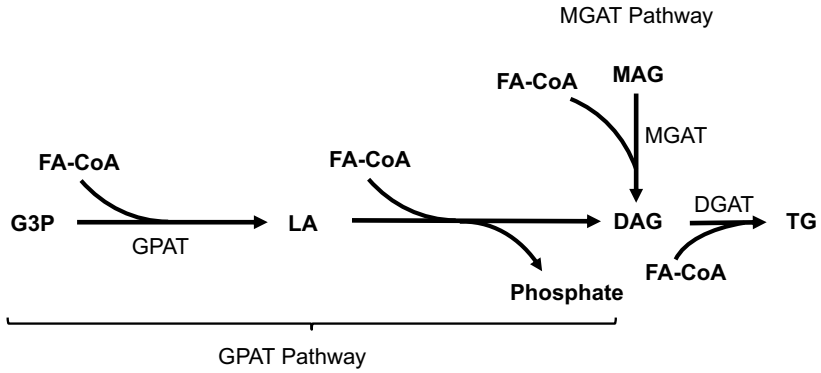

Figure 1.2. Fatty acid esterification to triglyceride. For TG synthesis via the GPAT pathway, glycerol-3-phosphate acyltransferase (GPAT) combines a fatty acyl-CoA with glycerol-3-phosphate, a glycolytic intermediate, to form lysophosphatidic acid (LA); the addition of another fatty acyl-CoA and removal of phosphate subsequently forms diacylglycerol (DAG). In the MAG pathway, DAG is formed by monoacylglycerol transferase adding a fatty acyl-CoA to monoacylglycerol (25). Following DAG formation by either pathway, diacylglycerol transferase (DGAT) forms TG by adding a fatty acyl-CoA to DAG.

1.2.3 FA Secretion

Certain cells can secrete lipids from intracellular stores into the plasma for transport to other tissues. From hepatocytes and enterocytes, lipids are secreted as TG in VLDL and chylomicrons, respectively. VLDL and chylomicron formation begins with translating apolipoprotein B (apoB) 100 or apoB48 mRNA. During translation, the growing apoB100 or apoB48 apolipoprotein is lipidated with TG, PL, and CE to form pre-VLDL or pre-chylomicrons, and with the addition of other apolipoproteins such as, apoA, apoC, and apoE, form mature VLDL and chylomicrons (26-29). Once secreted, lipoproteins deliver lipids to tissues that express intravascular lipases, such as lipoprotein lipase (LPL), hepatic lipase, and

endothelial lipase, that liberate FAs from lipoprotein-TG for uptake into cells, or to cells which express receptors, such as the low-density lipoprotein (LDL) receptor (LDL-R), for lipoprotein uptake through receptor mediated endocytosis (30, 31). Lipids are also secreted from adipose tissue. In adipocytes, FAs are first hydrolysed intracellularly from TGs by adipocyte triglyceride lipase (ATGL), hormone sensitive lipase (HSL), and monoglyceride lipase. Once liberated, FAs are exported from the cell, where they bind to albumin, and are transported in the systemic circulation to tissues for further metabolism.

1.2.4 FA Synthesis, Elongation, & Desaturation

The liver can synthesise FAs from non-lipid precursors (i.e. sugars, amino acids) via DNL. In this pathway, malonyl-CoA is first formed from acetyl-CoA and CO_2 by acetyl-CoA carboxylase (ACC). Next, malonyl-CoA undergoes successive rounds of elongation by fatty acid synthase (FAS) until palmitate, a 16-carbon SFA and the major product of DNL, is formed (32). Although DNL occurs primarily within hepatocytes in humans, malonyl-CoA formation occurs in most oxidative tissues as it regulates FA oxidation (21). Once formed, DNL-derived FAs mix with and are metabolised similarly to other intracellular FAs. FAs can be further modified by intracellular enzymes; for example, palmitate can be elongated by elongated FA elongase 6 (ELVOL6) to stearate (C18:0) or other very-long chain FAs, and desaturated by stearoyl-CoA desaturase (SCD) to the monounsaturated FAs (MUFAs) palmitoleate (C16:1n-7) and oleate (C18:1n-9; OA) (32, 33). However, humans do not express enzymes to form the polyunsaturated FAs (PUFAs) linoleate (C18:2*n*-6) and α-linoleate (C18:3*n*-3) from oleate, these FAs can only be obtained from the diet and are therefore known as essential FA.

1.3 Systemic Metabolism

Complex processes regulate systemic FA and glucose metabolism to balance the high metabolic demands of organs like the heart with preventing tissue damage from elevated

plasma nutrient concentrations. The liver has a central role in regulating metabolism as it coordinates the transition from the fasted to fed state, produces albumin, detoxifies drugs and ammonia, clears waste products, and synthesises bile acids and cholesterol. Most of these functions are performed by hepatocytes, which make up ~80% of the liver, the remaining ~20% is composed of supporting cells and extracellular space (34). The liver's dual blood supply supports its role in regulating systemic and postprandial metabolism as it receives oxygenated blood from the hepatic artery and nutrient-rich deoxygenated blood from the portal vein, which drains the majority of the gastrointestinal tract and pancreas. Therefore, following the absorption of dietary glucose and amino acids, these nutrients are carried, along with pancreatic hormones such as insulin and glucagon, directly to the liver. After passing the hepatocytes, blood is carried out of the liver by the hepatic vein which drains directly into the inferior vena cava then the right side of the heart.

1.3.1 Postprandial Glucose Metabolism

In the transition from fasted to fed state, the increased flux of nutrients to the liver and pancreas triggers a series of complex metabolic cascades to rapidly transition between energy storage and supply. Following the consumption of a mixed meal, dietary carbohydrates, proteins, and lipids are broken down throughout the digestive tract into sugars, amino acids, and FA for absorption. Sugars and amino acids are directly carried to the liver, with the increase in plasma glucose concentrations triggering insulin secretion from pancreatic β-cells. The increased portal plasma glucose concentration increases hepatocyte glucose uptake, which with increased hepatocellular insulin signaling, shifts hepatic glucose metabolism towards glycolysis and glycogenesis, away from glycogenolysis and gluconeogenesis, and promotes hepatic DNL (35, 36). However, as the liver is unable to take up, store, and utilise all meal-derived glucose, systemic plasma glucose and insulin concentrations rise. In cardiac and skeletal muscle and adipose tissue, increased insulin signaling promotes glucose uptake by

increasing plasma membrane glucose transporter type 4 (GLUT4) expression, this aids glucose uptake alongside import by the insulin-independent GLUT1 transporters (37-39). Insulin signaling also shifts oxidative metabolism in cardiac and skeletal muscle towards glucose and away from FAs and promotes storage of glucose as glycogen in muscle and as TG in adipose tissue (40, 41). Systemic glucose and insulin concentrations peak ~30-90min following the consumption of a meal before decreasing to pre-meal levels by ~240mins (42). The shift towards glucose oxidation and storage eventually decreases plasma glucose concentrations, which reduces further insulin secretion; plasma insulin concentrations decrease as the liver internalises and clears insulin bound to the insulin receptor (43). As glucose and insulin concentrations return to pre-meal levels, the decreased portal insulin-to-glucagon ratio shifts hepatic glucose metabolism towards the fasted response, this is characterised by increased glycogenolysis and gluconeogenesis and decreased glycogenesis (44). This metabolic shift enables the liver to secrete glucose into the plasma to maintain appropriate plasma glucose concentrations for the body's metabolic requirements.

1.3.2 Postprandial Lipid Metabolism

After consuming a lipid-containing meal, dietary fats, predominantly consumed as TG, are emulsified by bile acids, digested by lipases, and absorbed as FA and monoglycerides into enterocytes. Within enterocytes, TG is resynthesised and packaged for secretion into chylomicrons. Unlike sugars and amino acids, chylomicrons are secreted into and transported by the slow-flowing lymphatic system before entering the systemic circulation via the thoracic duct into the left subclavian vein. This results in chylomicrons bypassing the portal circulation and liver, where they are instead delivered to striated muscle and adipose tissue during their first circulation throughout the body. Plasma chylomicron concentrations peak ~180-300min following the consumption of a meal (45). During the postprandial period, dietary FAs are liberated from chylomicron-TG by intravascular lipases and taken up into cells via CD36 and

FABP (16, 30, 46, 47). In muscle, these FA can be oxidised, while in adipose tissue, they can be re-esterified into TG and stored. This shift towards storing dietary FA in adipose tissue is driven, in part, by postprandial insulin signaling which increases LPL expression, inhibits intracellular lipolysis, and promotes CD36 translocation to the plasma membrane (40, 48). During intravascular lipolysis, some lipase-liberated FAs escape tissue uptake and spillover into systemic circulation (i.e. spillover FA), and these FAs, along with partially hydrolysed chylomicron 'remnant' particles, are carried to the liver and heart where they are taken up and utilised by intracellular fat metabolism pathways (Fig. 1.3) (49-51).

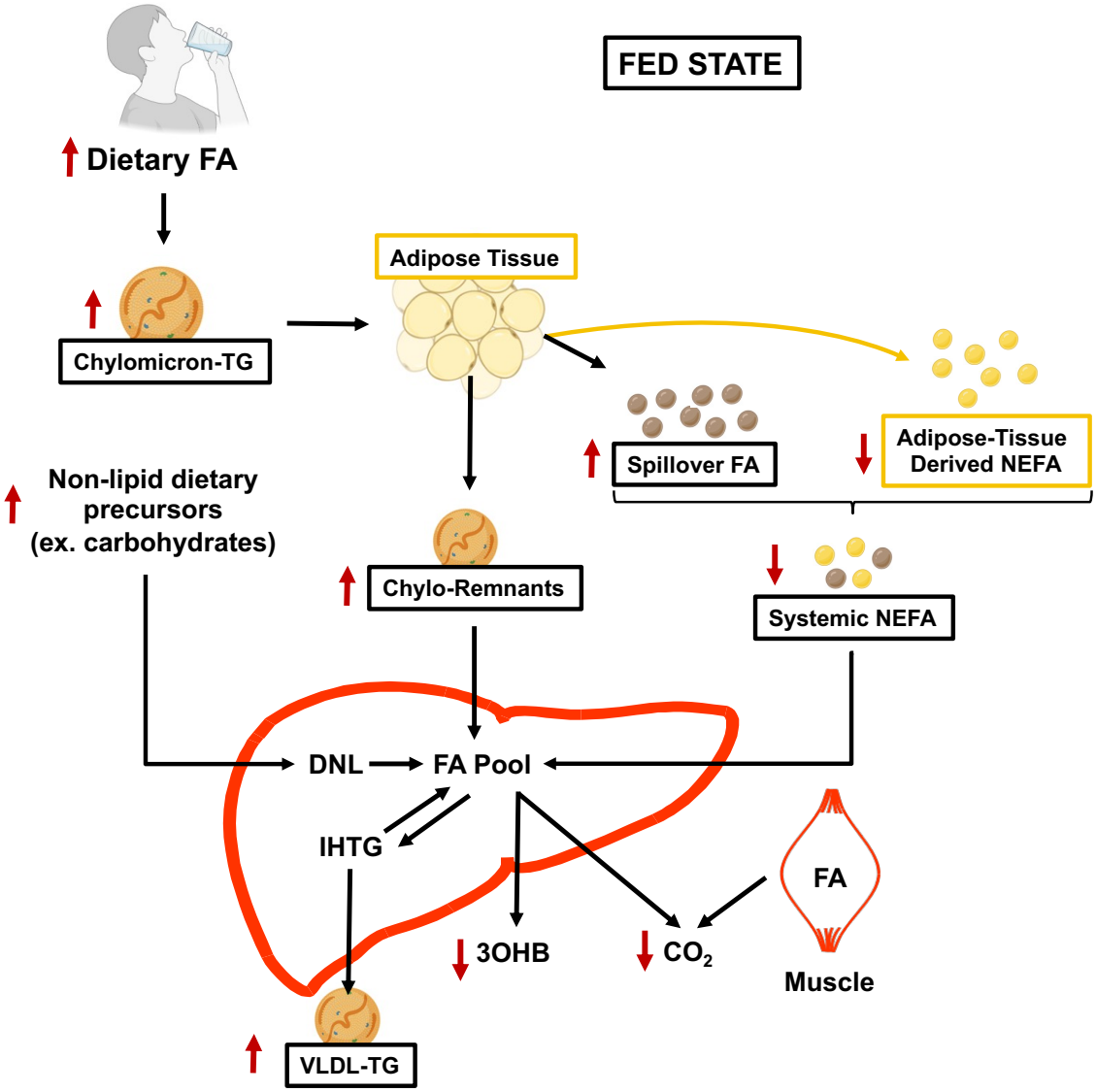

Figure 1.3. Overview of postprandial lipid metabolism. Abbreviations: 3OHB, 3-hydroxybutyrate; DNL, *de novo* lipogenesis; FA, fatty acid; IHTG, intrahepatic triglyceride; NEFA, non-esterified FA; TG, triglyceride; VLDL, very-low density lipoprotein.

As the body transitions from fed to fasted state, plasma insulin concentrations decrease which shifts systemic lipid metabolism away from lipid storage and towards mobilisation pathways (52). In adipose tissue, decreased insulin signalling enables HSL activation, which liberates FAs from TG and releases NEFA into plasma for transport to tissues like the heart and liver (Fig. 1.4) (53). NEFA uptake in the heart and liver are suggested to be proportional to plasma NEFA concentrations, therefore, increased plasma NEFA concentrations in the fasted period may promote hepatic and cardiac FA uptake and metabolism (54, 55). Lipid is also mobilised from the liver as VLDL-TG. In non-hepatic tissues, FAs are liberated from VLDL-TG by intravascular lipases and taken up to support that tissue's metabolic requirements. This process reduces VLDL TG content and forms the smaller intermediate-density lipoproteins (IDL) and LDL; compared with VLDL, they are enriched with CE and PL and lower in TGs (56). As with chylomicrons, some lipase-liberated FAs from VLDL-TG escape tissue uptake and spillover, and some VLDL-TG passes through tissues partially hydrolysed creating VLDL 'remnant' particles; both are delivered to the liver and heart (49, 56). Collectively, chylomicrons and VLDL are termed TG-rich lipoproteins (TRLs), and as such, chylomicron-remnants and VLDL-remnants are termed TRL-remnants. Spillover FAs are taken up into cells by FA transporters, while TRL-remnants, IDL, and LDL are cleared from the plasma by receptor-mediated endocytosis; any FAs liberated from these lipoproteins via endosomal lipolysis are recycled into the intracellular FA pool (14-17, 57). As the fasting period continues, hepatic ketogenesis also increases (20). This shift in systemic and hepatic metabolism towards lipid mobilisation supports systemic metabolic demands during the fasted period until the next meal.

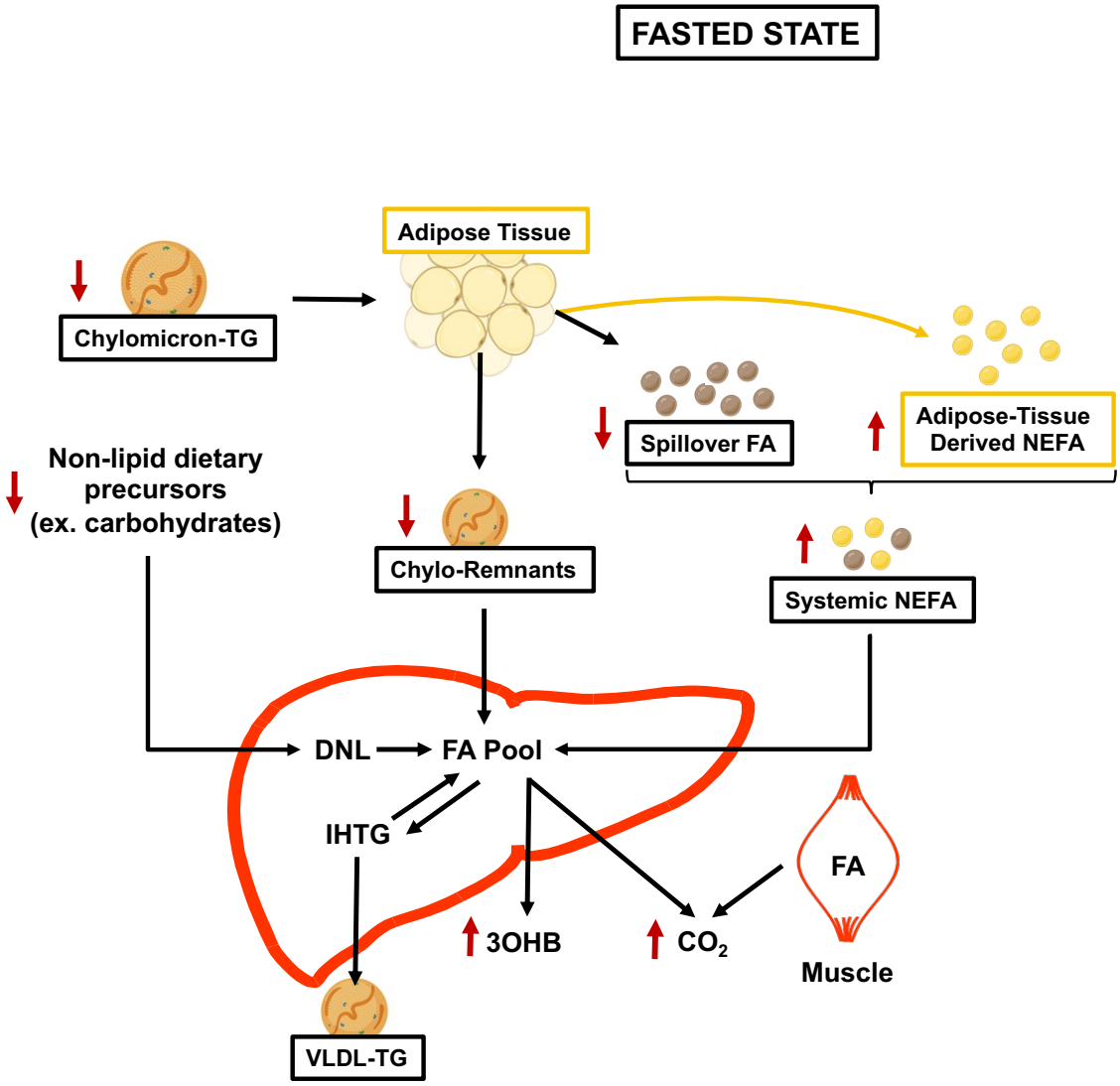

Figure 1.4. Overview of human lipid metabolism in the fasted state. Abbreviations: 3OHB, 3-hydroxybutyrate; DNL, *de novo* lipogenesis; FA, fatty acid; IHTG, intrahepatic triglyceride; NEFA, non-esterified FA; TG, triglyceride; VLDL, very-low density lipoprotein.

1.4 Hepatic Fat Metabolism

1.4.1 Hepatic Fat Metabolism Under Physiological Conditions

IHTG content is determined by a complex balance between the fat that enters the liver from dietary sources (as TRL-remnants and spillover FA) and adipose tissue (as NEFA), the amount synthesised via DNL, and the amount removed by oxidation (the citric acid (TCA) cycle and ketogenesis) and secretion (Figure 1.3-1.4). The sources of hepatic FAs, as well as the partitioning of FAs into different intrahepatic pathways is influenced by multiple

parameters including the body's nutritional (fed vs. fasted) (58) and hormonal state (59), hepatic and/or extrahepatic-tissue disease status (i.e. insulin resistance, MASLD) (33, 58, 60), and the amount, and potentially type of, dietary fat consumed (6, 9, 61).

Insulin has a major role in regulating hepatic FA metabolism by modulating FA flux to, and partitioning within, the liver. Following a meal, insulin inhibits adipose-tissue lipolysis to reduce FA flux from adipose-tissue to the liver; this is demonstrated by a decreased contribution of adipose-tissue-derived FA to VLDL-TG from ~75% in the fasted state to ~45% in the fed state (58). Within hepatocytes, the postprandial shift in hepatocellular FA metabolism toward DNL and FA esterification and away from oxidation is primarily driven by insulin (54, 55). Following a meal, insulin, via Akt/protein kinase B (PKB), activates sterol regulatory element binding protein 1c (SREBP1c) to upregulate DNL and FA esterification by increasing FAS, ACC2, and GPAT expression (62-64). Independent of insulin, increased hepatic glucose delivery, such as after an acute high-carbohydrate diet, contributes to the postprandial upregulation of DNL and FA esterification by, respectively, activating carbohydrate response element binding protein (ChREBP) to upregulate FAS and ACC2 expression, and providing G3P (via increased glycolysis) for GPAT-mediated FA esterification (36, 65-69). Upregulation of ACC2 increases malonyl-CoA formation, which inhibits CPT1 and reduces hepatic FA oxidation, this reciprocal regulation between FA synthesis and oxidation prevents futile cycling in the liver (54). Taken together, these findings suggest hepatic insulin signalling is a major driver of hepatocellular lipid synthesis and storage, and is supported by findings showing that patients with loss-of-function mutations in the insulin receptor are protected from hepatic steatosis despite presenting with markers of severe insulin resistance and hyperglycaemia (70).

In the fasted period, the relative absence of insulin and glucose, coupled with increased metabolic demands and FA delivery, shifts hepatic FA metabolism towards oxidation and away from DNL and TG esterification (52). Reduced insulin signaling increases adipose-tissue

lipolysis, and hepatic NEFA delivery, uptake, and *β*-oxidation. The increased acetyl-CoA and NADH from *β*-oxidation inhibit glucose oxidation by inhibiting pyruvate dehydrogenase and enter the TCA cycle to form citrate. Subsequently, increased citrate concentrations promote flux through the TCA cycle and further inhibit glucose metabolism by inhibiting glucose entry into glycolysis via phosphofructokinase-1 inhibition (71). Increased intracellular FAs also activate peroxisome proliferator-activated receptor alpha (PPARα), a transcription factor which upregulates genes involved in FA uptake, *β*-oxidation, ketogenesis, lipoprotein metabolism, and mitochondrial biogenesis (72, 73). Taken together, these FA-induced intracellular changes increase the overall FA metabolic capacity and acutely inhibit hepatic glucose metabolism in the fasted state.

1.4.2 Dysregulated Hepatic Fat Metabolism in the Pathogenesis of Hepatic Steatosis

It is not fully clear how elevated IHTG accumulation develops, especially in context of MASLD, though it is likely due to imbalances between the delivery, synthesis, and removal of FA from the liver. Steatotic liver disease, which, until recently, was termed non-alcoholic fatty liver disease (NAFLD), is now reclassified as MASLD (1). Although terminology has changed from NAFLD to MASLD (1), I will refer to the terminology/definition used by the authors of the respective studies for the purposes of this thesis. Increased IHTG content is a hallmark of NAFLD/MASLD and a risk factor for the disease progressing to non-alcoholic steatohepatitis (NASH)/metabolic dysfunction-associated steatohepatitis (MASH) and cirrhosis; these conditions characterised by hepatic inflammation, fibrosis, and eventually, liver failure (74). Therefore, understanding the mechanisms which contribute to increased IHTG content may help improve the understanding of how to prevent MASH and cirrhosis. Although it has been consistently demonstrated that overconsuming dietary fat, as excess calories, increases IHTG content (6, 52), the amount of dietary fat entering the liver depends on several factors, including the quantity (75-77), frequency (78), and potentially composition (61, 79) of the dietary fat

consumed, along with an individual's phenotype (i.e. adiposity, insulin resistance, etc.) and genotype (33, 80-83). One proposed mechanism explaining how IHTG accumulation increases with adiposity suggests that individuals with elevated adiposity have a reduced ability to store dietary fat in adipose tissue which leads to increased IHTG content (84). In support of this, patients with partial lipodystrophy have a genetic mutation that limits their ability to store fat in adipose tissue, and accordingly, present with severe IHTG accumulation (81). This suggests impaired adipose tissue fat storage and metabolism may have a role in IHTG accumulation.

Increased adipose tissue lipolysis alone may not explain the increased IHTG accumulation in individuals with obesity as plasma NEFA concentrations, a marker of adipose tissue lipolysis, do not correlate with BMI (85, 86). Indeed, the rate of appearance (R_a) of NEFA per kilogram fat mass is negatively correlated with fat mass, suggesting that lipolysis decreases with increased adiposity (86). However, total R_a NEFA and R_a NEFA per kilogram lean mass are positively correlated with fat mass, and this suggests that, despite a decrease in adipose-tissue lipolysis, NEFA delivery to non-adipose tissues (like the liver and heart), increases with adiposity (86). This discrepancy may be explained by the absolute increase in adipose tissue mass in obese individuals which may override the suppression of lipolysis and lead to increased NEFA delivery to non-adipose tissues. As NEFA uptake into non-adipose tissues strongly correlates with plasma NEFA levels, in individuals with obesity, increased NEFA uptake into cells may match the increased hepatic NEFA delivery and normalise plasma NEFA levels (54, 55). While this may explain increased hepatic lipid delivery in the fasted state, there is evidence of altered postprandial metabolism in obese individuals, as obese, compared with lean, adipose tissue has decreased postprandial FA trafficking (80). Following a meal, if FA uptake into adipose tissue is reduced, this may inappropriately increase hepatic dietary fat delivery as TRL-remnants or spillover FAs and further contribute to IHTG accumulation.

Elevated flux through hepatic DNL may contribute to IHTG accumulation. Using stable-isotope tracer methodologies, Donnelley *et al.* reported that in individuals with NAFLD, ~23% of VLDL-TG FA came from DNL; higher than the ~5% of DNL-derived FA in VLDL-TG from individuals without NAFLD (58, 60). Further, in individuals with NAFLD, the proportion of DNL-derived FAs in VLDL-TG did not differ between the fed and fasted state suggesting that constitutively elevated fasting DNL may contribute to IHTG accumulation (60). It is suggested by some that insulin resistance and hyperinsulinemia precede IHTG accumulation (33, 87); this would lead to reduced peripheral glucose uptake and hyperglycaemia, which increases insulin-independent glucose uptake into hepatocytes and could drive DNL activation via ChREBP (88).

Decreased lipid removal from the liver, through impaired FA oxidation or VLDL-TG secretion, may also contribute to IHTG accumulation. However, human studies investigating FA oxidation report conflicting results in patients with MASLD (69, 87, 89, 90). In some studies, people with IHTG accumulation are reported to have reduced hepatic FA oxidation secondary to increased hepatic DNL and/or hyperinsulinemia (33, 69). Alternatively, increased dietary FA delivery as TRL-remnants or spillover FAs may increase hepatic FA uptake which, in a PPARα-mediated manner, could increase FA oxidation (87, 90, 91). While the discrepancy in FA oxidation findings in MASLD patients may be explained by differences in methodology used to measure FA oxidation or patient characteristics between studies, there is emerging evidence that the FA composition of a person's diet may influence FA oxidation findings as dietary PUFAs, compared with SFAs, have been suggested to preferentially enter oxidation pathways (92). Although differences in the patient's background dietary FA composition may potentially explain the conflicting FA oxidation findings it remains unclear how FA composition impacts FA oxidation findings under conditions where FA oxidation may be suppressed, such as when hepatic DNL is elevated.

Alterations in hepatic VLDL-TG secretion could modulate IHTG content, however, relatively few studies have investigated the contribution of this pathway to IHTG accumulation in humans. Genetic studies have revealed that transmembrane 6 superfamily member 2 (TM6SF2) mutations reduce VLDL-TG secretion and increase IHTG accumulation, indicating that impaired hepatic VLDL-TG secretion increases IHTG content (83). However, in individuals with NAFLD, VLDL secretion rates are increased, with VLDL particles containing more TG compared with age- and BMI-matched individuals without NAFLD (93, 94). Further, while VLDL secretion positively correlates with IHTG content, secretion rates plateau when IHTG reaches ≥10% (94, 95). This suggests VLDL secretion may increase as a compensatory mechanism to remove excess TG from the liver. However, as individuals with IHTG accumulation may have reduced capacity for lipid storage in adipose tissue and VLDL delivery to peripheral tissues may exceed their oxidative capacity, the VLDL-remnants would recirculate to the liver, thereby contributing to IHTG accumulation.

1.4.3 Summary

Dysregulated hepatic fat metabolism likely contributes to IHTG accumulation; however, the exact mechanisms by which IHTG accumulates in the context of MASLD remains unclear. Further, it remains unclear how dietary fat composition interacts with hepatic FA metabolism pathways to influence IHTG accumulation.

1.5 Cardiac Metabolism

1.5.1 Cardiac Metabolism Under Physiological Conditions

The heart has one of the highest metabolic demands in the body, requiring a constant ATP supply to support its contractile activity to pump oxygenated, nutrient rich blood to, and remove waste products from, peripheral tissues. About 95% of cardiac ATP production occurs

through mitochondrial oxidative metabolism, with the remaining 5% is generated by substrate-level phosphorylation in glycolysis and TCA cycle (96). While the heart can oxidise a variety of metabolic substrates, ~60% of cardiac ATP production is derived from FA oxidation, ~30% from glucose oxidation, and the remaining ~10% from lactate, ketone, and amino acid oxidation (97-101). FAs are the preferential cardiac fuel source under most conditions as FA oxidation produces more ATP per molecule compared with glucose oxidation (102). However, as FAs are a less oxygen-efficient fuel source than glucose, the heart must be able to rapidly switch between FA and glucose oxidation to delicately balance limited oxygen supply with high ATP demands (102). The heart can store glucose as glycogen and FAs as TG; however, only ~10% of glucose and ~15% of FAs taken up into cardiomyocytes are stored, indicating the heart is highly dependent on adequate nutrient delivery to meet its metabolic demands (101, 103-105). In the heart, ATP can be rapidly generated around the myofilament from phosphocreatine (PCr) reserves (Fig. 1.5). However, as cardiac PCr concentrations can be rapidly used up, PCr more likely functions to buffer ATP concentrations during rapid increases in cardiac workload rather than as a protective mechanism against impaired nutrient delivery (106). Taken together, myocardial nutrient supply is fundamental to supporting cardiac function.

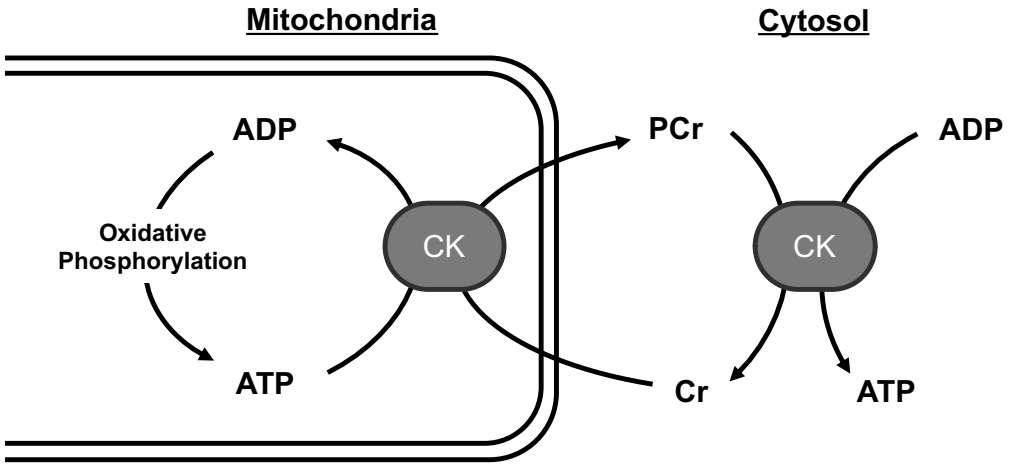

Figure 1.5. Cardiac Phosphocreatine Shuttle. Abbreviations: ADP, adenosine diphosphate; ATP, adenosine triphosphate; Cr, creatine; PCr, phosphocreatine; CK, creatine kinase.

1.5.1.1 Regulation of Cardiac Metabolism

Although FAs and glucose are constantly supplied to the heart, intricate mechanisms regulate myocardial substrate selection to ensure cardiac ATP demands are met in response to changes in substrate supply (following fasting and feeding) or workload (107). Under physiological conditions, the main determinants of myocardial substrate selection are plasma substrate availability and cardiac insulin signaling (107). During the fasting period, relatively low plasma insulin concentrations increase adipose-tissue lipolysis, myocardial FA delivery, uptake, and mitochondrial FA oxidation. When plasma glucose and insulin concentrations increase postprandially, cardiac insulin signaling stimulates GLUT4 translocation to the sarcolemma to increase myocardial glucose uptake and increases malonyl-CoA formation to reduce FA oxidation (21, 38). In the heart, insulin also increases CD36 translocation to the sarcolemma, which increases postprandial cardiac FA uptake (108). Independent of insulin and other hormones, the oxidation of one fuel source (i.e. FAs) inhibits oxidation of the other fuel source (i.e. glucose); this is a major intracellular mechanism regulating myocardial substrate selection (Fig. 1.6) (71). Hormones other than insulin also modulate cardiac metabolism, for example, adrenaline and noradrenaline increase cardiac contractility, heart rate, and promote glycogenolysis, TG lipolysis, and oxidative metabolism (109-112). The heart's ability to switch between fuel sources is referred to as metabolic flexibility and is vital in ensuring adequate myocardial ATP production.

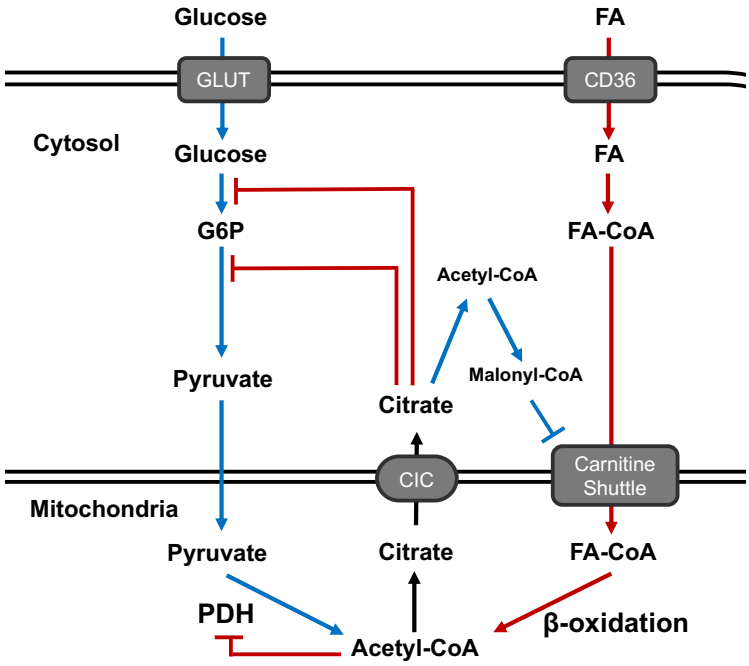

Figure 1.6. Reciprocal Inhibition between FA and Glucose Oxidation (i.e. Randle Cycle). When fatty acids (FAs) are abundant (red), FA oxidation inhibits glucose metabolism by *i)* increasing mitochondrial acetyl-CoA and NADH concentrations, which inhibit pyruvate dehydrogenase (PDH), the rate limiting enzyme of glucose oxidation, and *ii)* through forming citrate, which inhibits phosphofructokinase-1, the rate limiting enzyme of glycolysis. In contrast, when glucose is abundant (blue), glucose oxidation inhibits FA metabolism through forming malonyl-CoA, which inhibits mitochondrial FA uptake. Abbreviation: CIC, citrate carrier; GLUT, glucose transporter; CD36, cluster of differentiation 36/fatty acid translocase; G6P, glucose-6-phosphate.

1.5.2 Disrupted Cardiac Metabolism in the Pathogenesis of Cardiovascular Disease

Impaired ATP production, secondary to alterations in cardiac metabolism and a loss of metabolic flexibility contribute to CVD pathogenesis. For example, in heart failure with reduced ejection fraction (HFrEF), absolute myocardial ATP content and PCr/ATP, a biomarker of myocardial energetic reserve, are reduced by ~30% and ~50%, respectively (113, 114). Supporting this, most animal and some human studies report that myocardial metabolism in HFrEF shifts towards a more glycolytic, lower ATP-yielding, phenotype compared with the healthy heart (115-122). In some human studies, this shift towards glycolysis in the context of HFrEF is associated with decreased ability to oxidise FAs (118-122). In contrast, in T2D studies, myocardial metabolism shifts towards excessive FA uptake, oxidation, and TG accumulation (123-126). Both examples highlight that shifting myocardial substrate selection towards predominantly relying on glucose or FAs for ATP generation, without the ability to

switch to the alternative substrate, has detrimental effects on cardiac function. However, perturbations in cardiac metabolism develop before deteriorations in cardiac function suggesting that alterations in cardiac metabolism may have a pathogenic role in CMD development (124, 127).

Although obesity is not traditionally considered a CVD, there is evidence of abnormal cardiac metabolism and function in this population. Compared with age- and sex-matched controls, individuals with obesity have reduced cardiac PCr/ATP, which is associated with increased BMI, adiposity, and diastolic dysfunction (130, 131). Another marker of abnormal cardiac metabolism, increased myocardial TG content, is positively correlated with obesity and with markers of cardiac dysfunction, including left ventricular (LV) hypertrophy (LVH) and concentric LV remodeling (130). As cardiac FA uptake and metabolism are influenced by plasma FA availability, and dietary FA composition influences plasma FA composition, it could be speculated that dietary FA composition may impact cardiac metabolism and function.

1.6 Dysregulated Hepatic Lipid Metabolism & CVD Risk

As obesity is a risk factor for MASLD and CVD, and similar mechanisms may contribute to the development of IHTG accumulation and perturbed cardiac metabolism in obesity, there is interest in clarifying the relationship between hepatic steatosis and CVD risk. Recently, MASLD has been identified as an independent CVD risk factor and this risk is further increased if a patient has hepatic fibrosis (128-132). Even in individuals with a BMI <25 kg/m^2, a NAFLD diagnosis increases the risk of developing CVD, suggesting this relationship may be independent of obesity (133). Despite evidence linking hepatic steatosis with increased CVD risk, it remains unclear if MASLD increases CVD risk as a consequence of dysfunctional hepatic metabolism, or if the presence of increased IHTG accumulation identifies individuals with a more severe manifestation of metabolic syndrome, and it is this more severe underlying

systemic metabolic problem which increases CVD risk.

1.6.1 Evidence For Dysfunctional Hepatic Metabolism Increasing CVD Risk

Increased CVD risk in individuals with increased IHTG content but not defined as overweight or obese may be explained by alterations in hepatic metabolism and function, independent of systemic metabolic derangements (133). Patients with NAFLD have increased VLDL-TG secretion rates with larger VLDL-TG particles and reduced hepatic clearance of TRL-remnants and plasma NEFA, this may increase cardiac lipid delivery, promote excessive cardiac FA oxidation and impair metabolic flexibility (93, 94, 134). Further, these changes in hepatic lipoprotein metabolism may explain the hypertriglyceridemia, increased LDL and oxidised LDL, and decreased HDL (collectively termed "atherogenic dyslipidaemia") in individuals with NAFLD, and therefore, the increased risk of developing atherosclerotic CVD (131, 135). Alternatively, increased CVD risk in patients with MASLD may be mediated through the effects of specific FAs, such as palmitate, on the heart. Palmitate is the major product of hepatic DNL and once formed, is esterified into TG and secreted in VLDL. Hepatic DNL may be increased in individuals with MASLD, therefore, these individuals may have greater cardiac delivery of palmitate (60). Palmitate is reported to alter calcium and potassium currents in cardiomyocytes in a pro-arrhythmogenic manner, which may explain the increased rates of arrhythmias in patients with MASLD (136, 137). In addition to the detrimental changes on lipid metabolism, hepatic steatosis increases systemic and vascular inflammation, and endothelial dysfunction, all of which are independent CVD risk factors (138, 139). While relevant to the connection between hepatic steatosis and CVD risk, the details on the relationships between hepatic steatosis, inflammation, and endothelial function are beyond the scope of this thesis and have been comprehensively reviewed (139, 140). Together, this evidence suggests that changes in cardiac metabolism and function, originating from

derangements in liver metabolism secondary to IHTG accumulation, contribute to increased CVD risk in MASLD patients.

1.6.2 Evidence For Severe Systemic Metabolic Dysfunction Increasing CVD Risk

Greater insulin resistance, hyperinsulinemia, dyslipidaemia, and central adiposity are associated with increased IHTG accumulation (33, 141, 142). As all four metabolic derangements are also CVD risk factors, patients with increased IHTG accumulation, such that they meet MASLD diagnostic criteria, may have increased CVD risk due to this more severe metabolic phenotype (142-144). Supporting this, Luukkonen *et al.* investigated two patient groups with similarly elevated IHTG content, one group had multiple features of metabolic syndrome and were not carriers of the I148M variant in the patatin-like phospholipase domain containing protein 3 (*PNPLA3*) gene ("Metabolic NAFLD") and the other group had minimal features of metabolic syndrome and were carriers of the I148M variant in the PNPLA3 gene ("PNPLA3 NAFLD"). The "Metabolic NAFLD" group showed increased markers of insulin resistance, while the "PNPLA3 NAFLD" group did not, despite comparable total liver fat (145). Further, individuals with "PNPLA3 NAFLD" are at lower risk from developing CVD compared with individuals with "Metabolic NAFLD", despite similarly elevated liver fat (146, 147). This supports that systemic metabolic derangements, regardless of IHTG content, are needed to increase CVD risk. It could be argued that T2D is, in general, a disease with more severe manifestations of insulin resistance, hyperinsulinemia, dyslipidaemia, and central adiposity than MASLD, therefore, if perturbations in systemic metabolism are the primary driver of CVD in patients with elevated IHTG, then patients with T2D but without MASLD should have higher rates of CVD than patients with MASLD but without T2D. Indeed, the CVD incidence rate in patients with T2D but without MASLD is ~11.9 per 1000 person-years, which is higher than the ~8.5 per 1000 person-years in patients with MASLD but without T2D (148, 149). These studies support the suggestion that perturbations in systemic metabolism are

key mediators of increased CVD risk in patients with increased IHTG content.

1.6.3 Summary

Perturbations in both hepatic and systemic metabolism likely contribute to elevated CVD risk in individuals with increased IHTG content, especially as patients with both MASLD and T2D have higher rates of CVD than patients with only T2D or MASLD (150). As alterations in lipid metabolism appear to impact IHTG accumulation, cardiac metabolism, and CVD risk, and dietary fat is a major source of systemic FAs, changes in dietary fat content or composition could modulate systemic lipid metabolism, and by extension cardiac and hepatic metabolism and function, and CVD risk. Therefore, it is of interest to clarify the relationship between dietary FA composition, IHTG accumulation, and cardiac metabolism and function.

1.7 Dietary Fat Composition & Liver Fat Accumulation

1.7.1 Observational Studies Linking Dietary Fat Composition to Liver Fat Content

The effect of dietary fat composition on CMD risk was first described in the 1970s in the Seven Countries Epidemiological Study, which identified a positive association between SFA intake, total serum cholesterol, and CHD risk (151). While the relationship between cholesterol, SFA, and CHD has been well described and thoroughly reviewed (143, 152, 153), the relationship between dietary fat composition and the risk of developing CMDs, such as MASLD, remains unclear.

Most population-based observational studies have found that consuming excess calories or consuming a diet that exceeds the recommended intake of SFA, free sugars, and/or processed foods for the respective participant cohort studied is associated with increased circulating plasma-TG levels, hepatic steatosis, and insulin resistance (154-156). A limited number of cross-sectional studies that assessed dietary FA composition in individuals with and

without NAFLD have suggested that individuals with NAFLD and NASH consumed more total fat, SFA, and cholesterol, and less MUFA and PUFA, than age- and BMI-matched individuals without NAFLD (155, 157, 158). Further, in individuals diagnosed with NAFLD, this dietary pattern was associated with a higher degree of insulin-resistance and likelihood of hepatic steatosis progressing to NASH, compared with individuals with NAFLD who had consumed a diet lower in SFA and higher in MUFA and PUFA (159-161). Although self-reported food diaries and questionnaires are prone to reporter bias (162), these findings agree with more objective measures of *in vivo* intrahepatic and plasma FA composition (including quantifying IHTG FA composition in patients using MR spectroscopy and performing lipidomic and gas chromatography analysis on the FA composition of plasma lipid pools and liver biopsies); these studies have found that patients with NAFLD and NASH have increased SFA and decreased unsaturated FA in their circulating plasma TG and intrahepatic lipid pools compared with disease-free controls (163-167). Taken together, these observational studies indicate there is an association between dietary FA composition and IHTG quantity.

1.7.2 The Role of Intrahepatic FA Composition on Cardiometabolic Disease Risk

Although increased liver fat content is a CMD risk factor, IHTG FA composition, independent of IHTG quantity, may modulate CMD risk. In a study which characterised the liver lipidome of patients with elevated IHTG content, despite similarly increased liver fat content, differences in IHTG FA composition were observed between patients with "Metabolic NAFLD" compared with "PNPLA3 NAFLD" (145). The liver lipidome of patients with "Metabolic NAFLD" was enriched in saturated and monounsaturated TG, free FA, markers of *de novo* ceramide synthesis, and ceramides compared with patients without "Metabolic NAFLD" (145). In contrast, the liver lipidome of patients with "PNPLA3 NAFLD" was enriched in polyunsaturated TG, and not with ceramides, compared with individuals with "non-PNPLA3 NAFLD" (145). These findings agree with studies which performed lipidomic

analysis on liver biopsy samples and found the composition of hepatic lipids from obese patients with NAFLD or NASH were enriched with SFA, MUFA, and diacylglycerols (DAG) and deplete of PUFA compared with non-NAFLD obese controls (163, 165). Taken together, this suggests IHTG FA composition, independent of IHTG quantity, may influence CMD risk.

Although the consumption of dietary FAs differs between patients with NAFLD and disease-free controls, it has been reported that patients with NAFLD consume more free sugars and sugar-sweetened beverages than people without, suggesting that dietary sugars may also contribute to hepatic steatosis NAFLD (168-171). However, as sugars are substrates for hepatic DNL, excess sugar consumption could increase intrahepatic palmitate and contribute to CMD pathogenesis by modifying intrahepatic FA composition. In support of this, hepatic DNL was reported to not correlate with IHTG content in individuals with NAFLD, T2D, and disease-free controls; however, hepatic DNL correlated positively with the hepatic SFA fraction and did not correlate with the PUFA fraction (172). Further, the total IHTG content and the liver PUFA fraction were not associated with hepatic insulin sensitivity, whereas the hepatic SFA fraction had a strong, negative association with hepatic insulin sensitivity (172). Given these observations, it could be speculated that intrahepatic SFA quantity, rather than total intrahepatic fat quantity, may negatively contribute to hepatic insulin sensitivity and CMD risk, and that high rates of hepatic DNL, which are increased by dietary sugar consumption, alter intrahepatic FA composition to increase intrahepatic SFA quantity (172). However, as palmitate can be elongated into stearate (C18:0) and desaturated to palmitoleate (C16:1n-7) and oleate (C18:1n-9) (32), if an individual can elongate and/or desaturate newly made palmitate to oleate and/or palmitoleate, then the effects of a high rate of hepatic DNL on hepatic insulin sensitivity might be partly attenuated, and might thus attenuate CMD development and progression. Alternatively, if individuals with high rates of hepatic DNL consume a high-SFA diet, the increased intrahepatic SFA content may exceed the capacity of hepatic enzymes to

desaturate and elongate palmitate, which could promote intrahepatic SFA accumulation and potentiate the development and progression of insulin resistance and CMD.

Taken together, observational studies have identified that diets enriched with total fat, SFA, and free sugars, and lower in MUFA and PUFA are associated with increased IHTG accumulation, and that these dietary patterns may modify IHTG FA composition which can independently modulate CMD risk factors. However, as these studies have explored the effect of dietary patterns on IHTG accumulation, interventional studies are needed to characterise the effects of specific dietary FAs on these disease processes.

1.7.3 Interventional Studies on Dietary Fat Composition & Liver Fat Content

A limited number of interventional studies have investigated how dietary fat quantity and composition influence IHTG accumulation in cohorts of varying age, BMI, and disease status, and are summarised in Tables 1.2-1.4. To investigate the effect of dietary fat quantity, participants consumed diets with either less calories (hypocaloric), more calories (hypercaloric), or an equal number of calories (isocaloric) for their individual metabolic needs, and these may vary in macronutrient composition. For example, participants may consume high-fat low-carbohydrate (HFLC) diets, or low-fat high-carbohydrate (LFHC) diets. To study the effect of dietary fat composition, participants typically consume the same amount of fat but with varied composition. For example, some participants may consume a diet enriched in SFA and others a diet enriched in PUFA. There is currently no universally accepted definition for what constitutes a HFLC or LFHC diet, but it has been suggested that a HFLC diet is between 50-60% total energy (TE) fat and 20-30% TE carbohydrate, and a LFHC diet is 20-30% TE fat and 60-70% TE carbohydrate (173, 174). For the purposes of this thesis, I will refer to the type of diet consumed (e.g. HFLC, LCHF, SFA-enriched etc.) using the same terminology used by the authors of the discussed study.

1.7.3.1 Findings from Hypocaloric Studies

Hypocaloric studies have consistently reported that regardless of macronutrient (e.g. fat, carbohydrate) or dietary fat composition, decreased caloric intake reduces body weight and IHTG content (175-180) (Table 1.2). This decrease in IHTG accumulation has been observed in people who are overweight, obese, and/or have NAFLD or T2D, and who have undertaken hypocaloric interventions from 14 days for up to 2 years (Table 1.2) (181). In six studies that compared the effect of hypocaloric HFLC with hypocaloric LFHC diets on IHTG content, most reported similar reductions in body weight and IHTG across the two diet types and irrespective of macronutrient composition (175, 176, 179, 182-184). Recently, Schutte *et al.* (184) explored the effect of two 25% energy restricted LFHC diets on weight loss and IHTG content in 110 men and women with obesity aged 40-70 years. One diet was enriched in unsaturated FA, fibre, and plant-protein (high nutrient quality) and the other was enriched in SFA and free-sugars (low nutrient quality), and both were consumed for 12 weeks. They found no difference in the reduction of IHTG content between the two diet types, despite the high-nutrient-quality energy restricted diet resulting in a 2.1 kg greater weight loss ($p<0.01$) than the low-nutrient-quality energy restricted diet (184). These observations, along with other studies, indicate that dietary fat composition has minimal impact on changes in IHTG content when consuming a hypocaloric diet.

1.7.3.2 Findings from Hypercaloric Studies

Consuming a hypercaloric fat-enriched diet appears to increase IHTG accumulation to a greater extent than consuming a hypercaloric carbohydrate-enriched diet, despite both diets inducing similar weight gain (9-11, 185, 186). This suggests that in conditions of caloric excess, dietary fat quantity and/or composition influences the extent of IHTG accumulation (Table 1.3). For example, when overweight participants consumed an extra 1000kcal/day as

either SFA, unsaturated FA, or simple sugars for 3 weeks, IHTG content increased to a greater extent following the SFA diet, compared with the unsaturated FA or simple sugar diets despite similar weight gain (9). Further, after 3 weeks of consuming the SFA diet, markers of insulin resistance and plasma ceramides increased; these markers remained unchanged in those consuming the unsaturated FA or simple sugar-enriched diets (9). These findings indicate that increased SFA content, in the context of a HFLC hypercaloric diet, promotes a greater increase in IHTG content and increased CMD risk. Similar studies in lean and overweight participants, lasting between 3 days to 8 weeks, have found that overfeeding SFA, compared with overfeeding unsaturated FA or fructose, leads to greater levels of IHTG accumulation, fasting plasma total cholesterol, LDL, and apoB (10, 11) (Table 1.3). Taken together, these studies indicate the effects of weight gain on IHTG content are exacerbated by consuming increased SFA relative to unsaturated FA or sugar.

Table 1.2. Interventional hypocaloric human studies investigating dietary fat composition effects on intrahepatic triglyceride content.

Study	Participants	Intervention	Duration	Change in liver fat
Browning *et al.* 2011	18 M+F NAFLD. 45±12y 35±7kg/m^2	Low-CHO (<20g/d) diet vs Low-kcal (~1200-1500kcal/d).	14 d	Low-CHO: ↓from 22±13% to 10±7$^{\$}$% Low-kcal: ↓from 19±10 to 14±7$^{\$}$%
Haufe *et al.* 2011	102 M+F 30-60y§ 25-45kg/m^{2§}	Low-CHO (<90g/d) vs Low-fat (<20% TE)	6 m	Low-CHO: ↓~47*% Low-fat: ↓~42*% NSD between groups.
Kirk *et al.* 2009	22 M+F 43.6±2.5y 36.5±0.8 kg/m^2	High-CHO (>180g/d) vs Low-CHO (<60g/d)	~11 wk	Low-CHO: ↓38.0±4.5*% High-CHO: ↓44.5±13.5*%. NSD between groups.
Lewis *et al.* 2006	18 M+F 50y† (34-57y)‡‡ 44kg/m^2 †(40-51kg/m^2) ‡‡	VLCD (450-800 kcal/d)	6 wk	↓~43*%
Otten *et al.* 2016	70 F 50-70y§ 25-40 kg/m^{2§}	Paleo diet (40% TE fat) vs Low-fat diet (25-30% TE fat)	6 m 2 y	Paleo: ↓64*% 6 m, ↓50*% 2 y. Low-fat: ↓43*% 6m, ↓49*% 2 y.
Steven *et al.* 2016	30 M+F T2DM 25–80y§ 27–45 kg/m^{2§}	VLCD (625kcal/d); participants separated based on FPG at follow up. Responders: <7mmol/L. Non-responders: >7mmol/L	8 wk	Responders: ↓12.8±2.7$^{\wedge}$% to 2.2±0.2$^{\$}$% Non-responders: ↓8.2±1.1$^{\wedge}$% to 2.2±0.1$^{\$}$% NSD between groups.
Bian *et al.* 2014	43 M+F 51±3y 30.6±1.4 kg/m^2	6d low-CHO diet (-1000kcal/day, <20g CHO/d) vs. -1000 kcal/week as 30%TE fat (10% SFA, 10% MUFA, & 10% PUFA), 50%TE CHO until ~5% weight loss achieved	6d vs. 7m	6d low-CHO diet: from 11.1±1.3 to 8.4±1.3$^{\$}$% 7m 5% weight loss: from 10.8±1.5 to 7.8±1.4$^{\$}$% NSD between groups
Schutte *et al.* 2022	100 M+F 61y† (42-70y) ‡ 31.2±3.3$^{\#}$ kg/m^2	25% ER as a high-quality diet vs. Low-quality diet vs. No-ER habitual diet	12 wk	ER High-quality diet: ↓55*% ER Low-quality diet: ↓46*% Weight-neutral habitual diet: ↑24*% NSD between weight loss conditions

Crabtree *et al.* 2021	37 M+F 35±3y 30.9±0.7 kg/m^2	KD + ketone salt (70% TE fat) vs KD + placebo (67% TE fat) vs. Low-fat (25% TE fat) diet	6 wk	KD + ketone salt: ↓42*% KD + placebo: ↓32*% Low-fat diet: ↓52*% NSD between groups
Properzi *et al.* 2018	51 M + F 52 ±1.54$^¥$ y 30.8±0.7$^¥$ kg/m^2	LFHC diet (30% TE fat) vs. HFLC diet (45% TE fat)	12 wk	LFHC: ↓29*% HFLC: ↓30*% NSD between groups

Subject data presented as mean ± SEM unless otherwise stated: $^{\#}$ denotes standard deviation, †denotes median; ‡denotes range; ‡‡denotes interquartile range; $^{¥}$denotes pooled data; ↓ denotes a decrease in liver fat; ↑ denotes an increase in liver fat; $^{\wedge}$ denotes absolute change in liver fat; * denotes relative change in liver fat; $^{\$}$ denotes absolute liver fat at end of intervention; Abbreviations: CHO, carbohydrate; d, days; ER, energy restricted; FPG, fasting plasma glucose; F, Female; HFLC, high-fat low carbohydrate; KD, ketogenic diet; LFHC, low-fat high-carbohydrate; M, male; m, months; NAFLD, non-alcoholic fatty liver disease; NSD, no significant difference; Paleo, paleolithic; PUFA, polyunsaturated fatty acids; SFA, saturated fatty acids; TE, total energy; T2DM, type 2 diabetes mellitus; wk, weeks; y, years.

Table 1.3. Interventional hypercaloric human studies investigating dietary fat composition effects on intrahepatic triglyceride content.

Study	Participants	Intervention	Duration	Change in liver fat
Sobrecases *et al.* 2010	30 M 23.9±0.4y 22.6±0.2kg/m^2	StdD + Fru (3.5g/kg/FFM), SFA (+30% TE) vs. StdD +Fru+ SFA (3.5 g/kg/FFM & +30% TE)	7 d	Fru: ↑~16*% SFA: ↑~86*% Fru+SFA: ↑~133*%
Luukkonen *et al.* 2018	38 M+F 48±2y 31±1 kg/m^2	Extra 1000kcal/d as SFA vs. UnSFA vs. simple sugars	3 wk	SFA: ↑~55*% UnSFA: ↑~15*% Sugar: ↑~33*%
Rosqvist *et al.* 2014	37 M+F 20-38y§ 18-27 kg/m^{2§}	Habitual diet + High-SFA vs. high *n*-6 PUFA muffins	49 d	SFA: ↑0.56±1$^{\wedge}$% PUFA: ↑0.04±0.24$^{\wedge}$%
Rosqvist *et al.* 2019	60 M+F 42.3±9.5$^{\#}$y 28.3±3.5$^{\#}$ kg/m^{2§}	Habitual diet + High-SFA vs. High *n*-6 PUFA muffins	8 wk	SFA: ↑~53*% PUFA: ↓~2*%
van der Meer *et al.* 2008	15 M 25±6.6 y 23.4±2.5 kg/m^2	Habitual diet + 280 g/day fat (800 mL cream)	3 d	↑112*%

Subject data presented as mean ± SEM unless otherwise stated: $^{\#}$ denotes standard deviation, §denotes inclusion criteria or estimated range within which all participants are included; ↓ denotes a decrease in liver fat; ↑ denotes an increase in liver fat; $^{\wedge}$ denotes absolute change in liver fat; * denotes relative change in liver fat; Abbreviations: d, days; F, Female; Fru, fructose; M, male; m, months; PUFA, polyunsaturated fatty acids; SFA, saturated fatty acids; TE, total energy; UnSFA, unsaturated; wk, weeks; y, years.

1.7.3.3 Findings from Isocaloric Studies

In overweight and obese men and women, with and without NAFLD or T2D, consuming an isocaloric LFHC diet or low-SFA diet for between 2–16 weeks decreased IHTG content (61, 75-77, 187-191). In non-obese (BMI 18.5-27.5 kg/m^2), young (20-45 yr), otherwise healthy men and women, consuming a LFHC diet supplemented with one of three oils high in SFA, MUFA, or PUFA, did not change IHTG content (189). However, as baseline IHTG content in this cohort was on the lower end of the normal range (~1.0 ± 1.17%) and the participants were free from metabolic disease, this may explain the lack of observed difference (189). In contrast, isocaloric HFLC or high-SFA diets increase or do not change the IHTG content (61, 75-77, 187, 192, 193) (Table 1.4). To investigate the effect of specific dietary FAs on IHTG content, 61 overweight and obese participants consumed an isocaloric HCLF diet enriched with either SFA or PUFA for 10-weeks (61). In this study, IHTG content decreased by 16% following consumption of the PUFA-enriched diet and increased by 34% following consumption of the SFA-enriched diet (61). Using a randomised crossover study design, Basset-Sagarminaga *et al.* (187) compared the effect of a 2-week isocaloric low-glycaemic index (GI), low-SFA diet to a high-GI, high-SFA diet in 13 overweight and obese men and women. IHTG accumulation was significantly lower after following the low-GI, low-SFA diet compared with the high-GI, high-SFA diet; notably, changes in IHTG content were not correlated with changes in body weight (187). Moreover, following the consumption of a test meal at the end of the dietary intervention, the high-GI, high-SFA diet led to significantly greater postprandial TG and glucose concentrations compared with the low-GI, low-SFA diet (187). In a randomised crossover trial (RCT) of 16 overweight men comparing the effects of a 4-week isocaloric SFA-enriched diet with a free-sugar-enriched diet, consuming a SFA-enriched diet increased IHTG content to a greater extent and led to greater postprandial glucose and insulin excursions; changes in IHTG content did not correlate with changes in body weight

(192). Despite the variation in the design, duration, measured outcomes (e.g. plasma biochemical parameters), and participant populations among these hyper- and isocaloric intervention studies, they highlight the divergent effects of dietary SFA and of unsaturated FA on IHTG accumulation.

Findings from observational and interventional dietary studies demonstrate that dietary fat quantity and composition impact IHTG content, and by extension, CMD risk. It appears the consumption of SFAs and PUFAs lead to divergent effects on IHTG accumulation, which suggests there may be differences in the intrahepatic or systemic handling of specific dietary FA. However, it is unclear how dietary FA composition may impact IHTG accumulation in the context of a HFLC diet, and it unclear through which mechanism(s).

Table 1.4. Interventional isocaloric human studies investigating dietary fat composition effects on intrahepatic triglyceride content.

Study	Participants	Intervention	Duration	Change in liver fat
Bjermo *et al.* 2012	61 M+F 30-65y[§] 25-40kg/m^{2}[§]	*n*–6 PUFA enriched (15% TE) vs. SFA enriched (15% TE) diet	10 wk	*n*-6 PUFA: ↓0.9[^]% SFA: ↑0.3[^]%
Marina *et al.* 2014	13 M+F 18-55y[§] >27kg/m^{2}[§]	Low-fat (20% TE) vs. High-fat (55% TE) diet	4 wk	Low-fat:↓13.9±10.2[*]% High-fat: NSD
Utzschneider *et al.* 2013	35 M+F 69.3±1.6y 26.9±0.8kg/m^{2}	High-SFA (24%TE) vs. Low-SFA (7%TE) diet	4 wk	High-SFA: NSD Low-SFA: ↓19.8±6[*]%.
van Herpen *et al.* 2011	20 M 50-60y [§] >27kg/m^{2}[§]	Low-fat (20%TE) vs. High-fat (55%TE) diet	4 wk	Low-fat:↓~13[*]% High-fat: ↑~17[*]%
Westerbacka *et al.* 2005	10 F 43±5y 33±4 kg/m^{2}	Low-fat (16%TE) vs. High-fat (56%TE) diet	14 d	Low-fat: ↓20±9[*]% High-fat: ↑35±21[*]%
Parry *et al.* 2020	16 M 47.9±1.1y 27.7±0.4 kg/m^{2}	High-SFA (45%TE fat, 20%TE SFA) vs. High-sugar (20%TE fat, 20%TE sugar) diet	4 wk	SFA: ↑~39.0±10.0[*]% Sugar: NSD
Basset-Sagarminaga *et al.* 2023	13 M+F 67±6[#]y 29.5±1.9[#] kg/m^{2}	High-GI/SFA (15%TE SFA) vs. Low-GI/SFA (5%TE SFA) diet	2 wk	Post High-GI/SFA diet: 3.3±0.6[$]% Post Low-GI/SFA diet: 2.4±0.5[$]%
Della Pepa & Vetrani *et al.* 2020	43 M+F T2D 63±6[#]y 31.5±3.5[#] kg/m^{2}	High-MUFA (26.5%TE MUFA, 4.2%TE PUFA) vs. High-MUFA & PUFA diet (26.7%TE MUFA, 5.8%TE PUFA)	8 wk	MUFA alone: ↓1.4%±2.7[#^]% MUFA & PUFA: ↓4.0±4.5[#^]%
Stonehouse *et al.* 2021	64 M+F 20-45[§] y, 18.5-27.5[§] kg/m^{2}	Habitual diet + oil (PUFAs/SFAs/MUFA): Palm Olein Oil (4.2/13.5/15%TE); vs. Soybean Oil (14.4/8.8/9.4%TE) vs. Cocoa Butter (2.3/19.5/11%TE)	16 wk	Palm Olein Oil: NSD Soybean Oil: NSD Cocoa Butter: NSD

Bozzetto *et al.* 2012	17 M+F T2DM 58±6[#] 29.1±2.6[#] kg/m^2	High-CHO/low-GI (28% TE fat, 16% MUFA) vs. High-MUFA (42%TE fat, 27%TE MUFA) diet	8 wk	High-CHO/low-GI diet: NSD High-MUFA diet: ↓29[*]%
Errazuriz *et al.* 2017	43 M+F 62±12[#]y 30.9±3.8[#] kg/m^2	High-MUFA (46%TE fat, 22% MUFA) vs. High-fibre (28%TE fat, 7% MUFA) vs. Control diet (34%TE fat, 8% MUFA) diet	12 wk	High-MUFA: ↓18% ± 3[*^]% High-fibre: NSD Control: NSD

Subject data presented as mean ± SEM unless otherwise stated: [#] denotes standard deviation, [†]denotes median; [‡]denotes range; [‡‡]denotes interquartile range; [¥]denotes pooled data; [§]denotes inclusion criteria or estimated range within which all participants are included; ↓ denotes a decrease in liver fat; ↑ denotes an increase in liver fat; [^] denotes absolute change in liver fat;[*] denotes relative change in liver fat;[$] denotes absolute liver fat at end of intervention; Abbreviations: d, days; ER, energy restricted; FPG, fasting plasma glucose; F, Female; GI, glycaemic index; HFLC, high-fat low carbohydrate; LFHC, low-fat high-carbohydrate; M, male; m, months; NAFLD, non-alcoholic fatty liver disease; NSD, no significant difference; PUFA, polyunsaturated fatty acids; SFA, saturated fatty acids; TE, total energy; T2DM, type 2 diabetes mellitus; wk, weeks; y, years.

1.7.4 Proposed Mechanisms for the Handling of Dietary Fatty Acids

Several mechanisms from *in vivo* and *in vitro* studies have been proposed to explain the divergence in IHTG accumulation following the consumption of a SFA- compared with a PUFA-enriched diet. These include that SFA: 1) does not preferentially enter oxidation pathways relative to PUFA (92, 194); 2) causes the synthesis of biologically active lipids, such as ceramides or DAG (9, 145); 3) induces endoplasmic reticulum (ER) stress responses (195); or 4) undergoes different peripheral handling by extra-hepatic tissues (80).

In a small study (n=4 men) using stable-isotope tracers, DeLany *et al*. (194) showed whole-body FA oxidation decreased with increased FA-chain length and/or decreased FA saturation. By using ^{13}C-labelled FA, Parry *et al.* found the oxidation of dietary linoleate (PUFA) was greater than dietary palmitate (SFA) in healthy individuals consuming their habitual diet (92). *In vitro* studies further support that FA composition influences hepatocellular FA oxidation as linoleate-treated, compared with palmitate-treated HepG2 cells, have higher reactive oxygen species (ROS) production, suggesting that PUFAs promote higher rates of FA oxidation than SFAs or MUFAs (196). In line with these findings, Nagarajan *et al.* used stable isotope-labelled FA tracers to show Huh7 cells treated with a SFA- compared with a PUFA-enriched FA-mixture have lower β-oxidation rates (197). Rat hepatic CPT1, the rate-determining enzyme of mitochondrial FA oxidation, has a higher binding affinity and transport rate for PUFAs compared with SFAs (198). Although it remains unclear if human hepatic CPT1 has a higher binding affinity and transport rate for PUFA compared with SFA, it could be speculated that dietary PUFA, relative to SFA, are preferentially partitioned into mitochondrial oxidation pathways, which would reduce FA availability for TG synthesis and thus, IHTG accumulation.

Most other proposed intrahepatic mechanisms to explain the greater IHTG accumulation with consumption of a SFA- compared with PUFA-enriched diet, suggest that an

excess of intrahepatocellular SFA increases hepatocellular ceramides, DAGs, and/or ER stress, which leads to cellular derangements and IHTG accumulation (145, 195, 199). Indeed, the consumption of a SFA-enriched diet in overweight and obese men and women increases plasma ceramides (9, 11), and the livers of patients with NAFLD have a greater abundance of ceramides (145) and DAGs (165, 195, 199), which are positively associated with hepatic steatosis, insulin resistance, and inflammation (as reviewed in (200)). *In vitro* evidence also supports that palmitate, compared with oleate, may be preferentially partitioning towards ceramide- and DAG-synthesis rather than towards oxidation pathways as culturing HepG2 cells and primary rat hepatocytes with palmitate, compared with oleate, leads to greater ceramide and DAG accumulation (201, 202). Although *in vivo* and *in vitro* studies have shown hepatic ceramide and DAG accumulation is associated with insulin resistance and IHTG accumulation (200), most *in vitro* studies have characterised these responses in cells treated with only palmitate; this limits their generalisability as it is unrepresentative of physiological conditions when multiple FAs are present. For example, hepatocytes treated with only palmitate have less intrahepatocellular lipid accumulation than cells treated with oleate (202-207); this directly contrasts with *in vivo* human studies (9, 10, 61) and *in vitro* studies which report that adding oleate to palmitate-treated cells prevents palmitate-induced cell death and leads to greater intrahepatic lipid accumulation than with palmitate alone (205, 208). Nevertheless, *in vivo* studies have identified a positive association between increased IHTG accumulation and hepatic ceramides and DAGs accumulation, though, further studies are needed to clarify whether ceramide and DAG accumulation precedes or follows IHTG accumulation (145, 199). Overall, it is difficult to conclude, at present, if differences in FA partitioning towards bioactive lipid species synthesis contributes to or results from differences in IHTG accumulation following consumption of SFA compared with PUFA-enriched diets.

The effect of FA composition on extra-hepatic tissue fat metabolism is also thought to

influence IHTG accumulation by modulating FA flux to the liver. Elevated visceral adipose tissue-lipolysis has been suggested to increase IHTG accumulation (84). However, evidence from *in vivo* human studies showing that a SFA-enriched diet produces divergent effects on adipose tissue lipolysis compared with a PUFA-enriched diet is sparse (9). Further, FA trafficking is decreased in obese compared with lean adipose tissue (80), which might increase dietary fat delivery to the liver as TRL-remnants; evidence for an effect of dietary fat composition on this pathway is yet to be demonstrated in humans. Finally, hepatic TG secretion in VLDL is an important disposal route for IHTG. Huh7 cells cultured in SFA- or PUFA-enriched FA-mixtures take up the same proportion of FAs from the media and secrete the same amount of TG (197) suggesting that FA composition may not influence hepatic FA uptake and secretion, however, there is limited evidence for how dietary fat composition might influence this process in humans. To elucidate the mechanisms that underpin the differential handling of SFA compared with PUFA, further human studies and cellular *in vitro* models that capture the complexity of *in vivo* human FA metabolism are needed.

1.7.5 Summary

Diets with different FA compositions induce divergent effects on IHTG accumulation, with the consumption of SFA-enriched diets often leading to greater IHTG accumulation than sugar- or unsaturated-fat enriched diets. Despite growing evidence, it remains unclear if consuming a high-fat diet enriched with SFA or PUFA under isocaloric conditions influences IHTG accumulation. Further, the underlying mechanism explaining how these different dietary FAs may induce divergent effects on IHTG accumulation remain unclear.

1.8 Dietary Fat Composition and Cardiac Metabolism & Function

1.8.1 Dietary Fat Composition & Plasma CVD Risk Factors

The relationship between dietary fat composition and CVD risk has been extensively studied since the 1970s, where it was first reported that diets enriched in SFA are associated with increased plasma LDL and rates of CHD (209). Since then, longitudinal, cross-sectional, and mendelian randomisation studies, along with RCTs and meta-analyses have collectively shown that increased plasma LDL causes atherosclerotic CVD, and that increased consumption of dietary SFA, compared with PUFA, increases plasma LDL (143, 153, 210-213). A systemic review of 74 studies has shown that for every 1% TE of dietary SFA replaced with PUFA, there is a lowering of plasma total cholesterol by 0.064 mmol/L, plasma LDL by 0.055mmol/L, and plasma TG by 0.010 mmol/L (214). Further, overconsuming SFA, compared with unsaturated FA, induces proatherogenic effects on LDL such that each particle is more susceptible to aggregation, independent of LDL concentrations (215). In addition to modulating plasma lipids, increased consumption of dietary SFA, compared with PUFA, may increase plasma pro-inflammatory cytokine concentrations, pro-thrombotic coagulation factors, and blood pressure, all of which are CVD risk factors (216-221). Collectively, these findings indicate that increased consumption of dietary SFA, compared with PUFA, has negative effects of CVD risk, through the detrimental effects of SFA on CVD risk factors.

Given that increased consumption of dietary PUFAs exerts beneficial effects on plasma lipids, and that PUFAs represent a group of different FAs, there is interest in clarifying if certain PUFAs, such as omega–3 FAs, (which include eicosapentaenoic acid (EPA, 20:5*n*–3), docosahexaenoic acid (DHA, 22:6*n*–3), and α-linolenic acid (ALA, 18:3*n*–3)), exert different effects on CVD risk from omega–6 FAs, (which include linoleic acid (LA, 18:2*n*–6) and arachidonic acid (AA, 20:4*n*–6)). A recent meta-analysis of 86 RCTs reported that increased omega–3 FA consumption, provided to patients in most studies as a supplement, slightly

reduced plasma TG and mortality from CHD (222). However, the authors did not comment on how findings from omega–3 FA supplementation compared with increased omega–6 FA supplementation or consumption. This is highly relevant in the context of CMD as studies investigating the effects of dietary FA composition on cardiovascular-related outcomes have focused on EPA, DHA, and ALA (omega–3 FAs) supplementation, while studies investigating the effects of dietary FA composition on IHTG accumulation have focus on linoleate (an omega–6 FA) consumption (10, 61, 222, 223). Despite this difference, there may be a dose-dependent effect of omega–3 and omega–6, PUFAs on plasma lipids, with omega-3 PUFAs exerting lipid-lowering effects at lower concentrations (212, 223-226). Equally, increased omega–3 supplementation, similar to increased omega–6 PUFA consumption, reduces IHTG content (61, 227). This suggests that, with respect to CMD risk, the beneficial effects of increased consumption of PUFA, compared with SFA, on plasma lipids and IHTG accumulation may occur regardless of dietary PUFA omega–3 and omega–6 content.

1.8.2 Dietary Fat Composition and Cardiac Energetics & Function

As different dietary FAs appear to preferentially enter different intracellular and systemic FA handling pathways, dietary FA composition could influence cardiac energetics and function, and thereby CVD risk (92, 194). However, there are no studies to date which have examined the effect of dietary fat composition on *in vivo* human cardiac energetics. A handful of cross-sectional sectional studies have described the relationship between dietary or plasma FA composition and markers of cardiac function or structure, however, there are far fewer studies in this area than on the effects of dietary fat composition on IHTG accumulation. Similarly, while a limited number of RCTs on dietary FA composition and cardiac function have been carried out, they have focused on the effects of omega–3 PUFA supplementation in patients with heart failure or arrythmias (228, 229). Nevertheless, preliminary reports from human studies, along with findings from key animal and *in vitro* studies, support that PUFA,

compared with SFA, enriched diets may exert beneficial effects on cardiac metabolism and function.

Cross-sectional studies report that consuming a diet enriched with SFA, high-glycaemic index, and processed foods is associated with increased LV mass, decreased stroke volume (SV), and decreased LV ejection fraction (EF) (230). In contrast, consuming a diet with a higher unsaturated FA to SFA ratio is associated with a higher LV EF and SV (231). In patients with heart failure with a preserved ejection fraction (HFpEF), increased circulating plasma palmitate is associated with increased dyslipidaemia and a reduced distance achieved during a 6-minute walking test (marker of cardiopulmonary functional capacity), while increased circulating omega–3 PUFAs is associated with increased LVEF, reduced dyslipidaemia, and increased distance during a 6-minute walking test (232, 233). A prospective cohort study over 20 years reported that in 505 men, consuming a diet enriched with SFA at age 50 was positively associated with markers of LV diastolic dysfunction at age 70 (234). In a similar prospective cohort study over 20 years, a 1-standard deviation increase in the proportion of myristate (14:0), palmitate (16:0), stearate (18:0), oleate (18:1*n*–9), or EPA (20:5*n*–3) in the plasma CE fraction increased the risk of developing LVH at age 70 by 29-37%, while a 1-standard deviation increase in the proportion of LA (18:2*n*–6) the plasma CE fraction reduced the risk of developing LVH at age 70 by 24% (235).

RCTs have provided further support that increased PUFA consumption may induce beneficial effects on cardiac function. In a double-blind RCT, 43 patients with HFrEF receiving 1g/day or 4g/day of an omega–3 PUFA supplement, compared with placebo, had a dose-dependent increase in LVEF over 3 months (236). This is in line with a larger study of 133 patients with HFrEF which were randomised to receive a 2g/day omega–3 PUFA supplement or placebo; after 12 months, the PUFA-treated group had improved LVEF, exercise time, and reduced hospitalisation rates compared with placebo (237). In the only interventional study to

date investigating the effect of increased dietary FA consumption (and not supplementation) on markers of cardiac function, Carbone *et al.* showed in 9 patients with obesity and HFpEF that increasing dietary consumption of unsaturated FA for 12 weeks significantly improved exercise time and oxygen pulse without changes in BMI (238). While these studies suggest that increased intake of PUFA, compared with SFA, mediates beneficial effects on cardiac function, it would be of interest to investigate if increased intake of SFA, compared with PUFA, impairs cardiac function. Although no such studies have been performed in humans, two studies have been conducted in dogs and grizzly bears (239, 240). There were divergent cardiac and metabolic effects in dogs fed a HFLC diet supplemented with either lard (high-SFA) or salmon oil (high-PUFA) for 6 weeks (239). Although both groups consumed the same quantity of fat and had similar weight gain, compared with the other diet, dogs fed a lard-supplemented diet had reduced LV function, increased insulin resistance, and increased visceral fat, while dogs fed a salmon oil-supplemented diet had reduced myocardial TG content, and no markers of insulin resistance or cardiac dysfunction (239). Similar findings were observed in grizzlies; feeding grizzly bears a SFA-enriched diet for 5-months led to LV diastolic impairment, increased diastolic arterial blood pressures, and increased circulating pro-inflammatory cytokines compared with grizzly bears fed a PUFA-enriched diet (240). While no differences in cholesterol, HDL, and LDL were observed between the two diets in grizzly bears, evidence suggests that grizzlies are protected from developing atherosclerosis, which may explain why the SFA-, compared with PUFA-enriched diet, did not elevate plasma lipids as seen in humans (241). Although limited studies using different markers, designs, and species have assessed the relationship between dietary FA composition and cardiac function, taken together, the data suggest increased PUFA consumption mediates beneficial effects on cardiac function while increased SFA consumption induces deleterious effects on cardiac function.

1.8.3 Dietary FA Composition & Cardiac Function: Proposed Mechanisms

Several mechanisms have been proposed to explain the divergent effects of consuming a diet enriched or supplemented with PUFA, compared with SFA, on cardiac function; many mechanisms are similar to those proposed for explaining the divergence in IHTG accumulation following consumption of a SFA- compared with PUFA-enriched diet (section 1.7.4). If dietary SFA do not preferentially enter oxidation pathways compared with PUFA, consuming a SFA-enriched diet could impair myocardial energetics and reduce ATP content (92, 194). As impaired cardiac ATP production induces myocardial remodelling, it may explain the diastolic dysfunction and increased LVH in response to a SFA-enriched diet (235, 239, 240, 242). Alternatively, consuming a diet enriched with PUFA, compared with SFA, may protect the heart from dysfunction by increasing cardiolipin, an essential mitochondrial lipid required for mitochondrial oxidative metabolism. In a rat model of heart failure, feeding a diet enriched with linoleate, compared with no linoleate, restored cardiolipin levels and improved mitochondrial oxidative metabolism and LV function (243). Differences in dietary FA composition may exert different effects on cardiac function through divergent effects on cardiac metabolism.

Reduced partitioning of SFA, compared with PUFA, into oxidation pathways may increase intracellular SFA and result in the partitioning of SFA into alternative pathways, such as PL biosynthesis. Indeed, mice fed a SFA-enriched diet and cardiomyocytes cultured in SFA-enriched media have increased membrane PL FA saturation; in mice, this increased PL saturation positively correlates with diastolic dysfunction (244). Further, this diastolic dysfunction can be rescued by cardiomyocyte-specific overexpression of SCD1, an enzyme which desaturates palmitate to oleate and restores PL and membrane unsaturation (245). Although not investigated in these studies, it could be postulated that increased dietary PUFA consumption may protect the heart from diastolic dysfunction by maintaining PL and

membrane unsaturation. Similarly, increased dietary PUFA consumption may improve cardiac function through the interaction of dietary PUFA with cardiac ion channels (246). In general, dietary PUFAs inhibit cardiac excitatory calcium and sodium channels and activate inhibitory potassium channels, alter the time course of ion channel kinetics, alter the maximum ion channel conductance (247). This may explain the beneficial effect of dietary PUFA supplementation on reducing risk of sudden cardiac death (248). Taken together, dietary FA composition may influence both cardiac function and the risk of severe CVDs, such as sudden cardiac death, through effects on cardiomyocyte membrane fluidity and ion channel behaviour.

The partitioning of excess SFA into another lipid biosynthetic pathway, for example into ceramide and/or DAG formation, may explain the increase in plasma ceramides and DAG following consumption of a SFA-enriched diet (9, 145). As plasma ceramides and DAG increase, this may potentially, increase myocardial ceramide or DAG content. Increased myocardial ceramides inhibit the electron transport chain, impair mitochondrial dynamics, and induce apoptosis, similarly, increased myocardial DAG promote insulin resistance, ER stress, and apoptosis, all of which are cellular changes that could cause cardiac dysfunction and remodelling (249-253). As SFA-enriched diets lead to greater plasma, and potentially, greater myocardial ceramide and DAG content, the cellular and metabolic damage induced by these bioactive lipids may impaired cardiac function in response to SFA-enriched diets.

1.8.4 Summary

Dietary FA composition appears to induce divergent effects on cardiac function, with the consumption of SFA-enriched diets often leading to LV dysfunction, and consumption of PUFA-enriched diets improving LV function. Due to the limited number of studies, it is unclear if consuming an isocaloric high-fat diet enriched with SFA or PUFA directly influences cardiac metabolism and function in humans. Further, the cellular mechanisms explaining how these different dietary FAs may induce divergent effects on cardiomyocyte function remain unclear.

1.9 Thesis Aims

Although diet is a well-established modifiable risk factor for obesity, IHTG accumulation, and CVD, it remains unclear how dietary FA composition interacts with systemic and cellular FA metabolism to influence CMD pathogenesis and progression. The work described in this thesis aims to characterise how dietary fat composition impacts hepatic and cardiac metabolism and function during weight-neutral interventions. This will be achieved in three chapters, with the aim to address the following research questions:

1. Does acutely upregulating hepatic DNL with a high-carbohydrate diet impact the preferential partitioning of dietary palmitate (SFA) compared with dietary linoleate (PUFA) in humans free from diagnosed metabolic disease?

2. Does the FA composition (SFA- or PUFA-enriched) of an isocaloric high-fat diet differentially impact hepatic and cardiac metabolism and function in humans free from diagnosed metabolic disease independent of body weight?

3. Does FA composition, independent of FA quantity, impact cardiomyocyte metabolism and function in human induced pluripotent stem cell derived cardiomyocytes (hiPSC-CMs)?

Chapter 2

General Methods

2.1 Participant Recruitment & Screening

Participants were recruited from the Oxfordshire area by word of mouth and Oxford BioBank (http://www.oxfordbiobank.org.uk), a database of >10000 genotyped and phenotyped participants in Oxfordshire who have consented to be recruited and approached for future clinical research (254). Participants recruited for studies in Chapters 3 and 4 were free from diagnosed metabolic disease at the time of screening. This was defined as participants with BMI between 18.5 – 34.9 kg/m^2, blood pressure <140/90 mmHg, fasting plasma glucose <7.0mmol/L, fasting plasma TG <4.5mmol/L, fasting plasma total cholesterol <8.0mmol/L, and fasting plasma LDL-cholesterol <6.5mmol/L. While some of these values are greater than the accepted normal range, these participant characteristics are representative of the average UK adult which is the population where dietary modification may be utilised to reduce the risk of developing CMD. Studies were approved by the University of Oxford Medical Sciences Interdivisional Research Ethics Committee (R75046/RE001) and Northeast - Tyne & Wear South Research Ethics Committee (17/NE/0031). Prior to starting a study, participants underwent a screening visit where they gave written informed consent and were confirmed to meet the inclusion criteria for the respective study (sections 3.2.1 and 4.2.1). In Chapter 4, after consent was given, a fasting plasma sample was collected (described below) from each participant to determine individual background heavy water enrichment (section 2.6.3). Participants were free to withdraw at any point if desired.

2.2 Postprandial Study Days

On postprandial study days, participants arrived at the Oxford Centre for Diabetes, Endocrinology and Metabolism (OCDEM) clinical research unit (CRU) following an overnight fast of ~10h. Body weight and waist circumference were measured at the start of each study day. Waist circumference measurements were performed by a trained research nurse halfway

between the anterior-superior iliac spine and bottom rib. Participants were asked to avoid food naturally enriched in ^{13}C (e.g. cornflakes, foods rich in corn-starch, etc.) (255) in the 3-days leading up to the postprandial study day, and from consuming alcohol and undergoing strenuous exercise for 24h prior to the study day. A heated blanket was placed around the participant's arm and a Teflon catheter was inserted into an antecubital vein to allow for repeated blood sampling. A baseline fasting venous blood and breath sample (time 0) were collected to determine background tracer enrichment. In Chapter 4, a second Teflon catheter was inserted into the opposite antecubital vein to trace adipose-tissue derived NEFA. This was achieved by infusing [2,2-D_2]palmitate (0.04 μmol/kg/min) complexed to human albumin (Fig. 2.1). The infusion was allowed to equilibrate in the plasma NEFA pool for 45 min before collecting baseline (time 0) samples; as such, a -45 min plasma sample was collected to determine background [2,2-D_2]palmitate enrichment.

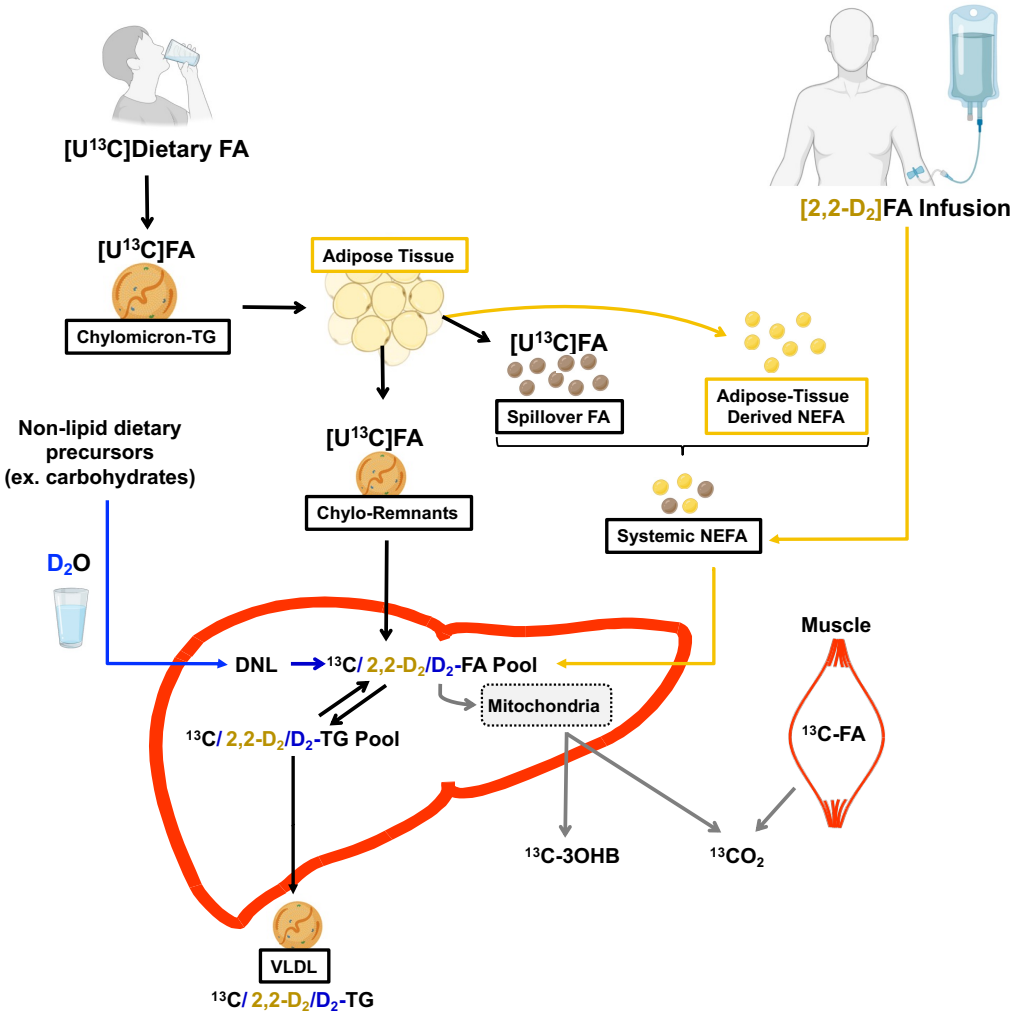

Figure 2.1 Overview of stable-isotope approaches to study in vivo human lipid metabolism. Abbreviations: 3OHB, 3-hydroxybutyrate; chylo, chylomicron; DNL, *de novo* lipogenesis; FA, fatty acid; NEFA, non-esterified fatty acid; TG, triglyceride; VLDL, very-low density lipoprotein.

After collecting the baseline samples, all participants were fed a mixed test meal containing 44g carbohydrate, 42g fat and 9.7g protein which was provided as 40g rice crispies, 200g skimmed milk, and a tracer-containing drink. The drink was made up fresh by combining 40g olive oil, 2.4g cocoa powder, 1.2g Xylitol, 0.4g emulsifier (Myverol 18-04k), 35.48g water, and 200mg [U^{13}C]FA tracer; all chemical reagents used throughout this thesis are listed in Appendix 1. In Chapter 3, [U^{13}C]palmitate or [U^{13}C]linoleate was added to the drink, whereas in Chapter 4, only [U^{13}C]palmitate was added to the drink. The [U^{13}C]FA tracer in the meal enables dietary FA tracing (Fig. 2.1). FA composition of the test meal was measured by gas chromatography (GC) (section 2.5) and found to be ~32% palmitate (16:0), 35% oleate

(18:1n-9), 27% linoleate (18:2n-6), 5% stearate (18:0) and 1% trace FA. After consuming the meal, blood and breath samples were collected at 30, 60, 90, 120, 180, 240, 300, and 360 min to measure tracer enrichment in plasma lipid pools, expired breath CO_2, and in Chapter 3, hepatic CO_2 (section 3.2.7). Breath samples were collected in EXETAINER® tubes (LabcoLtd, High Wycombe, UK). Blood samples were collected in heparinised tubes (Sarstedt, Leicester, UK), with plasma isolated by centrifugation at 3000g for 10min at 4˚C and stored at –20˚C until analysis.

2.2.1 Indirect Calorimetry

Indirect calorimetry was performed to determine fasting and postprandial whole-body VCO_2 production, VO_2 consumption, respiratory quotient (RQ), and resting energy expenditure (REE). For 10 minutes, participants freely respired into an airtight face mask (Cranlea Human Performance Limited, UK) attached to a calibrated indirect calorimeter (Metalyzer 3BR2, Cortex Biophysik). Results were recorded in 5sec intervals in Metasoft (v7.9.1, Cortex Biophysik).

2.2.2 Heavy Water Dosing

To assess fasting and postprandial hepatic DNL and fasting gluconeogenesis in Chapter 4, the incorporation of heavy water (D_2O)–derived deuterium (D) into VLDL-palmitate and fasting plasma glucose were measured (section 2.6.1 and 2.6.3, and 4.2.10, respectively). Participants were provided with D_2O to consume 10-12 hours prior to postprandial study visits to achieve 0.4% enrichment of the body water pool (4g/kg body water) with D_2O (70). The total D_2O dose, which was split into two doses to be consumed 2h apart to reduce the chance of participants experience side effects, was determined as follows:

$$\text{Men: } Volume\ of\ Heavy\ Water\ (mL) = Body\ Weight\ (kg) * 0.7 * 4$$

$$\text{Women: } Volume\ of\ Heavy\ Water\ (mL) = Body\ Weight\ (kg) * 0.65 * 4$$

A lower constant was used to calculate total body water content in women (256). After consuming the first D_2O dose and until the end of the postprandial study visit, participants were asked to drink 0.4% D_2O as required to minimise dilution of plasma D_2O. Plasma D_2O enrichment was measured by isotope-ration mass spectrometry (IRMS) for each postprandial study visit and in a plasma sample taken at screening to determine each individual participant's background D_2O enrichment (section 2.6.3).

2.3 Analytical Methods

2.3.1 Triglyceride-Rich Lipoprotein Isolation

Following each postprandial study day, plasma chylomicron- (Svedberg flotation rate (S_f) >400) and VLDL-rich fractions (S_f 20-400) were separated from samples at 0, 120, 180, 240, 300 and 360min by sequential flotation using density gradient ultracentrifugation (257). In tubes containing 6µL ethylenediaminetetraacetic acid (EDTA; 0.5 mol/L, pH 7.4), 3µL phenylmethylsulphonyl fluoride (PMSF; 10 mmol/L in propan-2-ol) and 15µL Trasylol (10,000 KIE/mL), 3mL plasma was added and gently inverted to mix. This was supplemented with 1.5mL NaBr (d1.42kg/L) to increase plasma density to d1.10kg/L. 4mL density-adjusted plasma was added to polyvinyl-alcohol (PVA)-coated Beckman Ultra-Clear centrifuge tubes (14 x 95mm) before sequentially adding 3mL NaCl (d1.063kg/L), 3mL NaCl (d.1.02kg/L), and 2.8mL NaCl (d1.002kg/L) drop wise to the PVA-coated centrifuge tubes to create a three-layer NaCl density gradient on the plasma. To isolate and collect the S_f >400 fraction, samples underwent ultracentrifugation in a SW40Ti swinging bucket rotor at 40000rpm and 15˚C for 32min (Optima L-70 Ultracentrifuge, Beckman Instruments, Palo Alto, CA) and the top 0.5-1mL was aspirated into pre-weighted tubes. To isolate and collect the S_f 20-400 fraction, tubes were topped up with 0.5-1mL NaCl (d1.006 kg/L) and further centrifuged for 16.5h at 40000rpm and 15˚C. The top 0.5-1mL was aspirated into pre-weighted tubes.

2.3.2 Biochemistry Analysis

In plasma, cell media, or isolated lipoproteins samples, glucose, NEFA, TG, glycerol, total and high-density lipoprotein (HDL) cholesterol, 3OHB, total apolipoprotein-B (ApoB), and lactate were measured on a semi-automatic analyser (iLab 480 clinical chemistry, Warrington, UK). Prior to running samples, the analyser was calibrated using in-house optimised protocols based on the manufacturer's instructions and validated with commercially available pre-determined quality controls and in-house aliquots of pooled plasma samples from previous studies. The analyser measures metabolite concentrations by spectrophotometry. In the analyser, the respective reagent for each analyte undergoes a reaction with the sample to produce a colorimetric product. The magnitude of colour change is measured at the appropriate wavelength and compared with a standard curve to determine the metabolite concentration.

2.3.3 Enzyme-linked immunosorbent assays (ELISAs)

Plasma insulin and C-peptide concentrations were quantified by enzyme-linked immunosorbent assays (Mercodia AB, Uppsala, Sweden) specific to each protein. Both assays are solid phase two-site enzyme immunoassays based on the direct sandwich technique. In the assays, insulin or C-peptide bind to anti-insulin or anti-C-peptide antibodies attached to the microplate wells and peroxidase-conjugated anti-insulin or anti-C-peptide antibodies in solution. Following washing steps, the unbound antigen and unbound enzyme-labelled antibody are removed, 3,3',5,5'-tetramethylbenzidine (TMB) is added, and a peroxidase-catalysed reaction occurs. The amount of product formed is directly proportional to the amount of peroxidase-catalysed antibody present, which is directly proportional to the amount of insulin or C-peptide in the sample. Finally, acid is added to quench the reaction and form a colorimetric endpoint that is read spectrophotometrically at 450nm (SPECTROstar Omega, BMG Labtech, Germany).

2.4 Lipid Extraction

To determine the FA composition and isotopic enrichment of individual plasma lipid pools, total lipids were extracted using the Folch method (258) and specific lipid fractions (TG, NEFA, and/or PL) were separated by solid-phase extraction (SPE) and methylated to form FA-methyl esters (FAMEs) (259, 260). Internal standards of a known concentration (glycerol triheptadecanoate (15:0) and/or heptadecanoic acid (17:0)) were added so FA concentrations could be calculated. FA composition (μmol/100 μmol total FAs) was determined by GC, while tracer enrichment was determined by GC-mass spectrometry (GC-MS) or GC-C-IRMS as appropriate.

2.4.1 Total Lipid Extraction

Into a glass vial, 500μL plasma, the internal standard aliquot, 5mL chloroform:methanol (2:1; v/v), and 1mL of 1M NaCL were added and vortexed. Samples were centrifuged (Beckman Instruments, Palo Alto, CA) at 800g for 5min at 15˚C to separate the aqueous top phase and organic lipid-containing bottom phase. The aqueous phase was aspirated and discarded while the organic phase was completely dried under nitrogen at 50˚C in a water bath evaporator (Zymark TurboVap LV Evaporator, Marshall Scientific, New Hampshire, USA).

2.4.2 Separation of Lipid Fractions Using Solid-Phase Extraction

Individual lipid fractions were separated by normal phase SPE using ISOLUTE SPE columns containing aminopropyl silica. In this purification, the sample is dissolved in a relatively non-polar organic solvent (liquid phase) and passed over the relatively polar aminopropyl silica (polar phase). Higher polarity lipids bind to aminopropyl silica and are retained within the column while lower polar lipids do not bind and pass through the column where they can be collected for further analysis. Silica-bound lipids in the column can be eluted

with a solvent of a different polarity to disrupt the lipid-silica interactions. Appropriate solvents for the liquid phase and elution steps depend on polarities of the specific lipids being isolated.

To isolate NEFA and PL fractions from TG and CE fractions, columns were prewashed twice with acetone and twice with chloroform and the dried total lipid sample was reconstituted in 1mL chloroform. Samples were added to the column under gravity, then washed twice with chloroform under vacuum. As NEFA and PL are more polar, they are retained within columns while the less polar TG and CE passed through the columns and were collected for further analysis. NEFA were eluted by washing twice with 2% acetic acid in diethyl ether (v/v). PL were eluted by washing twice with chloroform: methanol (3:2; v/v). All collected fractions were dried completely under nitrogen at 50˚C in a water bath evaporator (Zymark TurboVap LV Evaporator, Marshall Scientific, New Hampshire, USA).

To separate TG and CE fractions from each other, fresh columns were prewashed four times with hexane and the dried CE-TG fraction reconstituted in 1mL hexane. Samples were added to the column under gravity, then washed twice with hexane under vacuum. TG are more polar and retained within columns compared with CE which pass through. TG were eluted by washing twice with hexane: chloroform: ethyl acetate (100:5:5; v/v/v) and dried completely under nitrogen at 50˚C in a water bath evaporator.

2.4.3 Fatty Acid Methyl-Ester Synthesis

FAMEs were synthesised from isolated lipid fractions to reduce lipid polarity, liberate individual FAs from TG and PL, and lower FA boiling points for GC analysis. FAMEs were synthesised from TG and NEFA fractions by incubating samples for 1h at 80˚C with 400µL butylated hydroxytoluene (BHT):toluene (1:10; w/v) and 800µL 1.5% H_2SO_4:methanol (v/v). FAMEs were synthesised from the PL fraction by incubating samples for 2h at 80˚C with 400µL BHT:toluene (10mg BHT/100mL toluene) and 800µL 6% H_2SO_4:methanol (v/v). Following methylation, the reaction was quenched with 2mL neutralising solution (125mM

$KHCO_3$ and 125mM K_2CO_3 in water). To extract FAMEs, 2mL cyclohexane was added, samples were vortexed and centrifuged at 800g for 5min at 15˚C to separate the organic FAME-containing top phase and aqueous bottom phase. The organic phase was dried under nitrogen at 50˚C in a water bath evaporator and lipid fractions were reconstituted in chloroform with an external standard of known concentration (methyl tricosonate, 23:0).

2.5 Gas Chromatography

GC is a technique for separating and analysing vaporisable compounds based on the time it takes for a molecule to pass through a column. The sample is injected into an inert carrier gas (mobile phase) and carried through a column containing a polar molecule (stationary phase). As the column is gradually heated, molecules in the sample vaporise according to their boiling point, move from the stationary to mobile phase, and are carried to a detector for analysis. Samples were resolved using an Agilent 7890 GC (Agilent Technologies, Stockport, UK) on a 30m × 1.00µm × 0.530mm DB-WAX column (Agilent J&W GC Columns, 125-7032) with helium flowing at 2.0mL/min as the carrier gas. To separate FAMEs, the oven temperature was increased at 20°C per minute from 60˚C to 200°C and held for 12min, increased at 2°C per minute to 220°C and held for 2min, and increased at 1°C per min to 230°C and held for 25min. FA peaks from a sample were identified by comparing the retention time of sample FAMEs to a commercially available standard of 31 FAMEs, a representative chromatogram is shown in Fig. 2.2. FA concentration was determined by standardising the sample FA peak area to the peak area of the internal standard with a known concentration. Peak areas for all FA in a sample were added up, excluding the internal and external standards, and each FA species was expressed as a percent of the total FA area (molar percent; mol%).

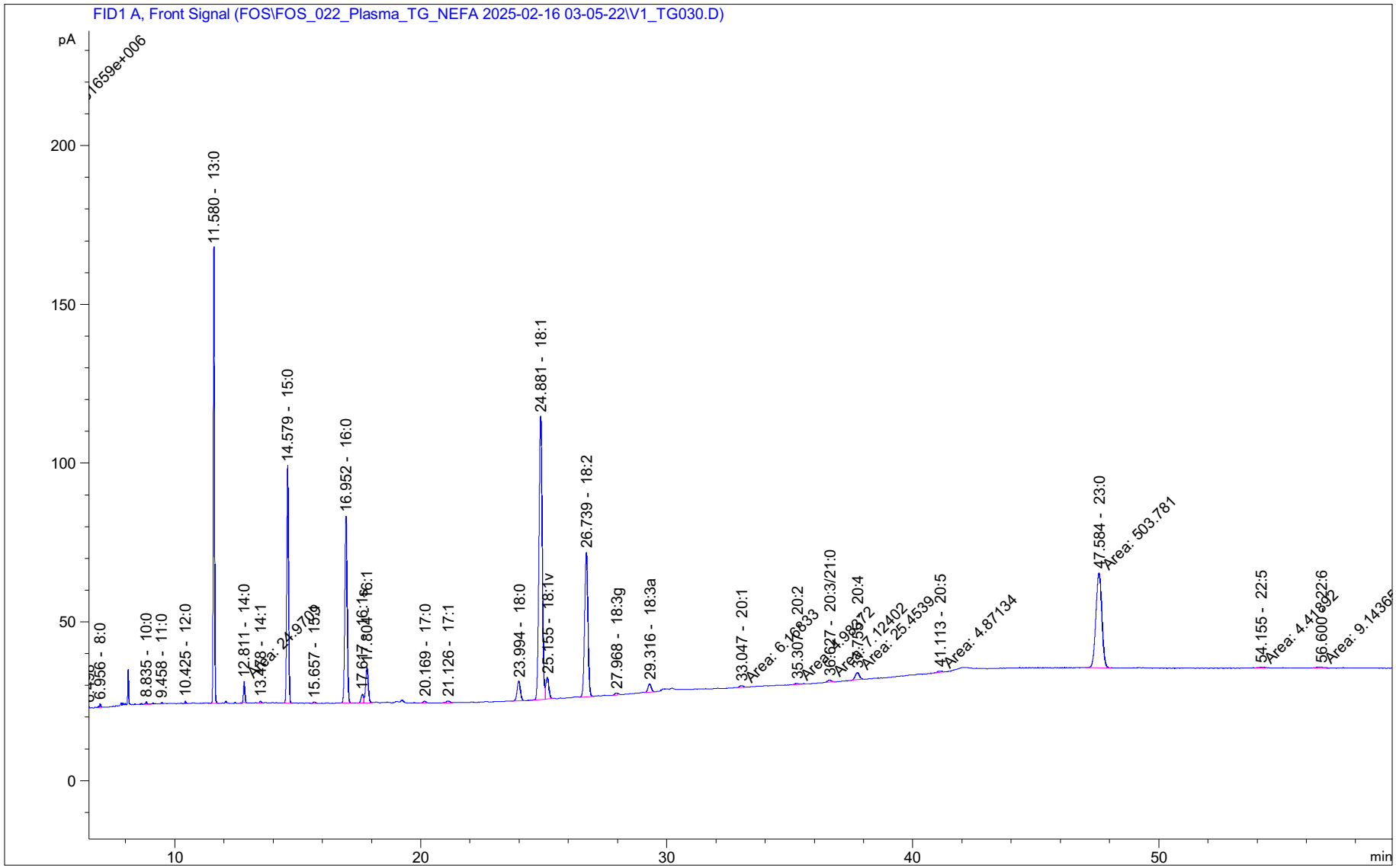

Figure 2.2 Representative gas-chromatography (GC) chromatogram. A plasma triglyceride sample collected from a participant was analysed by GC to determine the sample's fatty acid (FA) composition. Peaks corresponding to specific FA are labelled with the FA above the peak. The area under the curve for each FA-peak corresponds to the concentration of that specific FA in plasma-triglyceride.

2.6 Isotope Enrichment

Stable-isotope enrichment was measured in breath and plasma samples by GC-MS or GC-C-IRMS. In a GC-MS, the GC component separates compounds in a sample based on their retention time to provide purified molecules into the MS component. In the MS, the molecule is bombarded with electrons to ionise and break it into fragments with characteristic and reproducible mass-to-charge (m/z) ratios. These positively charged fragments are accelerated through a magnetic field, where depending on their mass, they defect and collide with a negatively charged detector that records the relative abundance of collisions and reports a mass spectrum (261). Selective ion monitoring was performed to detect palmitate-derived ions with a m/z of 270 (M+0), the unlabelled parent ion, 271 (M+1), to detect DNL-derived palmitate, 272 (M+2), to detect adipose-tissue derived palmitate, and 286 (M+16), to detect diet derived palmitate; a representative chromatogram is shown in Fig 2.2. Selective ion monitoring was performed to detect glucose-derived ions with a m/z of 319 (M+0), the unlabelled parent ion, and 320 (M+1), fasting gluconeogenesis-derived glucose. A tracer-tracee ratio (TTR) was calculated by dividing the tracer peak area by the parent ion peak area (e.g. 271/270).

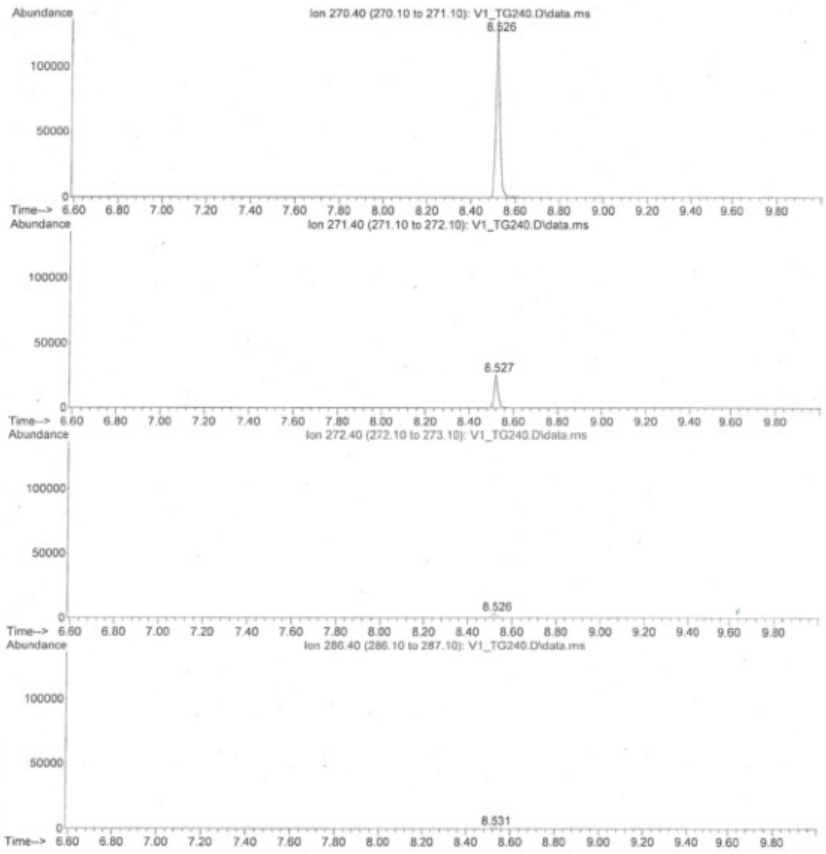

Figure 2.3. Representative gas-chromatography mass-spectrometry (GCMS) chromatogram. A plasma triglyceride sample collected from a participant which was fed [U^{13}C]palmitate in a test meal, infused with [2,2-D_2]palmitate-complexed to BSA, and provided D_2O to label DNL-derived [D_2]palmitate was analysed by GC-MS. From top to bottom, the chromatograms show the abundance of palmitate ions in the sample with a m/z of 270 (M+0), the unlabelled parent ion, 271 (M+1), the DNL-derived palmitate, 272 (M+2), the adipose-tissue derived FA, and 286 (M+16), the diet derived palmitate.

A GC-C-IRMS requires compounds of interest to be converted into CO_2, N_2, or H_2 gas for detecting ^{13}C, ^{15}N, and ^{2}H. Following separation by GC, a compound of interest is combusted into these low-molecular weight gases then analysed by IRMS. Results are reported as an isotope ratio of $^{13}C/^{12}C$, $^{15}N/^{14}N$, or $^{2}H/^{1}H$ ratios for each peak; however, no ^{15}N-containing tracers were used in this thesis. Each sample's isotope ratio is normalised to an internationally recognised standard (Vienna-PeeDee belemnite standard (VPDB) for $^{13}C/^{12}C$, or Vienna standard mean ocean water (VSMOW) and Standard Light Antarctic Precipitation (SLAP) for $^{2}H/^{1}H$); ratios are expressed as a delta value ($\delta^{13}C^{0}/_{00}$) and represent the difference in isotope enrichment between sample and standard. The $\delta^{13}C^{0}/_{00}$ was then converted to a TTR as follows (262, 263):

$$\text{TTR } (^{13}\text{C}/^{12}\text{C}) = (\frac{\delta^{13}\text{C}^{0}/_{00}}{1000} + 1) * 0.0112372 * {}^{17}/_{16}$$

2.6.1 Isotope Enrichment in Plasma Lipid Pools

In Chapter 3, [U^{13}C]palmitate and [U^{13}C]linoleate enrichment in plasma and lipoprotein fractions was determined by GC-C-IRMS (Delta Plus XP GC-IRMS; Thermo Electron, Bremen, Germany). FAMEs were separated in a 25m × 0.30µm × 0.32 mm CP-FFAP CB column (Variant Ltd, Oxford, UK) with constant 1.2mL/min flow of helium. The sample was injected using a splitless injection mode with the injector temperature of 250˚C. The initial oven temperature was held at 80˚C for 1min, increased by 25˚C per min to 200˚C, held for 15min, increased by 25˚C per min to 250˚C, then held for 7.6 min. Next, FAMEs underwent combustion at 940˚C in the presence of Pt/CuO/NiO catalysts to form $^{13}CO_2$ for IRMS analysis (92). In Chapter 4, [U^{13}C]palmitate, [2,2-D_2]palmitate, and [D_2]palmitate enrichment in plasma and lipoprotein fractions were determined by GC-MS using a 6890N GC and 5973N MS (Agilent Technologies, Stockport, UK) (264). FAMEs were resolved in a 30m × 0.25µm × 0.32 mm RTX-5 column (10224, Restek Thames, UK) with helium as the carrier gas. Samples were injecting using splitless mode with the injector temperature at 250˚C. The initial oven temperature was held at 50˚C for 1min, increased by 25˚C per min to 200˚C, increased by 10˚C per min to 230˚C, then held for 10 min. Dwell time was 100ms. The natural abundance of ^{13}C in all lipid fractions measured was accounted for by subtracting the TTR of the fasting sample (0), obtained before participants consumed the test meal, from each postprandial sample TTR. The natural abundance of [D_2]palmitate and [2,2-D_2]palmitate in lipoproteins was accounted for by subtracting the TTR of in-house unlabelled lipoprotein samples. The natural abundance of [2,2-D_2]palmitate in plasma NEFA was accounted for by subtracting the TTR of the –45 sample, obtained before starting the [2,2-D_2]palmitate infusion, from each plasma NEFA sample. Sample FA retention times were confirmed by comparing to a known standard

included on each run. The FA–TTRs were multiplied by the corresponding palmitate or linoleate concentrations in chylomicrons, VLDL, plasma TG, and NEFA to give plasma and lipoprotein tracer concentrations.

2.6.2 Isotope Enrichment in Expired Breath

Following [U^{13}C]fatty acid consumption, ^{13}C enrichment in expired CO_2 was measured by GC-C-IRMS, a representative chromatogram is shown in Fig. 2.3. Samples were delivered to the machine using a splitless injection mode, with a 40µL injection volume, and 110˚C injector temperature (262). CO_2 was separated from other gases in an 25m × 10µm × 0.32 mm PoraPLOT Q column (CP7551, Agilent Technologies, Stockport UK) with a constant 1.2mL/min flow of helium, the carrier gas. Oven temperature was kept constant at 35˚C for a total run time of 10min before IRMS analysis. TTRs were calculated from $\delta^{13}C^{0}/_{00}$ (section 2.6), and the fasting sample TTR was subtracted from each postprandial sample to account for the natural abundance of ^{13}C in expired CO_2. Whole-body meal-derived FA oxidation was calculated by multiplying CO_2 production (VCO_2, mmol/min) by $^{13}CO_2/^{12}CO_2$ TTR.

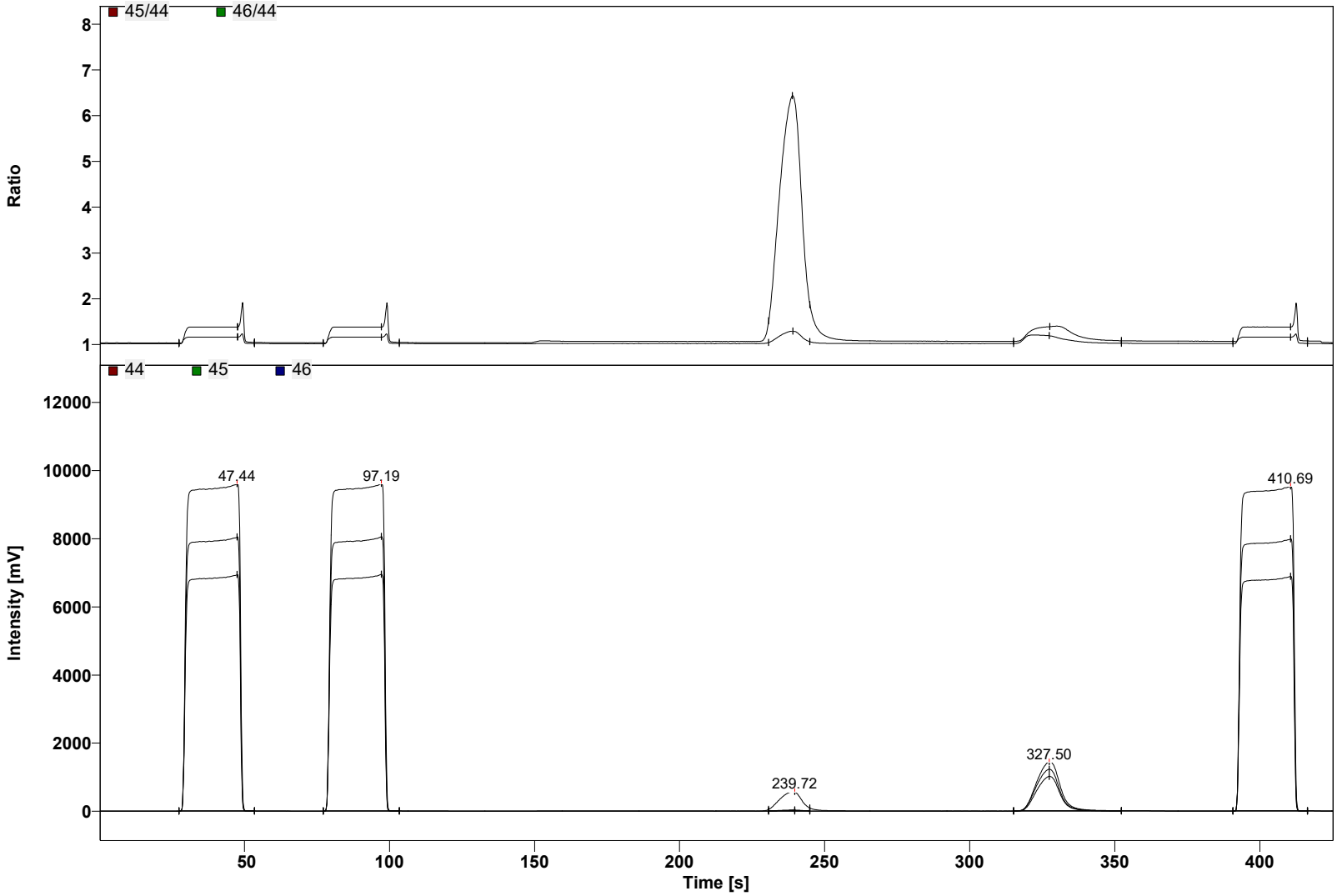

Figure 2.4 Representative gas-chromatography-combustion-isotope ratio mass spectrometry (GC-C-IRMS) chromatogram. A breath sample collected from a participant fed [U^{13}C]palmitate in a test meal was analysed by GC-C-IRMS. In the bottom chromatogram, the peak at 327.50s corresponds to CO_2, and the corresponding peak in the top chromatogram displays the $^{13}C/^{12}C$ ratio in expired CO_2.

2.6.3 Plasma Heavy Water Enrichment & DNL-Derived Palmitate

Plasma D_2O enrichment was measured by IRMS (Finnigan GasBench II Thermo Fisher Scientific, Paisley, UK) in plasma collected at screening to determine individual background D_2O enrichment, and on each study day at 0, 180, 240, and 360min. Prior to analysis, 300µL screening plasma or 10µL study day plasma were diluted with 200µL or 490µL deionised water in duplicate, respectively. SMOW standards of increasing D_2O concentration were prepared. A platinum catalyst was added to each sample before flushing for 5min with 2% hydrogen in helium and leaving to equilibrate for a minimum of 5h. After which, a sample of gas was injected into the IRMS, and the $^2H/^1H$ ratio measured ten times against the internal IRMS VSMOW value (265). To determine plasma D_2O enrichment in each sample, the last nine $^2H/^1H$ vs. SMOW measurements were averaged and SLAP corrected (266), then normalised to the VSMOW standards included on each run, the dilution factor, and the individual background plasma D_2O enrichment. Prior to each run, an H_3 factor test was performed to correct for the contribution of H_3^+ species to ^2H detection in the ion source at increasing H_2 pressures (267).

The percent newly synthesised palmitate in VLDL (i.e. DNL-derived palmitate) was determined using (70):

$$\%\ \text{Newly Synthesised Palmitate} = \frac{\text{Background Corrected } 271/270\ \text{ TTR in VLDL} - \text{TG}}{^2\text{H}/^1\text{H Plasma Water} * 22} * 100$$

Where, the observed enrichment, (TTR of VLDL-TG palmitate (section 2.6.1)) is divided by the maximum possible enrichment, plasma D_2O enrichment multiplied by 22, as 22 hydrogens on palmitate could be labelled during DNL.

2.7 Calculations

Fasting insulin resistance was approximated using the homeostatic model assessment for insulin resistance (HOMA-IR (268)):

$$\text{HOMA} - \text{IR} = \frac{\text{fasting plasma insulin (mU/L)} \ * \ \text{fasting plasma glucose (mmol/L)}}{22.5}$$

When participants did not consume heavy water so DNL could not be determined using stable-isotope tracers, fasting DNL was assessed by calculating the lipogenic index in the fasting plasma-TG fraction (68):

$$\text{Lipogenic Index} = \frac{Palmitate\ (16{:}\ 0)\ Concentration}{Lineoleate\ (18{:}\ 2\text{n} - 6)\ Concentration}$$

Stearoyl-CoA desaturase (SCD) activity was approximated by calculating the desaturation index in the fasting plasma-TG fraction (269).

$$\text{SCD Index} = \frac{Palmitoleate\ (16{:}\ 1\text{n} - 7)\ Concentration}{Palmitate\ (16{:}\ 0)\ Concentration}$$

Fasting and postprandial net whole-body fat and carbohydrate oxidation rates were calculated from VO_2 (L/min) and VCO_2 (L/min) measured by calorimetry, and *n,* which represents urinary nitrogen, a marker of protein oxidation, was assumed to be 0.2 g/min based on studies used to derive these equations (270):

$$\text{Fat Oxidation} = \ 1.67 * V_{CO_2} - \ 1.67 * V_{O_2} - \ 1.92 * n$$

$$\text{Carbohydrate Oxidation} = \ 4.55 * V_{CO_2} - \ 3.21 * V_{O_2} - \ 2.87 * n$$

Areas under the curve (AUCs) were calculated by the trapezoid method and were divided by the relevant time period to produce time-averaged values to provide an overview of the total postprandial excursion of a metabolite of interest.

2.8 Statistical Analysis

Data was analysed using Graphpad Prism (V10.9.1) Software for Mac (San Diego, California USA), SPSS (V30.0.0), or R (V4.5.0) on RStudio (V2024.09.1+394). The Grubb's test was used to check for outliers, which were removed if present. Data distribution was checked using the Shapiro–Wilk normality test and analysed using the appropriate parametric or non-parametric test. Comparisons between two groups of continuous data were assess using a t-test, comparisons between more than two groups were made using a one- or two-way ANOVA, as appropriate, followed by a Tukey's post-hoc test to determine which groups differed. Where the same sample or individual was compared, a paired or repeated-measures test was used. Statistical significance was set at $p<0.05$.

Chapter 3

Greater oxidation of dietary linoleate compared with palmitate in humans following an acute high-carbohydrate diet

The findings presented in this chapter have been published as Srnic N, Dearlove D, Johnson E, MacLeod C, Krupa A, McGonnell A, Frazer-Morris C, O'Rourke P, Parry S, Hodson L. Greater oxidation of dietary linoleate compared with palmitate in humans following an acute high-carbohydrate diet. Clin Nutr. 2024 Oct;43(10):2305-2315. doi: 10.1016/j.clnu.2024.08.028. 2024 Aug 24. The following were completed by others: the recruitment and sample collection for 10 of 20 participants were completed by Dr. Sion Parry and Dr. David Dearlove, the lipid extractions for 10 plasma samples were complete by Paige O'Rourke. The remaining participant recruitment, sample collection, processing and analysis, and data analysis was completed by me.

3.1 Introduction

MASLD is associated with obesity and starts with excessive IHTG accumulation (271), a risk factor for CVD and T2D. Accumulating evidence suggests dietary fat composition, independent of total dietary fat content and BMI influences IHTG accumulation (10, 11, 79). Most dietary intervention studies have reported greater IHTG accumulation in participants consuming SFA– compared with PUFA– or free–sugar enriched diet, despite comparable changes in body weight (10, 11, 61, 79, 192). Based on these observations, it is suggested that dietary PUFA are preferentially partitioned into oxidation pathways compared with dietary SFA (10). Supporting this, Parry *et al.* reported greater whole-body oxidation of dietary linoleate (PUFA) compared with dietary palmitate (SFA) in individuals consuming their habitual diet (92). While this may, in part, explain why consuming PUFA– rather than SFA–enriched diets are associated with lower IHTG content (10, 11, 79), it remains unclear if this preferential partitioning of dietary FA is maintained across different metabolic states.

Compared with individuals with normal IHTG content, those with elevated IHTG content may have altered hepatic fat metabolism, such as increased hepatic DNL, which

promotes FA esterification and may influence FA oxidation (60). After consuming an acute high-carbohydrate diet, hepatic DNL is consistently upregulated and markers of FA oxidation downregulated in humans (65, 67-69). However, in patients with MASLD (60, 272), where hepatic DNL may be chronically upregulated, FA oxidation findings are inconsistent (69, 87, 89). While differences in methodology used to assess FA oxidation or the duration an individual has had IHTG accumulation may explain this discrepancy, the dietary fat composition of an individual's habitual diet may also impact FA oxidation findings. It is currently unknown how alterations in hepatic metabolic state, such as an increase in hepatic DNL, may influence the oxidation of different dietary FA. Therefore, the aim of this study was to acutely upregulate hepatic DNL by having participants free from diagnosed metabolic disease consume a 3-day high-carbohydrate diet, in order to shift the metabolic state of the liver, and measure the preferential partitioning of dietary palmitate (SFA) or linoleate (PUFA) into oxidation pathways.

3.2 Materials and Methods

3.2.1 Participants

Male and female participants were recruited according to criteria in Table 3.1 and section 2.1.

Table 3.1. Participant Inclusion and Exclusion Criteria

Inclusion Criteria	Exclusion Criteria
Willing and able to give informed consent	Unwilling or unable to give informed consent
Male and female participants aged 18-50	Consumption of alcohol greater than, for males, 3-4 units of alcohol per day or 21-28 units of alcohol per week and, for females, greater than 2-3 units of alcohol per day or 14-21 units of alcohol per week

BMI >18.5 kg/m^2 and <35.0 kg/m^2	Gained or lost >5% body weight in the last 3 months
Free from diagnosed metabolic disease	History of an eating disorder
Not following a weight-loss diet	Inability to consume the high-carbohydrate diet
Not taking medications and/or supplements known to affect lipid and/or glucose metabolism	Pregnant or suspected pregnant or nursing
Not actively smoking (within last 3 mon.) or consuming other nicotine containing products	Participant has changed dose of a medication within the last three months
Plasma haemoglobin above 120g/L	Unable to undergo and/or tolerate cannulation
	History of bleeding disorders

3.2.2 Experimental Design

This was a randomised, crossover, double-blind study where each participant completed a fasting, baseline visit followed by two identical postprandial study days. A minimum of 14-days separated postprandial study days (Fig. 3.1). Prior to each postprandial study day, participants consumed a 3-day isocaloric high-carbohydrate diet (~75% TE carbohydrate, ~10% TE protein, ~15% TE fat) with all food provided. A representative example of the food provided for a single day of the three-day diet for an individual with a daily caloric expenditure between 2000-2250 kcal is listed in Table 3.2. The daily caloric requirement was calculated according to the Mifflin-St Jeor equation, and the quantity of food listed in Table 3.2 tailored to meet individual energy requirements (273). The fat composition of the 3-day isocaloric high-carbohydrate low-fat diet was ~4% TE from SFA, ~5% TE from MUFA, and ~2% TE from PUFA, and determined using Nutritics software (Nutritics Research Edition v6.02).

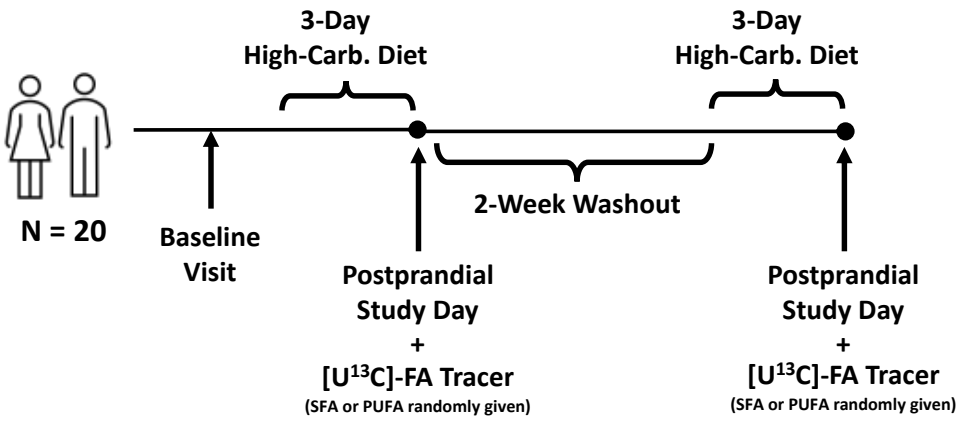

Figure. 3.1 Overview of Study Design.

Table 3.2. Representative One-Day Meal Plan of the High-Carbohydrate Diet

Meal/Food	*Amount (g)*	*kcal*	*Carb (g)*	*Protein (g)*	*Fat (g)*
Breakfast					
Milk skimmed	150	53	6.9	5.3	0.45
Coco pops	50	189	42	3.15	0.95
Snack 1					
Apple juice (fresh)	250	80	19.3	0.15	0.25
Tesco summer fruit cereal bars	19	52	10.5	0.87	0.8
Lunch					
Tesco cheese and tomato pasta (pre-packaged)	300	531	76	18.6	16.8
Banana	~100	86	20	1.2	0.1
Snack 2					
Wine gums	120	390	91	5.8	0.24
Cola	330	141	35.3	0	0
Dinner					
Tesco Italian vegetable lasagne (ready meal)	450	396	52	14.9	14.4
Low fat yoghurt	100	79	13.1	4.2	1.1
Peaches canned in syrup	410	233	56	2.1	0
Total (kcal/g)		**2230**	**422.1**	**56.27**	**35.09**
%TE			**75.7**	**10.1**	**14.2**

Abbreviations: kcal, kilocalories; Carb, carbohydrate; %TE, percent total energy.

On the two experimental postprandial study days, participants were fed, in random order, a standardised mixed test meal that was identical except for the addition of 200mg [U^{13}C]palmitate or [U^{13}C]linoleate, to trace whole-body FA oxidation (52). The order in which [U^{13}C]palmitate or [U^{13}C]linoleate were administered in the meal was random and determined by a researcher not involved in the study. Participants and researchers were blinded to isotope order until analysis.

3.2.3 Baseline Fasting Visit

Participants arrived at the OCDEM CRU after an ~10h overnight fast where a fasting venous blood sample was collected, and plasma isolated and stored (section 2.2).

3.2.4 Postprandial Study Days

After consuming the isocaloric 3-day high carbohydrate diet, participants arrived at the OCDEM CRU after an ~10h overnight fast for a postprandial study day (section 2.2). After consuming the tracer containing meal, blood and breath samples were collected at 30, 60, 90, 120, 180, 240, 300 and 360 min to measure ^{13}C enrichment in plasma lipid pools, expired breath CO_2, and hepatic CO_2 (Fig. 3.2, section 3.2.7). Indirect calorimetry was performed at 0, 120, and 360 min (section 2.2.1, Fig. 3.2).

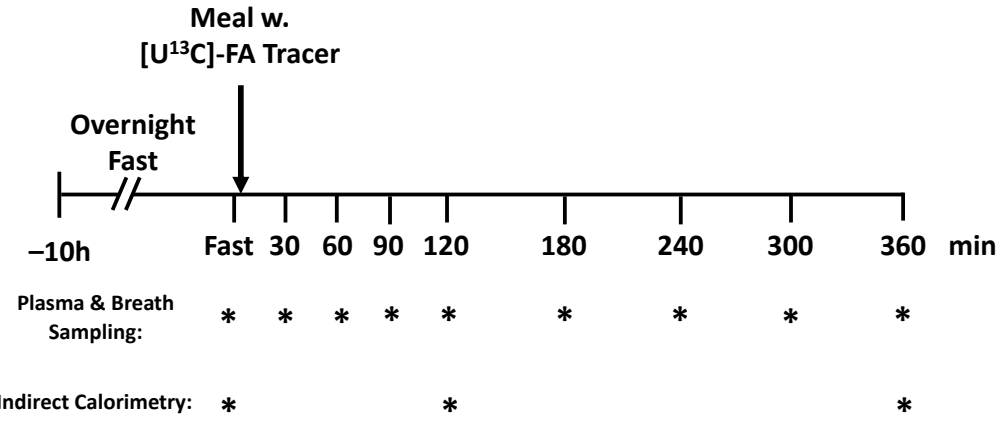

Figure. 3.2. Overview of Postprandial Study Day Protocol.

3.2.5 Analytical methods

Plasma glucose, NEFA, TG, glycerol, total and high-density lipoprotein (HDL) cholesterol, 3OHB, ApoB, and lactate were measured (section 2.3.2). Plasma insulin levels were quantified (section 2.3.3) and plasma chylomicron- and VLDL-rich fraction were isolated (section 2.3.1).

3.2.6 FA Composition and Isotopic Enrichment in Plasma Lipid Pools

To determine the FA composition and isotopic enrichment of individual plasma lipid pools, TG extracted from plasma lipid and lipoproteins, and NEFA extracted from plasma lipids, were used to synthesise FAMEs (section 2.4). FA composition was determined by GC (section 2.5) and [U^{13}C]palmitate and [U^{13}C]linoleate enrichment in plasma and lipoproteins pools was determined by GC-C-IRMS and used to calculate palmitate or linoleate concentrations (sections 2.6 and 2.6.1).

3.2.7 Isotopic Enrichment in Fatty Acid Oxidation Markers

Whole-body and hepatic dietary FA oxidation was determined by analysing ^{13}C enrichment in breath and hepatic CO_2 samples, these were then used to calculate peripheral FA oxidation by subtracting hepatic from whole-body fat oxidation (227). Whole-body meal-derived FA oxidation was determined by GC-C-IRMS (section 2.6.2).

As the liver is the predominant source of urea in humans and CO_2 derived from hepatic FA oxidation is used in urea synthesis (274), complete intrahepatic dietary FA oxidation was approximated using the method by Kloppenburg *et. al* (275). To liberate CO_2 from urea, 500µL of plasma was mixed with 1.5mL of deionised water, 25µL of 1M phosphoric acid, and 125µL of pentan-1-ol. Following a 30 min incubation at 37˚C, 1mL of working urease solution (100µL stock urease solution (3000 U/mL urease (Sigma-Aldrich U4002-100KU) dissolved in 500µL deionised water and 500µL glycerol, and 9.9mL EDTA) was added to each sample. Following

a further 15 min incubation at 37˚C, 750µL of 1M phosphoric acid was added to each sample and mixed for 30 min. Urea-derived CO_2 was transferred to EXETAINER® tubes (LabcoLtd, High Wycombe, UK) and ^{13}C enrichment was measured by GC-C-IRMS to calculate urea-derived $^{13}CO_2/^{12}CO_2$ TTRs (section 2.6.2). Hepatic CO_2 production was approximated by multiplying postprandial splanchnic respiratory quotients derived from a porcine model (due to limited *in vivo* human values) by the participant's body weight on the respective postprandial study visit (276). This was used to calculate postprandial hepatic $^{13}CO2$ production by multiplying the hepatic VCO_2 by urea-derived $^{13}CO_2/^{12}CO_2$ TTR.

3.2.8 Calculations

HOMA-IR, lipogenic index, desaturation index, and fasting and postprandial net whole-body fat and carbohydrate oxidation rates, and time-averaged AUC were calculated (section 2.7).

3.2.9 Power Calculation

A two-sided power calculation was performed in SPSS (V30.0.0) based on the findings by Parry *et al.* reporting the time-averaged AUC for ^{13}C appearance in expired CO_2 was 1.82 ± 0.66µmol/min (mean ± SD) following consumption of [U^{13}C]palmitate compared with 3.09 ± 2.19 µmol/min following consumption of [U^{13}C]linoleate in individuals consuming their habitual diet (92). Following the three-day high-carbohydrate diet, to detect a similar difference in ^{13}C appearance in expired CO_2 after consumption of [U^{13}C]palmitate or [U^{13}C]linoleate (power=0.80, α=0.05), 21 individuals would be required to achieve an effect size of 0.65.

3.2.10 Statistical Analysis

All data was analysed using Graphpad Prism (V10.9.1) Software for Mac (San Diego, California USA). Data distribution was checked using the Shapiro–Wilk normality test and analysed using the appropriate parametric or non-parametric test. Anthropometric measures,

fasting plasma biochemistry, and plasma FA composition, presented as mean ± SD if parametric or median (IQR) if non-parametric, were compared using a one–way repeated–measures analysis of variance (ANOVA)) with Tukey's post–hoc test or Friedman test with Dunn's multiple comparison post-hoc test as appropriate. Indirect calorimetry, presented as median (IQR), and time series plasma biochemistry and tracer data, presented as mean ± SD, was analysed first using a 2-way repeated measures ANOVA, and further with Tukey's post-hoc test if a tracer*time interaction effect was observed. In cases where data points were missing (representing 0.3% of all data points), they were either interpolated if the missing point was part of a postprandial data set where the data point before and after the missing data point were successfully measured (ie. time point 0 and 360 were not interpolated) and the rate of change of the data was linear (nadirs, peaks, and inflection points were not interpolated), or otherwise analysed with a mixed effects model with Bonferroni's post–hoc test. In cases where the data point from an assay or analytic machine was below the limit of detection for an assay, the lowest limit of detection was used in place. AUC and tracer recovery data, presented as mean ± SD, was analysed using a paired t-test or Wilcoxon matched-pairs test signed rank test. Statistical significance was set at $p<0.05$.

3.3 Results

3.3.1 Participant Characteristics

Twenty individuals (n=11 female) aged 26 (21–41) years (median (IQR)) free from diagnosed metabolic disease participated in the study and participant characteristics for all study visits are shown in Table 3.3. Over the course of the study, BMI, waist-hip ratio, or HOMA-IR did not change (Table 3.3).

Table 3.3. Participant Characteristics, Fasting Plasma Biochemistry, and Substrate Oxidation Rates.

	Baseline	***SFA*–Tracer**	***PUFA*–Tracer**
Sex (M/F)	9 / 11	-	-
Age (years)	26 (21 – 41)	-	-
BMI (kg/m^2)	24.1 ± 2.6	24.0 ± 2.6	23.9 ± 2.6
Waist-Hip Ratio	0.79 ± 0.07	0.79 ± 0.06	0.79 ± 0.06
Fasting Plasma Biochemistry			
Glucose (mmol/L)	4.7 (4.6 – 5.1)	4.9 (4.5 – 5.4)	4.8 (4.5 – 5.2)
Insulin (mU/L)	4.7 (2.8 – 7.4)	4.9 (4.1 – 7.2)	4.5 (3.7 – 6.4)
HOMA-IR	0.92 (0.58 – 1.44)	1.12 (0.80 – 1.35)	0.94 (0.80 – 1.35)
NEFA (µmol/L)	462 (307 – 649)	367 (337 – 466)	343 (266 – 528)
TG (mmol/L)	0.66 (0.52 – 1.09)	0.9 (0.71 – 1.18)*	0.87 (0.73 – 1.08)
3OHB (µmol/L)	42 (31 – 111)	35 (24 – 42)	35 (27 – 44)
Lactate (mmol/L)	0.61 (0.47 – 0.92)	0.73 (0.62 – 0.84)**	0.71 (0.61 – 0.82)**
Total Cholesterol (mmol/L)	3.8 (3.58 – 4.37)	3.73 (3.36 – 4.38)	3.72 (3.34 – 4.28)
HDL-Cholesterol (mmol/L)	1.38 ± 0.37	1.36 ± 0.46	1.32 ± 0.50
Non-HDL Cholesterol (mmol/L)	2.44 (2.24 – 3.09)	2.47 (1.96 – 2.80)	2.48 (2.22 – 2.86)
ApoB (mmol/L)	0.62 (0.54 – 0.76)	0.6 (0.49 – 0.64)	0.6 (0.52 – 0.67)
Plasma Fatty Acid Composition			
Lipogenic Index (16:0/18:2)	0.78 (0.56 – 1.16)	1.30 (1.03 – 1.65)**	1.23 (0.99 – 1.61)*
Desaturation Index (16:1/16:0)	0.14 (0.10 – 0.19)	0.19 (0.16 – 0.22)*	0.18 (0.13 – 0.23)*
Net Carbohydrate Oxidation Rates			
Fasting (g/min)	–	0.15 (0.13 – 0.24)	0.17 (0.13 – 0.22)
120 min (g/min)	–	0.17 (0.15 – 0.22)	0.20 (0.18 – 0.21)
360 min (g/min)	–	0.16 (0.09 – 0.21)†	0.11 (0.09 – 0.16)††
Net Fat Oxidation Rates			
Fasting (g/min)	–	0.03 (0.00 – 0.06)	0.02 (0.01 – 0.05)
120 min (g/min)	–	0.04 (0.02 – 0.05)	0.03 (0.02 – 0.05)
360 min (g/min)	–	0.05 (0.04 – 0.07)$^{\#\#\#}$	0.04 (0.03 – 0.08)$^{\#\#\,\dagger}$

Parametric data presented as mean ± SD, non-parametric data presented as median (IQR). Abbreviations: SFA, saturated fatty acid; PUFA, polyunsaturated fatty acid; BMI, body mass index; HOMA-IR, homeostatic model assessment of insulin resistance; NEFA, non-esterified fatty acid; TG, triglyceride; 3OHB, 3-hydroxybutyrate; HDL, high-density lipoprotein; ApoB, apolipoprotein B. *p<0.05, **p<0.01, *** p<0.001 compared with baseline visit; $^{\#\#}$ p<0.01 compared with fasting, $^{\#\#\#}$ p<0.001; †p<0.05, †† p<0.01 compared with 120 min.

3.3.2 Plasma Biochemistry

Compared with the baseline visit, the 3-day isocaloric high-carbohydrate diet increased fasting plasma TG, although this was only significant (p<0.05) on the SFA–tracer study day (Table 3.3). Fasting plasma lactate levels increased (p<0.01) after consumption of the high-carbohydrate diet on both study days when compared with baseline values but did not differ between the respective SFA– and PUFA–tracer study days (Table 3.3). There were no differences in fasting plasma glucose, insulin, NEFA, 3OHB, total cholesterol, HDL-cholesterol, non-HDL cholesterol, and ApoB concentrations between baseline and the SFA– and PUFA–tracer study days (Table 3.3).

The lipogenic index (ratio of 16:0/18:2n-6) in plasma TG was used as a marker of hepatic DNL (68) and the desaturation index (16:1n-7/16:0) as a marker of stearoyl–CoA desaturase activity (277). The fasting lipogenic index increased by ~65% (p<0.05) and the desaturation index increased by ~25% (p<0.05) on the both postprandial SFA– and PUFA–tracer study days compared with baseline (Table 3.3), suggesting consumption of the high-carbohydrate diet upregulated hepatic DNL and palmitate desaturation by SCD. Further, the lipogenic index was elevated to a similar extent on both study days suggesting a similar and reproducible elevation in hepatic DNL (Table 3.3).

On both postprandial study days, plasma glucose increased after consuming the test meal, peaking at 30mins before returning to fasting levels (p<0.001 effect of time, Fig. 3.3A). Although no tracer*time interaction was observed (p=0.30) and the [$U^{13}C$]palmitate and [$U^{13}C$]linoleate tracer was consumed in random order, the pattern of response differed between the postprandial study days with a greater excursion observed on the [$U^{13}C$]palmitate compared with [$U^{13}C$]linoleate study day (p<0.01 effect of tracer; Fig. 3.3A). There was a trend for a tracer*time interaction effect for plasma insulin (p=0.06), and no tracer*time interaction effects for plasma TG (p=0.79), NEFA (p=0.78), 3OHB (p=0.44), or lactate (p=0.69) over the course

of the postprandial period (Fig. 3.3B-F). During the postprandial study days, plasma insulin, TG, NEFA, 3OHB, and lactate all changed with time (all $p<0.001$, effect of time; Fig. 3.3B-F) and each metabolite followed a similar profile on both study days following consumption of the mixed test meal. The postprandial insulin and lactate excursions followed the postprandial glucose excursion, peaking at 30-60min and returning to baseline by ~180min (Fig. 3.3B, 3.3F), with the lactate profile likely reflecting glycolysis of dietary carbohydrate (42). Plasma-TG gradually increased over time following consumption of the mixed test meal, peaking at ~240 min (Fig. 3.3C), which coincided with peak chylomicronemia (Fig. 3.5A). Following consumption of the mixed test meal, plasma NEFA and 3OHB decreased from fasting, with the nadir occurring at ~90min, before increasing over the remainder of the study day (Fig. 3.3D, E). To determine if the order in which the tracers were administered influenced the metabolic response to a mixed test meal, postprandial plasma glucose, insulin, NEFA, TG, 3OHB, and lactate responses on the first study day were compared with the second study day and no order effect was observed (Fig. 3.4A-F)

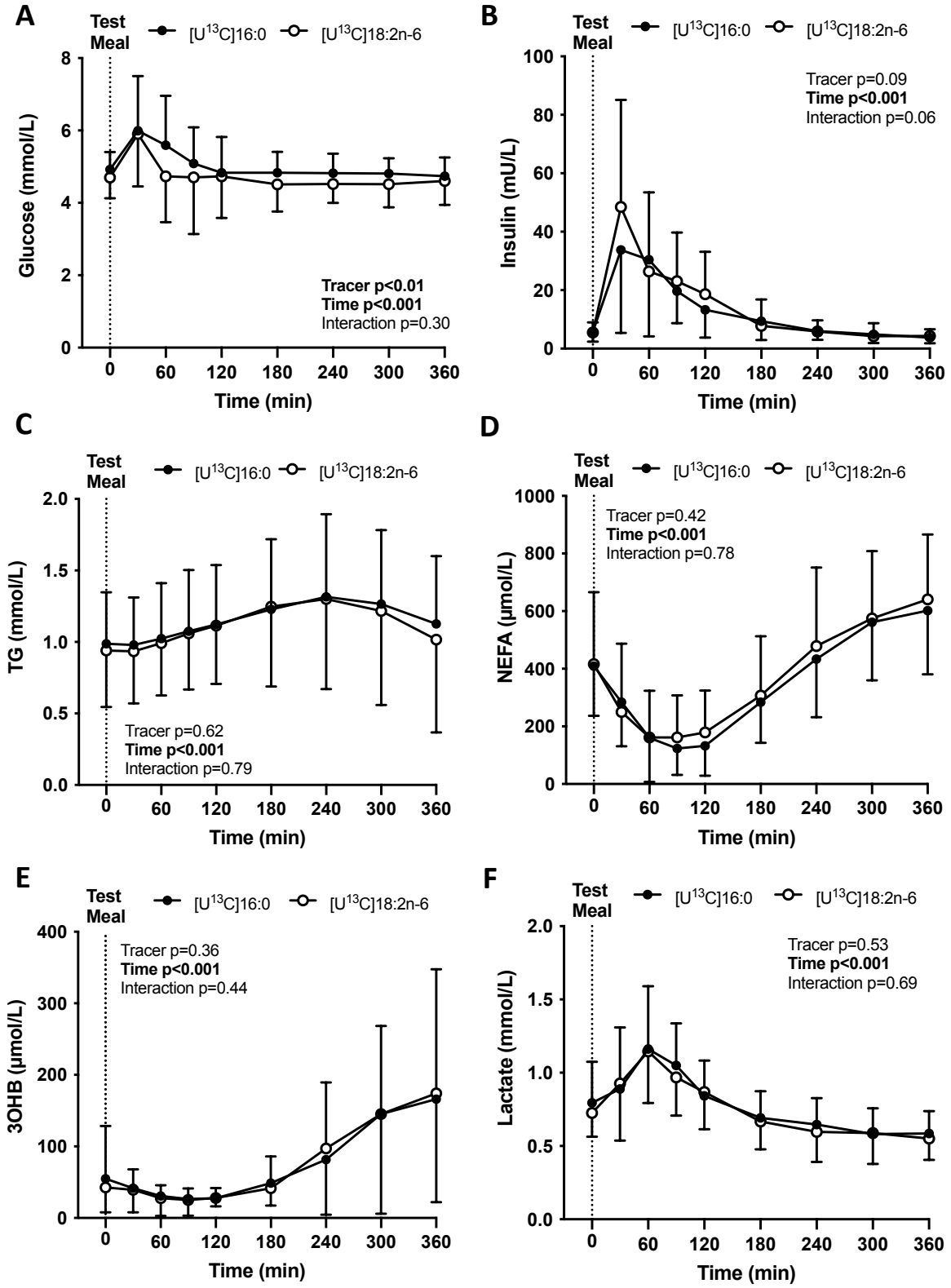

Figure 3.3 Plasma concentrations of (A) glucose, (B) insulin, (C) triglyceride (TG), (D) non-esterified fatty acid (NEFA), (E) 3-hydroxybutyrate (3OHB), and (F) lactate after consuming a 3-day high carbohydrate diet followed by a standardised mixed test meal containing either [$U^{13}C$]palmitate ([$U^{13}C$]16:0) or [$U^{13}C$]linoleate ([$U^{13}C$]18:2n-6). Plasma samples were collected every 30-60min for 6h. Data: mean ± SD, n=20. Analysed by a two–way repeated–measures ANOVA (A-D, F) or mixed effects model (E).

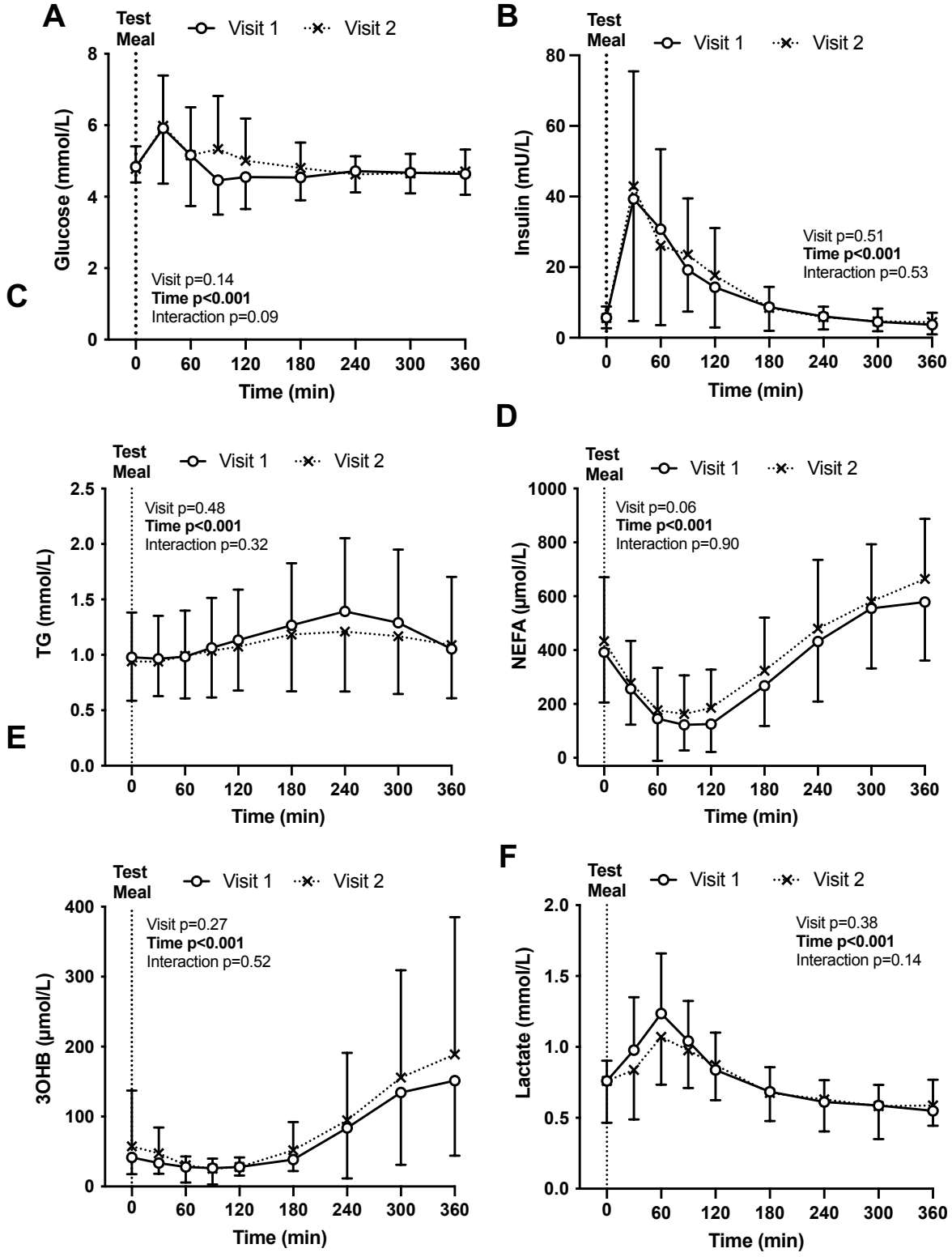

Figure 3.4 Plasma concentrations of (A) glucose, (B) insulin, (C) triglyceride (TG), (D) non-esterified fatty acid (NEFA), (E) 3-hydroxybutyrate (3OHB), and (F) lactate on the first or second visit after consuming a 3-day high carbohydrate diet followed by a standardised mixed test meal. Plasma samples were collected every 30-60min for 6h. Data: mean ± SD, n=20. Analysed by a two–way repeated–measures ANOVA (A-D, F) or mixed effects model (E).

3.3.3 Net Substrate Oxidation Rates

Net fat and carbohydrate oxidation were similar on both postprandial study days (Table 3.3). Net carbohydrate oxidation rates were increased at 120 min following consumption of the meal before decreasing at 360min (SFA, $p<0.05$; PUFA, $p<0.01$; Table 3.3). In contrast, following test meal consumption, net fat oxidation rates increased over the postprandial period from fasting to 360 min (SFA, $p<0.001$; PUFA, $p<0.01$) and from 120 min to 360 min (SFA, $p=0.06$; PUFA, $p<0.05$; Table 3.3).

3.3.4 Lipoproteins FA Composition

Plasma chylomicron-TG concentrations increased following test meal consumption ($p<0.001$ effect of time), peaking at ~240 mins (Fig. 3.5A), with no difference in time-averaged AUC chylomicron-TG between the respective tracer study days (Fig. 3.5B). There was minimal change in postprandial VLDL-TG concentrations (Fig. 3.5C) and no difference in VLDL-TG concentrations between the respective tracer study days (Fig. 3.5D). As an identical test meal was given on each study day, chylomicron-TG FA composition at peak chylomicronemia was measured and showed a similar FA composition on both study days, 33% palmitate, 19% linoleate, 43% oleate, and 5% stearate (Fig. 3.5E), which was reflective of the test meal.

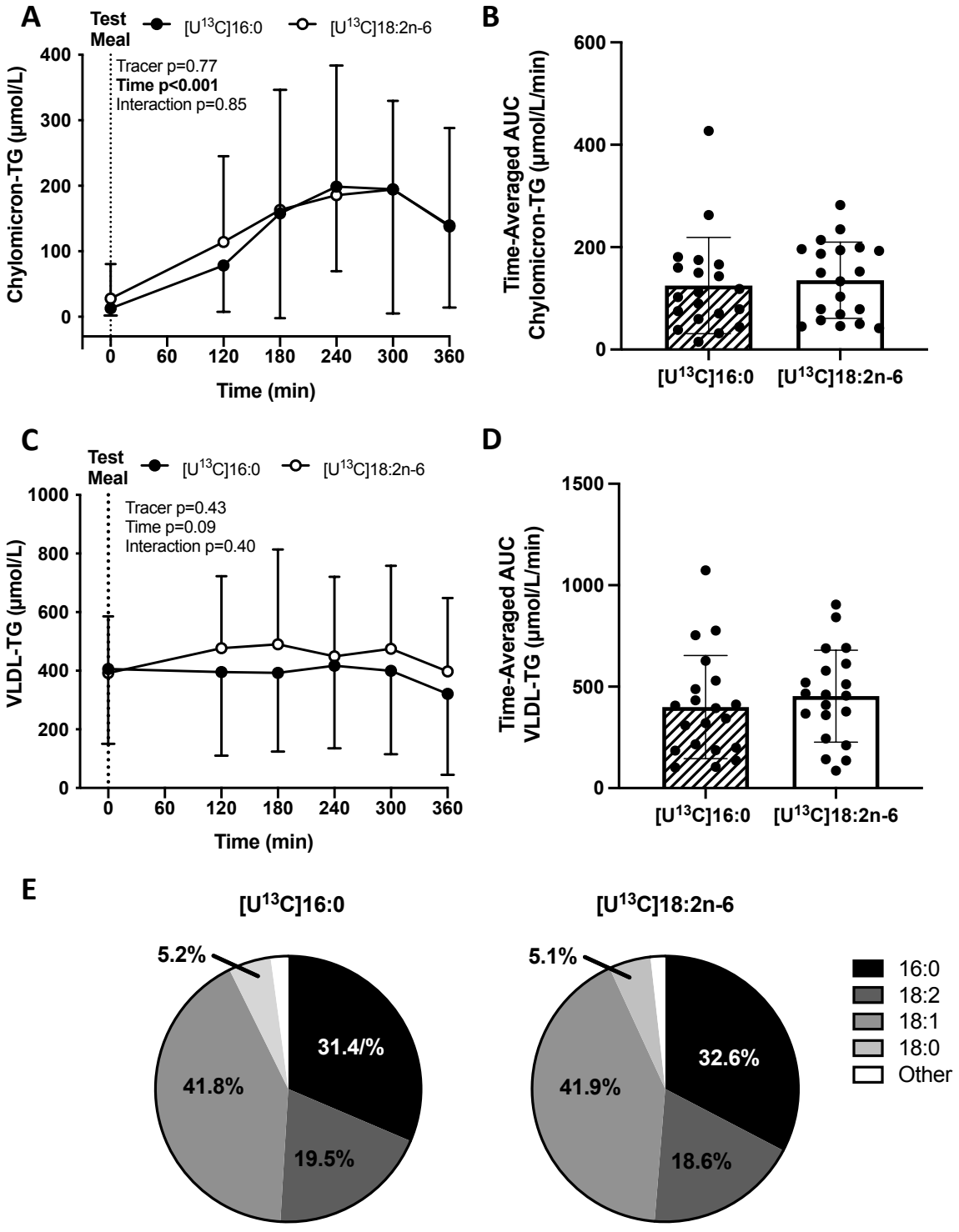

Figure 3.5. Postprandial TG-rich lipoprotein concentration and composition (A) plasma chylomicron-TG concentration, (B) time-averaged AUC chylomicron-TG, (C) plasma VLDL-TG concentration, (D) time-averaged AUC VLDL-TG, (E) chylomicron-TG fatty acid composition at peak chylomicronemia (t=240 minutes), after consumption of a 3-day high carbohydrate diet followed by a standardised mixed test meal containing either [U^{13}C]palmitate ([U^{13}C]16:0) or [U^{13}C]linoleate ([U^{13}C]18:2n-6. Plasma samples were collected every 30-60min for 6h. Analysed by a two–way repeated–measures ANOVA with Tukey's post–hoc test (A, C), Wilcoxon test (B), or paired t-test (D). Abbreviations: TG, triglyceride; VLDL, very-low density lipoprotein; AUC, area under the curve. Data: mean ± SD, n=20.

3.3.5 Tracer Incorporation into Plasma Lipid Fractions

Over the course of each study day, the appearance of ^{13}C from [U^{13}C]palmitate and [U^{13}C]linoleate increased in chylomicron-TG (p<0.001 effect of time; Fig. 3.6A). While there was no tracer*time interaction (p=0.18), the appearance of ^{13}C in chylomicron-TG was significantly greater following the consumption of [U^{13}C]palmitate (p<0.05 effect of tracer; Fig. 3.6A). The appearance of ^{13}C increased over time in the plasma NEFA pool following consumption of both tracers (p<0.001 effect of time; Fig. 3.6B). However, there was a greater increase following [U^{13}C]palmitate compared with [U^{13}C]linoleate consumption (p<0.001 effect of tracer; Fig. 3.6B) and there was a tracer*time interaction effect (p<0.001) as there was a greater ^{13}C appearance in plasma NEFA at 30min and 180-360min following [U^{13}C]palmitate consumption (Fig. 3.6B). While the appearance of ^{13}C in VLDL-TG increased over both study days (p<0.001 effect of time; Fig. 3.6C), it was not different between tracers and there was no tracer*time interaction (p=0.17; Fig. 3.6C). The appearance of ^{13}C into total plasma-TG increased during each study day (p<0.001 effect of time; Fig. 3.6D) and was greater following consumption of [U^{13}C]palmitate compared with [U^{13}C]linoleate (p<0.001 effect of tracer; Fig. 3.6D). A greater ^{13}C appearance into total plasma-TG from 60-360min following [U^{13}C]palmitate compared with [U^{13}C]linoleate consumption (tracer*time interaction effect, p<0.001; Fig. 3.6D) was observed. After consuming [U^{13}C]palmitate, time-averaged AUC for ^{13}C appearance in chylomicron-TG, plasma-NEFA, and plasma-TG were ~78%, ~116%, and ~123% greater, respectively, compared with [U^{13}C]linoleate (all p<0.05, Fig. 3.6E-G).

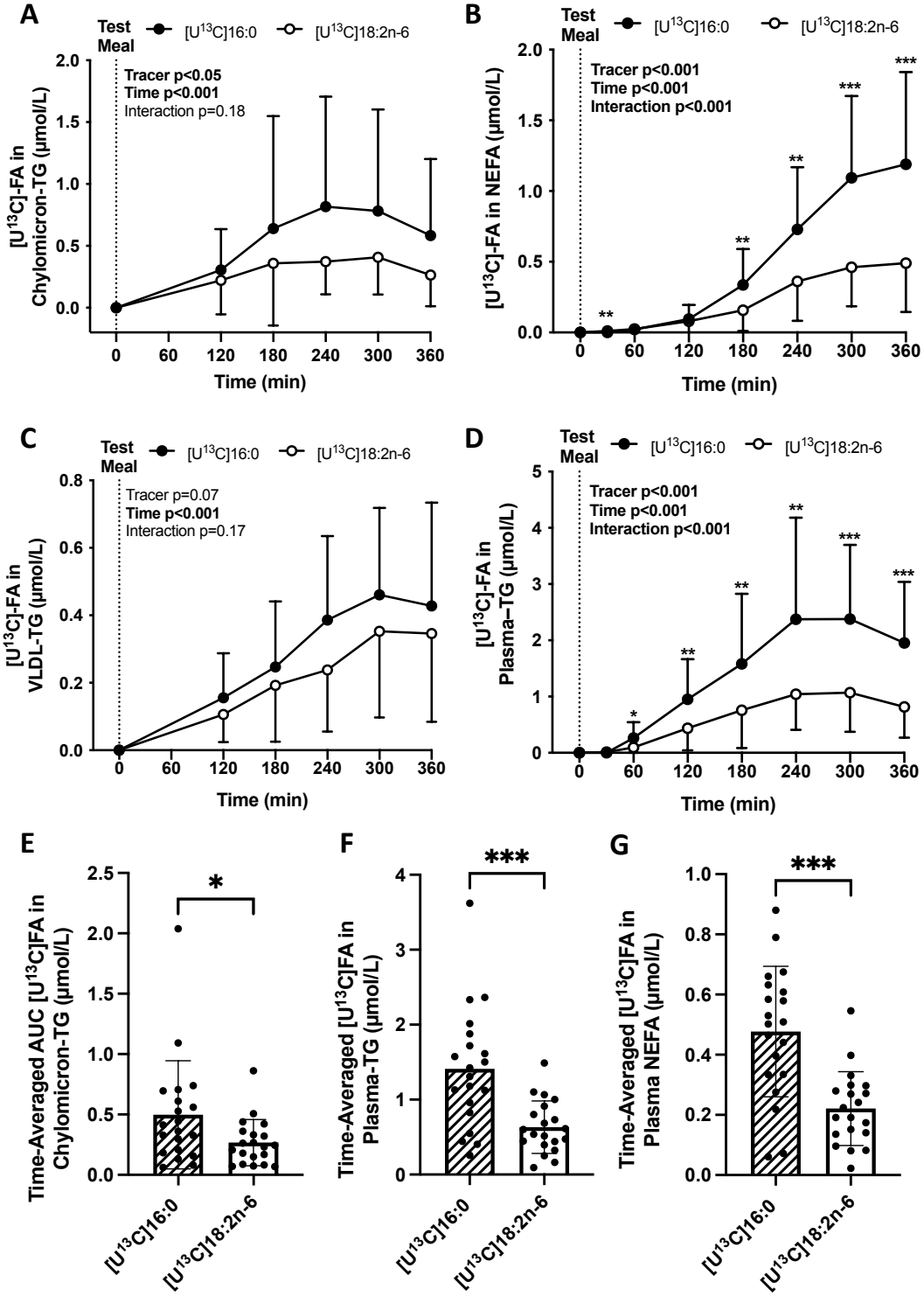

Figure 3.6. **Postprandial [U^{13}C]-tracer incorporation into (A) chylomicron-TG, (B) plasma NEFA, (C) VLDL-TG, and (D) plasma-TG, and time-averaged AUC of [U^{13}C]-tracer incorporation into (E) chylomicron-TG, (F) plasma-TG, and (G) plasma NEFA** after consumption of a 3-day high-carbohydrate diet followed by a standardised test meal containing either [U^{13}C]palmitate ([U^{13}C]16:0) or [U^{13}C]linoleate ([U^{13}C]18:2n-6). Plasma samples were collected every 30-60min for 6h. Analysed by a two–way repeated–measures ANOVA with Tukey's post–hoc test (A-D). Time-averaged AUC was calculated by the trapezoidal method and divided by the relevant time period, and data was analysed using a paired t-test (E-G). Abbreviations: TG, triglyceride; NEFA, non-esterified fatty acid; VLDL, very-low density lipoprotein; AUC, area under the curve. Data presented as mean ± SD, n=20. *p <0.05, **p<0.01, ***p<0.001 compared with alternative tracer study visit.

3.3.6 Whole-body and Hepatic FA Oxidation

To determine whole-body FA oxidation, ^{13}C appearance (from the labelled dietary–FA) into expired CO_2 was measured. The appearance of ^{13}C in expired CO_2 increased following consumption of the tracer-containing meal over the course of the postprandial study period ($p<0.001$ effect of time; Fig. 3.7A), and was greater following consumption of [U^{13}C]linoleate compared with [U^{13}C]palmitate ($p<0.01$ effect of tracer; Fig. 3.7A). There was a tracer*time interaction effect ($p<0.05$) demonstrating greater ^{13}C appearance in expired breath from 30-300min following [U^{13}C]linoleate compared with [U^{13}C]palmitate consumption (Fig. 3.7A). Time-averaged AUC showed a ~46% increase in $^{13}CO_2$ production following [U^{13}C]linoleate compared with [U^{13}C]palmitate consumption ($p<0.01$; Fig. 3.7B). Finally, the percent of ^{13}C recovered as expired $^{13}CO_2$ following [U^{13}C]linoleate consumption compared with [U^{13}C]palmitate was higher (5.08 ± 0.45% vs. 3.73 ± 0.43%, respectively; $p<0.01$; Fig. 3.7C).

^{13}C appearance in CO_2 liberated from plasma urea (227, 274, 276) was measured as a marker of complete intrahepatic FA oxidation. The appearnace of $^{13}CO_2$ in plasma urea increased during the postprandial study day ($p<0.001$ effect of time, Fig. 3.7D) and increased to a greater extent following consumption of [U^{13}C]linoleate compared with [U^{13}C]palmitate ($p<0.05$ effect of tracer; Fig. 3.7D). By subtracting hepatic $^{13}CO_2$ from whole-body $^{13}CO_2$, peripheral FA oxidation was estimated and ^{13}C appearance increased during the postprandial period ($p<0.001$ effect of time; Fig. 3.7E) and was greater following consumption of [U^{13}C]linoleate compared with [U^{13}C]palmitate ($p<0.01$ main effect of tracer, Fig. 3.7E).

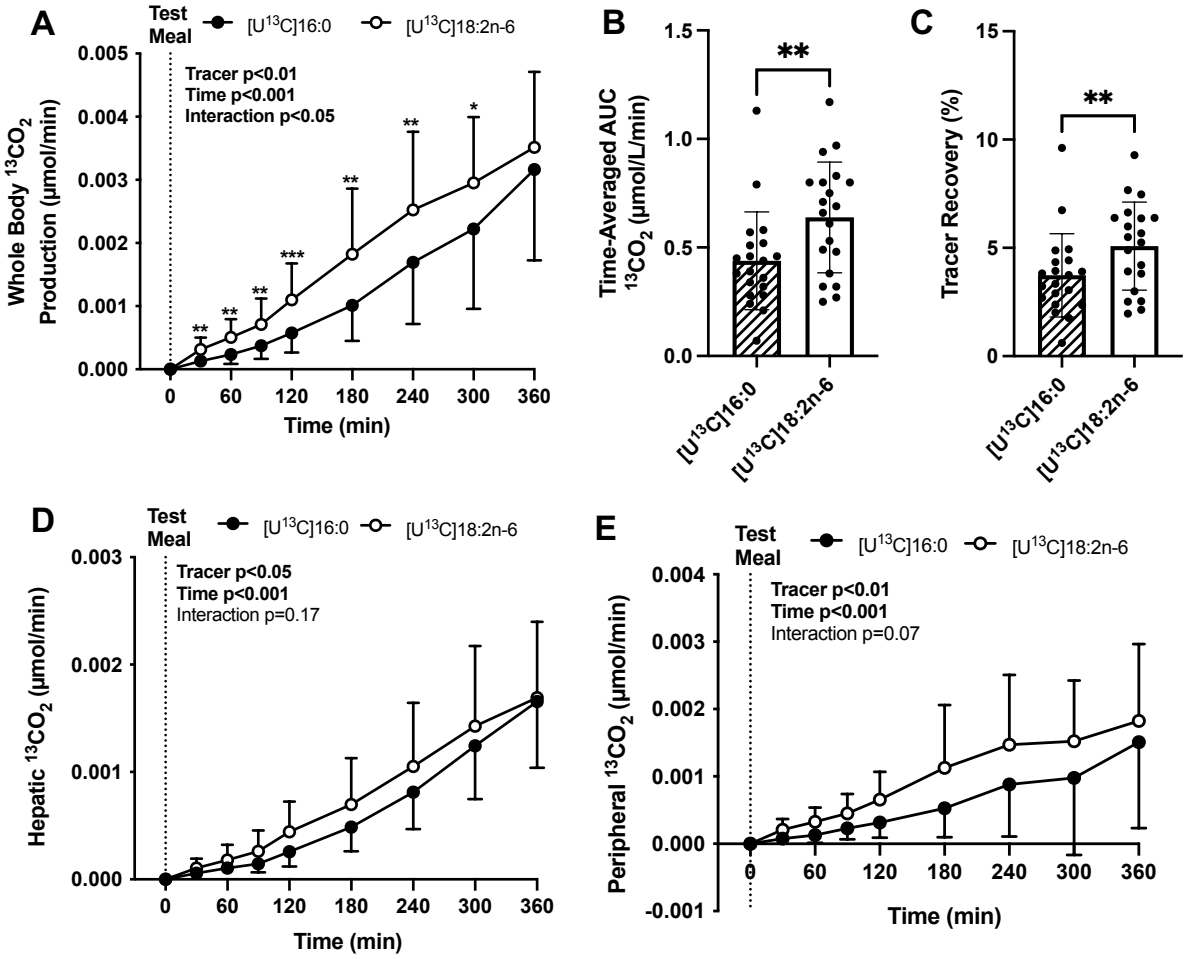

Figure 3.7. Markers of postprandial fatty acid oxidation in (A) expired $^{13}CO_2$, (B) time-averaged area under the curve (AUC) for expired whole-body $^{13}CO_2$, (C) the recovery of the dietary tracer at the end of the 6-h postprandial period, (D) postprandial hepatic $^{13}CO_2$, and (E) postprandial peripheral $^{13}CO_2$ after consumption of a 3-day high-carbohydrate diet followed by a standardised test meal containing either [U^{13}C]palmitate ([U^{13}C]16:0) or [U^{13}C]linoleate ([U^{13}C]18:2n-6). Samples were collected every 30-60min for 6h. Analysed by a two–way repeated–measures ANOVA with Tukey's post–hoc test (A, D, E) or Wilcoxon test (B, C). Time-averaged AUC was calculated by the trapezoidal method and divided by the relevant time period. Data presented as mean ± SD, n=20, *p<0.05, **p<0.01, ***p<0.001 compared with alternative tracer study visit.

As Parry *et al.* observed a sexual dimorphism in the partitioning of ^{13}C-labelled dietary FA (92), I wanted to determine if these differences were maintained when hepatic DNL was upregulated. The cohort was split by sex and time-averaged AUC for ^{13}C appearance in expired, hepatic, and peripheral CO_2 was compared for each person following consumption of [U^{13}C]palmitate or [U^{13}C]linoleate. There was significantly (p<0.05) greater ^{13}C appearance in expired CO_2 and peripheral CO_2 following [U^{13}C]linoleate consumption compared with [U^{13}C]palmitate consumption after the 3-day isocaloric high-carbohydrate diet in females, whereas for males, there was a trend for a greater ^{13}C appearance in expired CO_2 (p=0.07) and

peripheral CO_2 (p=0.06) following [U^{13}C]linoleate consumption compared with [U^{13}C]palmitate consumption (Fig. 3.8A-B). For hepatic CO_2, a trend (p=0.08) was observed for greater ^{13}C appearance in females following [U^{13}C]linoleate consumption compared with [U^{13}C]palmitate consumption, but there was no difference in males (p=0.31; Fig. 3.8C).

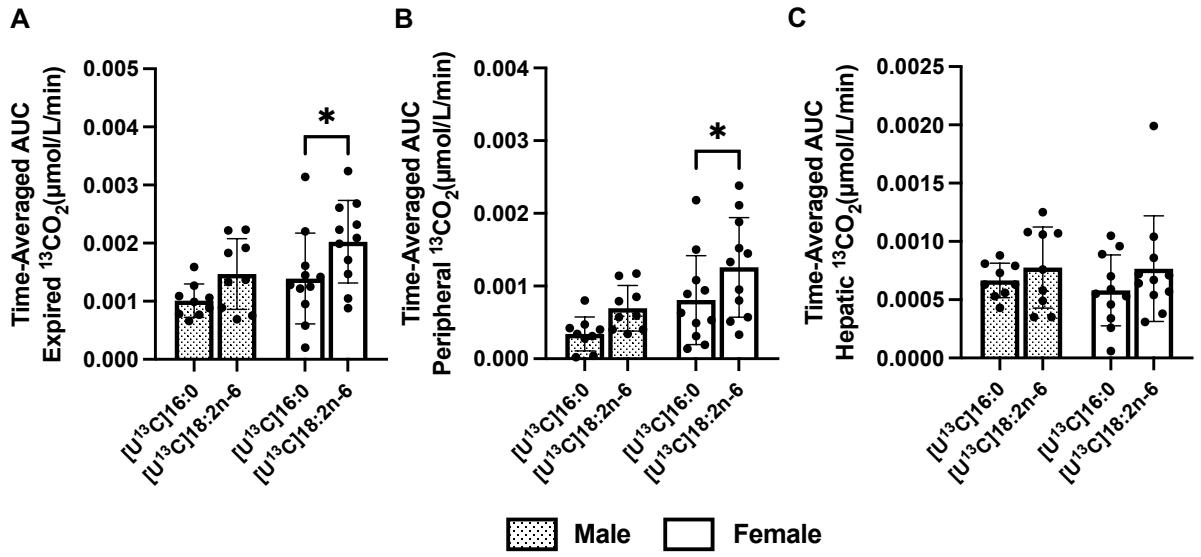

Figure 3.8. Time-averaged area under the curve (AUC) of (A) expired $^{13}CO_2$, (B) peripheral $^{13}CO_2$, and (C) hepatic $^{13}CO_2$ comparing male (shaded bars) and female (white bars) participants after consumption of a 3-day high-carbohydrate diet followed by a standardised test meal containing either [U^{13}C]palmitate ([U^{13}C]16:0) or [U^{13}C]linoleate ([U^{13}C]18:2n-6). Samples were collected every 30-60min for 6h. Data presented as mean ± SD, n=9 males, n=11 females. Time-averaged AUC was calculated by the trapezoidal method and divided by the relevant time period, and data was analysed using a paired t-test. * $p<0.05$ compared within sex between alternative tracer visit.

3.4 Discussion

A proposed mechanism for the divergent effects of dietary SFA and PUFA on IHTG accumulation is that they are preferentially partitioned into different intracellular pathways (92, 194). While Parry *et al*. previously reported greater whole-body oxidation of dietary linoleate (PUFA) compared with dietary palmitate (SFA) (92), it remains unclear if this preferential partitioning is maintained when the metabolic state of the liver is shifted from oxidation toward esterification. Therefore, hepatic DNL was acutely upregulated to investigate if hepatic metabolic state influences the partitioning of dietary SFA (palmitate) and PUFA (linoleate) in healthy participants. By consuming a high-carbohydrate (75% TE) diet for 3-days, the

lipogenic and SCD indices in plasma-TG notably increased, in agreement with others (65). Despite this intrahepatic metabolic shift, there was greater appearance of ^{13}C in markers of whole-body and hepatic FA oxidation following [U^{13}C]linoleate compared with [U^{13}C]palmitate consumption, and greater appearance of ^{13}C in plasma lipid pools following [U^{13}C]palmitate compared with [U^{13}C]linoleate consumption. Taken together, the data suggest that dietary PUFA, compared with SFA, remain preferentially partitioned into oxidation pathways in disease-free adults when the metabolic state of the liver is shifted away from oxidation.

3.4.1 Intrahepatic FA Partitioning

Previous human studies have shown the degree of FA saturation influences postprandial dietary FA oxidation (92, 278, 279). Although consuming an acute high-carbohydrate diet suppresses total dietary FA oxidation in humans (67, 280), the appearance of ^{13}C into expired CO_2 and urea-derived CO_2 was greater following consumption of [U^{13}C]linoleate compared with [U^{13}C]palmitate. CPT1, which catalyses the rate-determining step of mitochondrial FA oxidation and is expressed in hepatic and non-hepatic tissues, has a higher binding affinity and transport rate for PUFA compared with SFA (198). Thus, there may be greater mitochondrial uptake of PUFA, which would lead to greater β-oxidation and ^{13}C appearance from [U^{13}C]linoleate into expired CO_2 and urea. These findings suggest dietary fat composition may influence FA oxidation findings. As dietary fat composition is often not reported in studies, differences in composition may explain, in part, some of the inconsistent observations for FA oxidation in humans, when DNL is upregulated (69, 87, 89).

3.4.2 Other Factors Modulating FA Oxidation

Dietary FA oxidation findings may be also influenced by an individual's metabolic state (e.g. fed vs. fasted, presence of metabolic disease, etc.), intestinal absorption, transport in

circulation, and across cellular membranes (52, 194, 281, 282); however, it remains unclear how dietary fat composition interacts with these processes to modulate FA oxidation. Although greater appearance of ^{13}C-labelled FA in circulating chylomicron-TG and NEFA was observed following consumption of [U^{13}C]palmitate compared with [U^{13}C]linoleate, this could not be explained by greater plasma chylomicron-TG and NEFA concentrations on the SFA-tracer study day. Nelson *et al.* (283) observed in young, lean, individuals that the spillover of palmitate into the plasma NEFA pool is strongly positively correlated with plasma NEFA concentrations, whereas spillover of linoleate is inversely correlated with total plasma NEFA concentrations. Given total circulating NEFA concentrations were similar between study days, it is plausible the differences in ^{13}C-labelled FA appearance in chylomicron-TG and NEFA may be due to greater spillover of palmitate compared with linoleate, and linoleate being partitioned into other lipid pools, such as PL and CE synthesis (269), thus lowering the appearance of the linoleate tracer into the plasma NEFA pool. Additionally, Piche *et al.* observed the incorporation of ^{13}C-palmitate into the plasma NEFA pool is greater in females compared with males (284); thus, these findings may be influenced by the slightly higher number of females than males in the study.

As most fasting and postprandial biochemical parameters did not differ between postprandial study days, differences in the partitioning of ^{13}C-labelled FA into oxidation pathways and lipid pools are unlikely to be explained by differences in an individual's metabolic state. Hodson *et. al* found, when co-ingested, a similar appearance of dietary [U^{13}C]palmitate and [U^{13}C]linoleate into chylomicron-TG, and a higher incorporation of [U^{13}C]linoleate compared with [U^{13}C]palmitate in plasma PL and CE (269). While [U^{13}C]linoleate may have been preferentially partitioned into these lipid pools, ^{13}C enrichment was not measured in these lipid fractions in this study. Regardless, this would not explain the differences in the ^{13}C appearance in expired CO_2. Despite the greater appearance of ^{13}C-

labelled FA in chylomicron-TG and NEFA following consumption of [U^{13}C]palmitate compared with [U^{13}C]linoleate, suggesting a greater flux of SFA to the liver as TG-rich remnants and NEFA, greater ^{13}C appearance was observed in hepatic $^{13}CO_2$ following consumption of [U^{13}C]linoleate compared with [U^{13}C]palmitate. These observations support an intrahepatocellular mechanism that preferentially partitions PUFA, compared with SFA, into oxidation pathways.

3.4.3 Hepatic TG Secretion

Despite differences in ^{13}C appearance in CO_2 following consumption of the ^{13}C-labelled FAs, and the potentially greater flux of dietary SFA compared with PUFA to the liver, significant differences in ^{13}C-labelled FA appearance in VLDL-TG were not observed following consumption of the tracer containing meals. While there were similar VLDL-TG concentrations on the respective postprandial study days, differences between study days in VLDL-TG secretion and clearance rates cannot be excluded; although it is unlikely as the same test meal was given. Instead, as this study was powered to detect differences in ^{13}C appearance in expired CO_2, it may be underpowered to detect differences in ^{13}C-labelled FA appearance in VLDL-TG.

3.4.4 Plasma Glucose

Despite participants consuming an identical 3-day high-carbohydrate diet and mixed test meal on both study days, postprandial glucose excursions were greater following the meal containing [U^{13}C]palmitate compared with [U^{13}C]linoleate, with no difference in the postprandial insulin response and no order effect between study days. Menstrual cycle stage has previously been shown to influence plasma glucose concentrations in premenopausal females (285). As we did not match the postprandial days for stage in the menstrual cycle in female participants and nearly all female participants were premenopausal, it is plausible this,

in part, explains the small, but statistically significant, increase in postprandial plasma glucose. Further, differences in menstrual cycle stage may have impacted other metabolic findings, such as the desaturase index.

3.4.5 Limitations

This study is not without limitations. To upregulate hepatic DNL, participants consumed a 3-day high-carbohydrate diet, thus, it is plausible that in situations where hepatic DNL is constitutively upregulated (e.g. individuals with MASLD (60, 272)) observations may differ to what are reported here. It would be of interest to study such cohorts where DNL has been upregulated for longer periods. Our participants were younger and had BMIs that were typically lower than most adults at risk of CMD thus limiting the generalisability of our observations. Although participants were asked to maintain their habitual diet and lifestyle habits during the 2-week washout period, habitual diet was not controlled for and it is possible participants altered their diet. If participants increased dietary palmitate consumption, this may have influenced FA oxidation findings (286, 287); however, as the ^{13}C-FA tracers were given in random order, this would have influenced the oxidation findings of both palmitate and linoleate equally. Inclusion of individuals with moderate alcohol intake (14-21 units per week) may have influenced the findings, however, as this study was a crossover design, it would affect both linoleate and palmitate findings equally. Although limited differences in FA partitioning between sexes were observed, this study is likely underpowered to fully characterise these effects. Given males have a higher propensity for liver fat accumulation (288), it would be of interest to explore this further under conditions where lean mass could be accounted for and male and female participants could be matched for age and BMI. Within the liver, palmitate and linoleate can be elongated and desaturated to form stearate and arachidonate, respectively, which may, in part, explain some of the differences observed between [U^{13}C]palmitate and [U^{13}C]linoleate appearance in plasma lipid pools. However, ^{13}C

enrichment as stearate and arachidonate in plasma-TG and NEFA was undetectable which may be due to the limited time frame of the postprandial period in this study and the lipid fractions assessed. It would be of interest to explore these processes further in other lipid fractions, like plasma PL, which have a higher abundance of stearate and arachidonate, compared with plasma-TG and NEFA (13). It cannot be excluded the FA composition of the diet influenced, in part, the lipogenic and/or desaturase indices. However, given the low amount of dietary fat consumed over the 3-days prior to the study day and dietary palmitoleate is very limited (277), it is unlikely they had a large influence on these findings.

3.4.6 Conclusions

This study shows that following a dietary-induced upregulation of hepatic DNL, the preferential partitioning of dietary PUFA towards oxidation pathways and dietary SFA towards esterification pathways is maintained following consumption of a mixed-test meal. These findings help clarify how hepatic metabolic state interacts with dietary fat composition to influence the potential postprandial disposal of dietary fat from the liver, and in the long-term, effect IHTG accumulation.

Chapter 4

A Saturated, Compared with Polyunsaturated Fat, Enriched High-Fat Diet Induces Divergent, Weight-Independent Effects on Cardiometabolic Disease Risk in Humans: A Randomised Control Trial

The following aspects of this chapter were completed by others: recruitment and sample collection for 3 of 28 participants by Dr. Siôn Parry, mathematical modelling of insulin kinetics by Dr. Kieran Smith, acquisition of MRI/S data by trained radiographers at the Oxford Centre for Clinical Magnetic Resonance Research (OCMR), and the code to analyse spectroscopy data was created by Associate Prof. Ladislav Valkovic, Associate Prof. Chris Rodgers, and Dr. Ferenc Mozes. All remaining participant recruitment, sample collection, processing and analysis, and data analysis was completed by me.

4.1 Introduction

Increased IHTG content is a characteristic feature of MASLD and is associated with insulin resistance, a proatherogenic lipoprotein profile, and increased CVD risk (215, 271). Despite similar weight gain, overfeeding a SFA-, compared with PUFA- or sugar-enriched diet, increases IHTG accumulation to a greater extent, suggesting that dietary macronutrient composition may influence IHTG accumulation independent of changes in body weight (79). It is proposed dietary SFAs, compared with PUFAs, lead to divergent effects on IHTG accumulation due to differences in intrahepatic and systemic metabolism. It has been suggested, and I have shown in Chapter 3, that PUFAs preferentially enter oxidation pathways compared with SFAs, which may increase hepatic FA disposal; thus, consumption of a PUFA-enriched diet could decrease IHTG content, (92, 194, 289). In contrast, consumption of a SFA-enriched diet may increase adipose tissue lipolysis (79) and reduce systemic insulin sensitivity (192) which may increase IHTG content. However, most studies investigating the effects of dietary FA composition on IHTG accumulation have been conducted using hypercaloric diets, therefore, it is challenging to disentangle the effects of dietary FA composition from increased caloric intake and weight gain on IHTG content (10, 11, 79). Further, findings from studies which investigated the effects of dietary FA composition on IHTG content under isocaloric

conditions are inconsistent, with some studies reporting SFA-enriched diets increase IHTG content (61, 187, 192), and others showing no effect (77, 189); this may be due to differences in participant characteristics, the duration of experimental diet, or the amount of SFA consumed during different interventions. Further, no previous studies have directly compared how the FA composition of an isocaloric HFD impacts CMD risk in the absence of weight change. Therefore, the aim of this study was to compare the effects of two isocaloric HFDs - one enriched in SFA, and the other enriched in PUFA - on IHTG content, hepatic and whole-body fasting and postprandial metabolism, and cardiac metabolism and function in males and females free from diagnosed metabolic disease.

4.2 Materials and Methods

4.2.1 Participants

Male and female participants were recruited according to criteria in Table 4.1 and section 2.1. This trial was registered at clinicaltrials.gov NCT05962190.

Table 4.1. Participant Inclusion and Exclusion Criteria

Inclusion Criteria	Exclusion Criteria
Willing and able to give informed consent	Unwilling or unable to give informed consent
Male and female participants aged 30-65	Consumption of alcohol greater than, for males, 3-4 units of alcohol per day or 21-28 units of alcohol per week and, for females, greater than 2-3 units of alcohol per day or 14-21 units of alcohol per week
BMI >18.5 kg/m^2 and <35.0 kg/m^2	Gained or lost >5% body weight in the last 3 months
Free from diagnosed metabolic disease	History of an eating disorder or any other psychological condition that may affect the participants ability to adhere to study intervention/experimental diets
Not following a weight-loss diet	Inability to modify diet to consume a high-fat diet

Not taking medications and/or supplements known to affect liver and/or adipose tissue metabolism	Pregnant, suspected pregnant, or nursing
Not actively smoking (within last 3 mon.) or consuming other nicotine containing products	Participant has changed dose of a medication within the last three months
Plasma haemoglobin above 120g/L for females or 135g/L for males	Unable to undergo and/or tolerate cannulation
	History of bleeding disorders
	Standard contraindication(s) for magnetic resonance scan
	Donated or lost ≥250 mL of blood in the previous two months
	History of albumin and/or egg allergy
	Current anticoagulant treatment

4.2.2 Experimental Design

This was a randomised parallel-design, clinical trial where each participant completed an isocaloric dietary intervention under free-living conditions lasting up to 24 days. Following screening and providing consent to participate in the study, participants were randomised to one of two dietary interventions: *i)* a HFD enriched with SFA, or *ii)* a HFD enriched with PUFA. Prior to starting the dietary intervention, participants consumed a 7-day standardisation diet based on the UK Eatwell plate. During the standardisation diet and each week during the dietary intervention, participants completed 3-day diet diaries (two weekdays and one weekend day). Before starting (i.e. baseline) and after completing the dietary intervention (i.e. post-HFD), participants underwent a magnetic resonance imaging and spectroscopy (MRI/S) scan and postprandial study day with stable-isotope tracers (Fig. 4.1). The primary outcome was to investigate if the dietary FA composition of a HFD influenced IHTG accumulation. The secondary outcomes were to characterise if the dietary FA composition of a HFD impacted fasting and postprandial plasma biochemistry, systemic lipid metabolic pathways using stable-isotope tracers, postprandial plasma insulin kinetics, and cardiac metabolism and function. I

also investigated if there is a sexual dimorphism in fasting and postprandial metabolism following consumption of a SFA- or PUFA-enriched HFD.

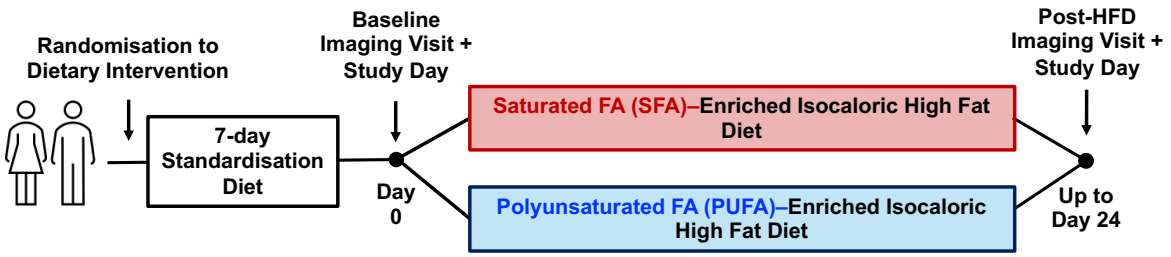

Figure 4.1. Overview of Experimental Design.

4.2.3 Experimental Diet

As there are no universally accepted definitions for HFDs, I used previous classifications (173, 174), with the target macronutrient composition for both SFA- and PUFA-enriched HFD being 50-60%TE from fat, 25-35%TE from carbohydrate, and 15%TE from protein. The target FA composition of the SFA- and PUFA-enriched HFD was determined in collaboration with Prof. Jennifer Carter based on the amount of SFA and PUFA typically consumed by UK adults in highest quintile of the UK Biobank. To reflect real-world intakes of dietary SFA and PUFA, participants consuming the SFA-enriched or PUFA-enriched HFD were advised to consume >15%TE from SFA or >10%TE from PUFA, respectively. To achieve these targets, participants randomised to consume the SFA-enriched HFD were advised to increase consumption of meat and meat products from land animals, dairy products (i.e. butter, cream, and hard cheeses), food items containing coconut, fast-food items, and were provided with some snacks (>70% dark chocolate, savoury biscuits, and cheese). Participants randomised to consume the PUFA-enriched HFD were advised to increase consumption of oily fish, nuts, seeds, sunflower and hemp seed oil, and were provided with some snacks (nuts, diet bars, and crisps fried in sunflower oil). Further, participants following both diets were advised to reduce consumption of carbohydrates (bread, rice, and pasta) to ensure the diet was isocaloric and minimise changes in bodyweight. Diet diaries were analysed with Nutritics

software (Nutritics Research Edition v6.02). The change in FA composition of fasting plasma-TG, measured by GC, was used as a biomarker of dietary FA intake. Participants were asked to maintain their habitual physical activity levels, alcohol intake, and bodyweight throughout the standardisation diet and dietary intervention, and each week, a member of the research team contacted each participant to support adherence. An intervention lasting up to 24 days is based on previous work showing this diet duration balances participant compliance with maximising change in metabolic parameters (290, 291).

4.2.4 Postprandial Study Days

At baseline and after consuming a HFD for up to 24 days, participants arrived at the OCDEM CRU for a postprandial study day after consuming D_2O the night before (section 2.2, 2.2.2). On the study day, the [2,2-D_2]palmitate infusion was started and allowed to equilibrate before consuming the [U^{13}C]palmitate containing meal, after which, repeated blood and breath samples were collected for 6h (Fig. 4.2). Indirect calorimetry was performed at 0 and 120min (section 2.2.1, Fig. 4.2). At the end of each postprandial study day, a dual energy x-ray absorptiometry (DEXA) scan (GE (Lunar iDXA, General Electric, Chesire, United Kingdom) was performed by a trained research nurse and analysed with Encore software (version 11.0; GE. Medical Systems, Madison, WI, USA) to measure body composition and visceral adipose tissue.

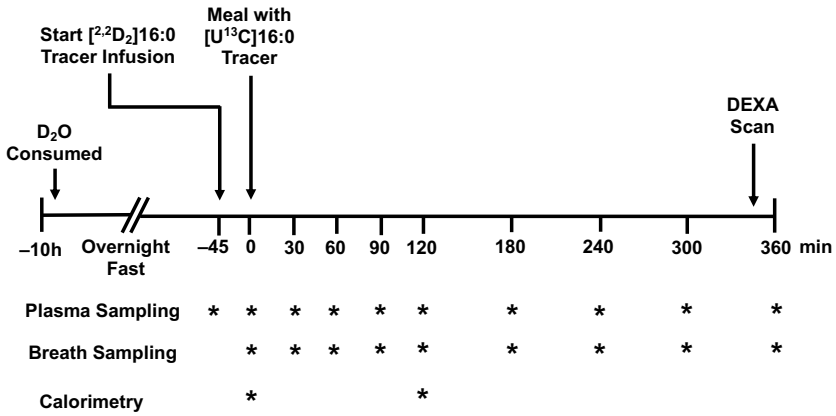

Figure 4.2. Overview of Postprandial Study Day Protocol.

4.2.5 MRI/S Scans

At baseline and after consuming a HFD, participants underwent an MRI/S scan at OCMR. Prior to each scan, participants fasted for at least 6h. All scans were performed using a 3-Tesla MR scanner (PRISMA, Siemens Healthineers, Erlangen, Germany) with participants in the supine position and at an end-expiration breath-hold. An electrocardiogram (ECG)-trigger at end-diastole for MRS scans and retrospective ECG-gating during cine acquisitions for MRI scans was used to reduce respiration and cardiac activity motion artefacts.

4.2.5.1 Proton (1H)-MRS

IHTG and myocardial TG content were measured by ^{1}H-MRS. Following acquisition of anatomical images, water-suppressed and non-water-suppressed stimulated echo acquisition mode (STEAM) measurements quantified IHTG content in a single voxel (20 x 20 x 20 mm^3) in the posterior left liver lobe and myocardial TG content in the mid-interventricular septum (voxel: 22 x 18 x 32 mm^3) (Fig. 4.3A-B) (292). Voxel position in the liver was recorded during each participant's baseline scan to match during post-HFD scans. Water-suppressed hepatic spectra were acquired over 3 breath holds with 6 acquisitions each, water-suppressed cardiac spectra were acquired over 5 breath holds with 6 acquisitions each. Three water-unsuppressed spectra were obtained within one breath hold after the respective cardiac and hepatic water-suppressed acquisitions and used as internal references during analysis. Sequence parameters for the hepatic ^{1}H-MRS were as follows: echo time 10 ms, retention time 760 ms, mixing time 7 ms, and repetition time at least 2,000 ms for water-suppressed scans and at least 4,000 ms for non–water-suppressed scans. Sequence parameters for the cardiac ^{1}H-MRS were as follows: echo time 40 ms, retention time 610 ms and repetition time at least 2,000 ms for water-suppressed scans and at least 4,000 ms for non–water-suppressed scans. Spectra were analysed using in-house script in Matlab (v. R2022b, The MathWorks Inc., USA) and the Advanced Method for Accurate, Robust, and Efficient Spectral tracking (AMARES) in the OXSA toolbox

(293). IHTG and myocardial TG content were calculated as the percent lipid peak relative to water peak (Fig. 4.3C).

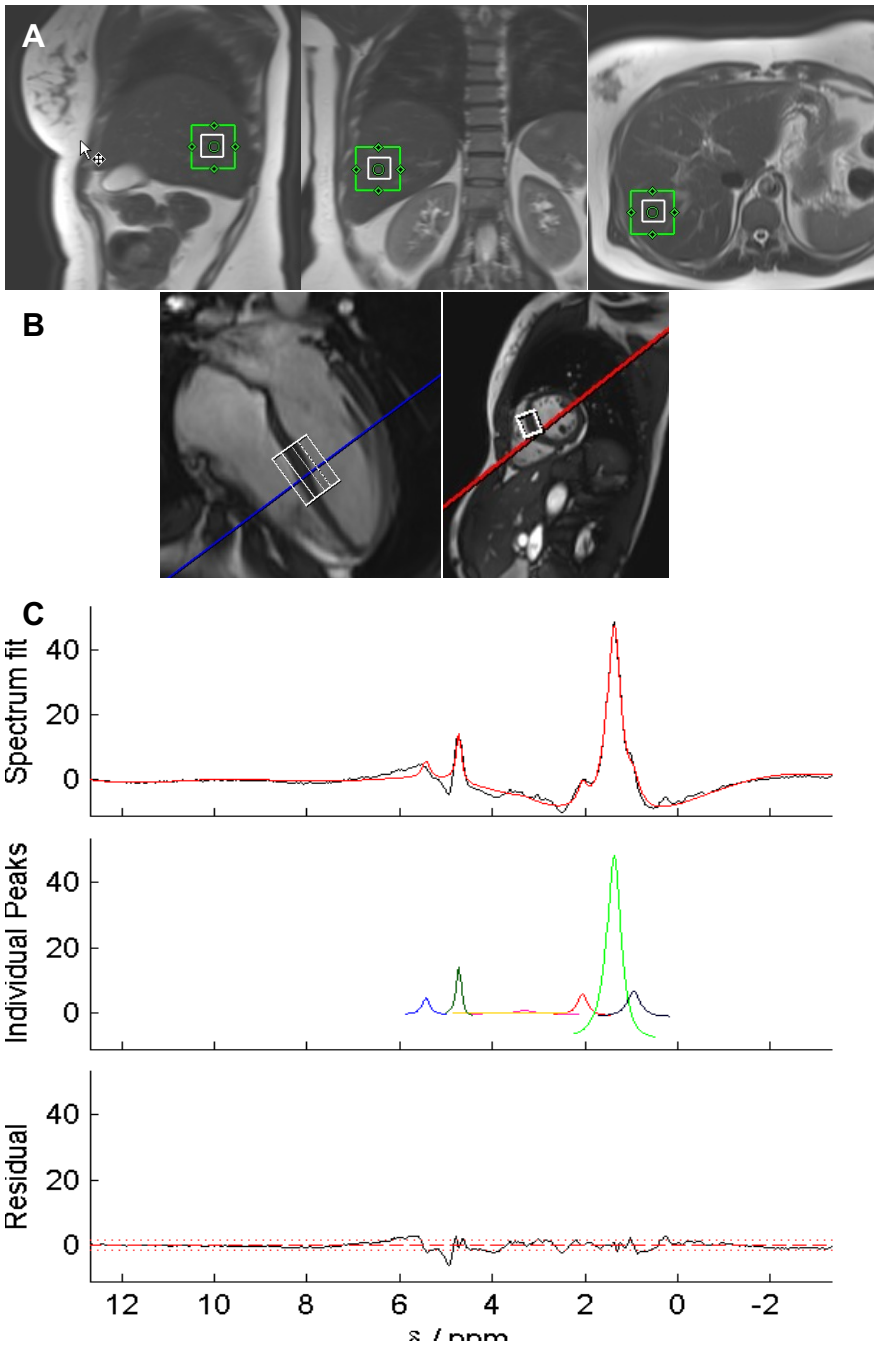

Figure 4.3. Representative H-MR spectroscopy images. (A) Voxel position in the posterior left lobe of the liver during hepatic H-MRS. (B) Voxel position in the mid-interventricular septum during cardiac H-MRS. (C) Representative H-MR spectra with the lipid peak represented by the light green peak and the suppressed water peak represented by the dark green peak.

4.2.5.2 31-Phosphorus-MRS

Myocardial PCr/ATP was measured by ^{31}P-MRS using a surface ^{1}H/^{31}P flex coil (Rapid

Biomedical, Rimpar, Germany) and slice-selective depth-resolved surface-coil spectroscopy (DRESS) sequence. After obtaining planning images, positions of phenylphosphonic acid (PPA) fiducial and cod-liver oil phantoms were located, and coil loading was measured by ten free induction decay inversion recovery curves with an increasing inversion delay (50-1500ms). The voxel (200 x 200 x 20mm^3) was placed over the myocardial interventricular septum and angled parallel to the coil. Saturation bands were placed over skeletal muscle in the chest wall and liver to reduce signal contamination from non-cardiac tissues. An optimising radiofrequency pulse, centred at 250Hz relative to PCr, was used to ensure uniform excitation (294). Spectra analysis was performed with in-house script in Matlab (v. R2022b, The MathWorks Inc., USA) using AMARES in the OXSA toolbox and prior knowledge of the expected myocardial phosphorus spectra (Fig 4.4) (293, 294). PCr/ATP results with a coefficient of variation greater than 30% were excluded.

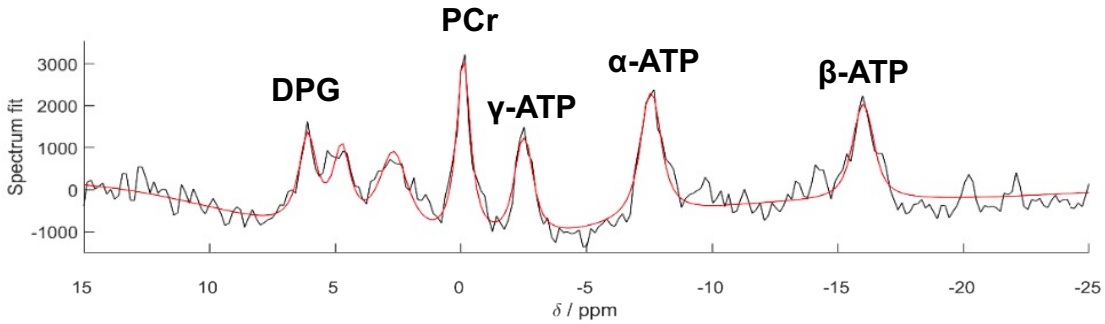

Figure 4.4. Representative myocardial ^{31}P spectrum. Black line indicates raw acquired spectral data with peaks of phosphorus-containing metabolites as labelled, red line represents AMARES spectral fitting.

4.2.5.3 Cardiac Volumes & Function by 1H-MRI

Cardiac volumes, mass, and function were measured using a 30-channel surface coil (Siemens Healthineers, Erlangen, Germany) with the following steady state free precession (SSFP) cine imaging parameters: slice thickness 7 mm, echo time 1.64 ms, retention time 54.60 ms, flip-angle 62°, and field of view 420 mm. After acquiring planning images, horizontal long axis (HLA), vertical long axis (VLA), and LV short-axis (SA) stack images were obtained (Fig. 4.5).

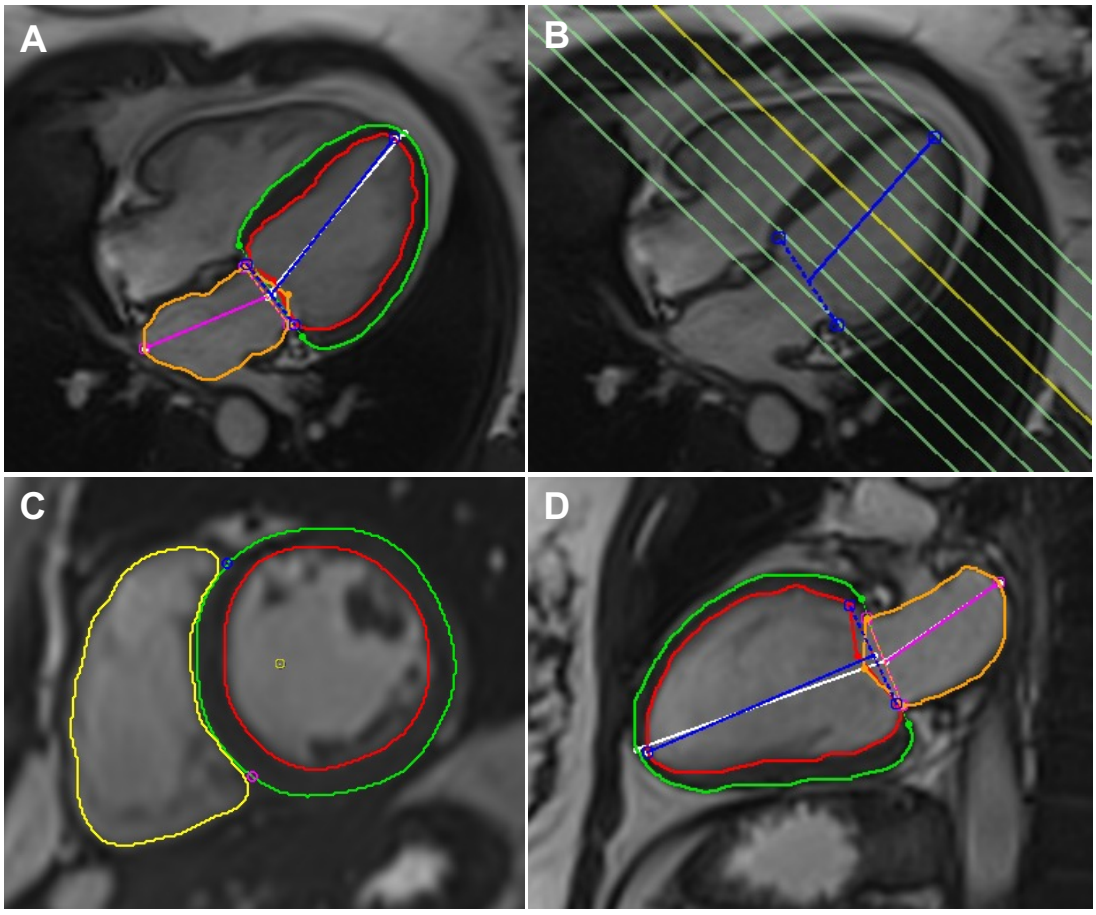

Figure 4.5. Representative cardiac H-MR images in the (A) horizontal long axis (B) locations of short axis images, (C) short axis, and (D) vertical long axis.

Analysis was performed using cvi42 v6.0.2 (Circle Cardiovascular Imaging Inc, Calgary, Alberta, Canada), where LV endocardial and epicardial borders in the SA stack, HLA, and VLA images, right ventricular (RV) endocardial borders in the SA stack, and left atrial endocardial borders in the HLA and VLA images were manually contoured (Fig 4.6). Scans were de-identified to blind the researcher during analysis. SV, EF, cardiac output (CO), LV myocardial mass, and LV mass-to-volume ratio were calculated as described (295). Peak diastolic filling rate was calculated by subtracting EDV between each phase, normalising to peak EDV, and dividing by repetition time (296). Global longitudinal and radial strain were measured in cvi42 using post-processing feature tracking.

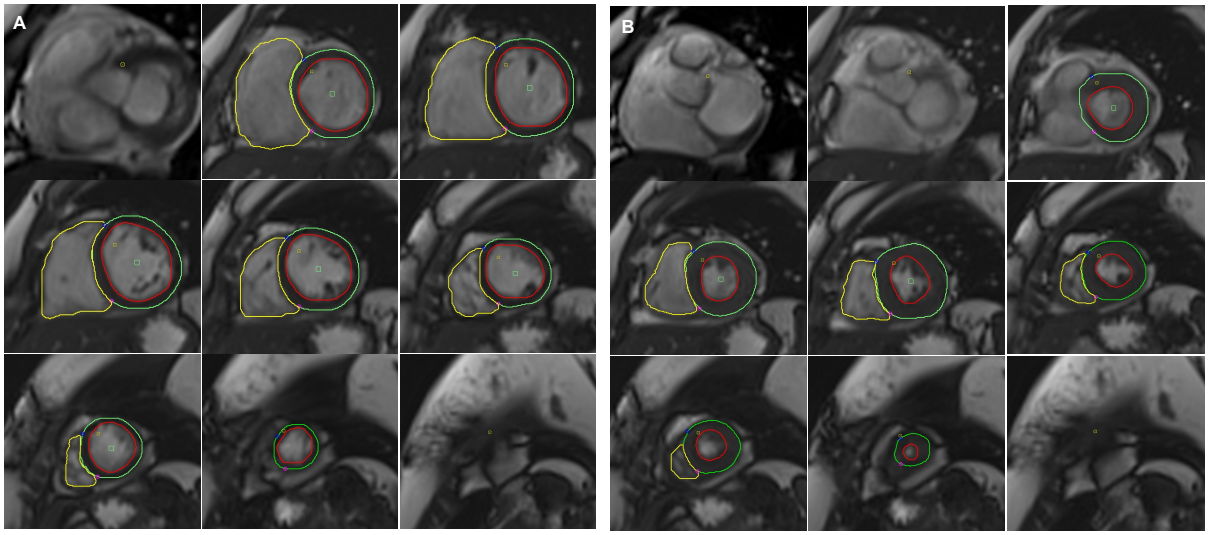

Figure. 4.6. Representative manual contours of the left and right ventricular endocardial and epicardial borders at (A) end diastole and (B) end systole

4.2.5.4 Aortic Distensibility

Aortic distensibility (AD) was measured using axial SSFP cine sequences (thickness 8 mm) acquired at the ascending and proximal descending aorta, and 12cm below the slice at the distal descending abdominal aorta (297). Brachial systolic and diastolic blood pressure was recorded during these acquisitions with a vicorder (Smart Medical Ltd., Cheltenham, UK), and used to determine aortic systolic and diastolic blood pressures by pulse-wave analysis. Maximal and minimal aortic areas at the ascending, proximal descending, and distal descending aorta were determined using a semi-automated Matlab code and used to calculate AD at all three locations (297, 298):

$$\text{AD} = \frac{\text{Max Aortic Area} - \text{Min Aortic Area}}{\text{Min Aortic Area}} \div \text{Aortic pulse pressure} \times 1000$$

4.2.6 Echocardiography

Transthoracic echocardiography was performed to assess diastolic cardiac function at OCMR after the MRI/S scan using a GE Vivid I system (GE, Boston, USA). Participants were positioned in the left lateral decubitus position and an apical 4-chamber view of the heart was obtained (Fig. 4.7A). Pulse wave doppler was used to measure peak trans-mitral early (E-wave)

and late diastolic flow (A-wave), and the flow deceleration time and slope from peak E-wave to the end of E-wave (Fig. 4.7B). Tissue doppler imaging (TDI) at the mitral annulus was performed to measure septal and lateral e'. These measurements were used to calculate E/A and E/e'.

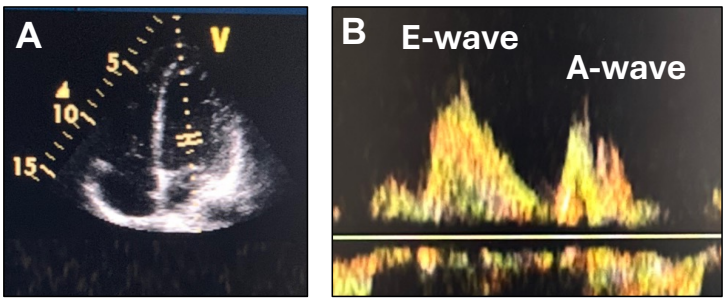

Figure. 4.7. Representative images of a (A) 4-chamber view of the heart and (B) trans-mitral flow.

4.2.7 Analytical methods

Plasma glucose, NEFA, TG, glycerol, total and HDL cholesterol, 3OHB, ApoB, and lactate were measured (section 2.3.2). Plasma insulin and C-peptide levels were quantified (section 2.3.3) and plasma chylomicron- and VLDL-rich fraction were isolated (section 2.3.1).

4.2.8 FA Composition and Isotopic Enrichment in Plasma Lipid Pools

The FA composition of plasma-TG, chylomicron-TG, VLDL-TG, and plasma NEFA were determined by GC (section 2.4, 2.5). [U^{13}C]palmitate and [2,2-D_2]palmitate enrichment in plasma TG, NEFA, chylomicron-TG, and VLDL-TG and [D_2]palmitate enrichment in VLDL-TG were determined by GC-MS and used to calculate palmitate tracer concentrations and percent of newly synthesised palmitate in VLDL-TG (section 2.6, 2.6.1, 2.6.3).

4.2.9 Isotopic Enrichment in Fatty Acid Oxidation Markers

Whole-body meal-derived FA oxidation was determined by measuring ^{13}C appearance in expired CO_2 by GC-C-IRMS (section 2.6.2).

4.2.10 Isotopic Enrichment in Fasting Plasma Glucose

Glucose was extracted from plasma by mixing plasma with ethanol, drying to completion, and adding 2% (w/v) methylhydroxylamine hydrochloride in pyridine. Samples were heated at 90˚C for 2h and cooled, before adding excess BSTFA+1% TCMS, heating for a further 15min at 120˚C, and drying to completion (299). Samples were reconstituted in decane and tracer enrichment measured by GC-MS (section 2.6). The proportion of fasting glucose derived from hepatic gluconeogenesis (fractional gluconeogenesis) was calculated using the "average" method where all hydrogens in glucose are assumed to have an equal chance of becoming labelled during gluconeogenesis (299, 300). Therefore, fractional hepatic gluconeogenesis was calculated by dividing the molar-percent enrichment of the glucose-derivative by the number of possible labelling sites and plasma D_2O enrichment (300). Fasting plasma glucose (FPG) derived from gluconeogenesis was determined by multiplying FPG by fractional gluconeogenesis. The difference between FPG derived from hepatic gluconeogenesis and total FPG was assumed to be from hepatic glycogenolysis.

4.2.11 Modelling Postprandial Insulin Kinetics

Deconvolution of plasma C-peptide concentrations, using population derived approximations of C-peptide kinetics, were used to mathematically model postprandial pre-hepatic insulin secretion rates (ISR) from fasting to 240min after consuming of a test meal (301). Postprandial insulin concentrations (I) were smoothed by cubic spline fitting and the derivative of insulin over time (∂I(t)/∂t) was calculated from the smoothed data in 5min intervals (MATLAB version R2022b, MathWorks Inc., USA). Insulin extraction and postprandial insulin clearance rates (ICR (t)) over a period (t) were calculated using a single pool model (302):

$$\text{Insulin Extraction}\ (t)\ =\ \text{ISR}(t) - (\frac{\text{dI}(t)}{\text{dt}}\ \times V)$$

$$\mathrm{ICR}(t) = \frac{\text{Insulin Extraction } (t)}{\mathrm{I}(t)}$$

where V, the distribution volume for insulin, is estimated as 141 mL/kg (303).

4.2.12 Calculations

HOMA-IR and fasting and postprandial net whole-body fat and carbohydrate oxidation rates were calculated (section 2.7).

Whole-body R_a NEFA was calculated as (304):

$$\mathrm{R}_a \text{ NEFA} = \frac{\text{Infusion Rate}}{\text{Background Corrected Plasma NEFA 272/270 TTR}}$$

4.2.13 Power Calculation

Luukkonen *et al.* (79) reported a ~50% greater increase in IHTG with SFA, compared with unsaturated FA, overfeeding. Pooling results from previous studies, the average IHTG content of our study cohorts is 3.6±1.8% (n=63 males and females, aged 45±6y, BMI 28±3 kg/m^2 (mean ± SD)). Therefore, to detect a 40% difference in IHTG between the SFA and PUFA-enriched HFD diets (power=0.80, α=0.05) 22 individuals would be required. To allow for a 15% drop-out rate and have an equal number of males and females in either group, 28 individuals were recruited. The work was planned with advice from an experienced statistician (Ruth Coleman, DTU OCDEM).

4.2.14 Statistical Analysis

All data was analysed using SPSS (V30.0.0) for Mac and figures created using Graphpad Prism (V10.9.1) Software for Mac (San Diego, California USA). Non-time series data is presented as mean ± SD if parametric or median (IQR) if non-parametric. Between group comparisons in baseline anthropometry, body composition, fasting plasma biochemistry, and changes in plasma-TG and VLDL-TG FA composition were made using an unpaired t-test

or Mann-Whitney test, as appropriate. A Fisher's exact test was used to compare data reported as counts. A paired t-test or Wilcoxon test was used to compare within group changes in macronutrient consumption during the dietary intervention, cardiac parameters, and sex differences in body composition and fasting plasma biochemistry in response to the dietary intervention. A two-way analysis of covariance (ANCOVA), where baseline and post-HFD values were matched by participant, and baseline values for each parameter were used as a covariate in the analysis of that parameter, was performed to compare the effect of dietary FA composition on IHTG accumulation, body composition, fasting plasma biochemistry, hepatic glucose production, blood pressures, and aortic distensibility before and after the dietary intervention. A Sidak's post–hoc test was performed if a significant (p<0.05) interaction effect was observed. Within diet comparisons of time-series plasma biochemistry, insulin kinetics, and tracer data, presented as mean ± SD if parametric or geometric mean ± 95% confidence interval if non-parametric, was analysed using a mixed-effects model with baseline and post-HFD values matched by participant. Between diet comparisons of time-series plasma biochemistry, insulin kinetics, and tracer data, presented as mean ± SD if parametric or median ± IQR if nonparametric, were made by subtracting the baseline value from the post-HFD value at each time point for each participant, and analysing the change from baseline to post-HFD between diets with a mixed-effects model. Statistical significance was set at p<0.05.

4.3 Results

4.3.1 Trial Conduct

Following screening, 31 participants were randomised to consume a SFA- or PUFA-enriched HFD (Fig. 4.8). One participant was withdrawn from the SFA-enriched HFD group as they started a glucagon-like peptide-1 (GLP-1) receptor agonist in between the screening visit and experimental HFD, one participant in the PUFA-enriched HFD group withdrew from

the study as they were unable to tolerate an MRI scan, and one participant who completed the PUFA-enriched HFD was not included in the analysis as their reported alcohol intake on the food diaries exceeded the acceptable amount in Table 4.1 (Fig. 4.8).

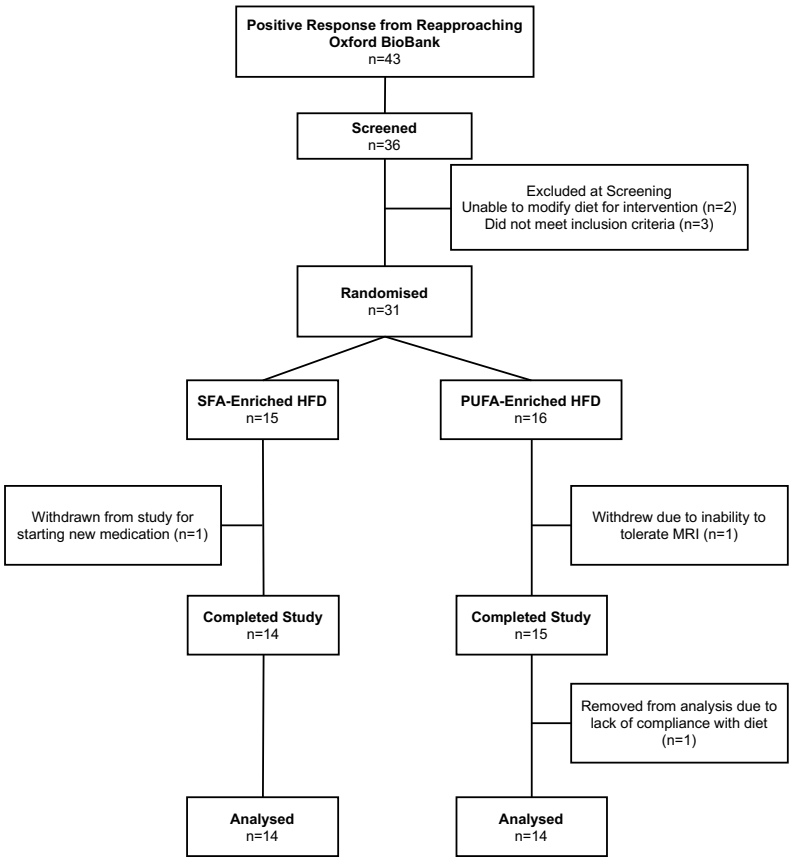

Figure 4.8. CONSORT Diagram.

4.3.2 Baseline Participant Characteristics & Plasma Biochemistry

Baseline anthropometry, four common single nucleotide polymorphisms (SNPs) associated with increased IHTG content, and fasting plasma biochemistry for the 28 participants included in analysis are shown in Table 4.2. Fourteen participants (n=7 female), aged 54 (50 – 57) years (median (IQR)), with a BMI of 28.0±4.3 kg/m^2 (mean ± SD) were analysed in the SFA-enriched HFD group, and 14 participants (n=7 female), aged 55 (50 – 59) years, with a BMI of 26.8±4.6 kg/m^2 were analysed in the PUFA-enriched HFD group. There were no baseline differences in age, BMI, body weight, fat mass, lean mass, waist-hip ratio, visceral fat, liver fat, or HOMA-IR between groups (Table 4.2). No differences in the proportion of individuals with SNPs at rs738409, rs641738, rs58542926, and rs1260326,

corresponding to mutations in *PNPLA3*, membrane-bound O-acyltransferase domain-containing protein 7 (*MBOAT7*), glucokinase regulatory protein (*GCKR*), and transmembrane 6 superfamily 2 (*TM6SF2*), respectively (82, 83, 305, 306), were observed between groups (Table 4.2). Baseline fasting plasma glucose, insulin, C-peptide, NEFA, 3OHB, TG, total-, HDL-, and non-HDL cholesterol, and apoB100 were similar between groups (Table 4.2).

Table 4.2. Baseline Participant Characteristics & Fasting Plasma Biochemistry

	***SFA*-Enriched Diet**	***PUFA*–Enriched Diet**	***p*-value**
Sex (M/F)	7/7	7/7	-
Age (years)	54 (50 – 57)	55 (50 –59)	*0.85*
BMI (kg/m^2)	28.0 ± 4.3	26.8 ± 4.6	*0.48*
Body Weight (kg)	82.6 ± 17.3	82.0 ± 15.6	*0.93*
Body Fat Mass (kg)	24.4 (20.9 – 38.9)	27.6 (17.8 – 33.2)	*0.40*
Body Lean Mass (kg)	49.9 ± 9.9	52.9 ± 11.6	*0.46*
Waist-Hip Ratio	0.89 ± 0.11	0.90 ± 0.10	*0.92*
Visceral Fat (g)	867 (309 – 1803)	700 (220 – 1844)	*0.60*
IHTG Content (%)	3.7 (2.2 – 7.1)	2.8 (1.8 – 9.1)	*0.81*
HOMA-IR	1.14 (0.85 – 1.94)	1.33 (0.68 – 2.07)	*0.59*
Genotype* [#] *(n=number)			
PNPLA3 (CC/CG/GG)	8 / 3 / 1	6 / 5 / 0	*0.52*
MBOAT7 (CC/CT/TT)	3 / 5 / 4	1 / 7 / 3	*0.64*
TM6SF2 (CC/CT/TT)	12 / 0 / 0	8 / 3 / 0	*0.09*
GCKR (CC/CT/TT)	6 / 6 / 0	6 / 3 / 2	*0.29*
Fasting Plasma Biochemistry			
Glucose (mmol/L)	5.6 ± 0.7	5.5 ± 0.5	*0.69*
Insulin (mU/L)	4.6 (3.3 – 9.8)	5.2 (2.7 – 8.1)	*0.95*
C-peptide (pmol/L) [a]	564 (463 – 780)	581 (360 – 987)	*0.81*
NEFA (µmol/L)	646 ± 172	520 ± 201	*0.08*
3OHB (µmol/L)	87 (36 – 159)	69 (27 – 110)	*0.26*
Triglyceride (mmol/L)	0.78 (0.67 – 1.20)	0.84 (0.53 – 1.64)	*0.70*
Total Cholesterol (mmol/L)	4.48 ± 0.87	4.78 ± 1.02	*0.26*
HDL-Cholesterol (mmol/L)	1.34 ± 0.43	1.40 ± 0.42	*0.71*
Non-HDL Cholesterol (mmol/L)	3.15 ± 0.78	3.38 ± 0.96	*0.48*
Apolipoprotein B100 (mmol/L)	0.76 ± 0.20	0.83 ± 0.30	*0.48*

Parametric data presented as mean ± SD, non-parametric data presented as median (IQR). Abbreviations: 3OHB, 3-hydroxybutyrate; BMI, body mass index; F, female; GCKR, glucokinase regulatory protein; HDL, high-density lipoprotein; HOMA-IR, homeostatic model assessment of insulin resistance; M, male; MBOAT7, membrane-bound O-acyltransferase domain-containing protein 7; NEFA, non-esterified fatty

acid; PNPLA3, patatin-like phospholipase domain-containing protein 3; PUFA, polyunsaturated fatty acid; SFA, saturated fatty acid; TM6SF2, transmembrane 6 superfamily 2; *p*-value represents output from unpaired student's t-test if data parametric, from Mann-Whitney test if data non-parametric, or from Fisher's exact test if data reported as counts, comparing values at baseline between groups. n=14 SFA, n=14 unless otherwise indicated. [a] n=13 SFA, n=13 PUFA, [#]n=12 SFA, n=11 PUFA.

Baseline postprandial plasma biochemistry was similar between groups with no group*time interaction effect for glucose (p=0.40), insulin (p=0.41), TG (p=0.71), NEFA (p=0.86), 3OHB (p=0.37), chylomicron-TG (p=0.76), and VLDL-TG (p=0.77) excursions, each metabolite changed with time (all p<0.01, effect of time; Fig. 4.9A-G) and followed a similar profile in both groups after consuming the mixed test meal. Plasma glucose and insulin increased following consumption of the test meal, peaking at 30-60mins before returning to fasting levels at ~180min (Fig. 4.9A-B). There was a trend for a greater postprandial plasma glucose excursion in the group randomised to consume a SFA-enriched HFD compared with a PUFA-enriched HFD (p=0.07, effect of group, Fig. 4.9A). After consuming the mixed test meal, plasma NEFA and 3OHB decreased from fasting, reaching a nadir at ~90min, before increasing for the remainder of the study day (Fig. 4.9D-E). Plasma-TG, chylomicron-TG, and VLDL-TG all increased following consumption of the mixed test meal, peaking at ~240-300min in both groups (Fig. 4.9C, F, G). Baseline fasting VLDL-TG FA composition was ~42% oleate (18:1*n*-9), ~25% palmitate (16:0), ~17% linoleate (18:2*n*-6), ~4% palmitoleate (16:*n*-7), and ~2.5% stearate (18:0) in both groups (Fig. 4.9H).

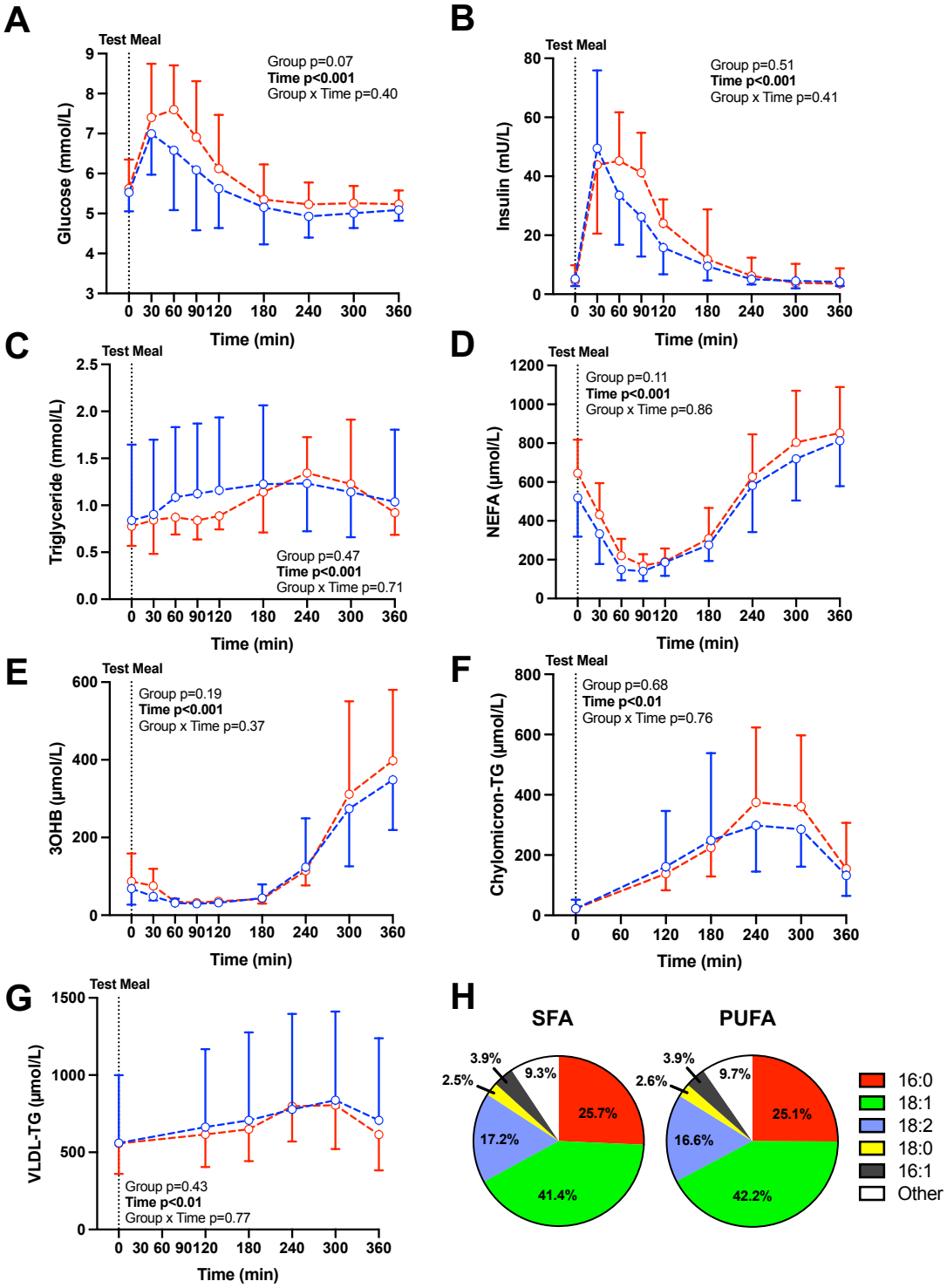

Figure 4.9. Baseline plasma concentrations of (A) glucose, (B) insulin, (C) triglyceride (TG), (D) non-esterified fatty acid (NEFA), (E) 3-hydroxybutyrate (3OHB), (F) chylomicron-TG, and (G) very-low density lipoprotein (VLDL)-TG following consumption a standardised mixed test meal, and (H) fasting VLDL-TG FA composition. Plasma samples were collected at fasting and every (A-E) 30-60min or (F-G) 60min from 2h for 6h and analysed by a mixed-effects model matching each participant pre- to post-high fat diet (HFD). Data presented as (A, D) mean ± SD, (B, C, E-G) geometric mean ± 95% confidence interval, or (H) mean; n=14 SFA; n=14 PUFA; red indicates baseline values pre-SFA-enriched HFD; blue indicates baseline values pre-PUFA-enriched HFD.

4.3.3 Dietary Intervention

During the 7-day standardisation diet (i.e. baseline) prior to the experimental diet, the group randomised to consume a SFA-enriched HFD had greater self-reported intake of carbohydrates (%TE) than the group randomised to consume a PUFA-enriched HFD (Table 4.3). Otherwise, there were no differences in baseline self-reported dietary intake between groups (Table 4.3). In both groups, median HFD duration was 21 days, with a range of 13–24 days (Table 4.3). One participant in the PUFA-enriched HFD group and two participants in the SFA-enriched HFD group consumed the diet for 13 days due to restrictions during the COVID-19 pandemic. Self-reported TE intake did not change during either HFD (Table 4.3). Participants consuming a SFA-enriched HFD reported to consume 51.0 (48.2 – 52.6) %TE from total fat and 24.0 (22.5 – 27.8) %TE from SFA during the dietary intervention, this was greater than the self-reported consumption of 35.9 (33.0 – 39.0) %TE from total fat and 12.1 (10.4 – 13.9) %TE from SFA at baseline (all $p<0.001$; Table 4.3). Self-reported consumption of carbohydrates in participants consuming the SFA-enriched HFD decreased to 32.4 (29.9 – 35.4) %TE from 45.4 (43.6 – 48.2) %TE at baseline ($p<0.001$; Table 4.3). During a SFA-enriched HFD, compared with baseline, there was a trend for participants to report consuming less omega-3 and omega-6 PUFAs ($p=0.09$) and no difference in self-reported MUFA, PUFA, or protein consumption (Table 4.3). Participants consuming a PUFA-enriched HFD reported consuming 51.9 (48.6 – 56.6) %TE from total fat, 16.0 (13.0 – 20.5) %TE from total PUFA, 2.6 (1.5 – 3.2) %TE from omega-3 PUFA, and 11.8 (8.8 – 16.1) %TE from omega-6 PUFAs during the dietary intervention; all of which were greater than at baseline where participants reported consuming 38.1 (34.4 – 42.2) %TE from total fat, 3.4 (2.6 – 5.5) %TE from total PUFA, 0.5 (0.2 – 1.0) %TE from omega-3 PUFA, and 2.3 (0.5 – 3.1) %TE from omega-6 PUFAs (all $p<0.001$; Table 4.3). Self-reported consumption of carbohydrates and SFA in participants consuming a PUFA-enriched HFD decreased to 30.4 (26.9 – 35.3) %TE and 9.5

(9.1 – 11.1) %TE during the dietary intervention from 41.1 (37.4 – 44.1) %TE and 12.9 (11.8 – 13.7) %TE at baseline, respectively (all $p<0.001$; Table 4.3). There was a trend for participants to report consuming more MUFAs ($p=0.09$) and less protein ($p=0.07$) during a PUFA-enriched HFD compared with baseline (Table 4.3).

Table 4.3. Dietary Intervention

	***SFA*-Enriched HFD**			***PUFA*–Enriched HFD**			***Comparison of Diets at Baseline (p-value)***
	Baseline	**HFD**	***Effect of Diet* (*p*-value)**	**Baseline**	**HFD**	***Effect of Diet* (*p*-value)**	
Diet Duration (days)	-	21 (13 – 24) [a]	-	-	21 (13 – 24) [a]	-	-
Energy (kcal)	2116 ± 460	2312 ± 627	*0.10*	2149 ± 534	2281 ± 516	*0.34*	*0.80*
Carbohydrates (%TE)	45.4 (43.6 – 48.2)	32.4 (29.9 – 35.4)	***<0.001***	41.1 (37.4 – 44.1)	30.4 (26.9 – 35.3)	***<0.001***	***0.007***
Fat (%TE)	35.9 (33.0 – 39.0)	51.0 (48.2 – 52.6)	***<0.001***	38.1 (34.4 – 42.2)	51.9 (48.6 – 56.6)	***<0.001***	*0.35*
SFA (%TE)	12.1 (10.4 – 13.9)	24.0 (22.5 – 27.8)	***<0.001***	12.9 (11.8 – 13.7)	9.5 (9.1 – 11.1)	***<0.001***	*0.60*
MUFA (%TE)	9.0 (6.4 – 13.2)	10.0 (7.0 – 13.9)	*0.17*	8.0 (5.8 – 11.1)	10.7 (9.7 – 11.6)	*0.091*	*0.32*
PUFA (%TE)	4.4 (2.4 – 5.5)	3.2 (1.9 – 4.1)	*0.12*	3.4 (2.6 – 5.5)	16.0 (13.0 – 20.5)	***<0.001***	*0.63*
Omega-3 PUFA (%TE)	0.4 (0.1 – 1.1)	0.2 (0.2 – 0.3)	*0.091*	0.5 (0.2 – 1.0)	2.6 (1.5 – 3.2)	***<0.001***	*0.62*
Omega-6 PUFA (%TE)	2.2 (1.4 – 4.2)	1.3 (0.9 – 1.8)	*0.094*	2.3 (0.5 – 3.1)	11.8 (8.8 – 16.1)	***<0.001***	*0.51*
Protein (%TE)	15.7 ± 3.1	15.2 ± 2.5	*0.63*	16.7 ± 2.8	15.3 ± 2.3	*0.072*	*0.38*

Parametric data presented as mean ± SD, non-parametric data as median (IQR), or as median (range) where indicated with [a]. Abbreviations: HFD, high-fat diet; kcal, kilocalories; MUFA, monounsaturated fatty acid; ω, omega; PUFA, polyunsaturated fatty acid; %TE, percent total energy; SFA, saturated fatty acid; effect of diet *p*-value represents output from within group comparisons made using student's paired t-test if data parametric or Wilcoxon test if data non-parametric, comparison of diets at baseline *p*-value represents output from between group comparison made using student's unpaired t-test if data parametric or Mann-Whitney test if data non-parametric; n=14 for each diet.

4.3.4 Biomarkers of Dietary FA Intake

The change in fasting plasma-TG FA composition was analysed as an objective biomarker of dietary FA intake. There was a relative increase in palmitate (16:0) and decrease in linoleate (18:2*n*-6) in plasma-TG after consuming a SFA-enriched HFD compared with baseline (both $p<0.05$, Fig. 4.10A). In contrast, there was a relative increase in linoleate (18:2*n*-6; $p<0.001$), and decrease in oleate (18:1*n*-9; $p<0.05$), palmitoleate (16:1*n*-7; $p<0.05$), palmitate (16:0; $p<0.001$), and myristate (14:0; $p<0.01$) in fasting plasma-TG after consuming a PUFA-enriched HFD compared with baseline (Fig. 4.10A). Compared with consuming a PUFA-enriched HFD, consuming a SFA-enriched, increased the proportion of stearate ($p<0.05$), palmitoleate ($p<0.01$), palmitate ($p<0.001$), and myristate ($p<0.05$) in fasting plasma-TG, while consuming a PUFA-enriched HFD, compared with SFA-enriched HFD, increased the proportion of linoleate ($p<0.001$) in fasting plasma-TG (Fig. 4.10A).

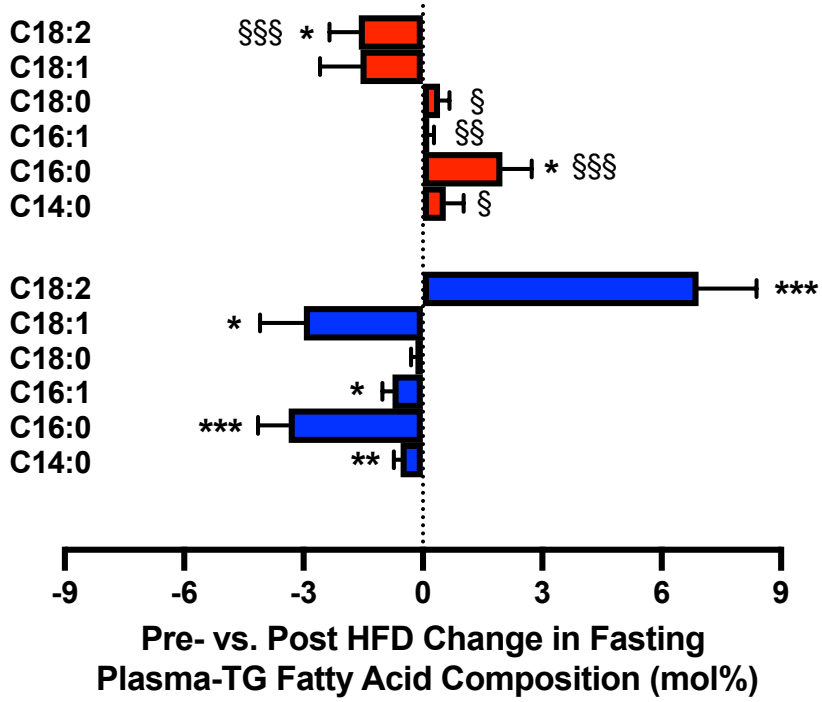

Figure 4.10 The change from baseline to post-high fat diet (HFD) in fasting plasma-triglyceride (TG) fatty acid composition after consuming a SFA- (red) or PUFA- (blue) enriched HFD. Within group analysis performed with a paired t-test; between group analysis performed with an unpaired t-test. Data presented as mean ± SD, (A) n=13 SFA; n=14 PUFA; (B) n=11 SFA; n=13 PUFA. * $p<0.05$, ** $p<0.01$, *** $p<0.001$ comparing the change from baseline to post-HFD within group, § $p<0.05$, §§ $p<0.01$, §§§ $p<0.001$ comparing the change from baseline to post-HFD between groups.

4.3.5 Dietary FA Composition Modulates Liver Fat Content Independent of Body Weight

Post-HFD body weight was within 1kg of baseline body weight in nearly every participant, confirming the dietary intervention was weight neutral (Fig. 4.11A). Similarly, there was no change in BMI, body fat mass, body lean mass, and visceral fat after either HFD compared with baseline (Table 4.4). Despite no change in body weight or body composition, dietary fat composition led to divergent effects on IHTG accumulation with a significant diet*time interaction effect (p<0.05; Fig. 4.11B). Compared with baseline, consuming a PUFA-enriched HFD reduced IHTG content by 19% (p<0.05), while consuming a SFA-enriched HFD tended to increase IHTG content by 17% (p=0.09; Fig. 4.11B). At the end of the dietary intervention, relative and absolute IHTG content was lower in the group which consumed a PUFA-enriched HFD compared with the group which consumed a SFA-enriched HFD (p<0.05; Fig. 4.11B and p<0.01; Fig. 4.11C).

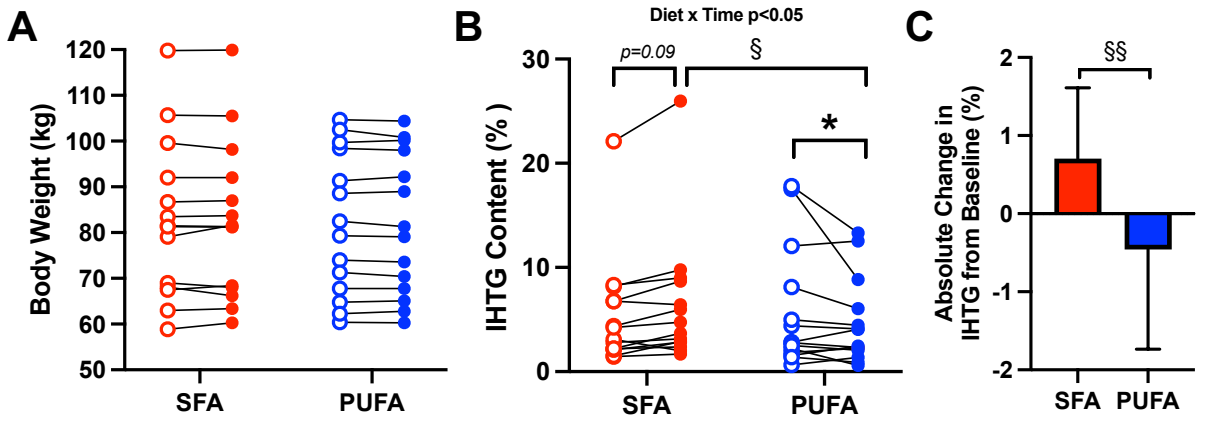

Figure 4.11. Dietary fat composition induces divergent effects on intrahepatic triglyceride (IHTG) content independent of changes in body weight. (A) Body weight and (B) IHTG content were measured before (empty circles) and after (filled circles) consuming a SFA-enriched (red) or PUFA-enriched (blue) HFD. (C) The absolute change in IHTG content after consuming a SFA-enriched (red) or PUFA-enriched (blue) HFD. Abbreviations: HFD, high fat diet; SFA, saturated fatty acid; PUFA, polyunsaturated fatty acid. Between group p-value represents output from 2-way ANCOVA where baseline and post-HFD values were matched by participant, and baseline values for each parameter were used as a covariate in the analysis of that parameter; if a significant interaction effect was present (diet*time p<0.05), a Sidak post-hoc test was performed with significance set at p<0.05 (A-B) data presented as individual points; (C) data presented as median ± IQR; n=14 SFA; n=14 PUFA; * p<0.05 comparing the change from baseline to post-HFD within group, § p<0.05, §§ p<0.01 indicates comparison between groups.

Table 4.4. Effects of Dietary Fat Composition on Body Composition, Fasting Plasma Biochemistry, & Substrate Oxidation Rates

	***SFA*-Enriched HFD**			***PUFA*–Enriched HFD**			***Between Group p*-value**
	Baseline	**Post-HFD**	***Within Group p*-value**	**Baseline**	**Post-HFD**	***Within Group p*-value**	
Body Composition							
BMI (kg/m^2)	28.0 ± 4.3	28.1 ± 4.3	-	26.8 ± 4.6	26.7 ± 4.5	-	*0.26*
Body Fat Mass (kg)	24.4 (20.9 – 38.9)	23.6 (20.5 – 38.6)	-	27.6 (17.8 – 33.2)	27.3 (17.9 – 32.1)	-	*0.90*
Body Lean Mass (kg)	49.9 ± 9.9	50.1 ± 9.9	-	52.9 ± 11.6	53.0 ± 11.7	-	*0.78*
Visceral Fat (g)	867 (309 – 1803)	883 (301 – 1922)	-	700 (220 – 1844)	706 (232 – 1742)	-	*0.87*
Fasting Plasma Biochemistry							
Glucose (mmol/L)	5.7 (5.3 – 6.0)	5.5 (5.3 – 5.8)	-	5.5 (5.2 – 5.9)	5.4 (5.1 – 5.7)	-	*0.87*
Insulin (mU/L)	4.6 (3.3 – 9.8)	5.3 (3.4 – 11.1)	*0.067*	5.2 (2.7 – 8.1)	4.8 (2.9 – 7.0)	*0.30*	***0.046***
C-peptide (pmol/L)	564 (463 – 780)	686 (580 – 764)	-	581 (360 – 987)	727 (393 – 975)	-	*0.66*
HOMA-IR	1.14 (0.85 – 1.94)	1.44 (0.85 – 2.74)	-	1.33 (0.68 – 2.07)	1.19 (0.68 – 1.73)	-	*0.09*
NEFA (µmol/L)	646 ± 172	503 ± 291	***<0.001***	520 ± 201	515 ± 232	*0.90*	***0.01***
3OHB (µmol/L)	87 (36 – 159)	87 (37 – 162)	-	69 (27 – 110)	73 (41 – 122)	-	*0.26*
Triglyceride (mmol/L)	0.78 (0.67 – 1.20)	0.84 (0.59 – 1.45)	-	0.84 (0.53 – 1.64)	0.76 (0.52 – 1.11)	-	*0.09*
Total Cholesterol (mmol/L)	4.48 ± 0.87	4.83 ± 0.69	***0.018***	4.78 ± 1.12	4.33 ± 0.97	***0.002***	***<0.001***
HDL-Cholesterol (mmol/L)	1.34 ± 0.43	1.49 ± 0.45	***0.006***	1.40 ± 0.49	1.39 ± 0.32	*0.94*	***0.038***
Non-HDL Cholesterol (mmol/L)	3.15 ± 0.78	3.34 ± 0.69	*0.14*	3.38 ± 0.98	2.94 ± 0.93	***<0.001***	***<0.001***
ApoB (mmol/L)	0.76 ± 0.20	0.81 ± 0.20	*0.16*	0.83 ± 0.34	0.75 ± 0.24	***0.009***	***0.006***

Net Carbohydrate Oxidation Rates							
Fasting (g/min) [#]	0.11 ± 0.06	0.12 ± 0.06	-	0.12 ± 0.07	0.13 ± 0.07	-	*0.85*
120 min (g/min) [#]	0.16 ± 0.06	0.16 ± 0.08	-	0.16 ± 0.06	0.17 ± 0.07	-	*0.86*
Net Fat Oxidation Rates							
Fasting (g/min) [#]	0.088 ± 0.012	0.082 ± 0.025	-	0.088 ± 0.026	0.092 ± 0.035	-	0.40
120 min (g/min) [#]	0.076 ± 0.012	0.080 ± 0.028	-	0.083 ± 0.025	0.092 ± 0.042	-	0.63

Parametric data presented as mean ± SD, non-parametric data presented as median (IQR). Abbreviations: 3OHB, 3-hydroxybutyrate; BMI, body mass index; HDL, high-density lipoprotein; HOMA-IR, homeostatic model assessment of insulin resistance; NEFA, non-esterified fatty acid; PUFA, polyunsaturated fatty acid; SFA, saturated fatty acid; between group *p*-value represents output from 2-way ANCOVA where baseline and post-HFD values were matched by participant, and baseline values for each parameter were used as a covariate in the analysis of that parameter; if a significant interaction effect was present (between group $p<0.05$), within group comparisons were made using a Sidak post-hoc test with significance set at $p<0.05$. n=14 SFA, n=14 PUFA unless otherwise indicated; [#]n=13 SFA, n=14 PUFA.

4.3.6 Fasting Plasma Biochemistry

Compared with baseline, consuming a SFA- or PUFA-enriched HFD led to divergent effects on fasting plasma biochemistry, with diet*time interaction effects for fasting plasma insulin ($p<0.05$), NEFA ($p<0.01$), total cholesterol ($p<0.001$), HDL-cholesterol ($p<0.05$), non-HDL cholesterol ($p<0.001$), and apoB ($p<0.01$; Table 4.4). Consuming a PUFA-enriched HFD reduced fasting total cholesterol ($p<0.01$), non-HDL cholesterol ($p<0.001$), and apolipoprotein B ($p<0.01$), while consuming a SFA-enriched HFD increased fasting total cholesterol ($p<0.05$) and HDL-cholesterol ($p<0.01$), reduced fasting NEFA ($p<0.001$), and showed a trend to increase fasting plasma insulin ($p=0.06$; Table 4.4). There was a trend for dietary fat composition to differentially modulate fasting plasma TG ($p=0.09$) and HOMA-IR ($p=0.09$), and no effect of dietary fat composition on fasting plasma glucose, C-peptide, and 3OHB (Table 4.4).

4.3.7 Net Substrate Oxidation Rates

Indirect calorimetry was measured on each study day at fasting and 120min following consumption of the mixed test meal and used to calculate net substrate oxidation rates. Net carbohydrate and fat oxidation rates at fasting and 120min after consuming a SFA- and PUFA-enriched HFD were similar to baseline (Table 4.4).

4.3.8 Postprandial Plasma Biochemistry

On the postprandial study day before and after consuming a SFA-enriched HFD, plasma glucose, insulin, TG, NEFA, 3OHB, and chylomicron-TG, all changed with time after consuming the mixed test meal (all $p<0.05$, effect of time; Fig. 4.12A-F,). There was a trend for a diet*time interaction effect for postprandial plasma glucose ($p=0.09$; Fig. 4.12A) and no diet*time interaction effect for postprandial plasma insulin (Fig. 4.12B). On the baseline study day, plasma glucose and insulin increased after consuming the test meal, peaked at 60min, and

returned to fasting levels by ~180-240mins (Fig. 4.12A-B). On the study day after consuming a SFA-enriched HFD, plasma glucose and insulin increased after consuming the test meal, with a biphasic excursion peaking at ~30min and ~120min, before returning to fasting levels by ~180-240mins (Fig. 4.12A-B). There was a diet*time interaction effect for postprandial plasma NEFA (p<0.05; Fig. 4.12D), where, at fasting (p<0.01), 180min (p=0.08), 240min (p<0.05), and 300min (p<0.01) after consuming the test meal, plasma NEFA concentrations were lower after consuming a SFA-enriched HFD compared with baseline, and at 90min after consuming the test meal, plasma NEFA concentrations were greater, after consuming a SFA-enriched HFD compared with baseline (p<0.05; Fig. 4.12D). Overall, there was a lower postprandial plasma NEFA excursion after the consuming a SFA-enriched HFD compared with baseline (p<0.01, effect of diet, Fig. 4.12D). Plasma-TG, 3OHB, and chylomicron-TG displayed similar postprandial excursions following test meal consumption at baseline and after a SFA-enriched HFD (Fig. 4.12C, E, F).

On the study day before and after consuming a PUFA-enriched HFD, plasma glucose, insulin, TG, NEFA, 3OHB, and chylomicron-TG all changed with time, following a similar excursion after a PUFA-enriched HFD compared with baseline (all p<0.05, effect of time; Fig. 4.13A-F). Plasma glucose and insulin increased following consumption of the test meal, peaking at 30-60mins before returning to fasting levels at ~180min (Fig. 4.13A-B). Plasma NEFA and 3OHB decreased after consuming the mixed test meal, with the nadir occurring at ~90min, before increasing for the remainder of the study day (Fig. 4.13D, E). Plasma-TG and chylomicron-TG increased following consumption of the mixed test meal, peaking at ~240-300min (Fig. 4.13C, F).

To assess the between-diet effects of a SFA- compared with PUFA-enriched HFD on time series data, such as postprandial plasma biochemistry, the baseline value was subtracted from the post-HFD value at each time point for each participant and the change from baseline

to post-HFD was compared between diets. The change in plasma glucose from baseline to post-HFD differed between diets (p<0.05 diet*time; Fig. 4.14A), where at 60 min after consuming the mixed test meal, consumption of a SFA-enriched HFD led to a decreased postprandial glucose excursion, while consumption of a PUFA-enriched HFD led to an increased postprandial glucose excursion compared with the respective baselines (Fig. 4.14A). There was a diet*time interaction effect for the change in plasma TG from baseline to post-HFD (p<0.05 diet*time; Fig. 4.14C); at fasting (p<0.05) and 60min (p=0.06), 90min (p<0.05), and 120min (p=0.08) after consuming the mixed test meal, consumption of a SFA-enriched HFD led to a greater postprandial TG excursion while consumption of a PUFA-enriched HFD led to a lower postprandial TG excursion compared with the respective baselines (Fig. 4.14C). There was no diet*time interaction effect for the change from baseline to post-HFD in plasma insulin (p=0.23), NEFA (p=0.21), 3OHB (p=0.50), and chylomicron-TG (p=0.19) (Fig. 4.14B, D-F). For the postprandial NEFA excursion, the change from baseline to post-HFD varied with time over the postprandial period (p<0.05, effect of time; Fig. 4.14D).

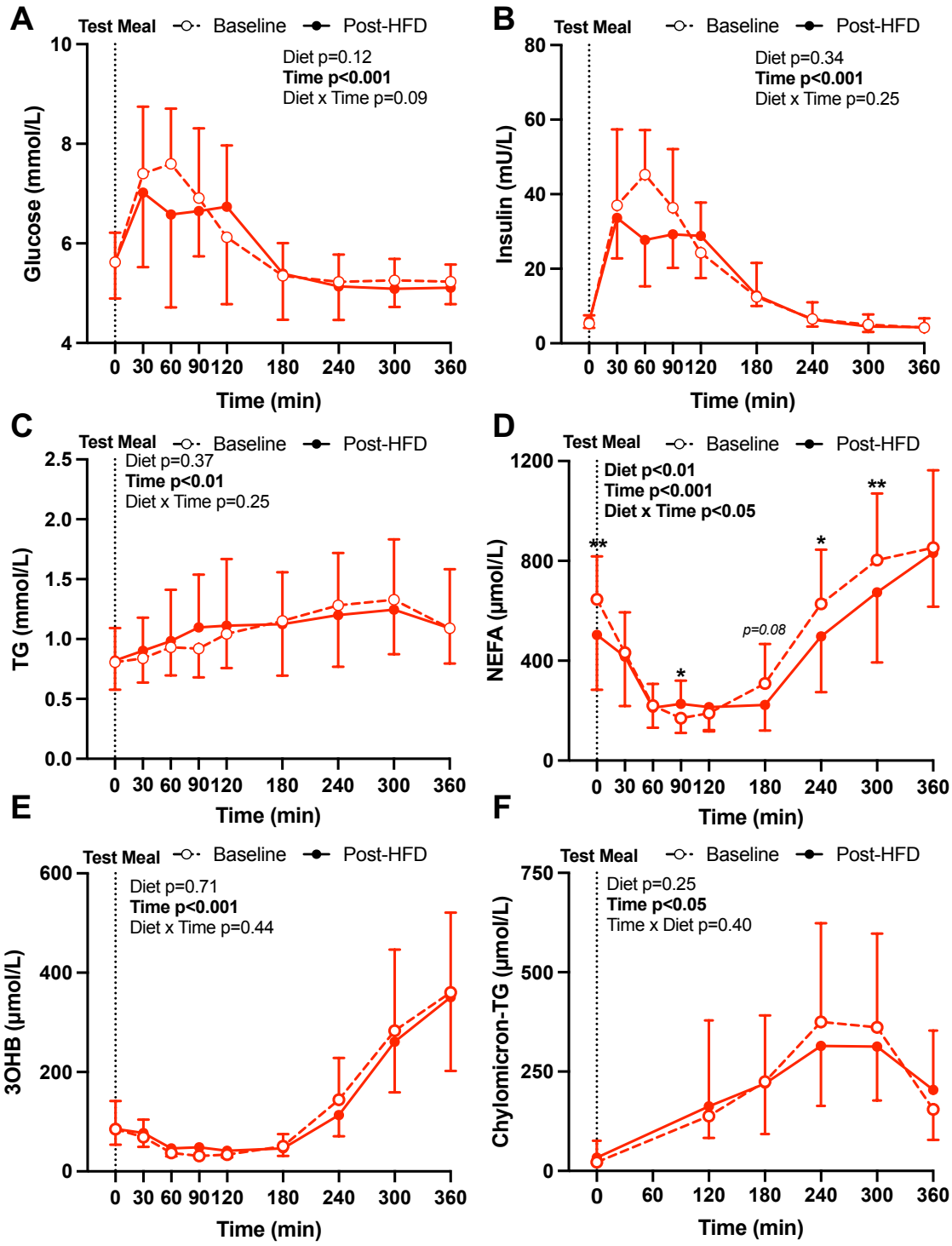

Figure 4.12. Plasma concentrations of (A) glucose, (B) insulin, (C) triglyceride (TG), (D) non-esterified fatty acid (NEFA), (E) 3-hydroxybutyrate (3OHB), and (F) chylomicron-TG following consumption a standardised mixed test meal before and after consuming a SFA-enriched HFD. Plasma samples were collected at fasting and every (A-E) 30-60min or (F) 60min from 120min for 6h and analysed by a mixed-effects model matching each participant pre- to post-HFD. Abbreviations: HFD, high fat diet; SFA, saturated fatty acid. Data presented as (A, D) mean ± SD, (B, C, E, F) geometric mean ± 95% confidence interval; n=14 SFA; n=14 PUFA; empty points (○) with hashed lines indicate baseline study visit, filled points (•) with solid lines indicate post-SFA-enriched HFD visit. * p<0.05, ** p<0.01 comparing the post-HFD value to the respective baseline value within group.

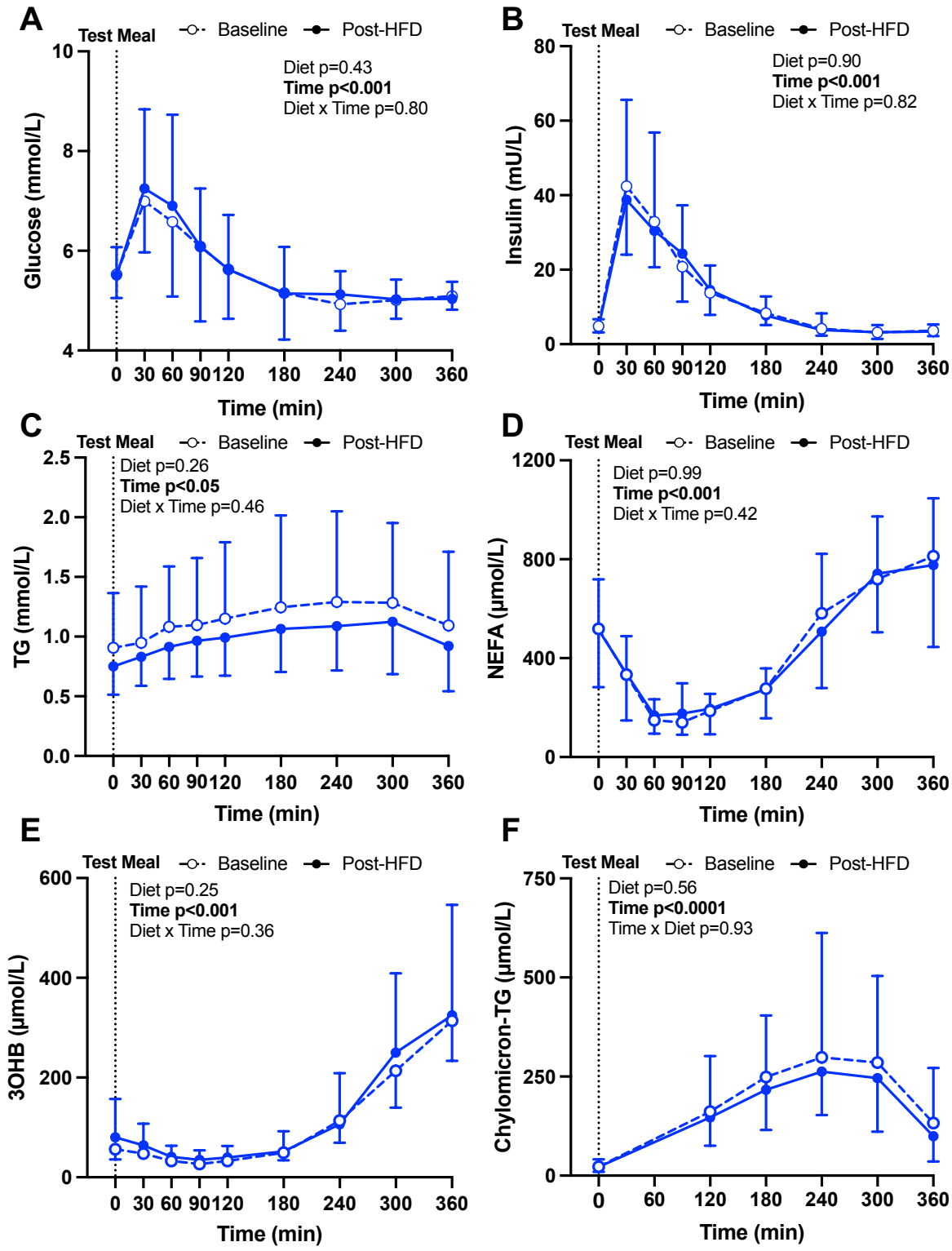

Figure 4.13. Plasma concentrations of (A) glucose, (B) insulin, (C) triglyceride (TG), (D) non-esterified fatty acid (NEFA), (E) 3-hydroxybutyrate (3OHB), and (F) chylomicron-TG following consumption a standardised mixed test meal before and after consuming a PUFA-enriched HFD. Plasma samples were collected at fasting and every (A-E) 30-60min or (F) 60min from 120min for 6h, and analysed by a mixed-effects model matching each participant pre- to post-HFD. Abbreviations: HFD, high fat diet; PUFA, polyunsaturated fatty acid. Data presented as (A, D) mean ± SD, (B, C, E, F) geometric mean ± 95% confidence interval; n=14 SFA; n=14 PUFA; empty points (○) with hashed lines indicate baseline study visit, filled points (•) with solid lines indicate post-SFA-enriched HFD visit.

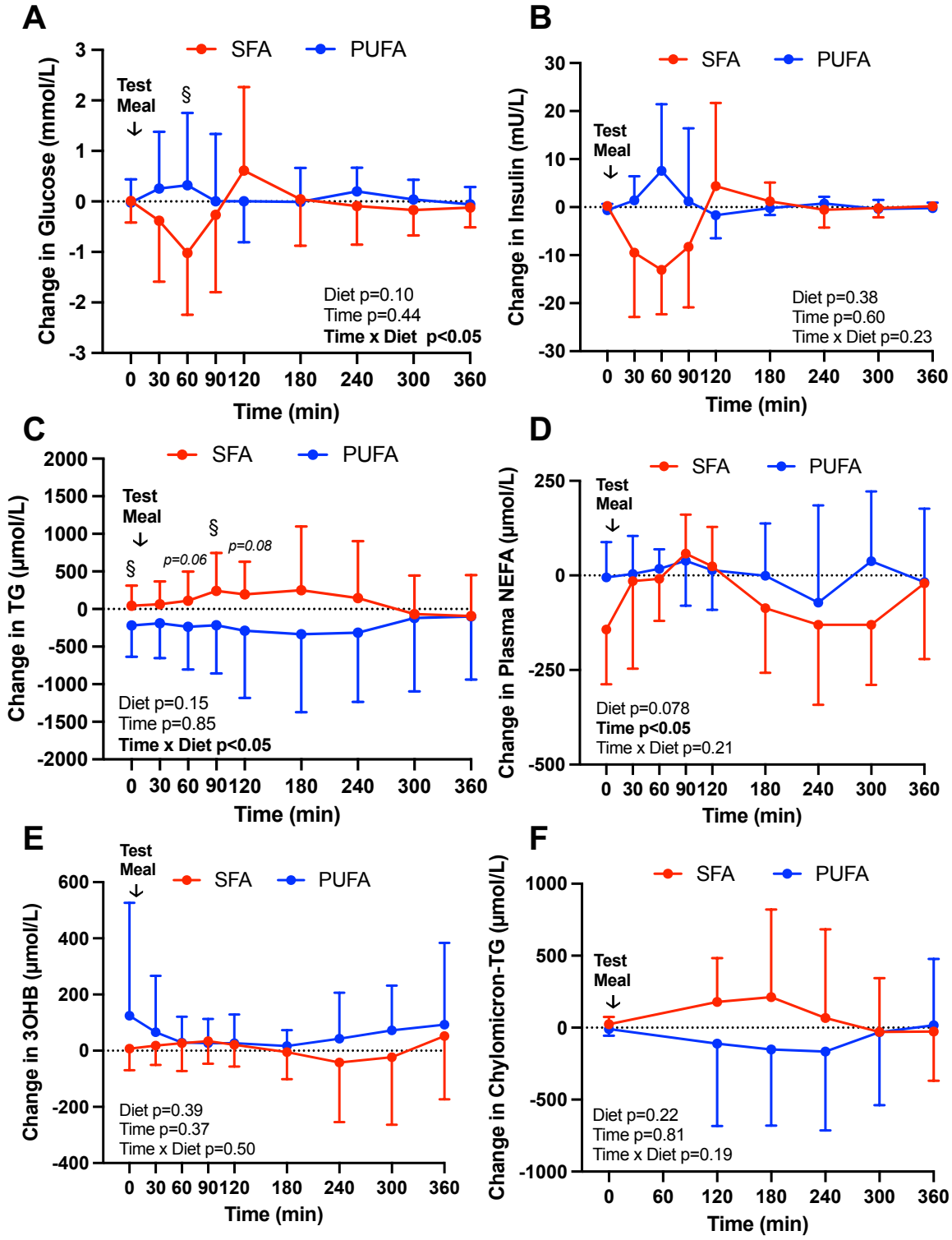

Figure 4.14. Change from baseline to post-HFD of plasma (A) glucose, (B) insulin, (C) triglyceride (TG), (D) non-esterified fatty acid (NEFA), (E) 3-hydroxybutyrate (3OHB), and (F) chylomicron-TG following consumption a standardised mixed test meal after following a SFA-enriched (red) or PUFA-enriched HFD (blue). The change from baseline to post-HFD was calculated for each participant at each time point, and the change from baseline between diets analysed by a mixed-effects model. Abbreviations: HFD, high fat diet; SFA, saturated fatty acid; PUFA, polyunsaturated fatty acid. Data presented as (A, D) mean ± SD or (B, C, E, F) median ± IQR; n=14 SFA; n=14 PUFA; § p<0.05 comparing the change from baseline to post-HFD between groups.

4.3.9 Fasting Hepatic Glucose Production

To explore if dietary FA composition modulates the relative contribution of hepatic gluconeogenesis and glycogenolysis to fasting plasma glucose, the proportion of newly synthesised glucose in fasting plasma glucose was measured before and after consumption of a SFA- or PUFA-enriched HFD. Dietary FA composition tended to induce divergent effects on markers of fasting gluconeogenesis with notable inter-person changes. There were trends for a diet*pre-/post-HFD interaction effect for fractional gluconeogenesis (p=0.07) and absolute amount of glucose derived from gluconeogenesis (p=0.06) (Fig. 4.15A-B) where consuming a SFA-enriched HFD may increase, while consuming a PUFA-enriched HFD may decrease, fractional gluconeogenesis and the amount of glucose derived from gluconeogenesis compared with baseline (Fig. 4.15A-B). There was no diet*pre-/post-HFD interaction for the effect of dietary FA composition on the absolute amount of glucose derived from hepatic glycogenolysis (Fig. 4.15C).

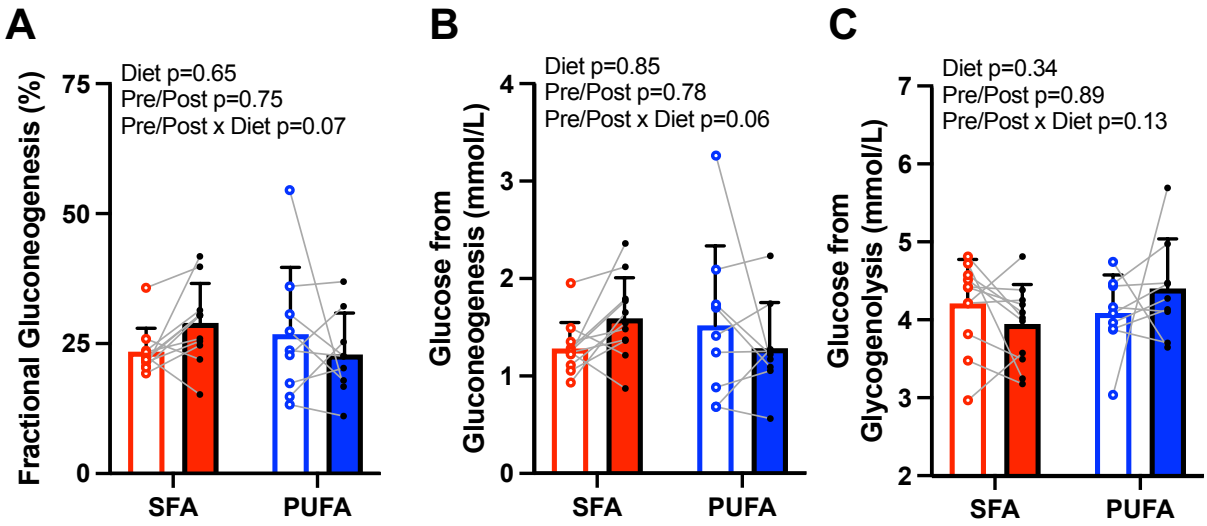

Figure 4.15. (A) Percent of fasting glucose synthesised from gluconeogenesis, and the concentration of fasting plasma glucose derived from (B) gluconeogenesis and (C) glycogenolysis before (empty bars) and after (filled bars) consuming a SFA-enriched HFD (red) or PUFA-enriched HFD (blue). Parameters were analysed by a 2-way ANCOVA with baseline-values as covariates and matching each participant pre- to post-HFD as appropriate. Abbreviations: HFD, high fat diet; SFA, saturated fatty acid; PUFA, polyunsaturated fatty acid. Data presented as (A-C) mean ± SD; n=11 SFA; n=9 PUFA.

4.3.10 Postprandial Insulin Kinetics

Following consumption of the mixed test meal, pre-hepatic ISR increased on each study day, peaking at ~30-60mins, before returning to fasting levels at ~240min (p<0.001 effect of time; Fig. 4.16A-B). Compared with the baseline study day, postprandial ISR was greater after consuming a PUFA-enriched HFD (p<0.05 effect of diet; Fig. 4.16B) and tended to be greater after consuming a SFA-enriched HFD (p=0.07 effect of diet; Fig. 4.16A). No diet*time interaction effect was observed for ISR after consuming either HFD compared with the respective baseline study day (Fig. 4.16A-B). However, the change in ISR from baseline to post-HFD differed between diets, where consuming a PUFA-enriched HFD induced a greater increase in ISR compared with consuming a SFA-enriched HFD (p<0.05, diet*time; Fig. 4.16C). On each study day, ICR sharply decreased after consuming the mixed test meal, reaching a nadir at ~30min, before gradually returning to fasting levels at ~240min (p<0.001 effect of time; Fig. 4.16D-E). Consuming a SFA- or PUFA-enriched HFD increased postprandial ICR compared with the baseline study visit (both p<0.05 effect of diet; Fig. 4.16D-E), and there was a trend for a diet*time interaction effect for ICR after consuming a SFA-enriched HFD (p=0.08, diet*time; Fig. 4.16D) and PUFA-enriched HFD (p=0.06, diet*time; Fig. 4.16E). The change in ICR from baseline to post-HFD did not differ between diets (p=0.56, diet*time; Fig. 4.16F), but did vary with time over the postprandial period (p<0.05 effect of time; Fig. 4.16F). Hepatic insulin extraction following a similar postprandial profile to ISR (both p<0.001 effect of time; Fig. 4.16G-H) and was greater after consuming both SFA- and PUFA-enriched HFD compared with the respective baseline study day (both p<0.05 effect of diet; Fig. 4.16G-H). However, there was no diet*time interaction effect for hepatic insulin extraction after consuming either HFD (Fig. 4.16G-H), and the change in insulin extraction from baseline to post-HFD did not differ between diets (p=0.30 diet*time; Fig. 4.16I). This data suggests that dietary FA composition induces divergent effects on ISR, with the

consumption of a PUFA-enriched HFD leading to a greater postprandial ISR compared with the consumption of a SFA-enriched HFD.

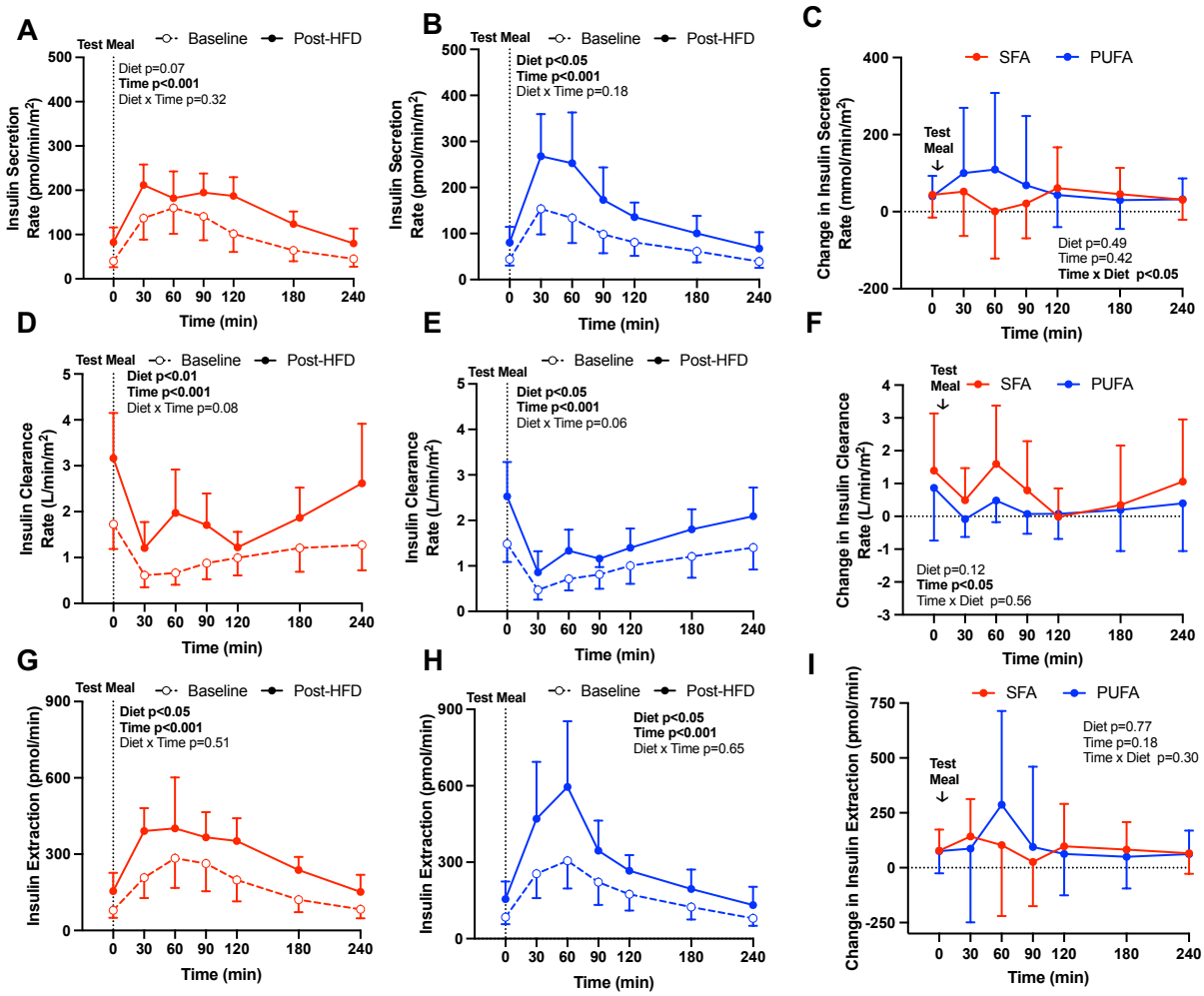

Figure 4.16. Postprandial plasma insulin kinetics. Following consumption of a standardised mixed test meal before and after consuming a (A, D, G) SFA- or (B, E, H) PUFA-enriched HFD, plasma insulin and C-peptide were measured at fasting and every 30-60min for 4h to mathematically model (A-B) pre-hepatic plasma insulin secretion rate, (D-E) insulin clearance rate, and (G-H) insulin extraction. (C, F, I) The change from baseline to post-HFD of (C) pre-hepatic plasma insulin secretion rate, (F) insulin clearance rate, and (I) insulin extraction after consuming a SFA- or PUFA-enriched HFD. Parameters were analysed by a mixed-effects model matching each participant pre- to post-HFD as appropriate. Abbreviations: HFD, high fat diet; SFA, saturated fatty acid; PUFA, polyunsaturated fatty acid. Data presented as (A-B, D-E, G-H) geometric mean ± 95% confidence interval; (C, F, I) mean ± SD; n=13 SFA; n=13 PUFA; empty points (○) with hashed lines indicate baseline study visit, filled points (•) with solid lines indicate post-HFD visit, red indicates SFA-enriched HFD; blue indicates PUFA-enriched HFD.

4.3.11 Plasma VLDL–TG

Over the course of each study day, VLDL-TG, indicated by the S_f 20-400 fraction, increased in the PUFA-enriched HFD group ($p<0.05$ effect of time; Fig. 4.17B) and trended to increase in the SFA-enriched HFD group ($p=0.059$ effect of time; Fig. 4.17A), peaking ~240-

300min after consuming the mixed test meal. The change in plasma VLDL-TG from baseline to post-HFD tended to vary with time over the postprandial period (p=0.053, effect of time; Fig. 4.17C). No diet*time interaction effect was observed for the postprandial plasma VLDL-TG profile within either diet (Fig. 4.17A-B), and the change in VLDL-TG from baseline to post-HFD did not differ between diets (p=0.75; Fig. 4.17C). Average fasting VLDL-TG particle size did not change after consuming either SFA- or PUFA-enriched HFD compared with baseline or between diets (Fig. 4.17D). The change in FA composition of fasting VLDL-TG was measured as a biomarker of intrahepatic TG FA composition. There was a relative increase in palmitate (16:0; p<0.01) and stearate (18:0; p<0.05) and decrease in linoleate (18:2n-6, p<0.01) in VLDL-TG after consuming a SFA-enriched HFD compared with baseline (Fig. 4.17E). In contrast, there was a relative increase in linoleate (18:2n-6; p<0.01), and decrease in palmitoleate (16:1n-7; p<0.01), palmitate (16:0; p<0.01), and myristate (14:0; p<0.05) in fasting VLDL-TG after consuming a PUFA-enriched HFD compared with baseline (Fig. 4.17E). Compared with a PUFA-enriched HFD, consuming a SFA-enriched HFD, increased the proportion of palmitoleate (p<0.01), palmitate (p<0.001), and myristate (p<0.05) in fasting VLDL-TG, while consuming a PUFA-enriched HFD, compared with SFA-enriched HFD, increased the proportion of linoleate (p<0.001) in fasting VLDL-TG (Fig. 4.17E). VLDL-TG FA composition was ~40% oleate (18:1n-9), ~28% palmitate (16:0), ~14% linoleate (18:2n-6), ~4% palmitoleate (16:n-7), and ~3% stearate (18:0) after consuming a SFA-enriched HFD, and was ~40% oleate (18:1n-9), ~22% palmitate (16:0), ~22% linoleate (18:2n-6), ~3% palmitoleate (16:n-7), and ~2.5% stearate (18:0) after consuming a PUFA-enriched HFD (Fig. 4.17F).

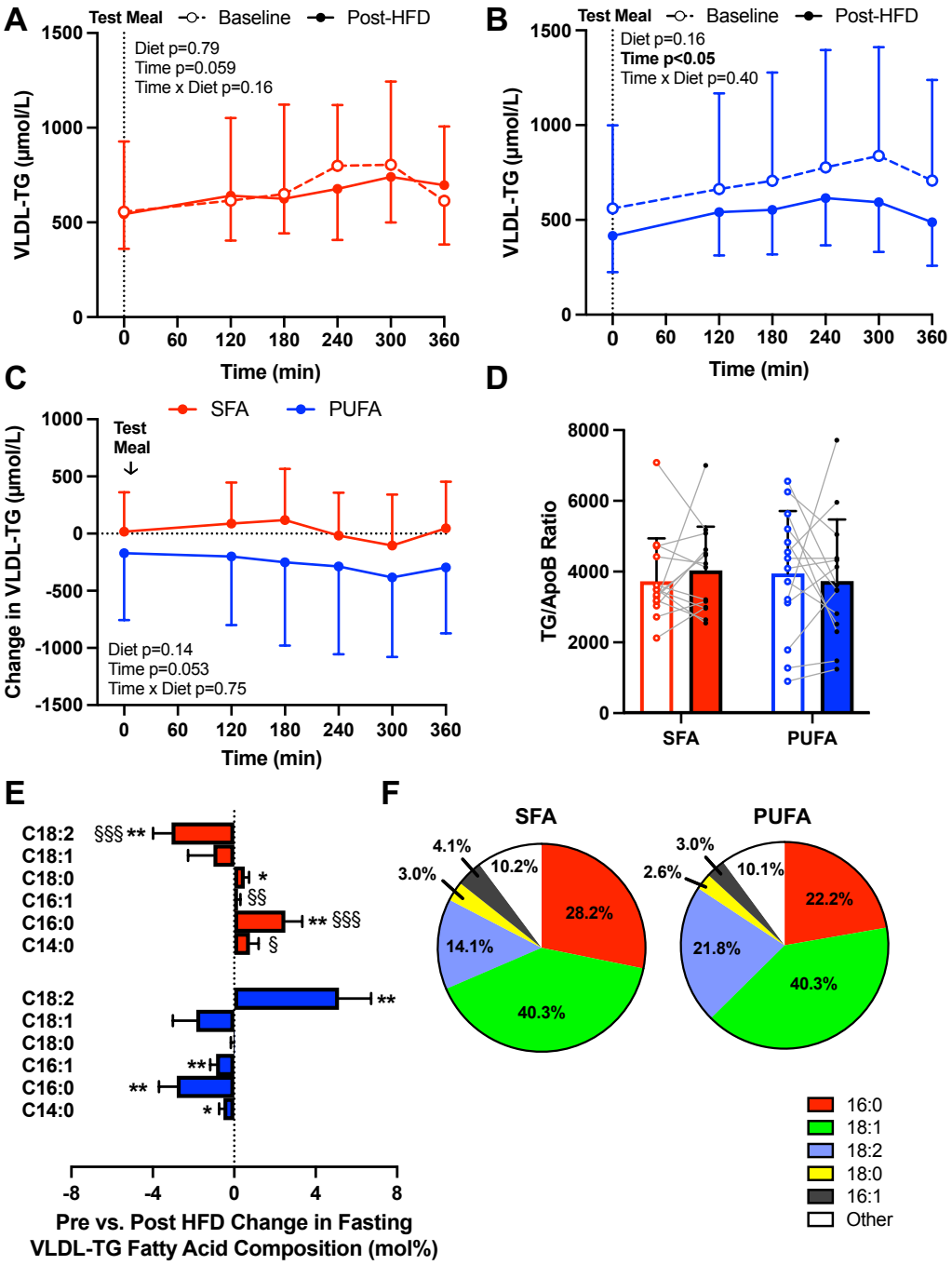

Figure 4.17. VLDL-TG Profile. (A-B) Postprandial plasma VLDL-TG concentrations following consumption of a standardised mixed test meal, before and after consuming a (A) SFA- or (B) PUFA-enriched HFD. (C) The change from baseline to post-HFD of plasma VLDL-TG after consuming a SFA- or PUFA-enriched HFD. (D) Average VLDL-TG particle size in fasting VLDL. (E) The change from baseline to post-HFD of fasting VLDL-TG FA composition and (F) fasting VLDL-TG FA composition after consuming a SFA- (left) or PUFA- (right) enriched HFD. Plasma samples were collected at fasting and every 60min from 2-6h and analysed by a (A-C, E) mixed-effects model or (D) 2-way ANCOVA with baseline values as covariates, matching each participant pre- to post-HFD as appropriate. Abbreviations: SFA, saturated fatty acid; PUFA, polyunsaturated fatty acid; VLDL-TG, very low-density lipoprotein triglyceride. Data presented as (A-B) geometric mean ± 95% confidence interval, (C-E) mean ± SD, (F) mean; n=14 SFA; n=14 PUFA; empty points (○)/bars with hashed lines indicate baseline study visit, filled points (•)/bars with solid lines indicate post-HFD visit, red indicates SFA-enriched HFD; blue indicates PUFA-enriched HFD.

4.3.12 Tracer Incorporation into Plasma-TG

Stable isotope tracer methodologies were used to investigate if changes in hepatic and systemic lipid metabolism may contribute to the divergence in IHTG accumululation following consumption of a SFA- compared with PUFA-enriched HFD. Before a study day, participants consumed D_2O to label endogenously synthesised FAs. During the study day, participants were infused with [2,2-D_2]palmitate and consumed [U^{13}C]palmitate to label adipose-tissue derived and dietary FA, respecitvely. Appearance of labelled FAs into different plasma lipid pools and expired CO_2 was quantified to characterise how dietary FA compostion may impact hepatic FA delivery and secretion, intrahepatic FA synthesis, and whole-body dietary FA oxidation.

Dietary FA composition may influence hepatic delivery of dietary and adipose-tissue derived FA, therefore, appearance of [U^{13}C]palmitate in plasma-TG, chylomicron-TG and plasma NEFA and [2,2-D_2]palmitate in plasma-TG and NEFA were measured, and R_a NEFA was calculated. Over the course of each study day, appearance of [U^{13}C]palmitate and [2,2-D_2]palmitate in plasma-TG increased (all $p<0.001$ effect of time; Fig. 4.18A-D). While there was no diet*time interaction for the appearance of [U^{13}C]palmitate and [2,2-D_2]palmitate in plasma-TG after consuming a SFA- or PUFA-enriched HFD (Fig. 4.18A-D), there was a trend for a lower appearance of [2,2-D_2]palmitate in plasma-TG after consuming a PUFA-enriched HFD ($p=0.056$ effect of diet; Fig. 4.18D). There was a trend for the change from baseline to post-HFD in the appearance of [U^{13}C]palmitate in plasma-TG to differ between diets ($p=0.06$ diet*time; Fig. 4.18E) and no diet*time interaction effect for change in appearance of [2,2-D_2]palmitate in plasma-TG from baseline to post-HFD (Fig. 4.18F).

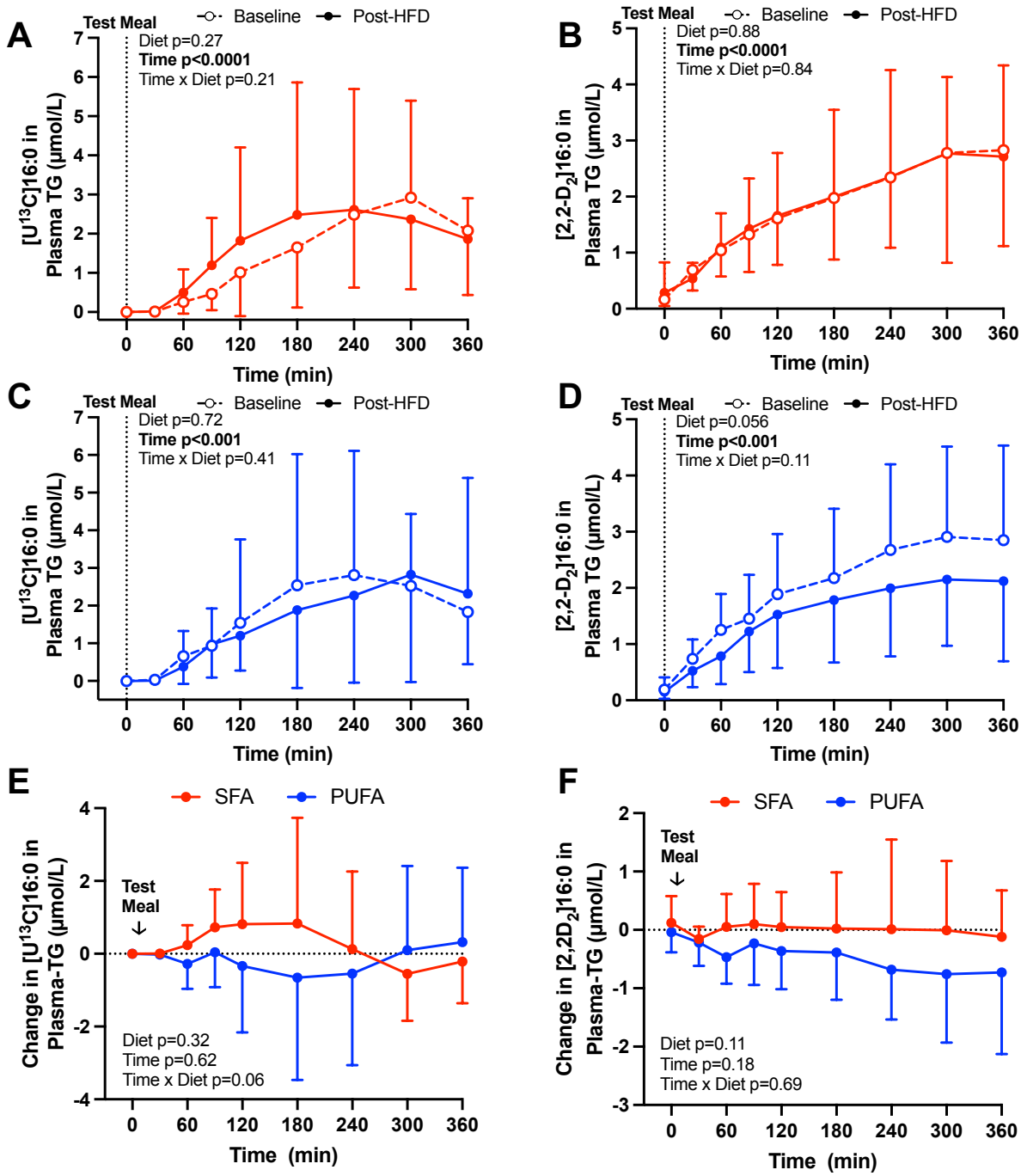

Figure 4.18. Postprandial incorporation of (A, C) [U^{13}C]palmitate and (B, D) [2,2-D$_2$]palmitate into plasma-triglyceride (TG) following consumption a standardised mixed test meal containing [U^{13}C]palmitate and intravenous [2,2-D$_2$]palmitate infusion before and after consuming a (A-B) SFA- or (C-D) PUFA-enriched HFD. (E-F) The change from baseline to post-HFD of (E) [U^{13}C]palmitate or (F) [2,2-D$_2$]palmitate in plasma-TG after consuming a SFA- or PUFA-enriched HFD. Plasma samples were collected at fasting and every 30-60min for 6h and analysed by a mixed-effects model matching each participant pre- to post-HFD as appropriate. Abbreviations: 16:0, palmitate; HFD, high fat diet; SFA, saturated fatty acid; PUFA, polyunsaturated fatty acid. Data presented as mean ± SD; (A, C, E) n=14 SFA; n=14 PUFA; (B, D, F) n=13 SFA; n=11 PUFA; empty points (○)/bars with hashed lines indicate baseline study visit, filled points (•)/bars with solid lines indicate post-HFD visit, red indicates SFA-enriched HFD; blue indicates PUFA-enriched HFD.

4.3.13 Dietary-FA Tracer Incorporation into Chylomicron-TG

[U^{13}C]palmitate appearance in chylomicron-TG increased during the study day in participants which consumed a PUFA-enriched HFD (p<0.05 effect of time; Fig. 4.19B) and tended to increase over the course the study day in participants which consumed a SFA-enriched HFD (p=0.07 effect of time; Fig. 4.19A). There was no diet*time interaction for the appearance of [U^{13}C]palmitate in chylomicron-TG after consuming a SFA- or PUFA-enriched HFD (Fig. 4.19A-B), but there was a trend for the change from baseline to post-HFD of [U^{13}C]palmitate in chylomicron-TG to differ between diets (p=0.08; Fig. 4.19C).

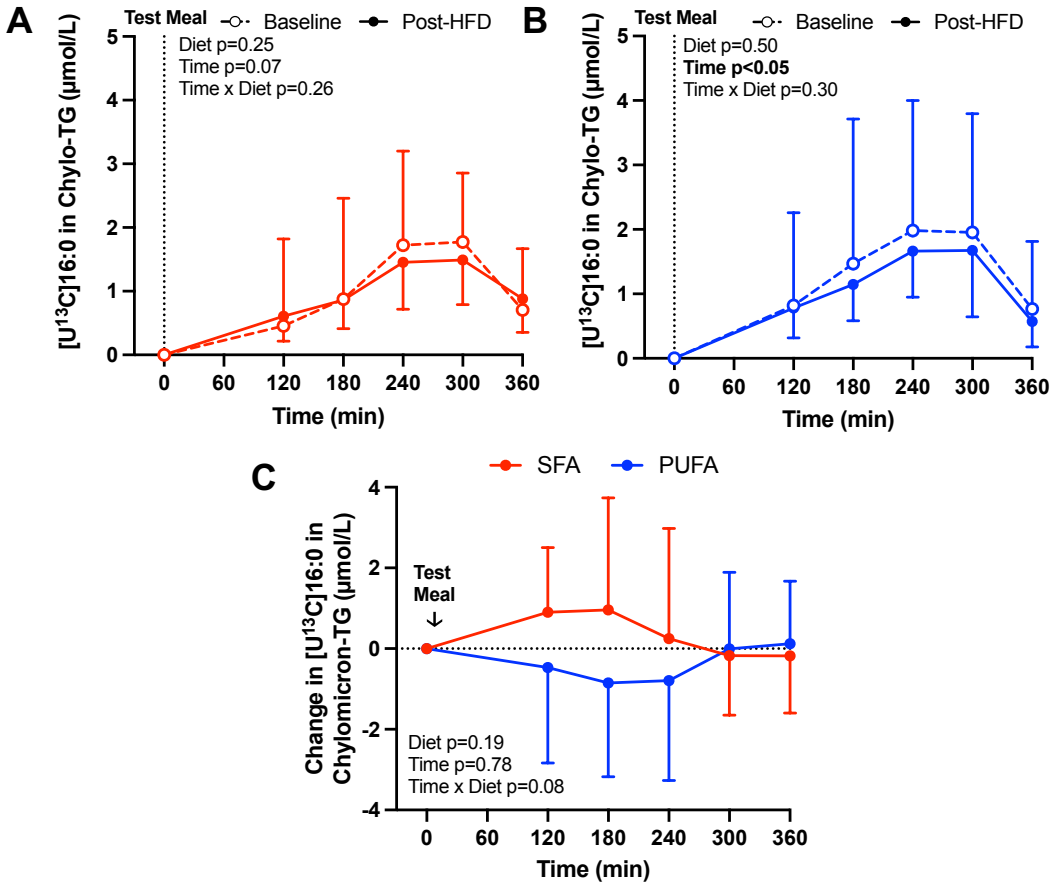

Figure 4.19. Postprandial incorporation of [U^{13}C]palmitate into chylomicron-TG following consumption a standardised mixed test meal containing [U^{13}C]palmitate before and after consuming a (A) SFA- or (B) PUFA-enriched HFD. (C) The change from baseline to post-HFD of [U^{13}C]palmitate in chylomicron-TG after consuming a SFA- or PUFA-enriched HFD. Plasma samples were collected at fasting and every 60min from 2-6h and analysed by a mixed-effects model matching each participant pre- to post-HFD. Abbreviations: 16:0, palmitate; chylo, chylomicron; HFD, high fat diet; SFA, saturated fatty acid; PUFA, polyunsaturated fatty acid; TG, triglyceride. Data presented as (A-B) geometric mean ± 95% confidence interval; (C) mean ± SD; n=14 SFA; n=14 PUFA; empty points (○) with hashed lines indicate baseline study visit, filled points (•) with solid lines indicate post-HFD visit, red indicates SFA-enriched HFD; blue indicates PUFA-enriched HFD.

4.3.14 Dietary-FA Tracer Incorporation into Plasma NEFA

The appearance of [U^{13}C]palmitate in plasma NEFA increased over the course of each study day (p<0.0001 effect of time; Fig. 4.20A-B). In participants who consumed a SFA-enriched HFD, there was a diet*time interaction effect for the appearance of [U^{13}C]palmitate in plasma NEFA (p<0.05; Fig. 4.20A), where compared with baseline, consuming a SFA-enriched HFD led to a greater appearance of ^{13}C in plasma NEFA at 60min (p=0.07), 90min (p<0.01), and 120min (p=0.05), and lower appearance of ^{13}C in plasma NEFA at 240min (p=0.08) and 300min (p<0.05) after consuming the mixed test meal (Fig. 4.20A). There was no diet*time interaction effect for the appearance of [U^{13}C]palmitate in plasma NEFA after consuming a PUFA-enriched HFD (Fig. 4.20B). Time-averaged AUC for ^{13}C appearance in plasma-NEFA did not change from baseline to post-HFD or between diets (Fig. 4.20C). The change from baseline to post-HFD of [U^{13}C]palmitate in plasma NEFA differed between diets (p<0.05 diet*time interaction; Fig. 4.20D). At 60min (p=0.05) and 90min (p<0.05) after consuming the mixed test meal, a SFA-, compared with PUFA-enriched HFD, led to a greater appearance of [U^{13}C]palmitate in plasma NEFA (Fig. 4.20D). At 300min post-test meal, a SFA-enriched HFD tended to decrease and a PUFA-enriched tended to increase [U^{13}C]palmitate appearance in plasma NEFA compared with the respective baseline (p=0.06; Fig. 4.20D).

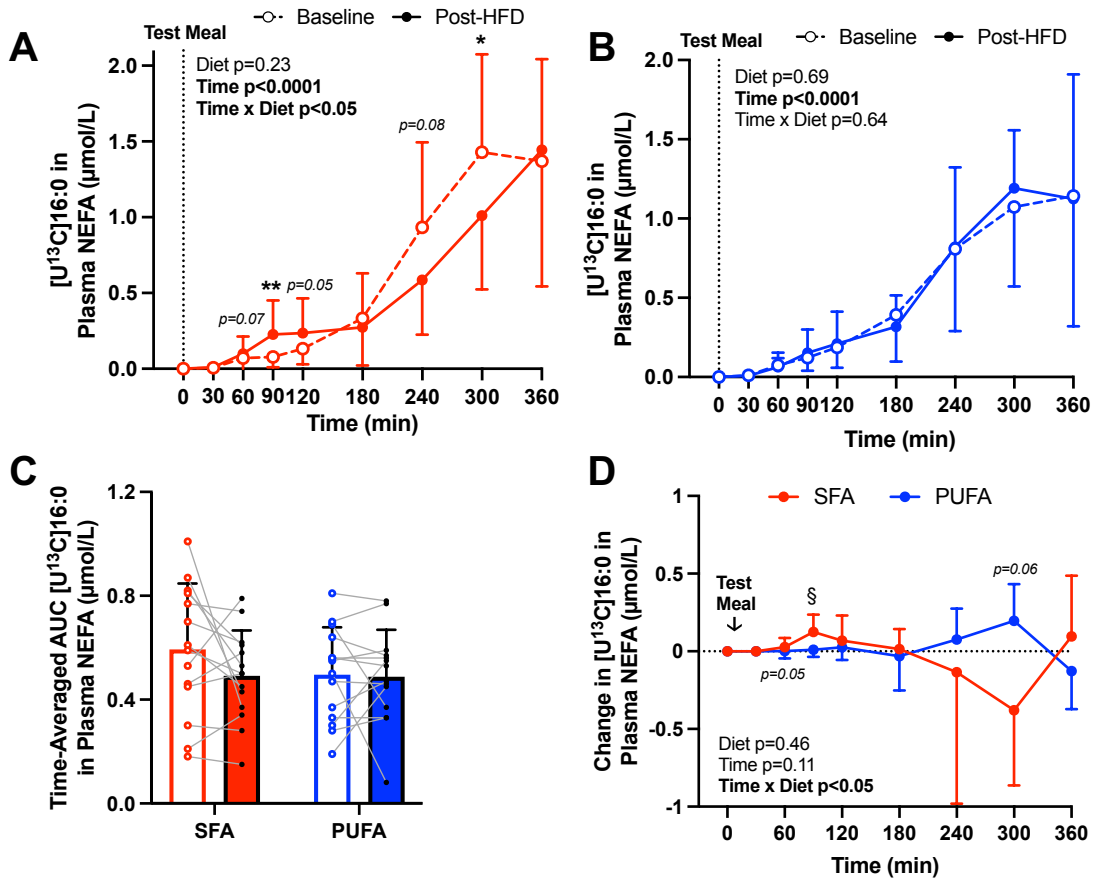

Figure 4.20. Postprandial appearance of [U^{13}C]palmitate in plasma NEFA following consumption a standardised mixed test meal containing [U^{13}C]palmitate before and after consuming a (A) SFA- or (B) PUFA-enriched HFD. (C) Time-averaged AUC of [U^{13}C]palmitate in plasma NEFA. (D) Change from baseline to post-HFD of [U^{13}C]palmitate in plasma NEFA after consuming a SFA- or PUFA-enriched HFD. Plasma samples were collected at every 30-60min for 6h and analysed by a mixed-effects model matching each participant pre- to post-HFD. Abbreviations: 16:0, palmitate; HFD, high fat diet; NEFA, non-esterified fatty acid; SFA, saturated fatty acid; PUFA, polyunsaturated fatty acid. Data presented as mean ± SD, n=14 SFA; n=14 PUFA; empty points (○)/bars with hashed lines indicate baseline study visit, filled points (•)/bars with solid lines indicate post-HFD visit, red indicates SFA-enriched HFD; blue indicates PUFA-enriched HFD; * p<0.05, ** p<0.01 comparing the post-HFD value to the respective baseline within group; § p<0.05 comparing the change from baseline to post-HFD between groups.

4.3.15 R_a NEFA & Incorporation of Adipose-Tissue Derived FA Tracer into Plasma NEFA

Over the course of each study day, R_a NEFA, a marker of adipose-tissue lipolysis, varied with time and followed the postprandial plasma NEFA profile (both p<0.0001 effect of time; Fig. 4.21A-B). There was no diet*time interaction effect for R_a NEFA after consuming a SFA- or PUFA-enriched HFD compared with the respective baseline study day (Fig. 4.21A-B). However, consuming a SFA-enriched HFD reduced postprandial R_a NEFA (p<0.05 effect of diet; Fig. 4.21A), and consuming a PUFA-enriched HFD tended to reduce postprandial R_a

NEFA (p=0.08 effect of diet; Fig. 4.21B) compared with each respective baseline. As the change within either diet from baseline to post-HFD was similar, there was no difference in R_a NEFA between diets (Fig. 4.21C).

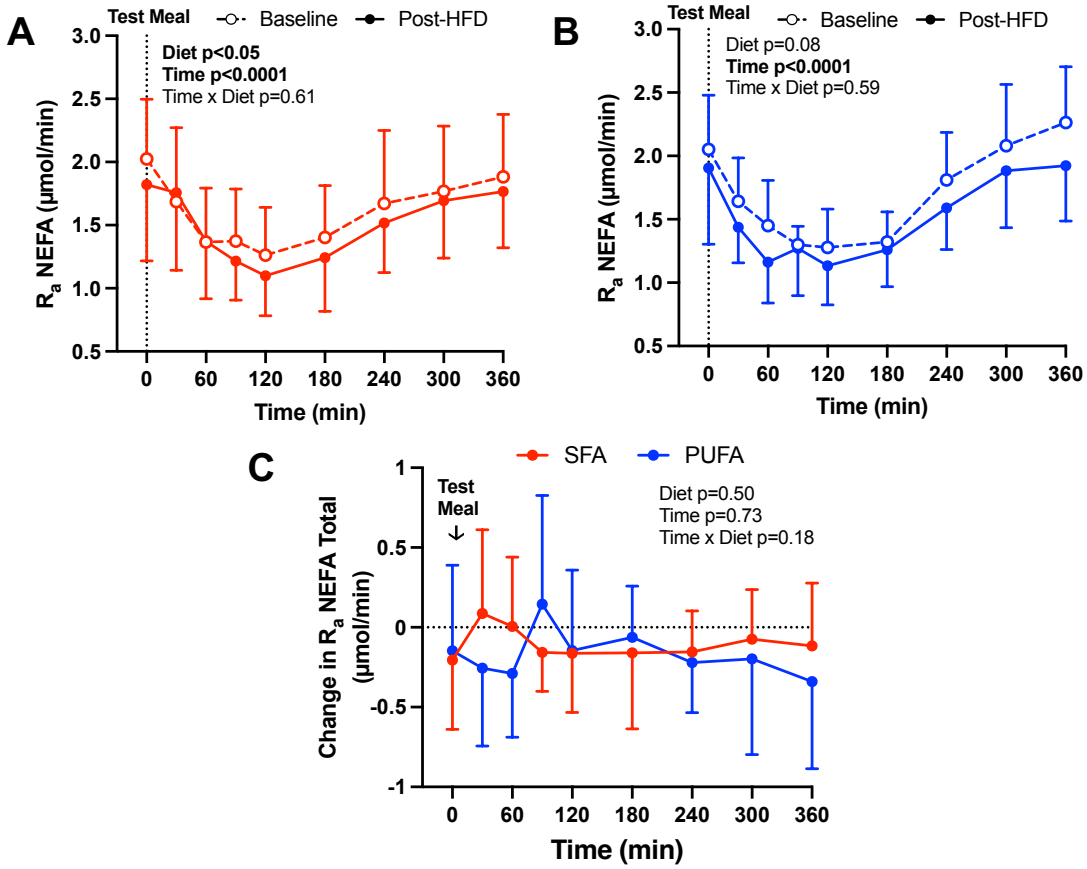

Figure 4.21. Postprandial R_a NEFA following consumption a standardised mixed test meal and intravenous [2,2-D_2]palmitate infusion before and after consuming a (A) SFA- or (B) PUFA-enriched HFD. (C) Change from baseline to post-HFD of R_a NEFA after consuming a SFA- or PUFA-enriched HFD. Plasma samples were collected every 30-60min for 6h and analysed by a mixed-effects model matching each participant pre- to post-HFD. Abbreviations: 16:0, palmitate; HFD, high fat diet; NEFA, non-esterified fatty acid; SFA, saturated fatty acid; PUFA, polyunsaturated fatty acid; R_a, rate of appearance. Data presented as mean ± SD, n=13 SFA; n=11 PUFA; empty points (○) with hashed lines indicate baseline study visit, filled points (•) with solid lines indicate post-HFD visit, red indicates SFA-enriched HFD; blue indicates PUFA-enriched HFD.

The appearance of [2,2-D_2]palmitate in the plasma NEFA pool, a marker of adipose-tissue derived FA, also followed the postprandial plasma NEFA profile (both p<0.0001 effect of time; Fig. 4.22A-B). There was no diet*time interaction effect for [2,2-D_2]palmitate in plasma NEFA after consuming a SFA- or PUFA-enriched HFD compared with the baseline study day (Fig. 4.22A-B), and the change of [2,2-D_2]palmitate in plasma NEFA from baseline

to post-HFD did not differ between diets (p=0.15; Fig. 4.22C). Despite the trend for consuming a PUFA-enriched HFD to reduce adipose tissue lipolysis, consuming a PUFA-enriched HFD increased the appearance of [2,2-D_2]palmitate in plasma NEFA compared with baseline (p<0.05 effect of diet; Fig. 4.22B). Further, consuming a PUFA-enriched, compared with SFA-enriched HFD, increased the appearance of [2,2-D_2]palmitate in plasma NEFA (p<0.05 effect of diet; Fig. 4.22C).

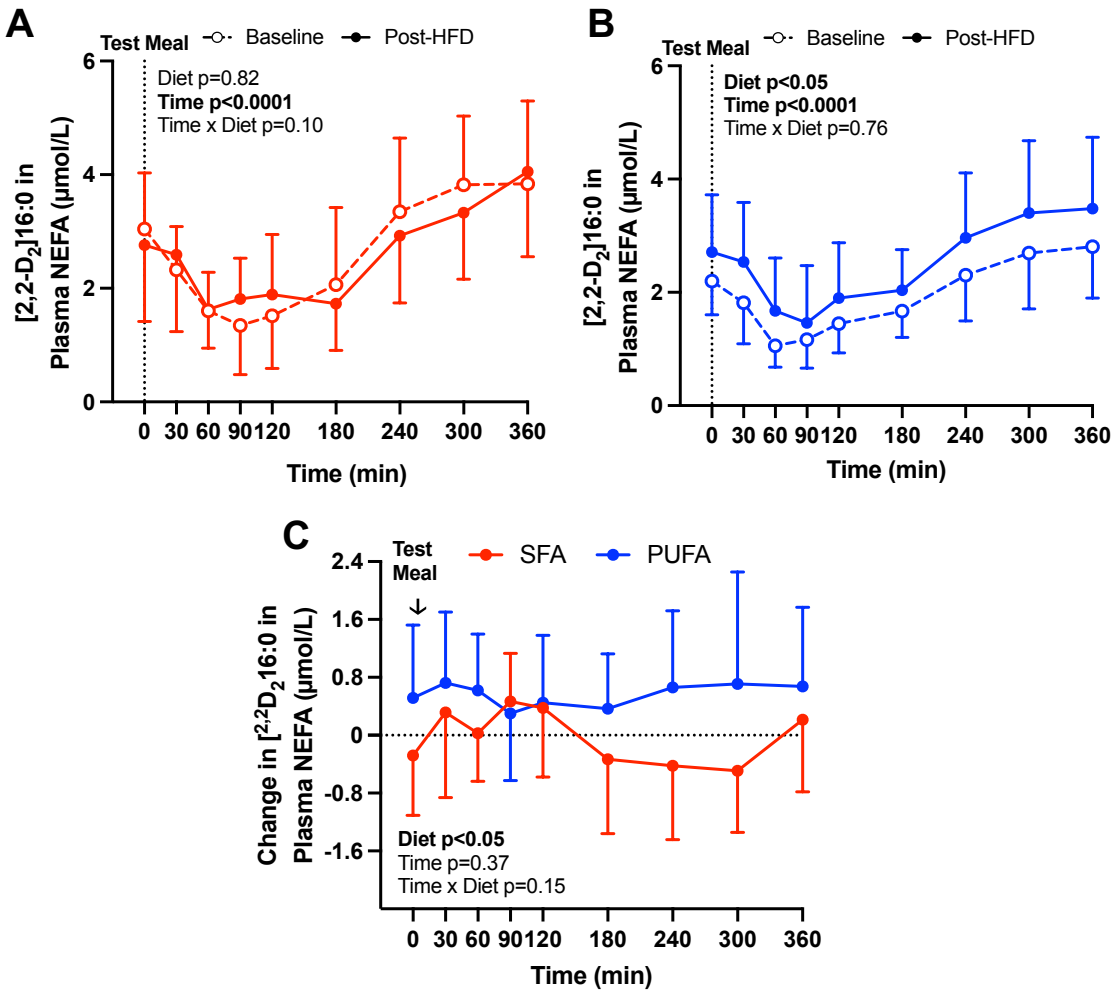

Figure 4.22. Postprandial appearance of [2,2-D_2]palmitate in plasma NEFA following consumption a standardised mixed test meal and intravenous [2,2-D_2]palmitate infusion before and after consuming a (A) SFA- or (B) PUFA-enriched HFD. (C) The change from baseline to post-HFD of [2,2-D_2]palmitate in plasma NEFA after consuming a SFA- or PUFA-enriched HFD. Plasma samples were collected every 30-60min for 6h and analysed by a mixed-effects model matching each participant pre- to post-HFD. Abbreviations: 16:0, palmitate; HFD, high fat diet; NEFA, non-esterified fatty acid; SFA, saturated fatty acid; PUFA, polyunsaturated fatty acid. Data presented as mean ± SD, n=13 SFA; n=11 PUFA; empty points (○) with hashed lines indicate baseline study visit, filled points (•) with solid lines indicate post-HFD visit, red indicates SFA-enriched HFD; blue indicates PUFA-enriched HFD.

4.3.16 Appearance of Dietary & Adipose-Tissue Derived FA Tracer into VLDL-TG

Appearance of [U^{13}C]palmitate and [2,2-D$_2$]palmitate in VLDL-TG was measured before and after consuming a SFA- or PUFA-enriched HFD to determined if differences in intrahepatic partitioning of dietary and adipose tissue-derived FA into VLDL-TG secretion pathways may contribute to the divergent effects of dietary FA composition on IHTG accumulation. Appearance of [U^{13}C]palmitate in VLDL-TG increased over the course of each study day (p<0.0001 effect of time; Fig. 4.23A-B), was not different after consuming a SFA- or PUFA-enriched HFD compared with baseline (Fig. 4.23A-B), and did not differ between diets (Fig. 4.23C).

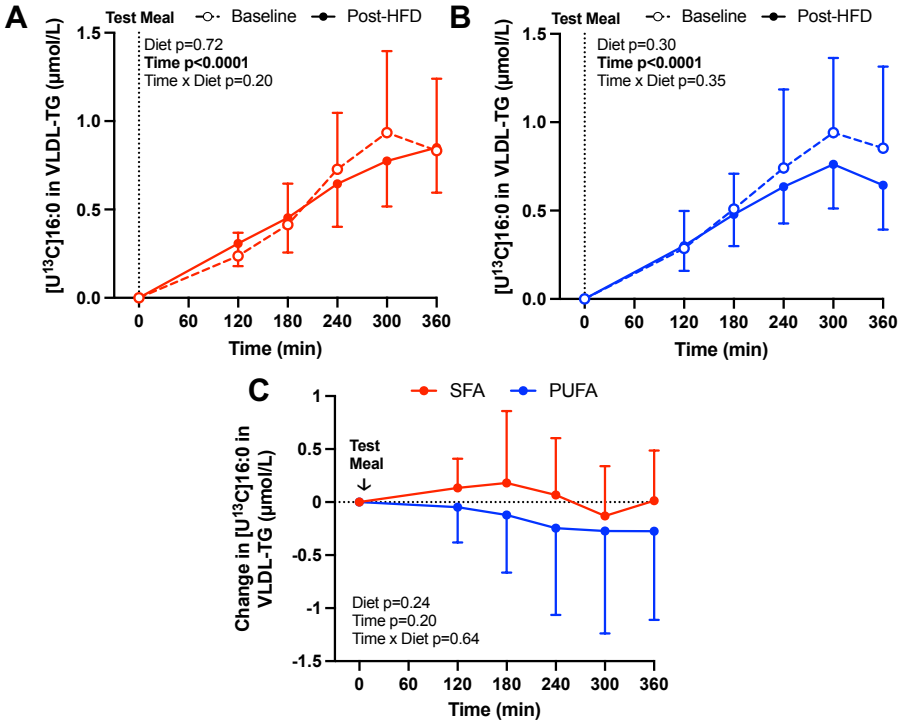

Figure 4.23. Postprandial incorporation of [U^{13}C]palmitate into VLDL-TG following consumption a standardised mixed test meal containing [U^{13}C]palmitate before and after consuming a (A) SFA- or (B) PUFA-enriched HFD. (C) The change from baseline to post-HFD of [U^{13}C]palmitate in VLDL-TG after consuming a SFA- or PUFA-enriched HFD. Plasma samples were collected at fasting and every 60min from 2-6h and analysed by a mixed-effects model matching each participant pre- to post-HFD. Abbreviations: 16:0, palmitate; HFD, high fat diet; SFA, saturated fatty acid; PUFA, polyunsaturated fatty acid; VLDL-TG, very low-density lipoprotein triglyceride. Data presented as (A-B) geometric mean ± 95% confidence interval, (C) mean ± SD; n=14 SFA; n=14 PUFA; empty points (○)/bars with hashed lines indicate baseline study visit, filled points (•)/bars with solid lines indicate post-HFD visit, red indicates SFA-enriched HFD; blue indicates PUFA-enriched HFD.

[2,2-D_2]palmitate appearance in VLDL-TG increased over the course of each study day (p<0.0001 effect of time; Fig. 4.24A-B), following a similar postprandial profile after consuming a SFA- or PUFA-enriched HFD compared with baseline (Fig. 4.24A-B). There was no difference in the change from baseline to post-HFD of [2,2-D_2]palmitate appearance in VLDL-TG between diets (p=0.37 diet*time; Fig. 4.24C), but there was a trend for the change of [2,2-D_2]palmitate in VLDL-TG to vary over time during the study day (p=0.055 effect of time; Fig. 4.24C). These data suggest that, compared with baseline, consuming a SFA- or PUFA-enriched HFD may not differentially impact the appearance of dietary and adipose-tissue derived FA into VLDL-TG.

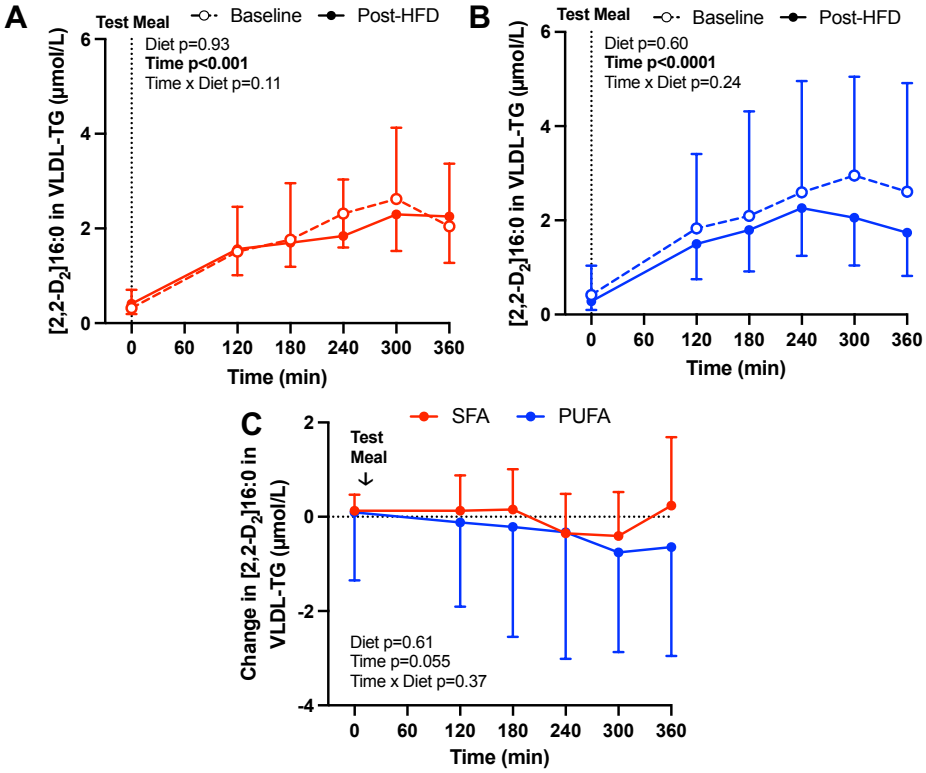

Figure 4.24. Postprandial appearance of [2,2-D_2]palmitate in plasma VLDL-TG following consumption a standardised mixed test meal and intravenous [2,2-D_2]palmitate infusion before and after consuming a (A) SFA- or (B) PUFA-enriched HFD. (C) The change from baseline to post-HFD of [2,2-D_2]palmitate in VLDL-TG after consuming a SFA- or PUFA-enriched HFD. Plasma samples were collected at fasting and every 60min from 2-6h and analysed by a mixed-effects model matching each participant pre- to post-HFD. Abbreviations: 16:0, palmitate; SFA, saturated fatty acid; PUFA, polyunsaturated fatty acid; VLDL-TG, very low-density lipoprotein triglyceride. Data presented as (A-B) geometric mean ± 95% confidence interval, (C) mean ± SD; n=13 SFA; n=11 PUFA; empty points (○)/bars with hashed lines indicate baseline study visit, filled points (•)/bars with solid lines indicate post-HFD visit, red indicates SFA-enriched HFD; blue indicates PUFA-enriched HFD.

4.3.17 Secretion of Endogenously Synthesised Palmitate in VLDL-TG

Increased flux through hepatic DNL may contribute to increased IHTG accumulation (60), therefore, appearance of newly synthesised palmitate in fasting and postprandial VLDL-TG was measured before and after consuming a SFA- or PUFA-enriched HFD. Although consuming a HFD increased the percent of newly synthesised palmitate in fasting VLDL-TG compared with baseline (p<0.05 effect of pre- to post-HFD; Fig. 4.25A), dietary FA composition did not have a divergent effect on this pathway (p=0.56 diet*pre-/post-HFD; Fig. 4.25A). Appearance of newly synthesised palmitate in VLDL-TG varied throughout postprandial period in participants which consumed a SFA-enriched HFD (p<0.05 effect of time; Fig. 4.25B), but not in participants which consumed a PUFA-enriched HFD (p=0.13 effect of time; Fig. 4.25C). No differences in the percent of newly synthesised palmitate in VLDL-TG were found after consuming a SFA- or PUFA-enriched HFD compared with baseline (Fig. 4.25B-C); further, the change from baseline to post-HFD of newly synthesised palmitate in VLDL-TG was similar between diets (Fig. 4.25D). This suggests the divergent effects of consuming a SFA- compared with PUFA-enriched HFD on IHTG accumulation may not be mediated through differential effects on hepatic DNL (Fig. 4.11B).

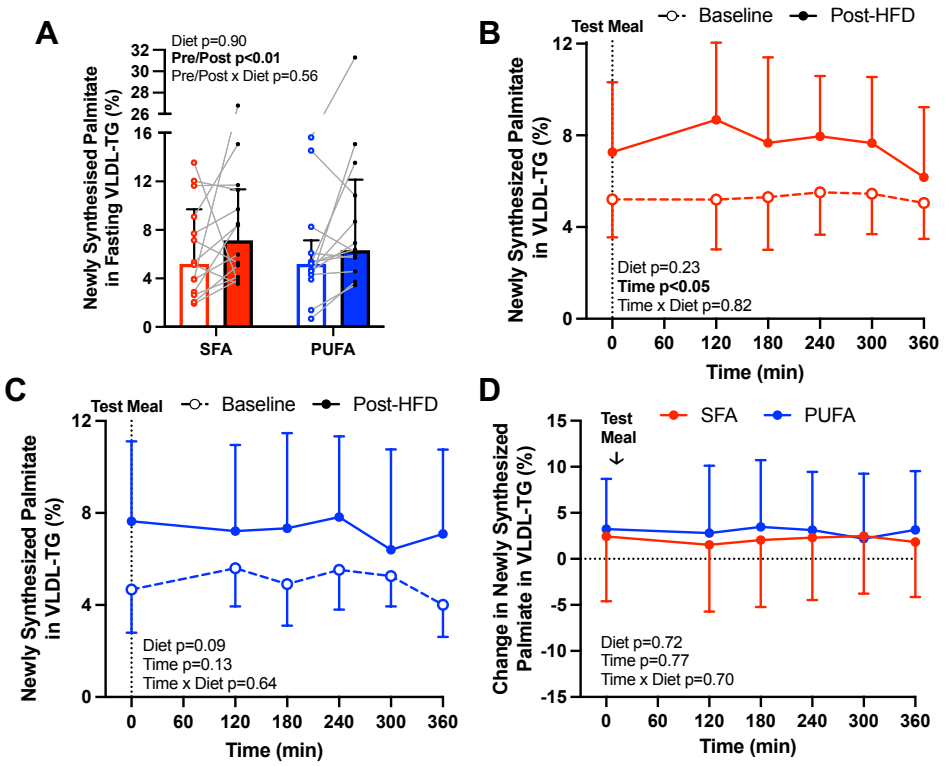

Figure 4.25. Appearance of newly synthesised palmitate in (A) fasting and (B-D) postprandial VLDL-TG following consumption of D_2O and a standardised mixed test before and after consuming a (B) SFA- or (C) PUFA-enriched HFD. (D) The change from baseline to post-HFD of newly synthesised palmitate in VLDL-TG after consuming a SFA- or PUFA-enriched HFD. Plasma samples were collected at fasting and every 60min from 2-6h and analysed by a mixed-effects model matching each participant pre- to post-HFD. Abbreviations: SFA, saturated fatty acid; PUFA, polyunsaturated fatty acid; VLDL-TG, very low-density lipoprotein triglyceride. Data presented as (A) median ± IQR, (B-C) geometric mean ± 95% confidence interval, (D) mean ± SD; n=14 SFA; n=13 PUFA; empty points (○)/bars with hashed lines indicate baseline study visit, filled points (•)/bars with solid lines indicate post-HFD visit, red indicates SFA-enriched HFD; blue indicates PUFA-enriched HFD.

4.3.18 Whole-body FA Oxidation

Appearance of ^{13}C (from the labelled dietary–FA) into expired CO_2 was measured to determine if differences in whole-body FA oxidation may explain the difference in IHTG accumulation after consuming a SFA- compared with PUFA-enriched HFD. Over the course of each study day, ^{13}C appearance in expired CO_2 increased after consuming the test meal containing [U^{13}C]palmitate (p<0.001 effect of time; Fig. 4.26A-B). Compared with the respective baseline study day, ^{13}C appearance in expired CO_2 tended to be lower after consuming a SFA-enriched HFD (p=0.07 diet*time; Fig. 4.26A), and unchanged after consuming a PUFA-enriched HFD (p=0.34 diet*time; Fig. 4.26B). There were no differences

in the percent of ^{13}C recovered as expired $^{13}CO_2$ following consumption of a mixed meal containing [U^{13}C]palmitate (Fig. 4.26C). However, between diets, the change from baseline to post-HFD of ^{13}C in expired CO_2 differed (p<0.001 diet*time interaction; Fig. 4.26D); at 300min (p=0.07) and 360min (p<0.05) following the test meal, consuming a PUFA-enriched HFD increased ^{13}C in expired CO_2 whereas consuming a SFA-enriched HFD decreased ^{13}C in expired CO_2 compared with the respective baseline (Fig. 4.26D). Taken together, these data suggest that consuming a PUFA-enriched, compared with SFA-enriched HFD, may increase FA disposal by increasing whole-body postprandial FA oxidation, and this increase in FA oxidation may explain the observed reduction in IHTG content after consuming a PUFA-enriched HFD.

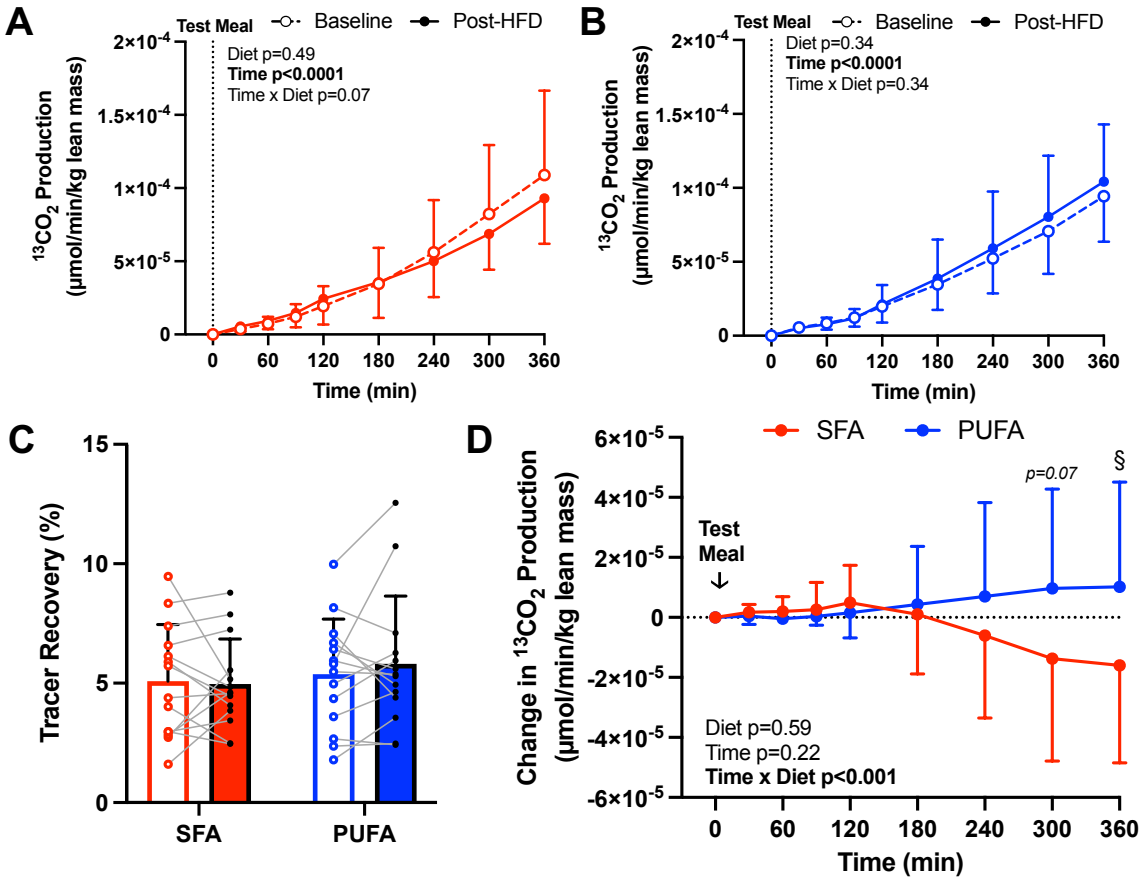

Figure 4.26. Markers of whole-body postprandial fatty acid oxidation in expired CO_2 following consumption of a standardised mixed test meal containing [U^{13}C]palmitate before and after consuming a (A) SFA- or (B) PUFA-enriched HFD. (C) The percent recovery of ^{13}C in expired CO_2 at the end of the 6-h postprandial period. (D) The change from baseline to post-HFD of ^{13}C in expired CO_2 after consuming a SFA- or PUFA-enriched HFD. Breath samples were collected every 30-60min from fasting for 6h and

analysed by a mixed-effects model with a Sidak post-hoc test, matching each participant pre- to post-HFD. Abbreviations: HFD, high fat diet; SFA, saturated fatty acid; PUFA, polyunsaturated fatty acid. Data presented as mean ± SD; n=14 SFA; n=14 PUFA; empty points (○)/bars with hashed lines indicate baseline study visit, filled points (•)/bars with solid lines indicate post-HFD visit, red indicates SFA-enriched HFD; blue indicates PUFA-enriched HFD. § indicates $p<0.05$ comparing the change from baseline to post-HFD between groups.

4.3.19 Sex Differences in Postprandial Metabolism

Pramfalk *et al.* (307) previously reported a sexual dimorphism in postprandial lipid metabolism. Therefore, I wanted to explore if the change from baseline to post-HFD in fasting and postprandial metabolism in males, compared with females, differed after consuming a SFA- or PUFA-enriched HFD. In line with previous studies (307), males, compared with females, had higher IHTG content, HOMA-IR, fasting plasma TG, total-cholesterol, and non-HDL cholesterol, visceral fat, and lean mass at baseline. Each group was split by sex, with baseline and post-HFD anthropometric, body composition, and fasting plasma biochemistry listed in Table 4.5 and Table 4.6 for the groups which consumed a SFA- or PUFA-enriched HFD, respectively.

Seven males aged 52±5 years with a BMI of 29.0±4.3 kg/m^2 and seven females aged 54±6 years with a BMI of 26.9±4.5 kg/m^2 consumed a SFA-enriched HFD (Table 4.5). At baseline, males had higher lean mass ($p<0.001$), visceral fat ($p<0.01$), fasting plasma insulin ($p<0.05$), and a trend towards increased HOMA-IR ($p=0.056$; Table 4.5) compared with females. Otherwise, there were no baseline differences in age, BMI, fat mass, liver fat, fasting plasma glucose, NEFA, TG, total-, HDL- and non-HDL cholesterol, and apoB between males and females randomised to consume a SFA-enriched HFD (Table 4.5). Consuming a SFA-enriched HFD reduced fasting plasma NEFA in both males and females compared with baseline ($p<0.05$; Table 4.5). In males, consuming a SFA-enriched HFD, compared with baseline, increased liver fat, fasting plasma total-cholesterol and HDL-cholesterol (all $p<0.05$; Table 4.5), and tended to increase fasting plasma non-HDL cholesterol ($p=0.07$), apoB ($p=0.05$), and insulin ($p=0.09$; Table 4.5). In females, there was a trend for consuming a SFA-

enriched HFD to increase fasting plasma total-cholesterol (p=0.07), HDL-cholesterol (p=0.08), and decrease visceral fat (p=0.09) compared with baseline (Table 4.5)

Seven males aged 51±10 years with a BMI of 28.4±3.5 kg/m^2 and seven females aged 56±4 years with a BMI of 25.2±5.2 kg/m^2 consumed a PUFA-enriched HFD (Table 4.6). At baseline, males, compared with females, had higher lean mass (p<0.001) and visceral fat (p<0.05; Table 4.5). Otherwise, there were no baseline differences in age, BMI, fat mass, liver fat, HOMA-IR, fasting plasma glucose, insulin, NEFA, TG, total-, HDL-, and non-HDL cholesterol, and apoB between males and females randomised to consume a PUFA-enriched HFD (Table 4.6). In males, consuming a PUFA-enriched HFD, compared with baseline, reduced HOMA-IR, fasting plasma insulin, total- and non-HDL cholesterol, and apoB100 (all p<0.05; Table 4.6). Consuming a PUFA-enriched HFD did not change body composition or fasting plasma biochemistry in females compared with baseline (Table 4.6).

Table 4.5 Anthropometry, Body Composition, & Fasting Plasma Biochemistry in Males and Females at Baseline and After Consuming an Isocaloric SFA-Enriched HFD

	Males			**Females**			
	Baseline	**Post-HFD**	***Within Sex Pre vs. Post HFD* (*p*-value)**	**Baseline**	**Post-HFD**	***Within Sex Pre vs. Post HFD* (*p*-value)**	***Comparison Males to Females at Baseline (p-value)***
Number	7	-	-	7	-	-	-
Age (years)	52 ± 5	-	-	54 ± 6	-	-	*0.50*
BMI (kg/m^2)	29.0 ± 4.3	29.1 ± 4.1	*0.64*	26.9 ± 4.5	26.9 ± 4.6	*0.83*	*0.43*
Body Fat Mass (kg)	30.5 ± 12.2	30.3 ± 12.0	*0.46*	28.7 ± 9.8	28.2 ± 10.0	*0.11*	*0.77*
Body Lean Mass (kg)	58.2 ± 6.7	58.2 ± 7.1	*0.89*	41.7 ± 3.0	41.9 ± 2.7	*0.32*	***<0.001***
Liver Fat (%)	6.8 (2.8 – 8.2)	6.4 (3.2 – 9.8)	***0.046***	2.2 (1.5 – 4.2)	2.8 (2.0 – 4.7)	*0.16*	*0.12*
Visceral Fat (g)	1927 ± 1082	1931 ± 1054	*0.89*	502 ± 381	468 ± 346	*0.09*	***0.006***
HOMA-IR	2.3 ± 1.6	2.8 ± 2.1	*0.15*	1.0 ± 0.3	1.0 ± 0.3	*0.51*	*0.056*
Fasting Plasma Biochemistry							
Glucose (mmol/L)	5.6 ± 0.9	5.8 ± 0.6	*0.61*	5.6 ± 0.5	5.5 ± 0.5	*0.24*	*0.90*
Insulin (mU/L)	8.7 ± 4.9	10.5 ± 6.5	*0.09*	4.0 ± 1.3	4.2 ± 1.2	*0.38*	***0.02***
NEFA (µmol/L)	592 ± 160	416 ± 239	***0.03***	699 ± 178	590 ± 173	***0.04***	*0.26*
Triglyceride (mmol/L)	1.14 ± 0.62	1.28 ± 0.59	*0.31*	0.71 ± 0.35	0.65 ± 0.31	*0.22*	*0.14*
Total Cholesterol (mmol/L)	4.5 ± 1.1	4.9 ± 0.9	***0.04***	4.5 ± 0.7	4.7 ± 0.5	*0.07*	*0.90*
HDL-Cholesterol (mmol/L)	1.2 ± 0.5	1.3 ± 0.5	***0.02***	1.5 ± 0.3	1.7 ± 0.3	*0.08*	*0.10*
Non-HDL Cholesterol (mmol/L)	3.4 ± 0.8	3.7 ± 0.7	*0.07*	2.9 ± 0.7	3.0 ± 0.6	*0.40*	*0.31*
Apolipoprotein B (mmol/L)	0.69 ± 0.39	0.77 ± 0.40	*0.05*	0.72 ± 0.15	0.71 ± 0.14	*0.92*	*0.87*

Parametric data presented as mean ± SD, non-parametric data presented as median (IQR). Abbreviations: BMI, body mass index; HDL, high-density lipoprotein; HFD, high fat diet; HOMA-IR, homeostatic model assessment of insulin resistance; NEFA, non-esterified fatty acid; PUFA, polyunsaturated fatty acid; SFA, saturated fatty acid; comparison of males to females at baseline *p*-value represents output from unpaired student's t-test if data parametric or from Mann-Whitney test if data non-parametric; within group comparisons were made using a paired student's t-test with significance set at $p<0.05$. n=7 males, n=7 females.

Table 4.6. Anthropometry, Body Composition, & Fasting Plasma Biochemistry in Males and Females at Baseline and After Consuming an Isocaloric PUFA-Enriched HFD

	Males			**Females**			
	Baseline	**Post-HFD**	***Within Sex Pre vs. Post HFD* (*p*-value)**	**Baseline**	**Post-HFD**	***Within Sex Pre vs. Post HFD* (*p*-value)**	***Comparison Males to Females at Baseline (p-value)***
Number	7	-	-	7	-	-	-
Age (years)	51 ± 10	-	-	56 ± 4	-	-	*0.28*
BMI (kg/m^2)	28.4 ± 3.5	28.3 ± 3.6	*0.51*	25.2 ± 5.2	25.1 ± 5.0	*0.65*	*0.20*
Body Fat Mass (kg)	27.2 ± 8.3	26.6 ± 8.4	*0.10*	24.3 ± 8.9	24.2 ± 2.2	*0.36*	*0.55*
Body Lean Mass (kg)	63.1 ± 6.6	63.3 ± 6.3	*0.33*	42.8 ± 2.5	42.7 ± 2.7	*0.67*	***<0.001***
Liver Fat (%)	5.0 (2.2 – 17.5)	4.5 (2.5 – 8.8)	*0.16*	2.5 (1.4 – 4.4)	2.3 (1.4 – 4.1)	*0.99*	*0.17*
Visceral Fat (g)	1743 ± 1250	1681 ± 1205	*0.43*	430 ± 403	466 ± 437	*0.29*	***0.02***
HOMA-IR	1.8 ± 1.4	1.4 ± 1.3	***0.02***	1.2 ± 0.7	1.4 ± 0.8	*0.27*	*0.35*
Fasting Plasma Biochemistry							
Glucose (mmol/L)	5.5 ± 0.6	5.4 ± 0.3	*0.39*	5.5 ± 0.4	5.6 ± 0.7	*0.70*	*0.95*
Insulin (mU/L)	7.4 ± 5.9	5.8 ± 5.6	***0.02***	4.9 ± 2.7	5.5 ± 2.5	*0.48*	*0.33*
NEFA (µmol/L)	466 ± 223	416 ± 197	*0.13*	574 ± 176	613 ± 234	*0.30*	*0.34*
Triglyceride (mmol/L)	1.39 ± 0.99	1.04 ± 0.91	*0.12*	0.89 ± 0.60	0.80 ± 0.38	*0.41*	*0.28*
Total Cholesterol (mmol/L)	5.1 ± 1.3	4.4 ± 1.0	***0.045***	4.5 ± 0.7	4.3 ± 1.0	*0.22*	*0.34*
HDL-Cholesterol (mmol/L)	1.3 ± 0.4	1.3 ± 0.3	*0.80*	1.5 ± 0.5	1.5 ± 0.3	*0.99*	*0.66*
Non-HDL Cholesterol (mmol/L)	3.7 ± 1.1	3.1 ± 1.0	***0.02***	3.1 ± 0.7	2.8 ± 1.0	*0.21*	*0.22*
Apolipoprotein B (mmol/L)	0.96 ± 0.35	0.80 ± 0.28	***0.05***	0.71 ± 0.19	0.69 ± 0.18	*0.70*	*0.12*

Parametric data presented as mean ± SD, non-parametric data presented as median (IQR). Abbreviations: BMI, body mass index; HDL, high-density lipoprotein; HFD, high fat diet; HOMA-IR, homeostatic model assessment of insulin resistance; NEFA, non-esterified fatty acid; PUFA, polyunsaturated fatty acid; SFA, saturated fatty acid; comparison of males to females at baseline *p*-value represents output from unpaired student's t-test if data parametric or from Mann-Whitney test if data non-parametric; within group comparisons were made using a paired student's t-test with significance set at $p<0.05$. n=7 males, n=7 females.

As a sexual dimorphism in the partitioning of dietary SFA, compared with dietary PUFA, into oxidation pathways was observed in Chapter 3, I compared if the change from baseline to post-HFD of ^{13}C appearance into expired CO_2 differed between males and females after consuming a SFA- or PUFA-enriched HFD. After consuming a SFA-enriched HFD, the change from baseline to post-HFD of ^{13}C in expired CO_2 differed between sexes (p<0.0001 diet*time; Fig. 4.27A). At 300min (p<0.05) and 360min (p<0.01) after consuming the test meal, compared with their baseline study visit, there was a decreased appearance of ^{13}C in expired CO_2 in females, but a minimal change in males (Fig. 4.27A). After consuming a PUFA-enriched HFD, the change from baseline to post-HFD of ^{13}C in expired CO_2 tended to differ between sexes (p=0.055 diet*time; Fig. 4.27B), when compared with the respective baseline study day, females had an increased appearance of ^{13}C in expired CO_2 and males had a minimal change from baseline (Fig. 4.27B). These data suggest the observed changes in whole-body dietary FA oxidation after consuming a SFA- or PUFA-enriched HFD are primarily driven by changes in females.

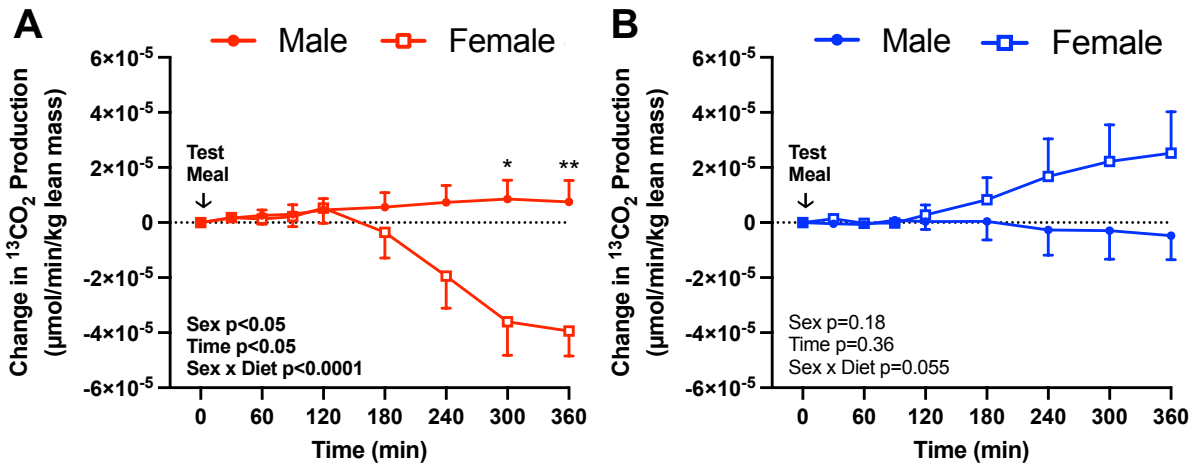

Figure 4.27. Change from baseline to post-HFD of ^{13}C appearance in expired CO_2 in males and females after consuming a (A) SFA-enriched or (B) PUFA-enriched HFD. Breath samples were collected every 30-60min from fasting for 6h and analysed by a mixed-effects model with a Sidak post-hoc test, matching each participant pre- to post-HFD. Abbreviations: HFD, high fat diet; SFA, saturated fatty acid; PUFA, polyunsaturated fatty acid. Data presented as mean ± SEM; n=7 males-SFA; n=7 females-SFA, n=7 males-PUFA, n=7 females-PUFA; empty squares (☐) indicate females, filled points (•) indicate males, red indicates SFA-enriched HFD; blue indicates PUFA-enriched HFD; * p<0.05, ** p<0.01 indicate comparisons between sexes.

The change from baseline to post-HFD of postprandial plasma biochemistry and incorporation of [U^{13}C]palmitate, [2,2-D_2]palmitate, and newly synthesised palmitate into plasma lipid pools after consuming a SFA- or PUFA-enriched HFD in males and females is shown in Appendix 2. In brief, there were no differences in postprandial plasma biochemistry and tracer incorporation into plasma lipid pools between males and females after consuming a PUFA-enriched HFD (Fig. S2.2, S2.4). However, consuming a SFA-enriched HFD led to greater postprandial plasma-TG, chylomicron-TG, and VLDL-TG excursions in males compared with females (Fig. S2.1). This may explain the greater appearance of [U^{13}C]palmitate in plasma-TG, chylomicron-TG, and VLDL-TG and [2,2-D_2]palmitate in plasma-TG and VLDL-TG in males compared with females after consuming a SFA-enriched HFD (Fig. S2.3). In contrast, females, compared with males, had a greater reduction in plasma NEFA in the later postprandial period (240-300min) after consuming a SFA-enriched HFD, which may explain the lower appearance of [U^{13}C]palmitate in plasma NEFA in females compared with males (Fig. S2.3). There were no differences between males and females in the change from baseline to post-HFD of newly synthesised palmitate in VLDL-TG after either HFD (Fig. S2.5). These findings support there may be sexual dimorphism in postprandial lipid metabolism, where consuming a SFA-, but not PUFA-enriched HFD, may lead to divergent postprandial responses in lipid metabolism between males and females.

4.3.20 Cardiac Metabolism & Function

Cardiac metabolism and function were assessed before and after consuming a SFA- or PUFA-enriched HFD to investigate if dietary FA composition directly impacts the heart. As the present study was not powered to investigate between group differences in cardiac parameters, only within group comparisons from baseline to post-HFD were made. Compared with baseline, consuming a PUFA-enriched HFD increased myocardial PCr/ATP (p<0.05),

while consuming a SFA-enriched HFD did not change myocardial PCr/ATP (Fig. 4.28). This suggests dietary FA composition may induce divergent effects on *in vivo* human cardiac energetics independent of changes in body weight.

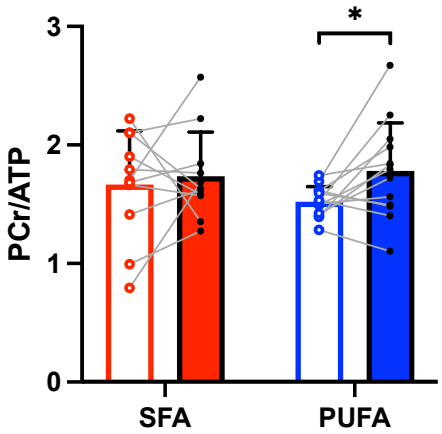

Figure 4.28. Myocardial phosphocreatine (PCr) to adenosine triphosphate (ATP) ratio before and after consuming a (red) SFA-enriched or (blue) PUFA-enriched HFD. Within group analysis performed by a paired t-test matching each participant pre- to post-HFD. Abbreviations: SFA, saturated fatty acid; PUFA, polyunsaturated fatty acid. Data presented as mean ± SD; n=11 SFA; n=13 PUFA; empty points/bars indicate baseline scan, filled points/bars indicate post-HFD scan; * indicates $p<0.05$ comparing change from baseline to post-HFD within group.

At baseline, the group randomised to consume a SFA-enriched, compared with PUFA-enriched HFD, had an increased deceleration slope ($p<0.05$; Table 4.7). Otherwise, there were no differences in baseline LV geometry, systolic or diastolic function, RV geometry and function, left atrial geometry and function, and myocardial TG content between groups (Table 4.7).

Table 4.7. Baseline Cardiac Structure and Function.

	***SFA*-Enriched Diet**	***PUFA*–Enriched Diet**	***p*-value**
LV Geometry			
End Diastolic Volume (mL)	153 (124 – 173)	153 (135 – 188)	*0.52*
End Systolic Volume (mL)	54 ± 18	63 ± 22	*0.26*
Stroke Volume (mL)	98 (81 – 111)	94 (84 – 113)	*0.98*
Myocardial Mass (g)	94 ± 25	104 ± 31	*0.36*
Myocardial Mass Index (g/m^2)	49 ± 10	52 ± 10	*0.39*
Mass-to-Volume ratio (g/mL)	0.63 ± 0.13	0.63 ± 0.10	*0.99*
LV Systolic Function			
Ejection Fraction (%)	64 ± 7	63 ± 5	*0.53*
Heart Rate (beats/min) [a]	60 ± 10	59 ± 13	*0.96*
Cardiac Output (L/min) [a]	5.86 ± 1.26	6.14 ± 1.34	*0.59*
Cardiac Output Index (L/min/m^2) [a]	2.95 ± 0.61	3.06 ± 0.47	*0.61*
Global Longitudinal Strain (%) [#]	-19.2 ± 2.5	-18.7 ± 1.6	*0.54*
Global Radial Strain (%) [#]	34.9 ± 7.2	32.8 ± 4.6	*0.39*
LV Diastolic Function			
Mitral E/A [$]	1.36 ± 0.36	1.32 ± 0.41	*0.94*
Deceleration Time (ms) [$]	216 (189 – 302)	232 (216 – 351)	*0.38*
Deceleration Slope (m/s^2) [$]	3.25 ± 0.94	2.45 ± 0.68	***0.041***
Mitral E/e' [$]	7.50 ± 1.86	7.11 ± 2.51	*0.67*
Peak Diastolic Filling Rate (mL/s)	2.97 ± 0.77	2.92 ± 0.90	*0.90*
RV Geometry & Function			
End Diastolic Volume (mL)	151 ± 33	174 ± 63	*0.24*
End Systolic Volume (mL)	57 ± 21	68 ± 30	*0.27*
Stroke Volume (mL)	95 (79 – 107)	96 (84 – 112)	*0.65*
Ejection Fraction (%)	66 (58 –70)	64 (59 – 66)	*0.55*
Cardiac Output (L/min)	5.54 ± 1.13	5.96 ± 1.63	*0.46*
Cardiac Output Index (L/min/m^2)	2.90 ± 0.63	3.08 ± 0.47	*0.42*
LA Geometry & Function			
Minimum Volume Index (mL/m^2)	13.4 (10.2 – 18.3)	11.2 (7.5 – 17.7)	*0.50*
Maximum Volume Index (mL/m^2)	39.8 (33.0 – 46.1)	37.7 (23.8 – 45.6)	*0.58*
Ejection fraction (%)	65 ± 7	66 ± 9	*0.84*
Metabolic Parameters			
Myocardial TG Content (%) [b]	1.5 ± 0.4	1.2 ± 0.3	*0.55*

Parametric data presented as mean ± SD, non-parametric data presented as median (IQR). Abbreviations: E/A, early to late ventricular filling velocity; E/e', peak early inflow velocity to peak early annular tissue diastolic velocity; PUFA, polyunsaturated fatty acid; SFA, saturated fatty acid; *p*-value represents output from student's unpaired t-test if data parametric or Mann-Whitney test if data non-parametric comparing respective values at baseline between groups. n=13 SFA, n=14 unless otherwise indicated. [a]n=13 SFA, n=13 PUFA; [#]n=12 SFA, n=13 PUFA; [$]n=10 SFA, n=11 PUFA; [b]n=12 SFA, n=10 PUFA

Compared with baseline, consuming a SFA-enriched HFD led to detrimental subclinical changes in LV systolic and diastolic function, independent of changes in body weight, as shown by increased deceleration time (p<0.05), and decreased global longitudinal strain (p<0.01), global radial strain (p<0.01), and deceleration slope (p<0.01; Table 4.7). In contrast, consuming a PUFA-enriched HFD, compared with baseline, reduced heart rate (p<0.05), LV CO (p<0.05), and tended to reduce RV and left atrial EF (both p=0.09; Table 4.7). Otherwise, consuming a SFA- or PUFA-enriched HFD for up to 24 days did not change LV geometry, RV and left atrial geometry and function, and myocardial TG content in participants free-from diagnosed CMD (Table 4.7).

Table 4.8. Effects of Dietary Fat Composition on Cardiac Structure and Function

	***SFA*-Enriched Diet**			***PUFA*–Enriched Diet**		
	Baseline	**Post-HFD**	***p*-value**	**Baseline**	**Post-HFD**	***p*-value**
LV Geometry						
End Diastolic Volume (mL)	153 (124 – 173)	153 (126 – 171)	*0.77*	153 (135 – 188)	154 (129 – 177)	*0.50*
End Systolic Volume (mL)	56 (41 – 65)	54 (46 – 67)	*0.64*	58 (50 – 75)	58 (44 – 69)	*0.95*
Stroke Volume (mL)	98 (81 – 111)	89 (81 – 114)	*0.84*	94 (84 – 113)	100 (84 – 112)	*0.90*
Myocardial Mass (g)	94 ± 7	96 ± 7	*0.34*	104 ± 8	107 ± 8	*0.37*
Myocardial Mass Index (g/m^2)	49 ± 3	50 ± 3	*0.32*	52 ± 3	54 ± 3	*0.13*
Mass-to-Volume ratio (g/mL)	0.62 (0.53 – 0.71)	0.61 (0.57 – 0.69)	*0.69*	0.61 (0.54 – 0.70)	0.64 (0.60 – 0.71)	*0.32*
LV Systolic Function						
Ejection Fraction (%)	64 ± 2	63 ± 2	*0.62*	63 ± 1	63 ± 1	*0.67*
Heart Rate (beats/min) [a]	60 ± 3	58 ± 2	*0.49*	59 ± 4	54 ± 3	***0.04***
Cardiac Output (L/min) [a]	5.86 ± 0.35	5.54 ± 0.46	*0.42*	6.14 ± 0.37	5.56 ± 0.31	***0.04***
Cardiac Output Index ($L/min/m^2$) [a]	2.95 ± 0.17	2.85 ± 0.20	*0.52*	3.06 ± 0.14	2.83 ± 0.11	*0.12*
Global Longitudinal Strain (%) [#]	-19.2 ± 0.7	-18.2 ± 0.7	***0.004***	-18.7 ± 0.4	-18.5 ± 0.5	*0.65*
Global Radial Strain (%) [#]	34.9 ± 2.1	31.3 ± 1.9	***0.005***	32.8 ± 1.3	32.0 ± 1.4	*0.58*
LV Diastolic Function						
Mitral E/A [$]	1.36 ± 0.11	1.35 ± 0.09	*0.96*	1.32 ± 0.12	1.42 ± 0.09	*0.59*
Deceleration Time (ms) [$]	216 (189 – 302)	260 (237 – 318)	***0.01***	232 (216 – 351)	215 (172 – 291)	*0.12*
Deceleration Slope (m/s^2) [$]	3.25 ± 0.31	2.42 ± 0.23	***0.001***	2.45 ± 0.21	2.89 ± 0.18	*0.06*
Mitral E/e' [$]	7.26 (6.08 – 9.10)	7.06 (6.10 – 8.07)	*0.43*	6.77 (4.53 – 9.57)	6.25 (5.23 – 9.44)	*0.73*
Peak Diastolic Filling Rate (mL/s)	2.97 ± 0.21	2.91 ± 0.21	*0.81*	2.92 ± 0.24	2.85 ± 0.19	*0.81*

RV Geometry & Function						
End Diastolic Volume (mL)	146 (126 – 183)	151 (127 – 175)	*0.83*	156 (128 – 204)	159 (140 – 190)	*0.85*
End Systolic Volume (mL)	50 (43 – 80)	57 (46 – 63)	*0.50*	61 (44 – 88)	61 (54 – 80)	*0.76*
Stroke Volume (mL)	95 (79 – 107)	88 (78 – 112)	*0.89*	96 (84 – 112)	101 (84 – 114)	*0.76*
Ejection Fraction (%)	66 (58 –70)	62 (59 – 65)	*0.41*	64 (59 – 66)	60 (57 – 66)	*0.09*
Cardiac Output (L/min)	5.54 ± 0.31	5.42 ± 0.41	*0.67*	5.96 ± 0.45	5.59 ± 0.31	*0.38*
Cardiac Output Index (L/min/m^2)	2.90 ± 0.17	2.81 ± 0.19	*0.52*	3.08 ± 0.13	2.85 ± 0.11	*0.08*
LA Geometry & Function						
Minimum Volume Index (mL/m^2)	13.4 (10.2 – 18.3)	12.8 (8.6 – 18.5)	*0.60*	11.2 (7.5 – 17.7)	16.5 (11.4 – 20.7)	*0.40*
Maximum Volume Index (mL/m^2)	39.8 (33.0 – 46.1)	40.5 (32.9 – 46.8)	*0.74*	37.7 (23.8 – 45.6)	49.4 (41.6 – 62.5)	*0.30*
Ejection fraction (%)	65 ± 2	65 ± 2	*0.72*	66 ± 3	61 ± 1	*0.09*
Metabolic Parameters						
Myocardial TG Content (%) [b]	1.5 ± 0.4	1.0 ± 0.2	*0.30*	1.2 ± 0.3	1.3 ± 0.3	*0.66*

Parametric data presented as mean ± SEM, non-parametric data presented as median (IQR). Abbreviations: E/A, early to late ventricular filling velocity; E/e', peak early mitral inflow velocity to peak early mitral annular tissue diastolic velocity; HFD, high-fat diet; PUFA, polyunsaturated fatty acid; SFA, saturated fatty acid; TG, triglyceride; *p*-value represent, if data is parametric, output from paired student's t-test, or if non-parametric, output from Wilcoxon matched-pairs signed rank test comparing values post-HFD to baseline within each group. n=13 SFA, n=14 unless otherwise indicated, [a]n=13 SFA, n=13 PUFA; [#]n=12 SFA, n=13 PUFA; [$]n=10 SFA, n=11 PUFA, [b]n=12 SFA, n=11 PUFA.

4.3.21 Blood Pressures & Aortic Distensibility

Blood pressures and AD responded differently following consumption of a SFA-, compared with PUFA-enriched HFD. There were diet*time interactions for systolic blood pressure (p<0.05), mean arterial pressure (p<0.05), and ascending AD (p<0.01; Fig. 4.29A, C-D). When compared with baseline, consuming a PUFA-enriched HFD reduced systolic blood pressure (p<0.001), mean arterial pressure (p<0.05), and ascending AD (p<0.05; Fig. 4.29A, C-D). After consuming a SFA-enriched HFD, systolic blood pressure, mean arterial pressure, and ascending AD were similar to baseline. Diastolic blood pressure, and proximal and distal descending AD were similar to baseline after consuming either HFD (Fig. 4.29A-E).

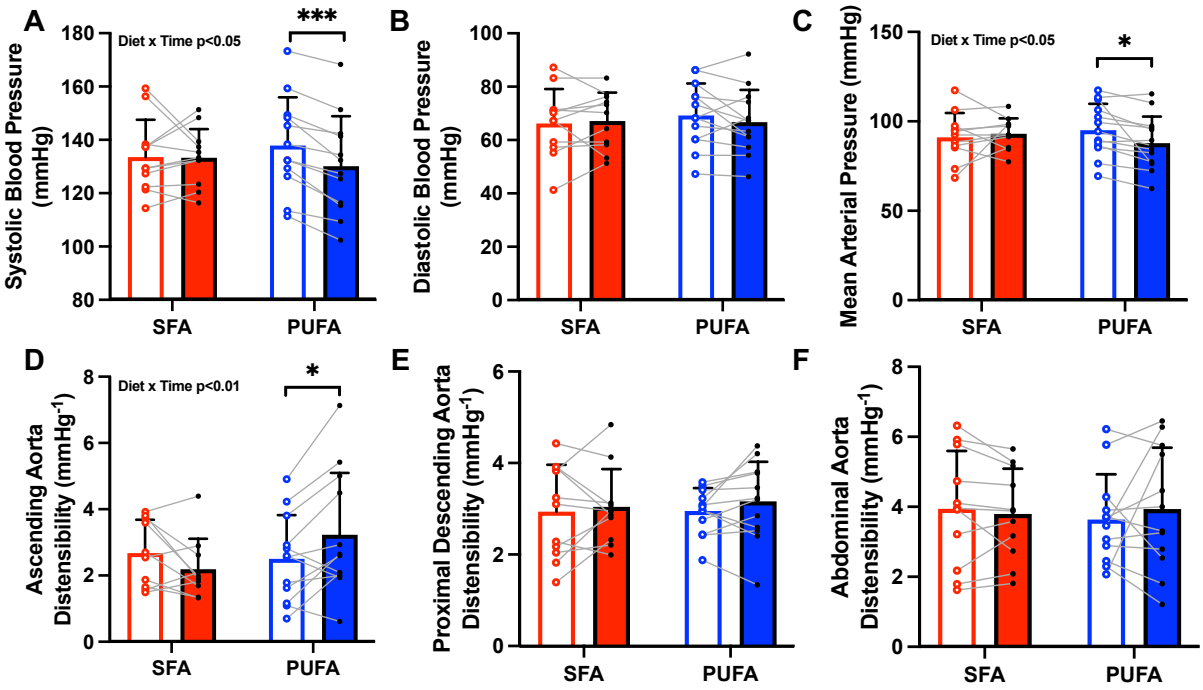

Figure 4.29. (A) Systolic, (B) diastolic, and (C) mean arterial blood pressure, and (D) ascending, (E) proximal descending, and (F) distal descending aortic distensibility before and after consuming a (red) SFA-enriched or (blue) PUFA-enriched HFD. Diet*time interaction p-value represents output from 2-way ANCOVA baseline values for each parameter were used as a covariate in the analysis of that parameter with pre- to post-HFD values matched by participant. If a significant interaction effect was present (diet*time p<0.05), within group comparisons were made using a Sidak post-hoc test with * indicating a significant (p<0.05) change from baseline to post-HFD within group. Abbreviations: SFA, saturated fatty acid; PUFA, polyunsaturated fatty acid. Data presented as mean ± SD; n=11 SFA; n=13 PUFA; empty points/bars indicate baseline scan, filled points/bars indicate post-HFD scan.

4.4 Discussion

To investigate if dietary FA composition impacts IHTG content, hepatic and systemic metabolism, and cardiac metabolism and function, participants free-from diagnosed metabolic disease underwent an MRI/S scan and postprandial study day with stable-isotope tracers before and after consuming an isocaloric SFA- or PUFA-enriched HFD under free living conditions for up to 24 days. Despite no change in body weight or body composition, consuming a PUFA-enriched HFD reduced IHTG content while consuming a SFA-enriched HFD tended to increase IHTG content. Further, consuming a PUFA-enriched HFD increased, while consuming a SFA-enriched HFD decreased markers of whole-body dietary FA oxidation. These findings suggest dietary FA composition induces divergent effects on whole-body FA oxidation, which may lead to divergent effects on IHTG content. In the current study, dietary FA composition impacted other CMD risk factors as consuming a PUFA-enriched HFD improved systolic and mean arterial blood pressures, myocardial PCr/ATP, markers of cardiac function, and increased ISR, while consuming a SFA-enriched diet adversely altered markers of cardiac function, insulin resistance, fasting and postprandial lipids. Taken together, these findings suggest dietary FA composition, independent of changes in body weight, impacts CMD risk.

4.4.1 Whole-Body FA Oxidation

Previous studies where participants consumed a SFA- or PUFA-enriched diet either did not assess FA oxidation, or used indirect calorimetry or plasma biomarkers to do so; these studies found minimal changes FA oxidation after consuming a PUFA-enriched, compared with SFA-enriched diet (11, 79, 187). In the current study, FA oxidation was assessed by measuring postprandial ^{13}C appearance (from a ^{13}C-labelled dietary FA) in expired CO_2 and it was observed that consuming a PUFA-enriched HFD increased, while consuming a SFA-enriched HFD decreased ^{13}C appearance in expired CO_2; this suggests dietary FA composition

leads to opposing effects on dietary FA oxidation. The findings in the current study agree with other studies which measured FA oxidation using stable-isotope tracers and support an inverse relationship between IHTG content and FA oxidation (227). As PUFAs activate PPARα to a greater extent than SFAs, consuming a PUFA-enriched HFD may increase FA oxidation capacity, which may explain the increased ^{13}C appearance in expired CO_2 after consuming a PUFA-enriched HFD (308). In contrast, *in vivo* studies in humans have shown consuming a single high-SFA, compared with high-PUFA, meal downregulates genes involved in oxidative phosphorylation, therefore, consumption of a SFA-enriched HFD may reduce FA oxidation capacity, which could explain the decreased ^{13}C appearance in expired CO_2 (309). Further, if consuming a SFA-enriched HFD delayed gastric emptying and/or absorption, this could delay delivery of the ^{13}C-labelled FA to peripheral tissues and contribute to the observed decrease ^{13}C appearance in expired CO_2.

4.4.2 Cardiac Metabolism, Function & Aortic Distensibility

Through utilisation of a radiotracer and PET imaging, Rosqvist *et al*. demonstrated that overconsuming SFA- and PUFA-enriched diets similarly increase myocardial palmitate uptake, this suggests dietary FA composition may not differentially impact cardiac FA uptake mechanisms (11). However, as SFAs and PUFAs appear to undergo differential intracellular handling such that PUFAs, compared with SFAs, preferentially enter oxidation pathways and upregulate FA oxidation genes, this may explain the increased myocardial PCr/ATP after consuming a PUFA-enriched HFD (92, 194, 289, 308). The minimal change in myocardial PCr/ATP after consuming a SFA-enriched HFD may result from the diet not influencing myocardial PCr/ATP or the diet reducing absolute levels of myocardial PCr and ATP, which would decrease myocardial energetic reserve but lead to a similar PCr/ATP ratio (113). In the current study, baseline myocardial PCr/ATP was slightly lower than typically reported in disease-free adults (310). Even though saturation bands were placed over the liver, the DRESS

sequence acquires data in a large slice and likely captures some hepatic signal which may lower the measured PCr/ATP values.

The reduction in systolic and mean arterial blood pressures, and ascending AD in participants after consuming a PUFA-enriched HFD may be explained by the reduced LV CO secondary to the reduced heart rate. As PUFAs inhibit calcium and sodium channels and activate potassium channels, this may explain the reduced heart rate in participants which consume a PUFA-enriched HFD (246, 247). After consuming a PUFA-enriched HFD, the degree of reduction in systolic blood pressure was similar to that observed in patients starting angiotensin converting enzyme inhibitors (311). The adverse subclinical changes in LV systolic and diastolic function after consuming a SFA-enriched HFD agree with findings from large animal studies that found when dogs and grizzly bears were fed a SFA-enriched, compared with PUFA-enriched diet, they have impaired LV systolic and diastolic function (239, 240). As consuming a PUFA-, but not SFA-enriched HFD, reduced systolic and mean arterial blood pressures this may reduce cardiac afterload and may, in part, help explain the observed divergent effects of dietary FA composition on cardiac function. Alternatively, increased myocardial SFA content, in response to consuming a SFA-enriched HFD, may impair cardiac energetics, inappropriately increase membrane phospholipid FA saturation, and/or increase cardiac ceramide content, all of which are linked with impaired cardiac function (79, 113, 244, 245, 312). Overall, the current work demonstrates, for the first time, that dietary FA composition impacts cardiac function in humans in the absence of body weight changes.

4.4.3 Glucose Metabolism & Insulin Kinetics

Findings presented here agree with some reports that consuming a SFA-, compared with PUFA-enriched diet increases markers of insulin resistance, and consuming a PUFA-, compared with SFA-enriched diet improves markers of insulin sensitivity (10, 61, 79, 192, 309, 313-317). However, changes in insulin resistance from baseline to post-intervention were not

as pronounced in this study as in previous studies, which may be due to participants in previous studies gaining weight, which likely exacerbates insulin resistance development, or consuming the experimental diet for longer (i.e. 6-10 weeks) (10, 61, 79, 192, 313). In the current study, there was sexual dimorphism in the glycaemic response to consuming a SFA-enriched diet and as some previous studies only investigated male participants (192, 309, 313, 314, 317), the difference in findings for markers of insulin resistance between studies may, in part, be explained by the inclusion of males and females in this study.

Dietary FA composition induced divergent effects on postprandial plasma glucose and ISR, where consuming a SFA-enriched HFD, compared with baseline, led to a prolonged postprandial glucose excursion, and consuming a PUFA-, compared with SFA-enriched HFD, induced a greater increase in ISR. In part, this may be explained by the consumption of a SFA-enriched HFD delaying gastric emptying and/or absorption, which would prolong glucose absorption, or the consumption of a SFA-enriched HFD increasing pancreatic β-cell SFA content and impairing insulin secretion; both could blunt the increase in ISR (318). In this study, consuming a SFA- or PUFA-enriched HFD did not lead to different effects on ICR and insulin extraction. As insulin is secreted from pancreatic β-cells and cleared by the liver, this suggests dietary FA composition may induce divergent effects on pancreatic β-cell function. Consuming a PUFA-enriched, compared with SFA-enriched HFD, could modulate release of incretins like gastric inhibitory peptide (GIP) and GLP1, hormones which promote glucose-dependent insulin secretion (319). Further, PUFAs reduce the threshold for glucose-stimulated insulin release by increasing calcium currents and reducing potassium currents in pancreatic β-cells (320-322). Taken together, this may explain the greater increase in ISR following an identical mixed test meal in participants which consumed the PUFA-enriched, compared with SFA-enriched HFD.

4.4.4 Lipid Metabolism

Consuming a SFA-enriched, but not PUFA-enriched HFD, altered the postprandial plasma NEFA profile, where during fasting and the later postprandial period, plasma NEFA concentrations were lower compared with baseline, but during peak insulin concentrations, reached a higher nadir. This postprandial plasma NEFA profile resembles the behaviour of adipose tissue from obese individuals, where there is blunted FA release and uptake following fasting and feeding compared with adipose tissue from lean individuals (80). Overfeeding studies suggest increased adipose-tissue lipolysis may contribute to increased IHTG content in response to consuming a SFA-enriched diet (79), however, adipose-tissue lipolysis was decreased in this study after consuming a SFA-enriched HFD. As participants gained weight during overfeeding studies but did not gain weight in the present study, this may, in part, explain the discrepancy in these findings. Consuming a SFA-enriched HFD reduced tracer appearance in chylomicron-derived spillover NEFA, which may be explained by the SFA-enriched HFD delaying gastric emptying and/or absorption of the tracer-containing test meal and therefore, the appearance of ^{13}C in the plasma NEFA pool. Despite no change in bodyweight, consuming a SFA-enriched, but not PUFA-enriched HFD may lead to detrimental changes in adipose tissue function and lipid metabolism, and it could be speculated that if a SFA-enriched HFD were consumed for longer, adipose tissue function may continue to change towards this obese-adipose tissue phenotype with adverse consequence on metabolic health.

4.4.5 Hepatic DNL

Compared with disease-free, lean controls, increased hepatic DNL has been reported in patients with MASLD and insulin resistance, and is often speculated to contribute to IHTG accumulation (323). In the current study, dietary FA composition did not have divergent effects on hepatic DNL despite leading to opposing effects on IHTG accumulation. This discrepancy

in the contribution of DNL to IHTG accumulation may be explained by participants with MASLD and IR having different intrahepatic metabolism than participants investigated in this study, who do not have diagnosed MASLD and insulin resistance (94). Alternatively, differences in participant's dietary macronutrient consumption between studies may explain the discrepancy in hepatic DNL findings. Broadly, two dietary patterns tend to be associated with increased IHTG accumulation – one enriched with sugars and one enriched with SFAs – (79, 324) and studies have shown that consuming a sugar-enriched, compared with SFA-enriched diet increases hepatic DNL (79, 192). Further, overfeeding dietary SFAs, compared with PUFAs, does not lead to divergent effects on hepatic DNL, which is in line with findings in this study. Taken together, this suggests hepatic DNL may contribute to IHTG accumulation in the context of a sugar-enriched, but not SFA- or PUFA-enriched diets.

4.4.6 Limitations

This study is not without limitations. Participants were advised to modify their habitual diet to meet target SFA-, PUFA-, and total fat intakes. Compared with studies which provided participants with specific snacks or all food, there may be increased inter-participant variability in the amounts of SFA-, PUFA-, or fat consumed (10, 11, 313). While changes in plasma-TG FA composition was used as a biomarker of dietary FA intake, changes in hepatic DNL, which produce SFAs, but not PUFAs, could impact this biomarker. However, as each participant's plasma lipid FA composition changed appropriately, with a minimal change in body weight from baseline, this indicates participants likely consumed the foods they reported to have consumed. The dietary intervention lasted up to 24-days to balance participant compliance with changes in metabolic parameters, however, it is unclear if my findings represent changes in metabolic health that would continue to develop if the participants continued to consume the diets or transient adaptations to the diet. During the standardisation diet and dietary intervention, physical activity or alcohol intake were not controlled for, and I cannot exclude

that a change in either or inclusion of individuals with moderate alcohol intake (14-21 units per week) influenced IHTG content. During study days, palmitate was used to trace the handling of dietary FAs, which may or may not reflect the handling of other FAs (92, 194, 289). However, using the same dietary FA tracer for both groups allowed for between group comparisons. In this study, individuals free-from diagnosed metabolic disease were investigated, it is unclear to what extent findings may be generalised to patient populations (e.g those with MASLD); it would be of interest to perform such studies.

4.4.7 Conclusion

Consuming a SFA-enriched, compared with a PUFA-enriched HFD for a relatively short period altered IHTG accumulation, plasma lipids, blood pressures, insulin kinetics, postprandial metabolism, and cardiac metabolism and function, independent of changes in bodyweight. If either HFD were continued, it could be speculated that over time, the effects on developing CVD, insulin resistance, MASLD, and/or T2D would be exacerbated. Further, preliminary data in this chapter suggests there is a sexual dimorphism in how diet influences CMD risk. This highlights that sex-specific dietary guidelines may be needed to appropriate manage CMD risk.

Chapter 5

Fatty acid composition, independent of quantity, induces divergent metabolic and nonmetabolic responses in human cardiomyocytes

5.1 Introduction

Dietary fat quantity and composition influence CMD risk; while there is substantial evidence linking dietary patterns enriched in total fat and SFA content with adverse changes in soluble CMD risk factors, there are few studies investigating the effects of dietary FA composition on cardiac metabolism and function (143, 152, 153). Yet, emerging evidence suggests that increased plasma FA, glucose, and insulin resistance induce cardiac dysfunction independent of other CMD risk factors and the presence of other CVDs (325). While this suggests that metabolic substrates, such as FA, have direct effects on the heart, the mechanisms linking alterations in plasma FA to cardiomyocyte dysfunction remain to be elucidated.

Chronically elevated plasma FAs increase myocardial FA availability (11). This shifts cardiac metabolism towards generating a greater proportion of ATP from FAs, which impairs cardiac ATP production and results in cardiac dysfunction (124, 126). Additionally, there is emerging evidence that FAs and their downstream metabolites modulate nonmetabolic cellular processes including epigenetic modifications, gene transcription, post-translational modifications, protein subcellular localisation, intracellular signalling cascades, and stress responses (326-330). Impairing nonmetabolic processes within cardiomyocytes may be a secondary mechanism by which increased plasma FAs contribute to cardiac dysfunction. Yet, these metabolic and nonmetabolic effects of FA on cardiomyocytes have been primarily characterised in response to different FA concentrations, few studies have investigated how FA composition impacts human cardiomyocyte function. As dietary FA composition influences plasma FA composition, and cardiac FA uptake is influenced by plasma FA availability, it is plausible that dietary FA composition could directly impact cardiomyocyte function.

I demonstrated in Chapter 4 that dietary FA composition induces divergent effects on *in vivo* human cardiac energetics and function. However, no previous studies have investigated

how the FA composition of a physiological concentration of FAs impacts cardiomyocyte physiology *in vitro*. Therefore, the aim of this study was to characterise, at a cellular level, how dietary FA composition, independent of FA quantity, impacts cardiomyocyte function. To model the cardiac effects of the SFA- and PUFA-enriched diets from Chapter 4, human inducible pluripotent stem cell (hiPSC) derived cardiomyocytes (hiPSC-CMs) were treated with a physiological concentration of a lipid-mix containing four FAs in different proportions such that one lipid-mix was enriched in SFA and the other in PUFA. Following the treatment period, cell stress markers, media metabolite uptake, and transcriptomic responses were compared between these two groups.

5.2 Materials & Methods

5.2.1 Cell Culture Methodology

5.2.1.1 hiPSC Maintenance & Differentiation into Cardiomyocytes

All experiments were conducting using IMR-90 cells gifted from Imperial College London by Prof. Sian Harding, these are an hiPSC cell-line derived from lung fibroblasts obtained from a 16-wk-old Caucasian female foetus (331). To start each experiment, cells were removed from liquid nitrogen, rapidly thawed, and suspended in phosphate buffered saline (PBS). Following centrifugation, the pellet was resuspended in TeSR-E8 media. Cells were seeded on 6-well plates coated with Matrigel to increase cell adherence and cultured as a 2D monolayer. Daily media changes were performed using TeSR-E8 media and cells were split at >90% confluence.

Differentiation into hiPSC-CMs was carried out by modulating Wnt-signalling and metabolically selecting for cardiomyocytes (332) (Fig. 5.1). At the start of differentiation (day 0; D0), Roswell Park Memorial Institute (RPMI) 1640 media supplemented with 1% B27

minus insulin (RB-) and 6μM CHIR99201 was added to each well (Fig. 5.1). CHIR99201 activates Wnt signalling to direct iPSCs towards a mesodermal lineage. On D2, media was replaced with RB- media, the following day (D3), media was changed to RB- media supplemented with 2.5μM Wnt-C59. Wnt-C59 inhibits Wnt signalling to direct mesodermal cell differentiation towards cardiac progenitor cells. From D5 to D11, media was changed every other day using RB- media, with evidence of beating beginning on D9. On D11, wells contained a mixture of hiPSC-CMs and non-cardiomyocytes (such as fibroblasts); therefore, a metabolic selection was carried out using RPMI 1640 without glucose supplemented with 1% B27 minus insulin to starve off glucose-dependent non-cardiomyocytes. Our group has shown from D15, wells contain predominantly hiPSC-CMs as ~80-85% of cells stain positive for alpha-actinin, a cardiomyocyte marker (333). Until starting the experimental protocol, media was changed every other day using RPMI 1640 supplemented with 1% B27 complete (RB+).

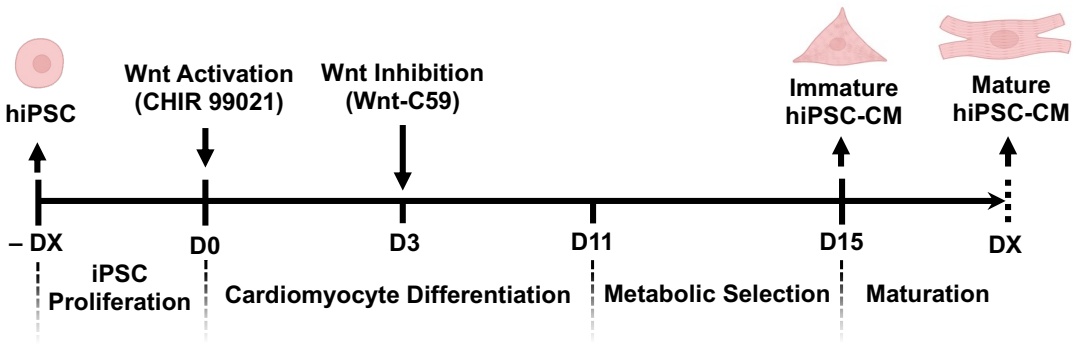

Figure 5.1. Overview of the protocol for differentiating human induced pluripotent stem cells (iPSCs) into cardiomyocytes (hiPSC-CMs).

At the end of differentiation, hiPSC-CMs from all wells were pooled and cell number and viability were assessed by loading a 1:1 mixture of hiPSC-CMs and 0.4% Trypan Blue into a Countess Automated Cell Counter (ThermoFisher Scientific). Cell number and viability were measured three times and averaged, aiming for >95% cell viability and enough cells such that >$6x10^5$ cells could be seeded per well in 12-well plates. In my experiments, cell viability was ~92%, which is acceptable, and $8x10^6$ hiPSC-CMs were seeded per well to ensure equal cell numbers per condition in further experiments. Following counting and reseeding, hiPSC-CMs

were left for 2-3 days before starting the experimental protocol with media changes performed every other day using RB+ media.

5.2.2 hiPSC-CM Experimental Protocol

hiPSC-CMs were incubated in media supplemented with either 400µM SFA-enriched or PUFA-enriched lipid-mix, no FA, or 76µM OA to investigate how FA composition impacts cardiomyocyte function. Media for the hiPSC-CM experimental protocol consisted of Dulbecco's Modified Eagle Medium (DMEM) (5.5mM glucose) with 10% inactivated horse serum, 5µg/mL vitamin B12, 0.5mM vitamin C, 0.82µM biotin, 50nM insulin, 0.5mM non-essential amino acids, 20U/mL penicillin/streptomycin, and, depending on the group, bovine-serum album (BSA) complexed to either no FA, 76µM OA, or 400µM SFA-enriched or PUFA-enriched lipid mix (Fig. 5.2). hiPSC-CMs were treated for 8 days with media changes every other day; this duration was chosen as our group has previously characterised hiPSC-CMs treated with 76µM OA for 8-days post-differentiation (333). Media aliquots were stored at -20˚C for further analysis, collected from fresh media and from cells after the first two days (D17-19) and last two days (D23-25) of the experimental protocol (Fig. 5.2).

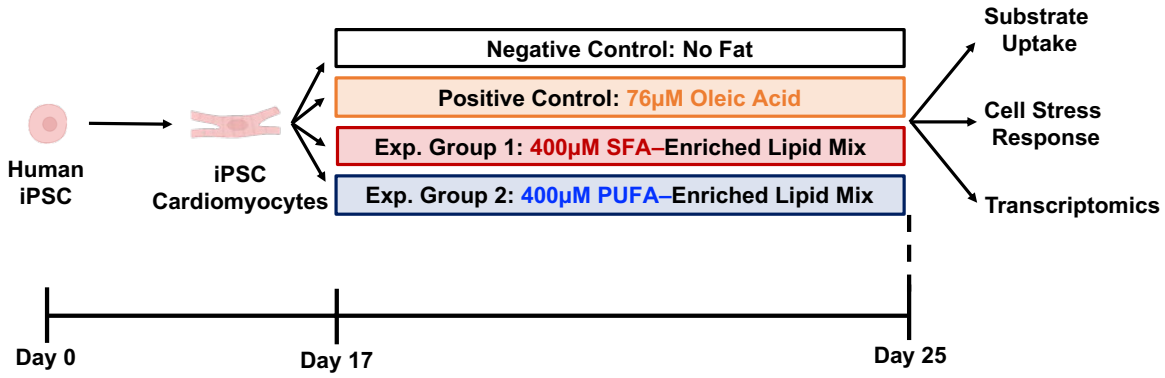

Figure 5.2. Overview of the experimental design to investigate the effect of media fatty acid composition on human induced pluripotent stem cell (iPSC) derived-cardiomyocyte cell physiology.

The FA-BSA solution was prepared by filtering 5% w/v BSA in DMEM/F-12 media, with no glucose and no phenol red. Three different 0.5M FA solutions were prepared on a 90˚C

heat block for each FA-containing experimental group. The OA group FA mixture was prepared by adding 281µL OA (1.77M) to 719µL ethanol (100%). The SFA-enriched FA mixture was prepared by dissolving 76.9mg palmitic acid in 884.4µL ethanol (100%) and adding 82µL OA (1.77M), 28µL LA (1.78M), and 5.57µL ALA (0.898M); a FA mixture containing 60% palmitate (SFA), 29% OA (MUFA), 10% LA (PUFA), and 1% ALA (PUFA) (Table 5.1). The PUFA-enriched FA mixture was prepared by dissolving 32.0mg palmitic acid in 786µL ethanol (100%) and adding 142.2µL OA (1.77M), 67.4µL LA (1.78 M), and 5.57µL ALA (0.898 M); a FA mixture containing 25% palmitate, 50% OA, 24% LA, and 1% ALA (Table 1). Each 0.5M FA mixture was added dropwise to 5% BSA at 30˚C to produce a 5mM stock FA:BSA solution. The stock solution was filtered and FA concentration measured using a plasma analyser (section 2.3.2) so the appropriate amount of each FA:BSA stock could be added to make media with 400µM SFA- or PUFA-enriched lipid mix, 76µM OA, or BSA with no FA.

Following the experimental protocol, each well was washed three times with PBS, and TRIzol Reagent or lysis buffer was added for ribonucleic acid (RNA) or protein extraction, respectively. Cells were collected and homogenised by pipetting with a 23G needle and stored at -80˚C until analysis.

Table 5.1. Lipid Composition of Saturated- and Polyunsaturated-Fatty Acid Enriched Lipid Mix

	SFA-Mix	PUFA-Mix
Palmitate	60%	25%
Oleate	29%	50%
Linoleate	10%	24%
α-Linoleate	1%	1%

Abbreviations: SFA, saturated fatty acid; PUFA, polyunsaturated fatty acid.

5.2.3 Quantification of Cellular Integrity & Metabolism

5.2.3.1 Analytical Methods

Glucose, NEFA, and lactate were measured in media placed on hiPSC-CMs and in media collected 48h later using a semi-automatic analyser (iLab 480 Clinical Chemistry, Warrington,

UK; section 2.3.2). Lactate dehydrogenase (LDH) release into the media was measured using an automated ABX Pentra 400 Chemistry Analyser (Monarch Laboratories, USA); the LDH reagent reacts with LDH in the media to form a colorimetric product so that LDH concentrations can be determined by spectrophotometry. All media measurements were performed in duplicate and averaged.

5.2.3.2 Protein Quantification

Protein concentrations were measured in hiPSC-CMs cell lysates collected in lysis buffer using a bicinchoninic acid (BCA) protein assay as per manufacturer's instruction. In this assay, a colorimetric product is formed in proportion to the sample's protein concentration and protein concentration is determined by spectrophotometry.

5.2.4 Quantification of Gene Expression

5.2.4.1 RNA Extraction

RNA was extracted from hiPSC-CM cell lysates collected in TRIZOL using the Qiagen RNEasy Mini-Kit following the manufacturer's instructions, including the optional DNase digestion. RNA concentration and purity were measured by Nanodrop UV spectrophotometry, aiming for RNA concentrations >100ng/µL and A260/280nm ratio 1.9–2.1. Extracted RNA was used for quantitative polymerase chain reaction (qPCR) analysis and bulk RNA-sequencing by Novogene.

5.2.4.2 cDNA Synthesis & Quantitative PCR

Complementary deoxyribonucleic acid (cDNA) was synthesised from extracted RNA using a high-capacity cDNA Reverse Transcription Kit as per manufacturer's instructions in a SensoQuest Basic Thermal Labcycler (Geneflow Limited, Lichfield, UK). For qPCR, 15ng cDNA (5ng/µL), 5µL SYBR Green MasterMix, and 1µL of forward and reverse primer

(600nM) were loaded into each well and run on a Step-One Plus Real-Time PCR system (Applied Biosystems, ThermoFisher Scientific). Genes of interest and respective forward and reverse primers are listed in Supplemental Table 3.1. Relative gene expression was quantified using the ΔΔCT method (334) by comparing the expression of a gene of interest, which may vary between experimental conditions, to a housekeeping gene, ubiquitin C (*UBC*), which was confirmed to not vary in expression between experimental conditions (Fig. S3.1). For each gene, the fold-change in gene expression for each sample was normalised to no-fat treated hiPSC-CMs if all experimental groups are presented or PUFA-enriched lipid-mix treated hiPSC-CMs if only lipid-mix treated hiPSC-CMs are presented; normalised values were used for further analysis and visualisation.

5.2.4.3 Transcriptomic Analysis

Bulk RNA-sequencing was performed by Novogene on RNA extracted from hiPSC-CMs. Novogene sequenced RNA samples using an Illumina paired-end 150-bp poly-A enrichment protocol, checked read quality, and aligned sample transcripts to the human genome to provide me with raw gene counts for further analysis. Each sample was sequenced to a depth of 30 million reads with 6 samples per group.

Transcriptomic analysis was performed in R (V4.5.0) with RStudio (V2024.09.1+394). Using the EdgeR package (V 4.4.2) (335), raw gene counts were filtered to remove genes with low expression, defined as a count-per-million below the minimum cutoff determined by the package's default settings, and normalised using the trimmed mean of M-values (TMM) method to adjust for differences in library size post-filtering (336). To visualise variation in gene expression between samples, principle component analysis (PCA) was carried out using FactoMineR (V2.11) and factoextra (V1.0.7) packages. To characterise differences in gene expression between groups, a mixed effects model was created with the limma package (V3.62.1) using filtered and normalised gene counts (337). Differences in gene expression

between experimental groups were considered a fixed effect, while differences in gene expression between samples within an experimental group were considered a random effect. Further, variation in gene expression due to sample position on a cell culture plate, a predictable variable, were controlled for in this model as a covariate. This approach increases the model's statistical power while allowing for random differences in gene expression between replicates. Using this model, three comparisons were investigated: *i)* hiPSC-CMs cultured in OA vs. no-fat, *ii)* lipid mix (group formed by combining SFA-enriched and PUFA-enriched lipid mix groups) vs. no-fat, and *iii)* SFA-enriched lipid mix vs. PUFA-enriched lipid mix. Differentially expressed genes were identified by a false discovery rate (FDR)<0.05.

Volcano plots were generated with the EnhancedVolcano package (V1.24.0), using an FDR<0.05 and $\log_2$ fold change (FC) <0.2 as cut-offs to visualise differentially expressed genes. Gene set enrichment analysis (GSEA) was performed to characterise differentially regulated pathways between conditions using the fgsea package (V1.32.0) and Molecular Signatures Database (MSigDB) hallmark gene set pathways (338). When analysing differentially regulated pathways between hiPSC-CMs treated with a SFA- or PUFA-enriched lipid mix, a secondary pathway analysis using the clusterProfiler package (V4.14.4) and Gene Ontology (GO) Biological Processes pathways (339, 340) was performed to confirm findings from the first pathway analysis. Differentially regulated pathways were identified by an FDR<0.05 and visualised using the ggplot2 package (V3.5.1). To predict which transcription factor(s) (TF) may be differentially active between treatment conditions, significantly upregulated genes from a transcriptomic comparison of interest were analysed using the Enrichr webtool and TRRUST Transcription Factor 2019 database (341, 342). The predicted TF activation was visualised using the Enrichr webtool's interactive software, with differentially active TF(s) identified by a p_{adj}<0.05 from Enrichr's internal enrichment calculation (343).

5.2.5 Statistical analysis

Transcriptomic data was analysed as described in section 5.2.5. The remaining data was analysed using Graphpad Prism (V10.9.1) Software for Mac (San Diego, California USA). The Shapiro–Wilk normality test was used to check data distribution, the Levene test was used to check if groups had equal variances, and the Grubb's test was used to check for outliers, which were removed if present. Protein and RNA concentration, media LDH, gene expression data, and media metabolite uptake and secretion data were presented as mean ± SEM if parametric or median (IQR) if non-parametric and analysed using the appropriate parametric or non-parametric test. Results with more than two groups were compared using *i*) a one–way repeated–measures analysis of variance (ANOVA)) with Tukey's post–hoc test if data distribution was normal and variance between groups equal, *ii*) Brown-Forsythe and Welch ANOVA test with a Dunnett T3 post-hoc test if data distribution was normal and variance between groups was not equal, or *iii*) Kruskal-Wallis test with Dunn's post-hoc if data distribution was not normal. Gene expression data with only two groups was analysed with a Welch's t-test. Statistical significance was set at $p<0.05$ or FDR<0.05 as appropriate.

5.3 Results

5.3.1 Effect of media FA composition on cell viability and stress responses

To determine if culturing hiPSC-CMs in different FA concentrations and compositions impacted cell viability, protein and RNA concentrations, and markers of cell death and stress were assessed. Protein (Fig. 5.3A) and RNA concentrations (Fig. 5.3B) were measured at the end of the experimental protocol, as decreases in either may indicate cell death; no reductions in either parameter were observed between conditions. In contrast, protein concentrations in PUFA-enriched lipid mix treated hiPSC-CMs were increased compared with no-fat treated hiPSC-CMs ($p<0.05$; Fig. 5.3A). To characterise cell death, LDH release into the media was

measured during the final 48h of the experimental protocol and no differences between conditions were observed (Fig. 5.3C) suggesting minimal cell death. To assess if culturing hiPSC-CMs in different lipid mixes activated cell stress responses, *BNIP3* expression, which increases in response to mitochondrial stress, was measured by qPCR and found to be comparable across groups (Fig. 5.3D). *BNIP3* expression in the OA-group is not reported due to an error when preparing the OA-group experimental media for the batch of cells used for this experiment; the cells did not beat and were therefore not viable for analysis. Taken together, these findings suggest culturing hiPSC-CMs in a physiological concentration of a FA lipid-mix, does not induce significant cell stress, dysfunction, or death responses.

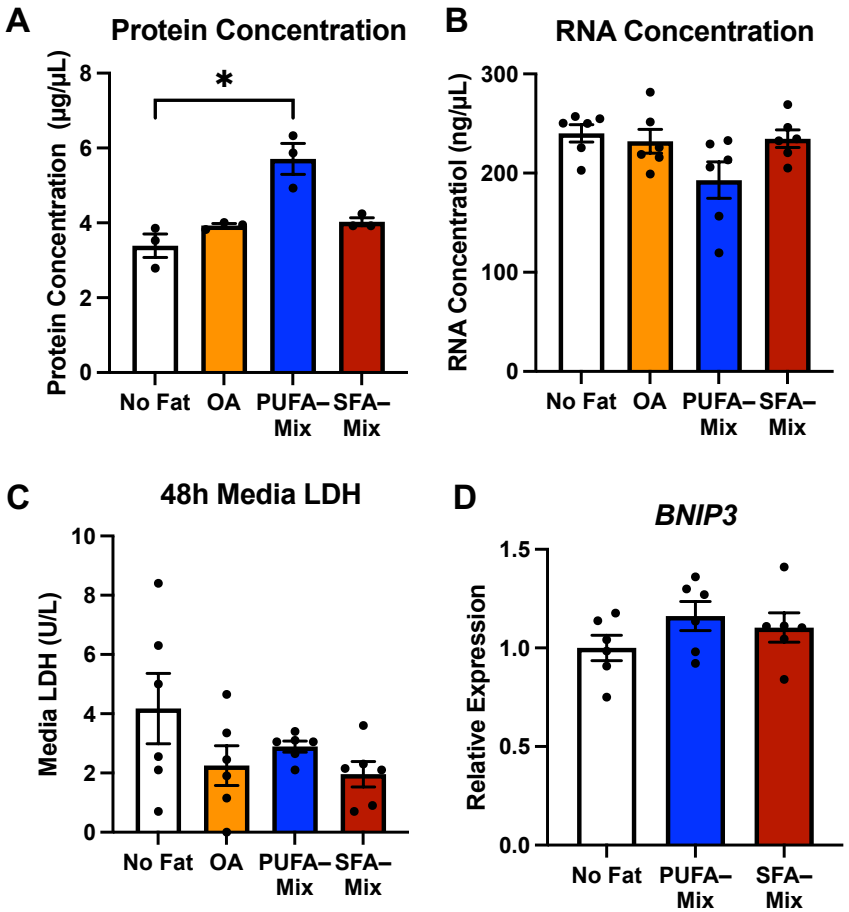

Figure 5.3. The effect of media fatty acid composition on hiPSC-CM cell stress responses. (A) protein concentration, **(B)** ribonucleic acid (RNA) concentration **(C)** lactate dehydrogenase (LDH) release into the media during the last 48h of the experimental protocol, and **(D)** *BNIP3* gene expression in hiPSC-CMs treated with no fatty acids, 76µM oleic acid (OA), or 400µM of a lipid mix enriched with polyunsaturated (PUFA) or saturated (SFA) fatty acids for eight days with media changes every other day. Data: mean ± SEM, n=6 per group, * $p<0.05$.

5.3.2 Effect of media FA composition on hiPSC-CM metabolic substrate uptake

To assess if FA composition impacts metabolic substrate uptake, in the first and last 48h of the 8-day experimental protocol, media FA, glucose, and lactate concentrations were measured before and 48h after being placed on hiPSC-CMs. Media metabolite concentrations after 48h on hiPSC-CMs were subtracted from the baseline metabolite concentration, a positive value indicated net uptake of the metabolite into hiPSC-CMs while a negative value indicated secretion from hiPSC-CMs.

In the first 48h of the experimental protocol, hiPSC-CMs incubated with OA and both FA lipid-mixes took up a comparable and greater amount of FA than no-fat treated hiPSC-CMs ($p<0.01$; Fig. 5.4A). However, in the last 48h of the experimental procedure, FA uptake in OA treated hiPSC-CMs was greater than no-fat treated hiPSC-CMs ($p<0.001$), and FA uptake in PUFA-enriched lipid-mix treated hiPSC-CMs was greater than in SFA-enriched lipid-mix ($p<0.05$) and no-fat treated hiPSC-CMs ($p<0.01$; Fig. 5.4B). Within the no-fat, OA, and SFA-enriched lipid-mix groups, FA uptake was decreased in the last 48h of the experimental protocol compared with the first 48h ($p<0.01$; Fig. 5.4C). Despite SFA- and PUFA-lipid-mix treated hiPSC-CMs experiencing the same cumulative FA exposure during the experimental protocol, media FA composition led to divergent effects on hiPSC-CM FA uptake as hiPSC-CMs treated with SFA-enriched lipid-mix reduced FA uptake while PUFA-enriched lipid-mix continued to take up FA (Fig. 5.4C).

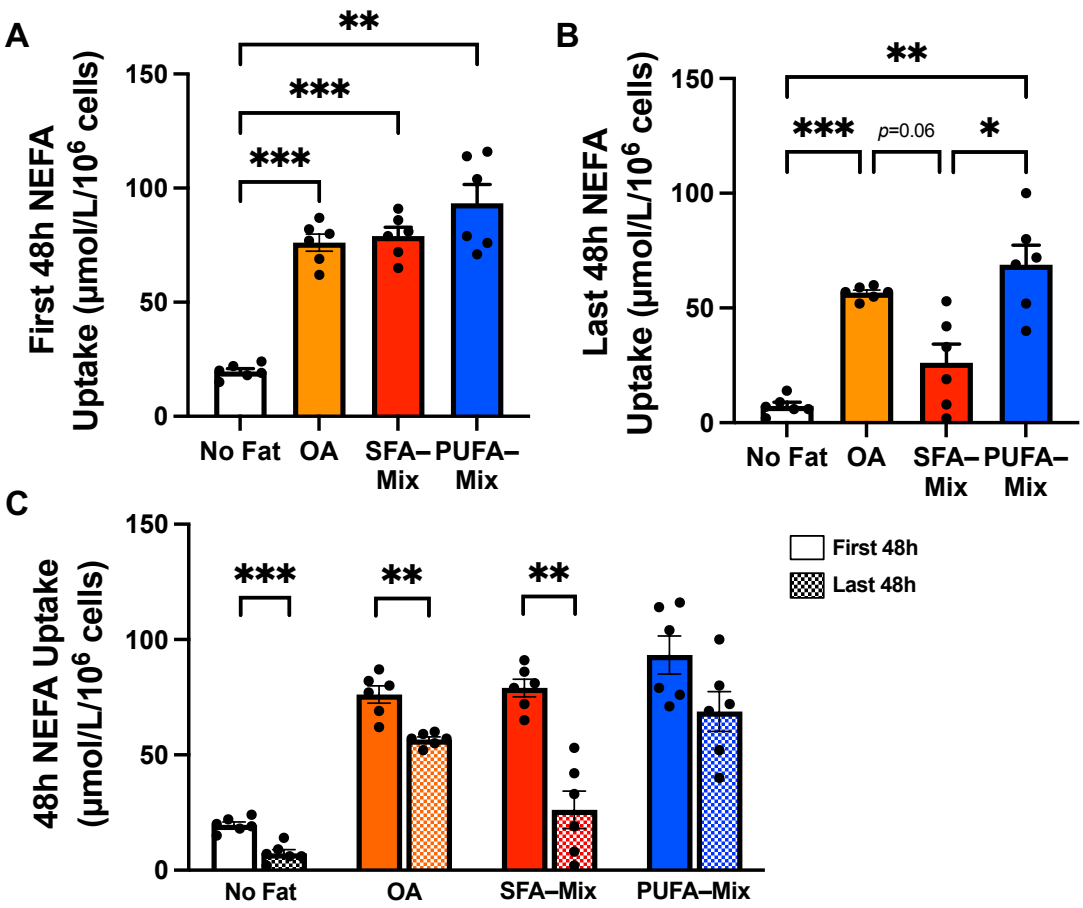

Figure 5.4. Effect of media fatty acid composition on hiPSC-CM fatty acid uptake. Non-esterified fatty acid (NEFA) uptake in the **(A)** first and **(B)** last 48h of the experimental protocol; **(C)** direct comparison of NEFA uptake in the first 48h (solid bars) with the last 48h (hashed bars) within each group in hiPSC-CMs treated with no fatty acids, 76µM oleic acid (OA), or 400µM saturated (SFA) or polyunsaturated (SFA) fatty acid-enriched lipid-mix for eight days with media changes every other day. Data: mean ± SEM, n=6 per group, *p<0.05, **p<0.01, ***p<0.001.

Glucose uptake was similar between all groups in the first (Fig. 5.5A) and last 48h (Fig. 5.5B) of the experimental procedure. Similarly, lactate production was comparable between all groups in the first (Fig. 5.5C) and last 48h (Fig. 5.5E) of the experimental protocol. While media FA composition modulated hiPSC-CM FA uptake, media FA composition did not differentially impact hiPSC-CM glycolytic metabolism under these conditions.

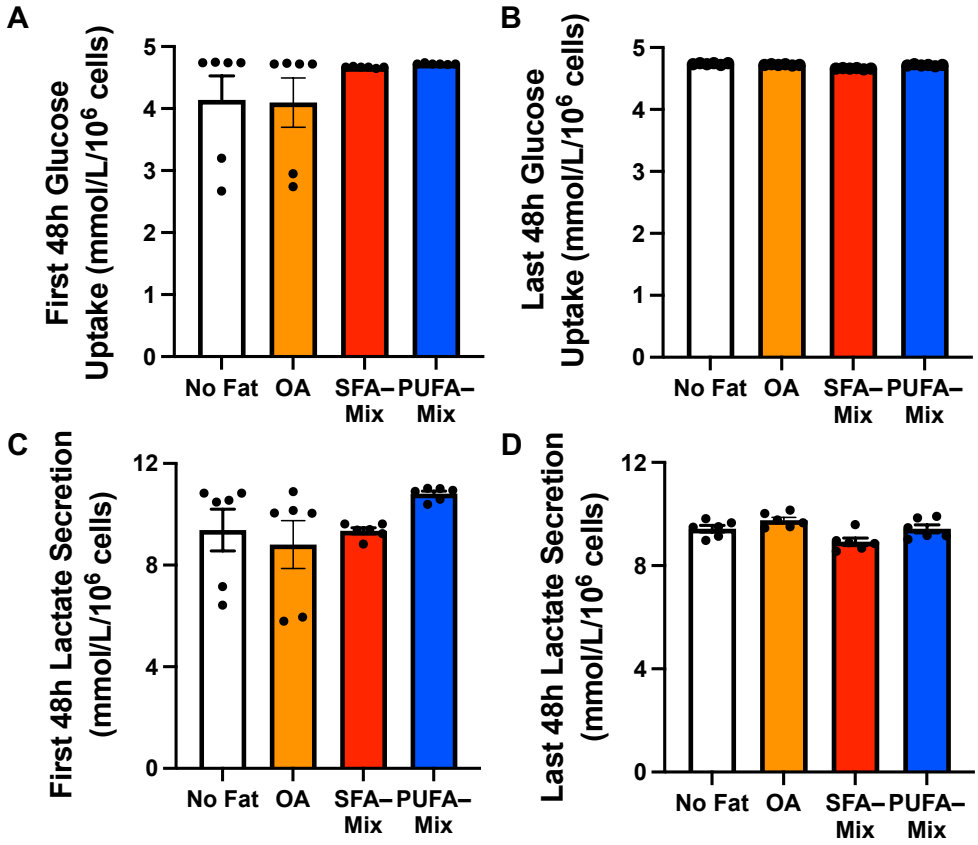

Figure 5.5. Effect of media fatty acid composition on hiPSC-CM glycolytic metabolism. Glucose uptake in the **(A)** first and **(B)** last 48h of the experimental protocol; lactate secretion in the **(C)** first and **(D)** last 48h of the experimental protocol in hiPSC-CMs treated with no fatty acids, 76μM oleic acid (OA), or 400μM saturated (SFA) or polyunsaturated (PUFA) fatty acid enriched lipid mix for eight days with media changes every other day. Data: mean ± SEM, n=6 per group.

5.3.3 Effect of media FA quantity and composition on hiPSC-CMs transcriptomic profiles

At the end of the 8-day experimental protocol, RNA was extracted from all hiPSC-CMs for bulk RNA sequencing. PCA suggested FA treatment was the primary source of variation in gene expression (dimension 1: 41.1%, Fig. 5.6). There is no clear identifier for the secondary source of variation (dimension 2: 19.8%, Fig. 5.6). PCA also showed FA composition may be as important as FA quantity in modulating hiPSC-CM gene expression responses, as SFA- and PUFA-enriched lipid-mix groups, which were treated with the same FA concentration but different FA composition, did not cluster together.

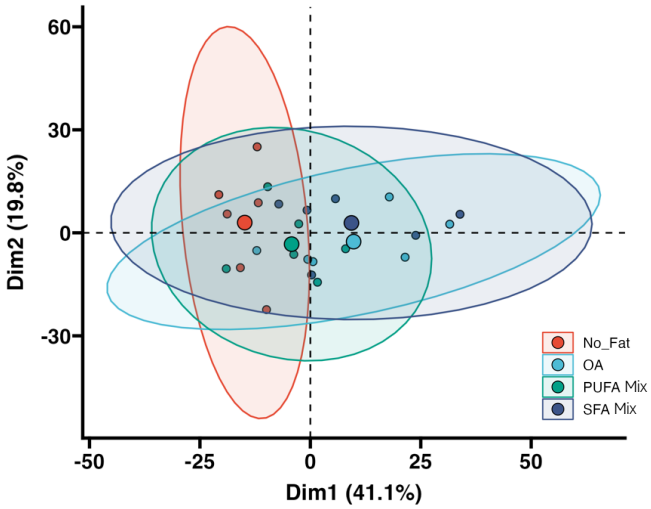

Figure 5.6. Principal component analysis of bulk RNA-sequencing from hiPSC-CMs treated with different fatty acid quantities and compositions. Bulk RNA transcriptomic analysis was performed on hiPSC-CMs treated with no fatty acids, 76µM oleic acid (OA), or 400µM of a lipid mix enriched with polyunsaturated (PUFA) or saturated (SFA) fatty acids for eight days with media changes every other day (n=6 per group).

For the following differential gene expression and pathway analysis, a comparison can only be made between two groups at a time. While the OA-treated hiPSC-CMs were included in previous figures as a well-characterised reference group, this group is not included in the following results section as the primary aim of this chapter was to investigate how FA composition modulates hiPSC-CM function. Nevertheless, the transcriptomic analysis of OA vs. no-fat treated hiPSC-CMs, displayed in Appendix 3, shows that hiPSC-CMs cultured using our standard protocol upregulate pathways in line with our previous observations, thereby increasing confidence in the analysis pipeline (333). In the following results, two comparisons were analysed: hiPSC-CMs cultured in lipid mix vs. no-fat, to characterise the effect of FA quantity, and hiPSC-CMs cultured SFA- vs. PUFA-enriched lipid-mix, to characterise the effect of FA composition, on hiPSC-CM transcriptional responses.

5.3.4 Transcriptomic responses of hiPSC-CMs treated with lipid-mix compared with no fat.

To investigate how media FA quantity impacts hiPSC-CM transcriptomic responses, SFA- and PUFA-enriched lipid mix groups were combined to form a "lipid-mix" group where hiPSC-CMs were treated with 400µM lipid-mix and differential gene expression analysis was

carried out. Differentially expressed genes were identified by an FDR<0.05 and FC>2 (lipid-mix) or <2 (no-fat) and visualised using a volcano plot (Fig. 5.7A). The top upregulated genes in the lipid-mix compared with no-fat group are all involved in FA metabolism (Fig. 5.7A, Table S3.2) while the top five upregulated genes in the no-fat compared with lipid mix group appear unrelated (Fig. 5.7A, Table S3.2). In hiPSC-CMs treated with lipid-mix compared with no-fat, 1296 genes were significantly upregulated, 1168 genes were significantly downregulated, and 7592 genes were unchanged (Fig. 5.7B). Findings from this transcriptomic comparison were validated by confirming greater *PDK4* expression in hiPSC-CMs treated with lipid-mix compared with no-fat via qPCR (Fig. 5.7C).

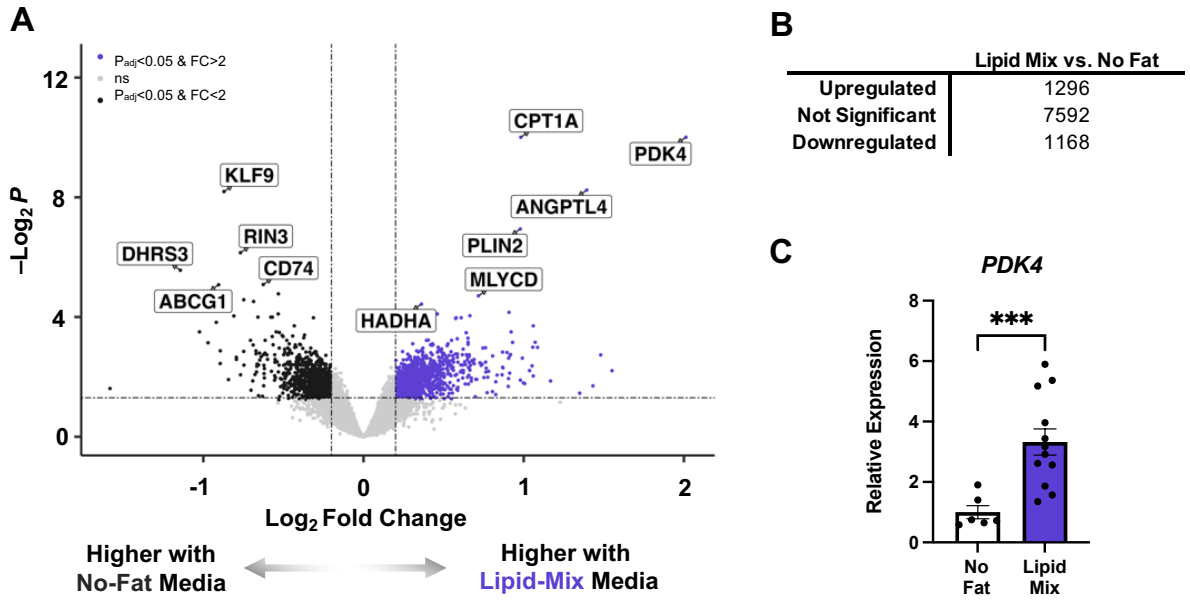

Figure 5.7. Transcriptional profiles of hiPSC-CMs treated with lipid-mix compared with no fat. Transcriptomic analysis was performed on hiPSC-CMs treated with 400µM lipid mix compared with no fat for eight days with media changes every other day. Data was visualised using a **(A)** volcano plot with individually differentially expressed genes (fold change (FC) > 2 and FDR < 0.05) indicated by a purple dot if upregulated with OA or dark grey dot if upregulated with no-fat. **(B)** total number of differentially expressed genes in each condition. **(C)** *PDK4* expression measured by quantitative-PCR, data: mean ± SEM, n=6 no-fat, n=12 lipid mix, ***p<0.001.

Predicted TF activation on the 1296 significantly upregulated genes suggests hypoxia-inducible factor 1α (HIF1α), activating transcription factor 4 and 6 (ATF4; ATF6), circadian locomotor output cycles kaput (CLOCK), aryl hydrocarbon receptor nuclear translocator-like protein 1 (ARNTL), ataxia telangiectasia mutated (ATM), PPARα, myocyte enhancer factor 2c

(MEF2C), and von Hippel-Lindau tumor suppressor (VHL) are the most likely human TFs active in lipid-mix treated hiPSC-CMs (Fig. 5.8).

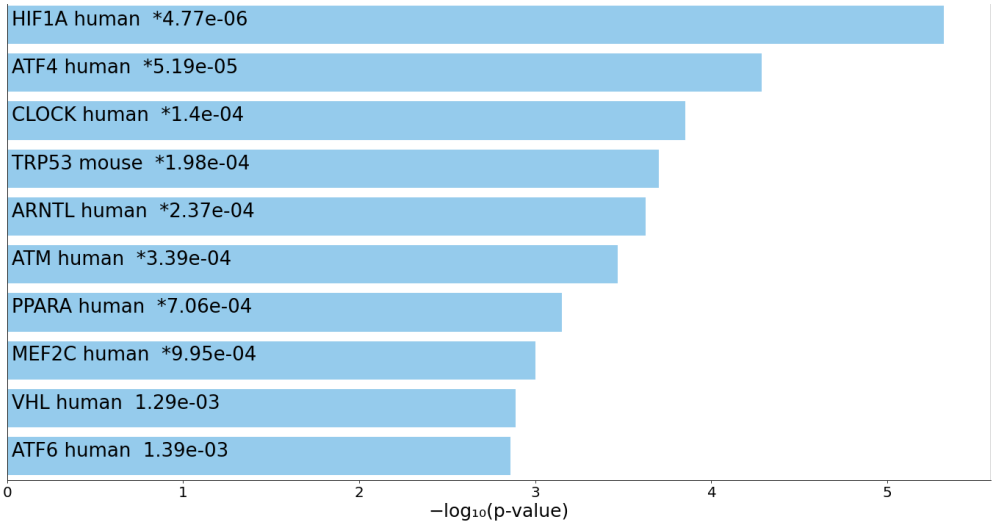

Figure 5.8. Predicted transcription factor activation in hiPSC-CMs treated with a lipid-mix compared with no fat. Transcriptomic analysis was performed on hiPSC-CMs treated with 400µM lipid mix (n=12) compared with no fat (n=6) for eight days with media changes every other day. Significantly upregulated genes in lipid-mix treated hiPSC-CMs were provided to the Enrichr webtool and analysed using the TRRUST 2019 transcription factor database. Transcription factors predicted to be significantly active are shown by a blue bar, p_{adj} is shown next to the transcription factor.

Gene set enrichment analysis (GSEA) using the hallmark pathways showed that comparing lipid-mix to no-fat treated hiPSC-CMs, metabolic pathways (hypoxia, oxidative phosphorylation, glycolysis, and FA metabolism) are the biggest cluster of significantly upregulated pathways, followed by pathways involved in cell stress responses (hypoxia and unfolded response) and cellular structure (mitotic spindle) (Fig. 5.9). In hiPSC-CMs treated with no-fat compared with lipid mix, epithelial-to-mesenchymal transition, DNA repair, IFNα response, and IFNγ response pathways are significantly upregulated (Fig. 5.9). These findings suggest hiPSC-CMs treated with lipid-mix compared with no-fat primarily upregulate genes and pathways involved in cellular metabolism.

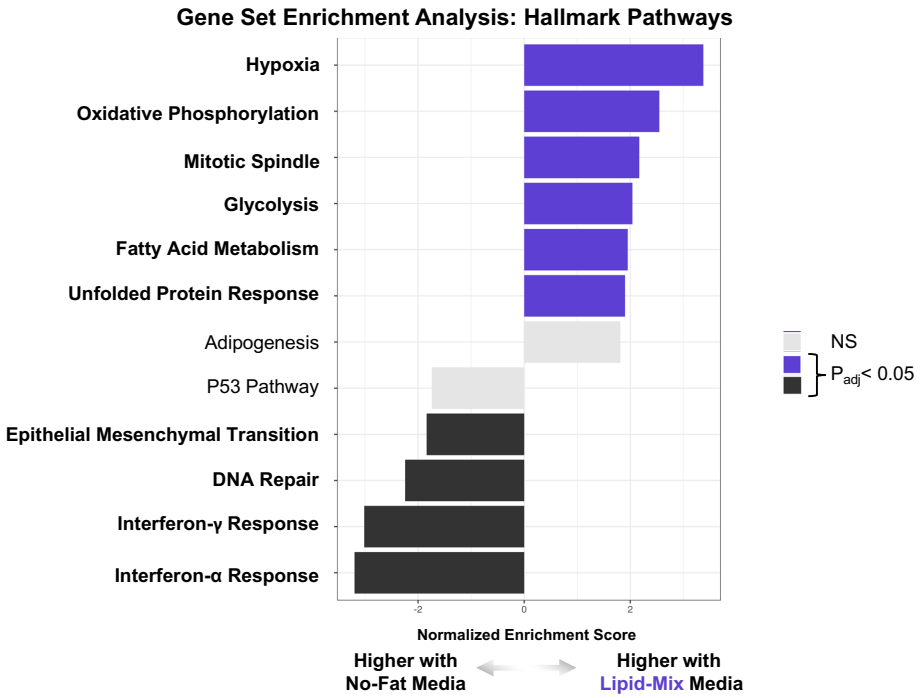

Figure 5.9. Pathway analysis of hiPSC-CMs treated with lipid mix compared with no fat. Gene set enrichment analysis was performed with hallmark pathways using the differentially expressed gene list generated by transcriptomic analysis of hiPSC-CMs treated with 400µM lipid mix compared with no fat. Significantly differentially regulated pathways (p_{adj}<0.05) between conditions are indicated by bold text and purple blocks if upregulated in response to lipid mix or dark grey blocks if upregulated in response to no fat, n=6 no fat, n=12 lipid mix.

5.3.5 Transcriptomic responses of SFA- compared with PUFA-enriched lipid-mix treated hiPSC-CMs

Transcriptomic analysis was performed on hiPSC-CMs treated with the same physiological concentration of a SFA- or PUFA-enriched lipid mix to investigate if media FA composition, independent of FA concentration, impacts cardiomyocyte function. Top upregulated genes in PUFA-enriched lipid-mix treated hiPSC-CMs are involved in sarcomere structure (*MYH3*) and regulation (*MLYK3*), cytosolic lipid droplet formation (*FITM2*), and cellular adhesion (*CLSTN2*) (Fig. 5.10A, Table S3.2). In SFA-enriched lipid-mix treated hiPSC-CMs, the top upregulated genes are involved in solubilising FAs (*FABP5*), extracellular matrix structure (*MFAP4*), cell proliferation (*CDKN1C*), cardiomyocyte differentiation (*IRX4*), and cardiac remodelling (*DLK1*) (Fig. 5.10A, Table S3.2). Overall, 573 genes were upregulated in SFA- compared with PUFA-enriched lipid mix treated hiPSC-CMs, 475 genes were

upregulated in PUFA- compared with SFA-enriched lipid mix treated hiPSC-CMs, and 9008 genes were unchanged (Fig. 5.10B). This transcriptomic comparison was validated by qPCR confirming greater *CD36* (Fig. 5.10C) and *ACLS4* (Fig. 5.10D) expression in hiPSC-CMs treated with PUFA- compared with SFA-enriched lipid-mix.

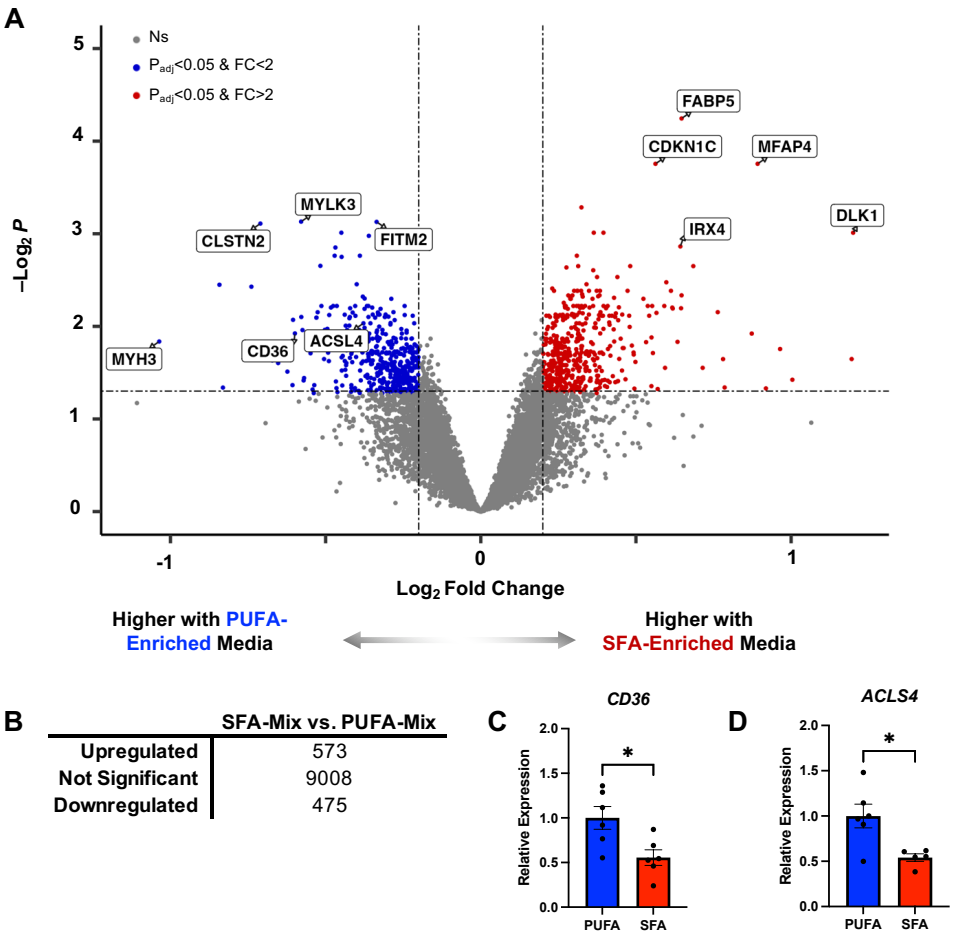

Figure 5.10. Transcriptomic profiles of hiPSC-CMs treated with SFA-enriched compared with PUFA-enriched lipid-mix. Transcriptomic analysis was performed on hiPSC-CMs treated with 400µM of a saturated (SFA) or polyunsaturated (PUFA) enriched lipid-mix for 8d with media changes every other day. Data was visualised using a **(A)** volcano plot with individually differentially expressed genes (fold change>2 and FDR<0.05) upregulated in SFA-enriched lipid mix (red dots), or PUFA-enriched lipid mix (blue dots); **(B)** total number of differentially expressed genes in each condition; **(C)** *CD36* or **(D)** *ACLS4* expression measured by qPCR, data: mean ± SEM, (C) n=6 per group (D), n=6 PUFA, n=5 SFA (one outlier removed), **p*<0.05.

Predicted TF activation suggested ETS translocation variant 4 (ETV4), nuclear receptor 4A1 (NR4A1), HIF1α, nuclear factor-κB subunit 2 (NFKB2), and DNA methyltransferase 3α (DNMT3α) are the most likely human transcription factors activated in SFA- compared with PUFA-enriched lipid-mix treated hiPSC-CMs (Fig. 5.11A). In PUFA- compared with SFA-

enriched lipid-mix treated hiPSC-CMs, PPARα is predicted to be the most likely activated human transcription factor (Fig. 5.11B).

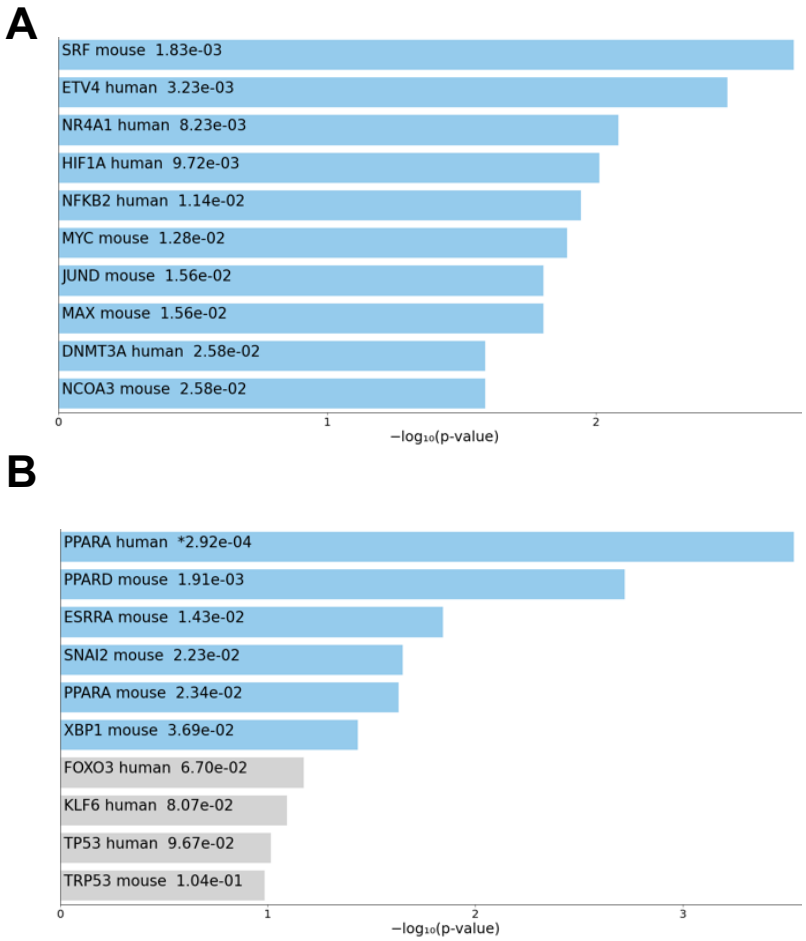

Figure 5.11. Predicted transcription factor activation in hiPSC-CMs treated with (A) SFA-enriched or (B) PUFA-enriched lipid mix. Transcriptomic analysis was performed on hiPSC-CMs treated with 400μM of a saturated (SFA) or polyunsaturated (PUFA) enriched lipid-mix for eight days with media changes every other day. Significantly upregulated genes in each condition were provided to the Enrichr webtool and analysed using the TRRUST 2019 transcription factor database. Transcription factors predicted to be significantly active are shown by a blue bar, p_{adj} is shown next to the transcription factor.

GSEA using the hallmark pathways showed ribosomal biogenesis (Myc Targets V1) and oestrogen receptor signalling (oestrogen response late and early) were upregulated in SFA- compared with PUFA-enriched lipid-mix treated hiPSC-CMs (Fig. 5.12A). In PUFA- compared with SFA-enriched lipid-mix treated hiPSC-CMs, FA metabolism was upregulated (Fig. 5.12A). A secondary pathway analysis using the gene ontology (GO) biological processes pathways supports that ribosomal biogenesis, translation, and rRNA metabolism pathways were upregulated in SFA- compared with PUFA-enriched lipid-mix treated hiPSC-CMs (Fig.

5.12B). Oestrogen receptor signalling and FA metabolism related pathways were not detected in this secondary analysis (Fig. 5.12B). Despite this, FA metabolism pathways are likely upregulated in PUFA-enriched lipid-mix treated hiPSC-CMs as findings from GSEA using hallmark pathways align with predicted TF analysis and qPCR data. These findings suggest media FA composition induces divergent transcriptional responses in hiPSC-CMs, such that incubating cells in a SFA-enriched media activates ribosomal metabolism pathways while incubating cells in a PUFA-enriched media upregulates FA metabolism pathways.

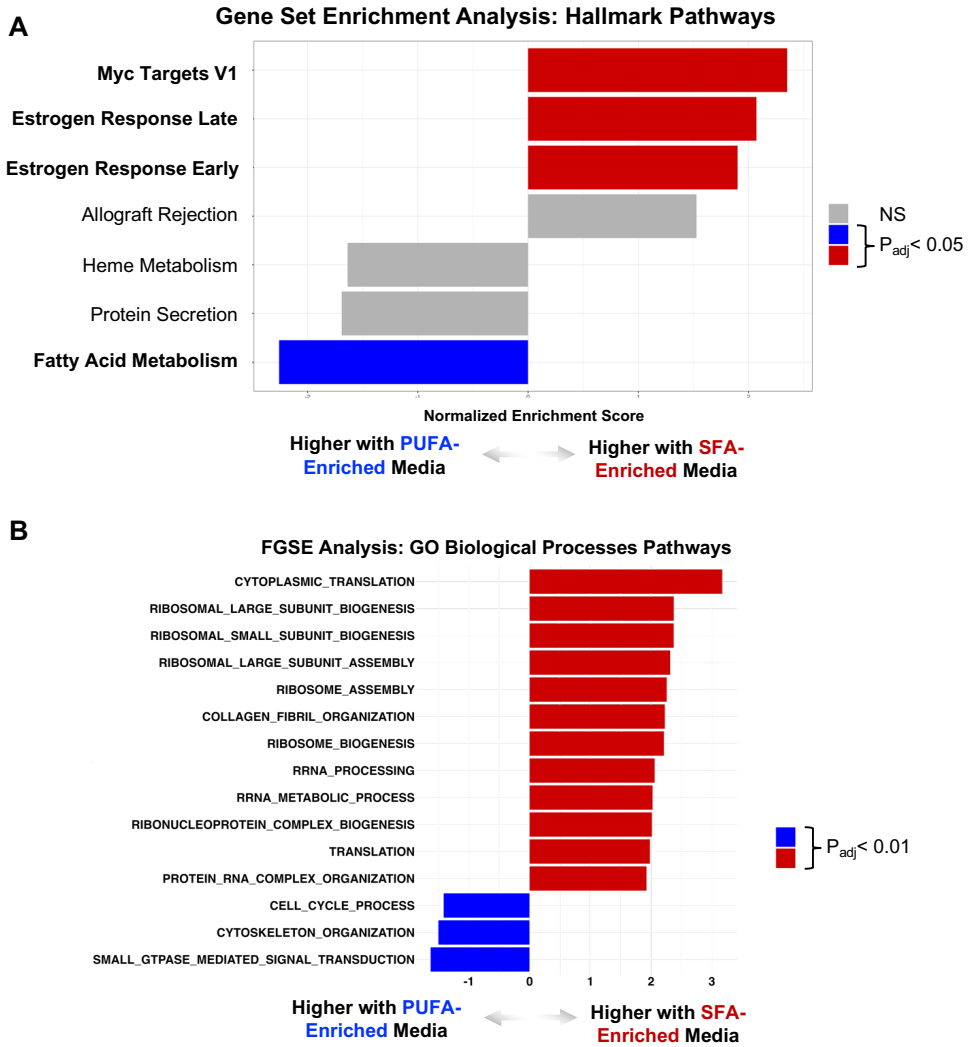

Figure 5.12. Pathway analysis of hiPSC-CMs treated with SFA-enriched compared with PUFA-enriched lipid mix. Gene set enrichment analysis was performed with **(A)** hallmark pathways or **(B)** Gene Ontology (GO) biological processes pathways using the differentially expressed gene list generated by transcriptomic analysis of hiPSC-CMs treated with 400µM saturated fat (SFA)-enriched or polyunsaturated fat (PUFA)-enriched lipid mix. Significantly differentially regulated pathways (p_{adj}<0.05 hallmark pathway analysis; p_{adj}<0.01 GO biological processes pathways) between conditions are indicated by bold text and red blocks if upregulated in response to SFA-enriched lipid mix or blue blocks if upregulated in response to PUFA-enriched lipid mix, n=6 per group.

To check the Myc Targets V1 and FA metabolism hallmark pathways were differentially regulated because of differences in media FA composition, as opposed to increased FA quantity, I compared how the 10% of genes with the lowest adjusted p-value in these pathways clustered on the volcano plot comparing SFA- vs. PUFA-enriched lipid mix treated hiPSC-CMs to how the same genes clustered on the volcano plot comparing lipid-mix vs. no fat treated hiPSC-CMs. Using this criteria, the top 10% of genes all displayed a positive fold change (Fig. 5.13A). In contrast, on the volcano plot comparing lipid-mix vs. no fat treated hiPSC-CMs, the same group of genes had a relatively equal mix of positive and negative fold changes (Fig. 5.13B). Similarly, in the volcano plot comparing SFA- vs. PUFA-enriched lipid mix treated hiPSC-CMs, the top 10% of genes with the lowest adjusted p-values in the FA metabolism pathway all displayed a negative fold change (Fig. 5.14A), while on the volcano plot comparing lipid-mix vs. no fat treated hiPSC-CMs, the same group of genes had a mix of positive and negative fold changes (Fig. 5.14B). This suggests the upregulation of ribosomal metabolism in SFA-enriched lipid mix treated hiPSC-CMs and FA metabolism in PUFA-enriched lipid mix treated hiPSC-CMs is driven by differences in FA composition, independent of FA quantity.

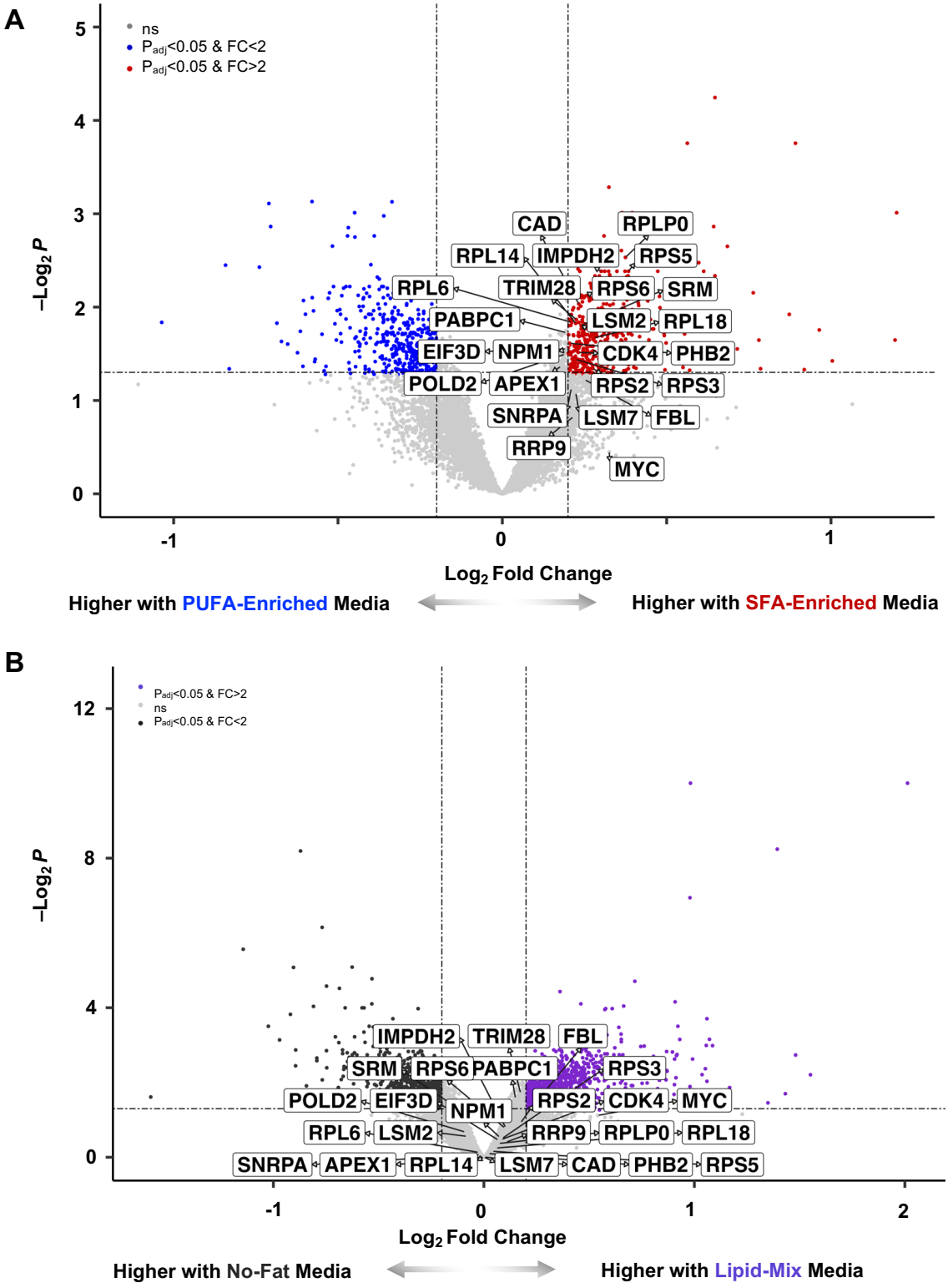

Figure 5.13. Volcano plot visualising genes in the Myc targets V1 hallmark pathway. Transcriptomic and gene set enrichment analysis using the hallmark pathways was performed on hiPSC-CMs treated with 400µM saturated fat (SFA)- or polyunsaturated fat (PUFA)-enriched lipid mix or no fat. The Myc targets V1 pathway was significantly upregulated in hiPSC-CMs treated with SFA- compared with PUFA-enriched media, so genes in this pathway were ranked according to the extent to which they were upregulated by SFA-enriched media. The 10% of genes with the lowest p_{adj}-value were visualised in a volcano plot comparing hiPSC-CMs treated with **(A)** SFA- vs. PUFA-enriched lipid mix (n=6 per group) or **(B)** lipid-mix (n=12) vs. no-fat (n=6).

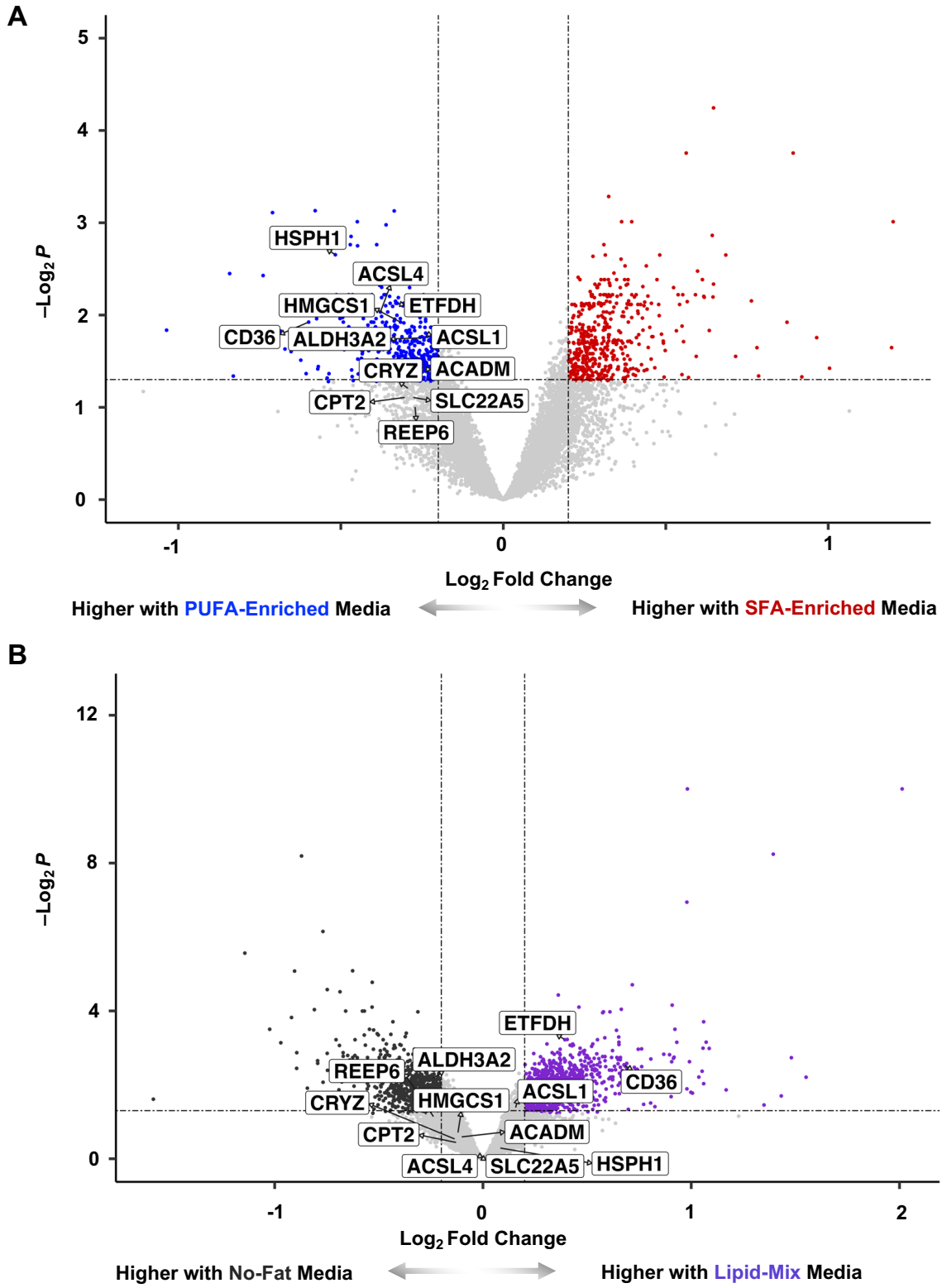

Figure 5.14. Volcano plot visualising genes in the fatty acid metabolism pathway. Transcriptomic and gene set enrichment analysis using the hallmark pathways was performed on hiPSC-CMs treated with 400µM saturated fat (SFA)- or polyunsaturated fat (PUFA)-enriched lipid mix or no fat. The fatty acid metabolism pathway was significantly upregulated in hiPSC-CMs treated with PUFA- compared with SFA-enriched media, so genes in this pathway were ranked according to the extent to which they were upregulated by PUFA-enriched media. The 10% of genes with the lowest p_{adj}-value were visualised in a volcano plot comparing hiPSC-CMs treated with **(A)** SFA- vs. PUFA-enriched lipid mix (n=6 per group) or **(B)** lipid-mix (n=12) vs. no-fat (n=6).

5.4 Discussion

While dietary FA composition modulates soluble CMD risk factors (143, 153, 344), it remains unclear if FA composition, independent of FA quantity, directly impacts cardiomyocyte function. In Chapter 4, I showed dietary FA composition has divergent effects on *in vivo* human cardiac energetics and function, therefore in this chapter, I aimed to further characterise this phenotype by incubating hiPSC-CMs with different FA mixtures, at a physiological concentration, to model the SFA- and PUFA-enriched HFDs. hiPSC-CMs treated with a PUFA-enriched lipid mix continued to take up FA from the media and upregulated FA metabolism pathways, while hiPSC-CMs treated with a SFA-enriched lipid mix reduced FA uptake and upregulated pathways involved in protein translation and ribosomal biogenesis. These results were independent of FA quantity and do not appear to be driven by or in response to cell stress. Taken together, these findings support that FA composition has direct effects on cardiomyocytes, with SFAs and PUFAs inducing divergent cellular responses.

5.4.1 Media FA Composition & hiPSC-CMs FA Metabolism

Previous studies have reported different FAs induce divergent effects on cardiomyocytes gene expression, including genes involved in FA metabolism (308, 345-348). Lockridge *et al.* showed that culturing adult rat cardiomyocytes for 24h with 400μM oleate or linoleate, compared with palmitate, led to a greater number of FA metabolism related genes being differentially expressed (345). This may be explained by oleate and linoleate activating PPARα to a greater extent than palmitate (308). While most studies have been conducted in rodents or rodent cell lines using a single FA or oleate/palmitate mixture for a short duration (≤ 24h), it does not fully model human CMD pathogenesis and may limit translatability. However, the transcriptomic findings in this chapter, generated using human iPSC-derived cardiomyocytes cultured with a physiological FA mixture for a longer period than previous

studies, support a PPARα-mediated upregulation of FA metabolism in human cardiomyocytes cultured in a PUFA- compared with SFA-enriched lipid-mix.

hiPSC-CMs cultured in a PUFA-enriched lipid-mix continued to take up FA during the experimental period while SFA-enriched lipid-mix cultured hiPSC-CMs reduced FA uptake. Incubating neonatal rat cardiomyocytes for 20h in 500μM palmitate, compared with oleate, reduces FA oxidation, increases myocardial TG, and decreases AMPK activity (349). Chabowski *et al.* showed in isolated rat cardiomyocytes and intact perfused hearts that activating AMPK increases the expression and targeting of key FA-transport proteins, CD36 and FABPpm, to the plasma membrane (350). Therefore, as SFA-enriched lipid-mix treated hiPSC-CMs were exposed to a greater palmitate concentration, this may have reduced AMPK signalling and decreased plasma membrane CD36 and FABPpm targeting and FA uptake. Alternatively, palmitate increases CD36 ubiquitination *in vitro* which would induce CD36 degradation and reduce FA uptake (351). This may function as a negative feedback mechanism preventing excessive FA uptake and lipid overload when FA delivery exceeds oxidation requirements, however, the mechanisms linking FA composition to differences in cardiomyocyte FA uptake remain to be elucidated.

5.4.2 Media FA Composition & hiPSC-CM Cell Stress Responses

Numerous studies have linked myocardial palmitate accumulation with increased cell stress responses, including ceramide and DAG formation, mitochondrial stress, oxidative stress, and apoptosis (253, 346, 347, 349, 352, 353). Indeed, our group previously cultured matured hiPSC-CMs in 300μM palmitate for 6 days to create an insulin-resistant hiPSC-CM model (354). However, palmitate-induced cell stress responses were not observed in the present study likely due to the presence of other FAs in the lipid mix. Miller *et al.* reported adding 100μM oleate to the media when culturing rat ventricular cardiomyocytes prevented oxidative stress and apoptosis caused by culturing cells in 500μM palmitate (352). Adding PUFAs to cell

media also rescues the pro-apoptotic effects of palmitate on cardiomyocytes (347, 353). It has been proposed unsaturated FA activate PPARα to increase FA esterification and lipid droplet formation, this directs palmitate towards storage as TG, reducing the amount available for bioactive lipid synthesis and cell stress responses. While adding 50μM and 250μM oleate rescued lipotoxicity induced by 500μM palmate in a skeletal muscle cell line, adding 500μM oleate, such that the total FA concentration was 1mM, diminished the protective effects of oleate (348). This suggests the FA quantity and composition both modulate cell stress responses; however, it is unclear how hiPSC-CMs would response to greater concentrations of SFA- or PUFA-enriched lipid-mixes.

Findings suggesting increased oestrogen receptor signalling in SFA-enriched lipid-mix treated hiPSC-CMs may be a false hit as these pathways did not appear in the secondary pathway analysis and conflict with TF analysis which predicts mouse oestrogen-related receptor-α to be active in PUFA- and not SFA-enriched lipid-mix treated hiPSC-CMs. hiPSC-CMs cultured with a SFA-enriched lipid mix upregulate ribosomal biogenesis and protein translation transcriptional pathways compared with hiPSC-CMs cultured with a PUFA-enriched lipid mix. Lockridge *et al.* reported adult rat cardiomyocytes cultured for 24h with 400μM palmitate significantly upregulated genes in the Gene Ontology "translation" pathway, while oleate and linoleate had no effect on this pathway (345). Cardiac FA oxidation is required for myocardial protein synthesis, as translation initiation requires ATP and a majority of cardiac ATP production occurs through FA oxidation (355). In contrast to the findings in this chapter, it could be expected that cardiomyocytes exposed to greater SFA/palmitate concentrations would reduce protein synthesis as SFAs lead to less FA oxidation compared with PUFAs (92). However, in hearts perfused without FAs and therefore with reduced FA oxidation, ribosomal subunits accumulate (356), this suggests ribosome biogenesis may be upregulated as a compensatory mechanism for the decrease in translation initiation. Therefore, upregulated

ribosomal biogenesis in SFA-enriched lipid-mix treated hiPSC-CMs with may be a compensatory response to the decreased FA uptake and oxidation in these cells compared with PUFA-enriched lipid-mix treated hiPSC-CMs.

5.4.3 FA Quantity Regulates hiPSC-CMs Metabolism & Hypoxia Signalling

Compared with hiPSC-CMs treated with no-fat, lipid-mix treated hiPSC-CMs upregulate cellular metabolism and maturation pathways. This is in line with studies showing a dose-dependent relationship between FA concentration, cardiomyocyte FA metabolism gene expression, and hiPSC-CM maturity (333, 345). Hypoxia signalling was the top differentially regulated pathway in hiPSC-CMs treated with lipid mix; a pathway where, in response to decreased intracellular oxygen, HIF1α degradation is inhibited to increase the expression of genes involved in anaerobic metabolism and cell stress responses (330). Hass *et al.* showed that culturing hiPSC-derived retinal pigment epithelial cells (highly oxidative cells, like cardiomyocytes) in greater media volumes induces hypoxic responses due to oxygen's poor media-solubility and inability to diffuse to cells (357). However, this is an unlikely explanation for my findings as no-fat treated hiPSC-CMs were cultured with the same media volumes as fat-treated hiPSC-CMs, therefore, they would have also experienced this hypoxic effect and the pathway would not appear differentially regulated. Instead, this hypoxic pathway may be a false positive. Although FA-treated hiPSC-CMs are more mature than hiPSC-CMs matured without FA (333), they still display a highly glycolytic, foetal phenotype, shown by the 2:1 ratio of media lactate secretion to glucose uptake. The anaerobic metabolism phenotype coupled with ROS-induced cell stress responses in FA-treated hiPSC-CMs may be inappropriately identified as hypoxic signalling. To clarify this finding, measuring HIF1α protein expression in future studies would be beneficial to assess whether hypoxia signalling is truly active in FA-treated hiPSC-CMs under cell culture conditions.

5.4.4 Limitations

Findings were generated using hiPSC-CMs from a single hiPSC lineage, results should be replicated in hiPSC-CMs from a different lineage and sex to ensure outcomes are not sex-specific or driven by SNPs in IMR-90s. This *in vitro* model lacked several physiological parameters that impact *in vivo* cardiac metabolism including nutrient and hormonal fluctuations between fed and fasted state, FA delivery as TRLs, and the 3D tissue environment; however, as this was a preliminary study, a simpler approach was deemed more appropriate. The SFA- and PUFA-enriched lipid mixes were composed of four major FAs found in the human diet, while they represent ~90% of circulating FA in human plasma-TG, the lipid mix did not include FAs, such as EPA and DHA, which have established effects on CMD risk, and short and medium chain FAs which may have different effects on cardiomyocyte physiology (212, 225, 358). Future studies with lipid mixes containing different FAs and ratios are needed to fully characterise the relationship between FA composition and CMD risk.

5.4.5 Conclusion

In this chapter, hiPSC-CMs were treated with a physiologic concentration of a SFA- or PUFA-enriched lipid mix to investigate whether FA composition, independent of concentration, induces divergent responses. These findings suggest FA composition influences metabolic and nonmetabolic response in hiPSC-CMs, as hiPSC-CMs treated with a PUFA-enriched lipid mix upregulate FA metabolism pathways and continue taking up FA while hiPSC-CMs cultured in a SFA-enriched lipid mix reduce FA uptake and upregulate ribosomal biogenesis. These results highlight that dietary FA composition has direct effects on the heart and may implicate FA composition in the pathogenesis of CVD, independent of other soluble CVD risk factors.

Chapter 6

General Discussion

6.1 Overview & Integration of the Main Findings

An individual's diet is a modifiable lifestyle risk factor associated with obesity, where consuming excess calories or certain macronutrients may increase CMD risk (77, 79). Independent of changes in body weight, overfeeding studies consistently show that consuming a SFA-enriched, compared with PUFA-enriched diet adversely impacts IHTG accumulation, insulin signalling, and promotes a proatherogenic lipoprotein profile (10, 11, 79, 215, 309). Further, differences in intracellular or systemic handling of SFAs and PUFAs may explain their divergent effects on IHTG accumulation. However, as these studies have typically been conducted utilising hypercaloric experimental diets, it is difficult to disentangle the effects of weight gain from dietary FA composition on CMD risk. Therefore, the overarching aim of this thesis was to investigate if, during the consumption of a weight-neutral diet, SFAs, compared with PUFAs, undergo differential intracellular handling and if consuming a SFA- or PUFA-enriched HFD impacts hepatic and cardiac metabolism and function.

To investigate if dietary FA composition impacts CMD risk, participants free-from diagnosed metabolic disease were studied before and after consuming an isocaloric SFA- or PUFA-enriched HFD. Bodyweight did not change over the course of either HFD. However, consuming a PUFA-enriched HFD decreased, while consuming a SFA-enriched HFD increased, IHTG content. Using stable-isotope tracer methodologies, I showed these divergent effects of dietary FA composition on IHTG content may be mediated by changes in FA oxidation as consuming a PUFA-enriched HFD increased and SFA-enriched HFD decreased the appearance of ^{13}C (from a ^{13}C-labelled dietary FA tracer) in expired CO_2. Further, dietary FA composition impacted other CMD risk factors, with reduced blood pressures and plasma lipids, and increased myocardial PCr/ATP after consuming a PUFA-enriched HFD, and increased plasma lipids and markers of insulin resistance and cardiac dysfunction after consuming a SFA-enriched diet. Taken together, these findings suggest dietary FA

composition, independent of body weight, impacts systemic, hepatic, and cardiac metabolism.

The finding that dietary FA composition modulates IHTG content through effects on FA oxidation is in line with previous studies, and with findings from Chapter 3, which suggest dietary PUFA, compared with SFA, may be preferentially partitioned into oxidation pathways (92, 194, 227) . In Chapter 3, participants consumed a high-carbohydrate diet for 3-days to acutely upregulate hepatic DNL and shift the metabolic state of the liver away from oxidation and towards esterification. Despite this shift in hepatic metabolism and a potentially greater flux of palmitate than linoleate to the liver, there was a greater appearance of ^{13}C in markers of whole-body and hepatic FA oxidation following consumption of [U^{13}C]linoleate compared with [U^{13}C]palmitate. The results from Chapter 3, along with previous studies, suggest there may be intracellular mechanisms which preferentially partition dietary PUFA, compared with SFA, into oxidation pathways to promote FA disposal (54, 92, 278). As these studies have been primarily conducted in healthy participants, it would be of interest to investigate if in patient populations with metabolic disease (i.e. MASLD, insulin resistance) SFAs, compared with PUFAs, are preferential partitioning into different intracellular metabolic pathways.

Although dietary FA composition impacts CVD risk through effects on plasma CVD risk factors, it is unclear if dietary FA composition directly impacts the heart. Therefore, in Chapter 5, hiPSC-CMs were treated with a physiological concentration of a SFA- or PUFA-enriched lipid-mix for 8-days to investigate if media FA composition, independent of total FA concentration, impacts cardiomyocyte metabolism, cell stress responses, and transcriptomic responses. hiPSC-CMs treated with a PUFA-enriched lipid mix upregulated FA oxidation pathways and took up a greater proportion of FAs from the media than hiPSC-CMs cultured with a SFA-enriched lipid mix. Further, these changes were independent of FA concentration and cell stress responses. If these *in vitro* findings are representative of *in vivo* changes following consumption of a PUFA-enriched HFD, then the increased myocardial PCr/ATP in

humans observed in Chapter 4 may be mediated by increased cardiac FA uptake and/or oxidation. In contrast, hiPSC-CMs cultured in a SFA-enriched lipid-mix reduced FA uptake with increased SFA exposure. If this is also representative of *in vivo* striated muscle behaviour, then consuming a SFA-enriched HFD may lead to reduced FA uptake into skeletal and cardiac muscle, promote larger TRL-remnants formation, increase hepatic lipid flux, and augment IHTG accumulation. Further, reduced FA uptake into striated muscle would reduce FA oxidation and therefore, may contribute to the observation of reduced ^{13}C appearance (from the dietary FA tracer) in expired CO_2 following consumption of a SFA-enriched HFD in Chapter 4. Taken together, these findings suggest dietary FA composition may directly impact cardiac FA handling, metabolism, and function and may modulate CVD risk.

6.2 Effects of Dietary FA Composition on Metabolic Tissues

As treating hiPSC-CMs with a SFA-, but not PUFA-enriched lipid mix leads to decreased FA uptake, it would be of interest to study if the binding site of CD36 has different affinities or transport capacities for FAs with a different degree of saturation. Further, it would be of interest to characterise if CD36 has allosteric FA-binding sites which regulate its activity and if intracellular FA composition regulates CD36 trafficking to the plasma membrane. FA composition may also influence FA uptake and metabolism through effects on TRL metabolism. For example, the FA composition of a meal may influence LPL activity, which could impact FA concentrations within tissues and FA transport into cells (359). There is also emerging evidence that SNPs in *LPL* (and other genes) may interact with dietary FA composition to impact an individual's CMD risk (360). This suggests certain dietary patterns or macronutrients may have different effects on an individual's CMD risk depending on their genetic background. As a result of these findings and others, there is increasing interest in improving our understanding of gene-diet interactions to personalise dietary and nutrition advice.

Although the effects of dietary FA composition on the heart and liver were investigated in this thesis, there is emerging evidence that alterations in skeletal muscle and adipose tissue physiology may precede cardiac and hepatic manifestations of metabolic syndrome (361, 362). Therefore, further work is needed to understand how dietary FA composition impacts the function and metabolism of skeletal myocytes and adipocytes. As adipocytes partition a greater proportion of FAs towards esterification and storage over oxidation pathways, future work could investigate if SFAs, compared with PUFAs, are preferentially partitioned towards storage pathways within adipocytes and if this induces divergent effects on adipose tissue function. Alternatively, different macronutrient compositions may induce different lipid droplet patterns within hepatocytes and these lipid droplet patterns may be associated with altered cellular function (227). Therefore, it is of interest to determine if a divergence in lipid droplet pattern occurs in adipocytes in response to different FA compositions, and if it is associated with changes in adipose tissue function.

6.3 Sexual Dimorphism in the Effects of Dietary FA Composition on CMD Risk

Compared with males, CMD risk and prevalence is lower in pre-menopausal females but potentially higher in post-menopausal females; however, the mechanisms explaining this difference remain unclear (363). One proposed mechanism, and in agreement with the findings throughout this thesis, suggests that females tend to partition FAs into oxidation pathways, while males tend to partition FAs into esterification pathways (307). In Chapter 3, and in agreement with the observations of Parry *et al.* (92), females, but not males, had greater ^{13}C appearance in expired and peripheral CO_2 after consumption of dietary [U^{13}C]linoleate, compared with [U^{13}C]palmitate. In Chapter 4, changes in whole-body dietary FA oxidation after consuming a SFA- or PUFA-enriched HFD were primarily driven by females. Compared with males, skeletal muscle in females has greater expression of FA oxidation genes, capacity for β-oxidation, and has more lipid droplets that are smaller and in closer proximity to

mitochondria (307, 364-366). Taken together, this cellular organisation and gene expression profile suggests that females have a greater capacity to change FA oxidation in response to an intervention and this may, in part, explain the greater change in ^{13}C appearance in expired CO_2 in females compared with males after consuming a SFA-enriched HFD. While differences in FA oxidation may contribute to the sexual dimorphism in CMD risk, there may also be differences in adipose tissue function, hepatic DNL, and VLDL-TG production (307, 367, 368). Therefore, further studies are needed to clarify how sex, lipid metabolism, and menopause interact with each other to cumulatively influence CMD risk.

6.4 Broader Implications

Dietary modifications are a preventative and first-line therapeutic option to reduce a patient's risk of developing CMD, and are often utilised alongside pharmacologic approaches. However, there is often limited success due to challenges associated with making dietary modifications long-term and mixed information on the optimal dietary pattern to reduce CMD risk. Despite this, dietary changes can notably modify CMD risk. In Chapter 4, in an experimental research setting, participants were advised on how to modify their habitual diet to consume either a SFA- or PUFA-enriched HFD, and it was observed that consumption of a PUFA-enriched HFD for up to 24 days reduced systolic blood pressure by ~7mmHg, non-HDL cholesterol by ~15%, and IHTG content by ~20%. Given that starting an angiotensin-converting-enzyme inhibitor, statin, or a GLP-1/glucagon dual receptor agonist is expected to reduce systolic blood pressure, LDL-cholesterol, and IHTG content by ~8mmHg, ~40%, and ~45%, respectively, the magnitude of change observed after consuming a PUFA-enriched HFD with minimal change in bodyweight is clinically relevant (311, 369, 370). Among the growing number of pharmacological options, the work presented in this thesis supports that dietary modifications remain a clinically relevant option for mitigating CMD risk.

Appendix 1: Chemical Reagents

Supplementary Table 1.1. Chemical Reagents

Experiment	Reagent	Company	Catalogue Number
Postprandial Study Days	[2,2-D_2]palmitate	Cambridge Isotope Laboratories Inc	DLM-3773-1
	Human albumin	Octapharma	5400971
	[$U^{13}C$]palmitate	Cambridge Isotope Laboratories Inc	CLM-409-0.1
	[$U^{13}C$]linoleate	Cambridge Isotope Laboratories Inc	CLM-8835-PK
	D_2O	Cambridge Isotope Laboratories Inc	DLM-4-1L
	Rice Crispies	Kellogg	Commercially Available
	Skimmed Milk	Tesco	Commercially Available
	Olive Oil - Light	Tesco	Commercially Available
	Cocoa Powder	Tesco	Commercially Available
	Myverol (Emulsifier)	Surfachem	Myverol 18-04k
	Xylitol	Tesco	Commercially Available
Triglyceride Rich Lipoprotein Isolation	Ethylenediaminetetraacetic acid (EDTA)	Sigma-Aldrich	E8008
	Phenylmethylsulphonyl fluoride (PMSF)	Sigma-Aldrich	P7626
	Trasylol	Sigma Pharmacy	93482
	Ultra-Clear centrifuge tubes (14 x 95mm)	Beckman Inc.	344060
Analytical Methods	Glucose reagent	Werfen	18250840
	NEFA reagent	Randox	FA115
	Triglyceride reagent	Werfen	18255640
	Glycerol reagent	Randox	GY105
	HDL-C reagent	Randox	CH2655
	Total Cholesterol reagent	Werfen	18250540
	Total apolipoprotein-B100 reagent	Randox	LP3839
	Lactate reagent	Randox	LC3980
	Lactate dehydrogenase reagent	HORIBA ABX SAS	1220001824
	Bicinchoninic acid protein assay	ThermoFischer Scientific	23225
Lipid Extraction	Glyceryl triheptadecanoate	Sigma-Aldrich	T2151- 100MG
	Heptadecanoic acid	Sigma-Aldrich	H3500-1G
	1,2-diheptanoyl-sn-glycero-3-phosphocholine	Sigma-Aldrich	P4148-100MG

	ISOLUTE SPE columns	Biotage Ltd.	470-0010-A
	Methyl tricosonate	Sigma-Aldrich	T9900-1G
Isotope Enrichment Analysis	FAME Mix RM-6	Thames Restek	RE35027
	StdB FAME mix	Merck Life Science UK Ltd	18919-1AMP
	Platinum catalyst	ThermoFischer Scientific	1091831
hiPSC Maintenance	Phosphate Buffered Saline	Sigma Aldrich	D8537
	TeSR-E8 media	StemCell Technologies	05990
	Matrigel	Corning	356234
hiPSC-CM Differentiation	RPMI 1640 media	ThermoFisher Scientific	11875085
	B27 minus insulin	ThermoFisher Scientific	A1895601
	CHIR99201	Tocris Bioscience	4423
	Wnt-C59	Tocris Bioscience	5148
	RPMI 1640 without glucose	ThermoFisher Scientific	11879020
	B27 complete	ThermoFisher Scientific	17504044
	0.4% Trypan Blue	ThermoFisher Scientific	15250061
hiPSC-CM Experimental Protocol	DMEM 5.5mM glucose	Gibco	11885084
	Inactivated horse serum	Gibco	26050088
	Vitamin B12	Merck	V2876
	Vitamin C	Merck	A92902
	Biotin	Merck	B4639
	Insulin	Merck	I9278-5ML
	Non-essential amino acids	Gibco	11140035
	Penicillin/streptomycin	Gibco	15070063
	Bovine serum albumin	Sigma-Aldrich	A9418
	DMEM/F-12 media, with no glucose and no phenol red	Gibco	A2494301
	Oleic Acid	Cayman Chemical	90260
	Palmitic Acid	Sigma Aldrich	P0500
	Linoleic Acid	Cayman Chemical	90150
	α-linoleic acid	Cayman Chemical	90210
	TRIzol Reagent	Invitrogen	15596026
RNA Extraction	Qiagen RNEasy Mini-Kit	Qiagen	74104
cDNA Synthesis	high-capacity cDNA Reverse Transcription Kit	ThermoFisher Scientific	4374966
	SYBR Green MasterMix	ThermoFisher Scientific	4309155

Abbreviations: DMEM, Dulbecco's Modified Eagle Medium; FAME, Fatty acid methyl ester; RPMI, Roswell Park Memorial Institute;

Appendix 2. Chapter 4 Supplementary Data

2.1 Sexual Dimorphism in the Change in Plasma Biochemistry and Tracer Incorporation into Plasma Lipid Pools after Consumption of a SFA- or PUFA-Enriched HFD

The change from baseline to post-HFD of postprandial plasma biochemistry and incorporation of [U^{13}C]palmitate, [2,2-D_2]palmitate, and newly synthesised palmitate into plasma lipid pools after consuming a SFA- or PUFA-enriched HFD between males and females was compared. After consuming a SFA-enriched HFD, there was an interaction effect for the change from baseline to post-HFD between sexes for postprandial plasma glucose (p<0.05), TG (p<0.0001), NEFA (p<0.001), chylomicron-TG (p<0.05), and VLDL-TG (p<0.001) (Fig. S2.1A, C-F). Females compared with males, had lower plasma glucose at 60min and lower NEFA at 240min and 300min after consuming the test meal on the post-HFD study day compared with the baseline study day (all p<0.05; Fig. S2.1A). Males, compared with females, had a higher plasma TG excursion at 120min (p=0.05), 180min (p<0.01), and 240min (p<0.05), higher chylomicron-TG excursions at 120min (p=0.06), 180min (p<0.05), and 240min (p=0.05), and higher VLDL-TG excursions at 180min (p<0.01) and 240min (p<0.05) after consuming the test meal on the post-HFD study day compared with the baseline study day (Fig. S2.1C, E-F). The change from baseline to post-HFD in plasma insulin did not differ between sexes after consuming a SFA-enriched HFD (Fig. S2.1B). After consuming a PUFA-enriched HFD, there were no differences in postprandial plasma biochemistry between males and females (Fig. S2.2A-F).

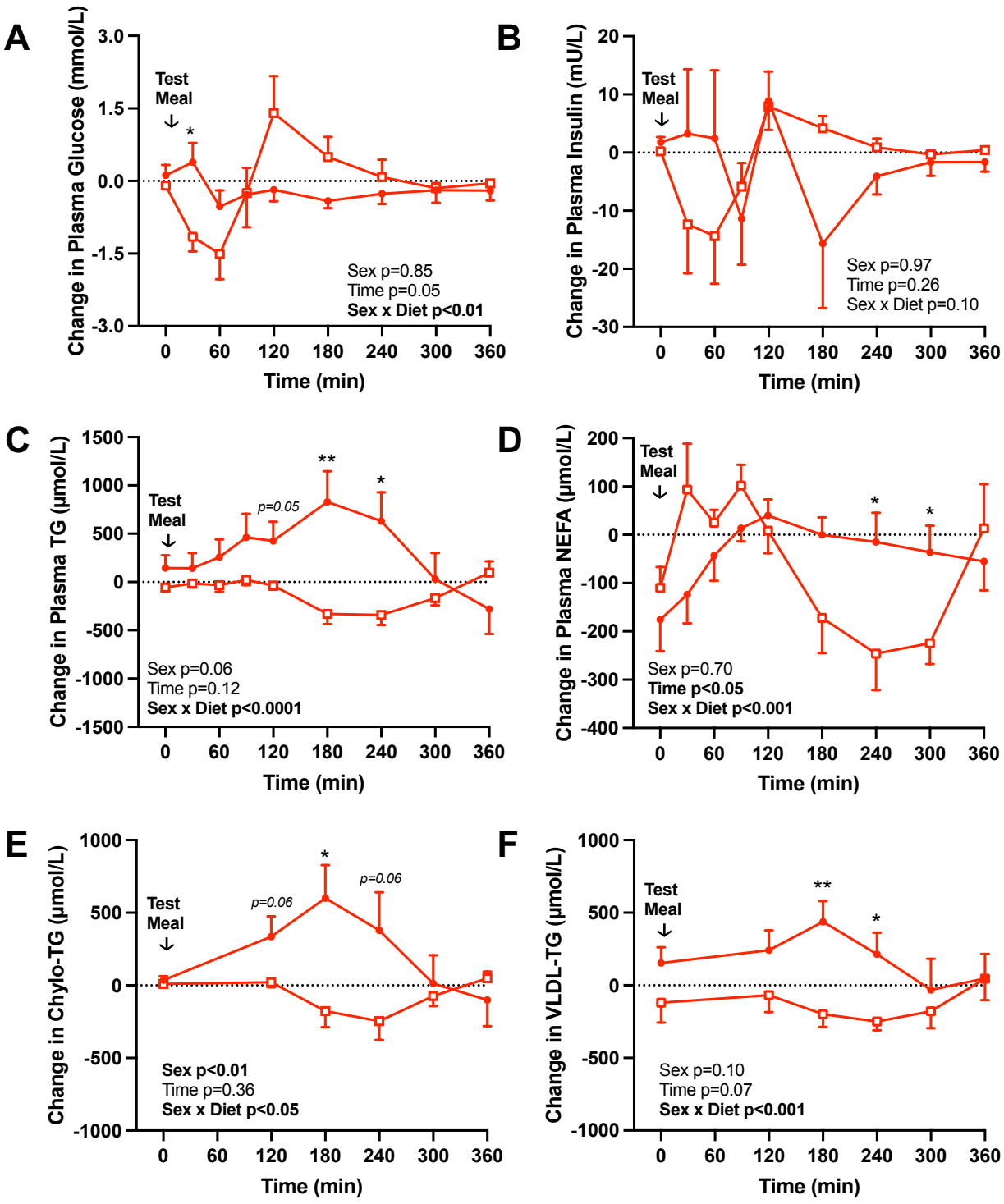

Figure S2.1 Change from baseline to post-HFD of postprandial plasma (A) glucose, (B) insulin, (C) triglyceride (TG), (D) non-esterified fatty acids (NEFA), (E) chylomicron (chylo)-TG, and (F) very-density lipoprotein (VLDL)-TG in males (•) and females (☐) after consuming a SFA-enriched HFD. Samples were collected at fasting and every (A-D) 30-60min or (E-F) 60min from 2h for 6h and analysed by a mixed-effects model with a Sidak post-hoc test, matching each participant pre- to post-HFD. Abbreviations: HFD, high fat diet; SFA, saturated fatty acid. Data presented as mean ± SEM; n=7 males; n=7 females; * $p<0.05$, ** $p<0.01$ indicate comparisons between sexes.

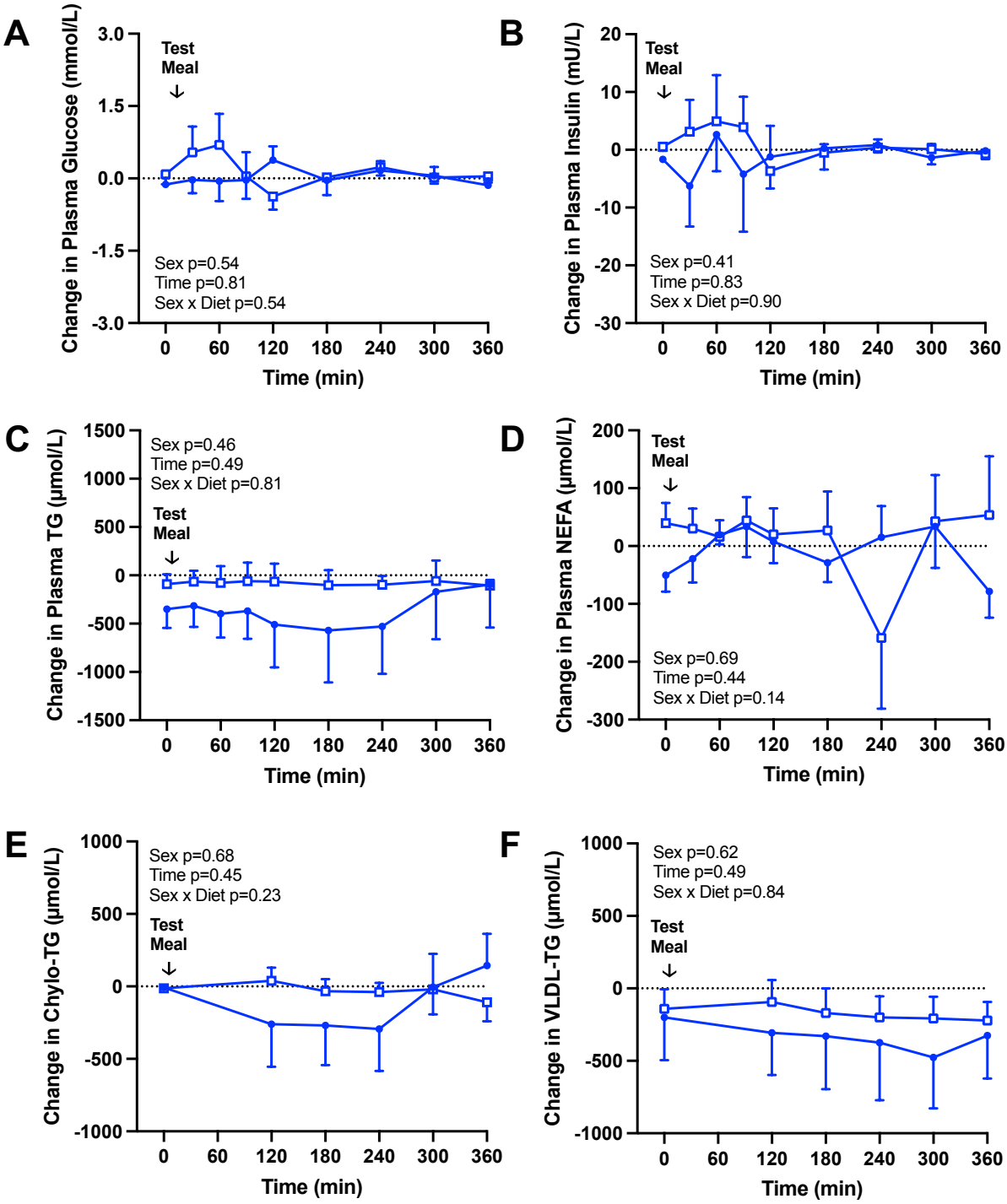

Fig. S2.2 Change from baseline to post-HFD of postprandial plasma (A) glucose, (B) insulin, (C) triglyceride (TG), (D) non-esterified fatty acids (NEFA), (E) chylomicron (chylo)-TG, and (F) very-density lipoprotein (VLDL)-TG in males (•) and females (☐) after consuming a PUFA-enriched HFD. Samples were collected at fasting and every (A-D) 30-60min or (E-F) 60min from 2h for 6h and analysed by a mixed-effects model, matching each participant pre- to post-HFD. Abbreviations: HFD, high fat diet; PUFA, polyunsaturated fatty acid. Data presented as mean ± SEM; n=7 males; n=7 females.

After consuming a SFA-enriched HFD, there was an interaction effect for the change from baseline to post-HFD between sexes in the appearance of [U^{13}C]palmitate in plasma-TG (p<0.0001), chylomicron-TG (p<0.01), plasma NEFA (p<0.001), and VLDL-TG (p<0.01) and the appearance of [2,2-D_2]palmitate in plasma-TG (p<0.05) and VLDL-TG (p<0.05) (Fig. S2.3.A-E, H). Males, compared with females, had greater postprandial incorporation of [U^{13}C]palmitate into plasma-TG and VLDL-TG and [2,2-D_2]palmitate incorporation into VLDL-TG at 180min and 240min, after consuming a SFA-enriched HFD compared with baseline (all p<0.05; Fig. S2.3A, D, H). Similarly, ther was greater postprandial incorporation of [U^{13}C]palmitate into chylomicron-TG at 120min (p=0.08), 180min (p<0.05), and 240min (p=0.06), in males, compared with females, after consming a SFA-enriched HFD compared with baseline (Fig. S2.3B). In contrast, females, compared with males, had lower appearance of [U^{13}C]palmitate into plasma NEFA at 180min, 240min, and 300min in response to the consumption of a test meal after consming a SFA-enriched HFD compared with respective baselines (all p<0.05; Fig. S2.3C). The change from baseline to post-HFD in R_a NEFA and incorporation of [2,2-D_2]palmitate in plasma NEFA did not differ between sexes (Fig. S2.3.F-G). After consuming a PUFA-enriched HFD, there were no differences in the appearance of [U^{13}C]palmitate or [2,2-D_2]palmitate in plasma-TG, chylomicron-TG NEFA, or VLDL-TG between males and females (Fig. S2.4.A-F). There were also no differences between males and females in the appearance of newly synthesised palmitate in VLDL-TG after consuming a SFA- or PUFA-enriched HFD compared with the respective baseline (Fig. S2.5.A-B). Taken together, this suggests there is a sexual dimorphism in the postprandial lipid metabolic response to consuming a SFA- compared with PUFA-enriched HFD. It appears that in males, compared with females, consuming a SFA-enriched diet leads to a greater increase in the transport of dietary FA, but not adipose-tissue derived FA, into the liver, and an increased secretion of dietary and adipose-tissue derived FA out of the liver.

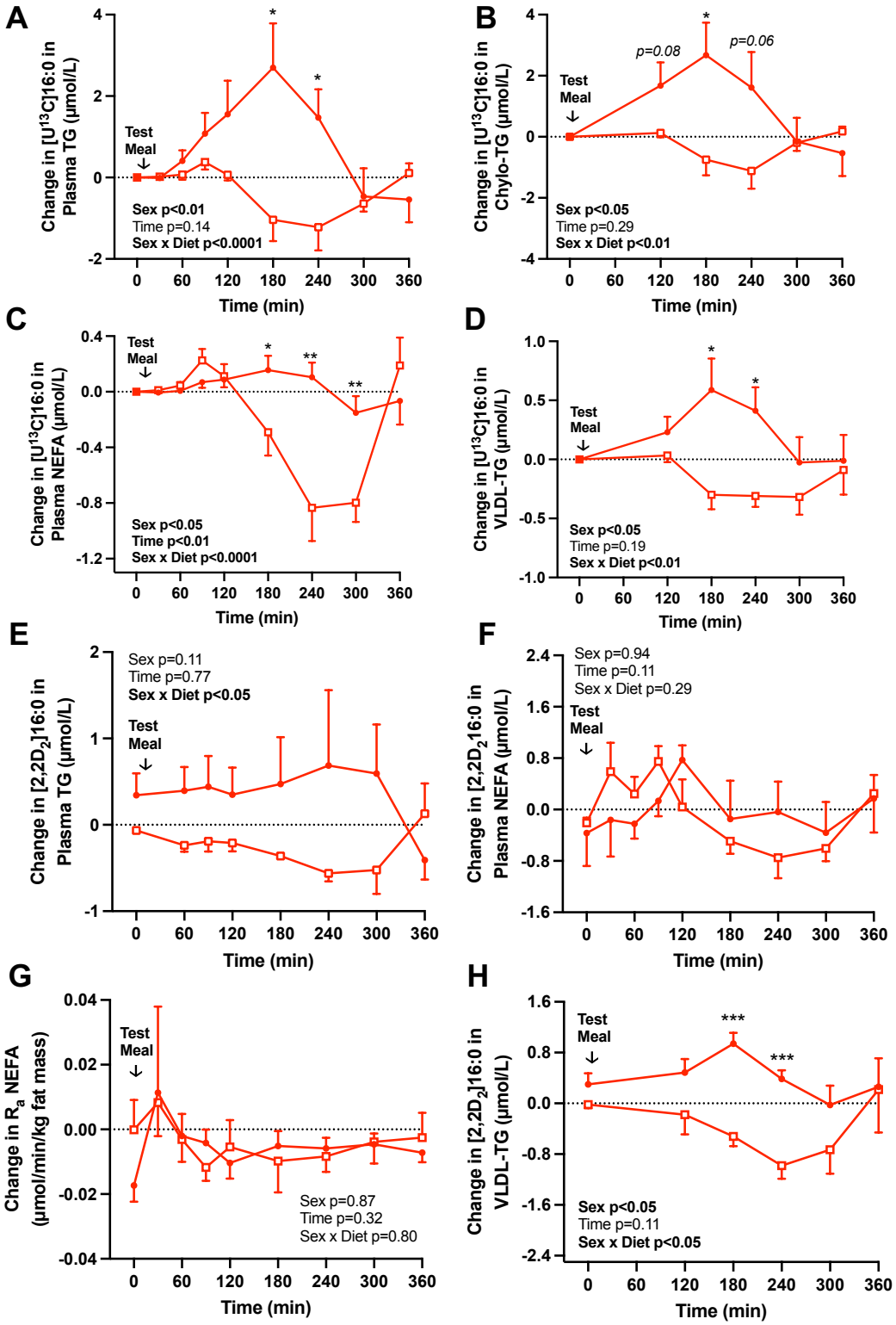

Fig. S2.3 Change from baseline to post-HFD of postprandial [U^{13}C]palmitate incorporation into plasma (A) TG, (B) chylomicron (chylo)-TG, (C) non-esterified fatty acids (NEFA) and (D) very-low density lipoprotein (VLDL)-TG and [2,2-D$_2$]palmitate incorporation into plasma (E) TG (F) NEFA, and (H) VLDL-TG, and (G) R$_a$ NEFA in males (•) and females (□) after consuming a SFA-enriched HFD. Samples were collected at fasting and every (A, C, E-G) 30-60min or (B, D, H) 60min from 2h for 6h and analysed by a mixed-effects model with a Sidak post-hoc test, matching each participant pre- to post-HFD. Abbreviations: HFD, high fat diet; SFA, saturated fatty acid. Data presented as mean ± SEM; n=7 males; n=7 females; * p<0.05, ** p<0.01; *** p<0.001 indicate comparisons between sexes.

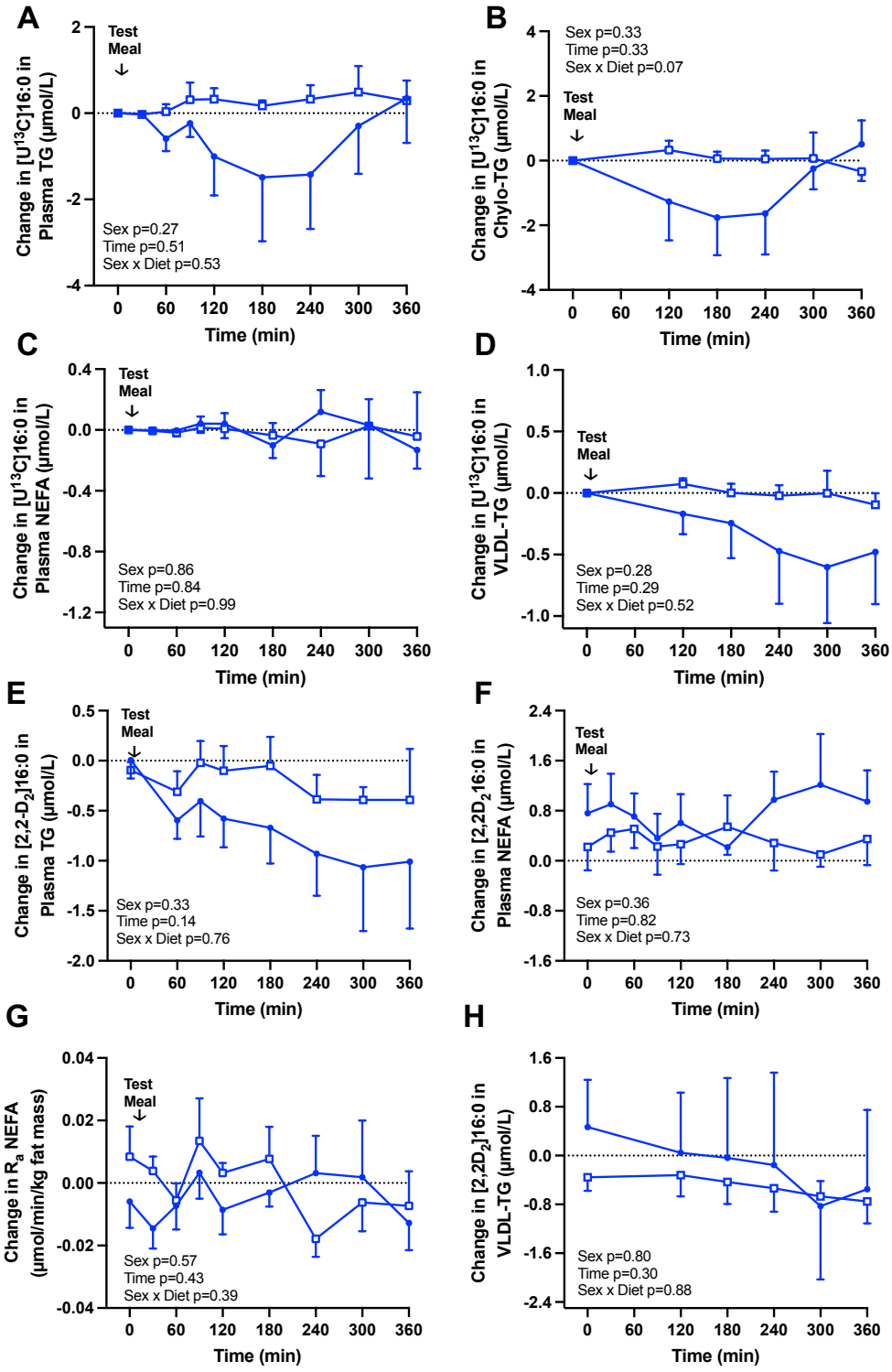

Fig. S2.4 Change from baseline to post-HFD of postprandial [U^{13}C]palmitate incorporation into plasma (A) TG, (B) chylomicron (chylo)-TG, (C) non-esterified fatty acids (NEFA) and (D) very-low density lipoprotein (VLDL)-TG and [2,2-D$_2$]palmitate incorporation into plasma (E) TG (F) NEFA, and (H) VLDL-TG, and (G) R$_a$ NEFA in males (•) and females (☐) after consuming a PUFA-enriched HFD. Samples were collected at fasting and every (A, C, E-G) 30-60min or (B, D, H) 60min from 2h for 6h and analysed by a mixed-effects model, matching each participant pre- to post-HFD. Abbreviations: HFD, high fat diet; PUFA, polyunsaturated fatty acid. Data presented as mean ± SEM; n=7 males; n=7 females.

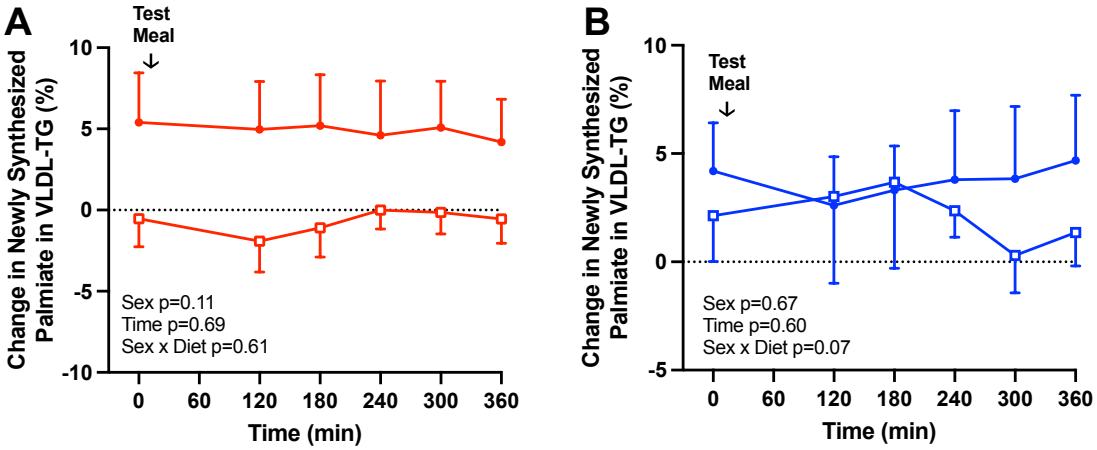

Fig. S2.5 Change from baseline to post-HFD of newly synthesised palmitate in postprandial very-low density lipoprotein (VLDL)-triglyceride (TG) in males (•) and females (☐) after consuming a (A) SFA- or (B) PUFA-enriched HFD. Samples were collected at fasting and every 60min from 2h for 6h and analysed by a mixed-effects model matching each participant pre- to post-HFD. Abbreviations: HFD, high fat diet; SFA, saturated fatty acid; PUFA, polyunsaturated fatty acid. Data presented as mean ± SEM; n=7 males; n=7 females.

Appendix 3. Chapter 5 Supplementary Data

Supplementary Table 3.1. qPCR Primer Sequences

Gene	Sequence (Direction)
UBC	CCTGGTGCTCCGTCTTAGAG (fwd) TTTCCCAGCAAAGATCAACC (rev)
BNIP3	GAATTTCTGAAAGTTTTCCTTCCA (fwd) TTGTCAGACGCCTTCCAATA (rev)
PDK4	TGGTCCAAGATGCCTTTGAGT (fwd) GTTGCCCGCATTGCATTCTT (rev)
CD36	TTGCAAAACGGCTGCAGGTC (fwd) TCACCAATGGTCCCAGTCTCAT (rev)
ACLS4	TTGGCACAACAGAAAGGGGT (fwd) ATCGCTCCAATTTCATGGCA (rev)

Abbreviations: Fwd: forward; Rev, reverse.

Supplementary Table 3.2. Top Differentially Expressed Genes from Transcriptomics

Gene	Gene Name	Function of Protein Encoded by Gene	Upregulated In
PDK4	Pyruvate dehydrogenase 4	Inhibits pyruvate dehydrogenase to promote FA oxidation	OA, compared with No Fat, treated hiPSC-CMs
CPT1A	Carnitine palmitoyl transferase 1	Promotes FA entry into mitochondria	
PLIN2	Perilipin 2	Promotes formation of cytosolic lipid droplets	
ANGPTL4	Angiopoietin-like 4	Inhibits lipoprotein lipase	
IRS2	Insulin receptor substrate 2	Part of insulin signaling cascade	
KATNB1	Katanin regulatory subunit B1	Involved in microtubule polymerisation	No Fat-treated, compared with OA, treated hiPSC-CMs
RAMP1	Receptor activity modifying protein 1	Involved in calcitonin-gene related peptide signaling	
ADI1	Acireductone dioxygenase 1	Enzyme involved in methionine salvage	
CBR1	Carbonyl reductase 1	Reduces lipid peroxidation products	
TMEM25	Transmembrane protein 25	Function unknown in human cardiomyocytes	
MLYCD	Malonyl-CoA decarboxylase	Breaks down malonyl-CoA into acetyl-CoA	Lipid Mix, compared with No Fat, treated hiPSC-CMs
HADHA	Hydroxyacyl-CoA dehydrogenase trifunctional multienzyme complex subunit alpha	Enzyme involved in β-oxidation	
KLF9	Krueppel-like factor 9	Transcription factor involved in cell differentiation	No Fat, compared with Lipid Mix, treated hiPSC-CMs
DHRS3	Dehydrogenase/reductase 3	Dehydrogenase involved in retinoic acid metabolism	
RIN3	Ras and Rab Interactor 3	A guanine nucleotide exchange factor	
ABCG1	ABC binding cassette protein G1	Cholesterol membrane transporter	
CD74	HLA-DR antigens-associated invariant chain	Receptor for migration inhibitory factor (MIF)	
MYH3	Myosin heavy chain 3	Encode myosin-3, part of the cardiac sarcomere	PUFA-, compared with SFA-enriched lipid mix, treated hiPSC-CMs
MLYK3	Myosin light chain kinase 3	Regulates cardiac sarcomere contraction	
FITM2	Fat Storage Inducing Transmembrane Protein 2	Promotes cytosolic lipid droplet formation	
CLSTN2	Calsyntenin 2	Involved in cellular adhesion	

FABP5	Fatty acid binding protein 5	Solubilises and binds FA	SFA-, compared with PUFA-enriched lipid mix, treated hiPSC-CMs
MFAP4	Microfibril associated protein 4	Contributes to the extracellular matrix structure	
CDKN1C	Cyclin dependent kinase inhibitor 1C	Regulates cell cycle progression	
IRX4	Iroquois homeobox 4	Involved in cardiomyocyte differentiation	
DLK1	Delta like non-canonical Notch ligand 1	Regulates cardiomyocyte-induced fibroblast remodeling	

Abbreviations: FA: fatty acid; hiPSC-CM: human induced pluripotent stem cell derived cardiomyocyte; OA: oleic acid; PUFA: polyunsaturated fatty acid; SFA: saturated fatty acid

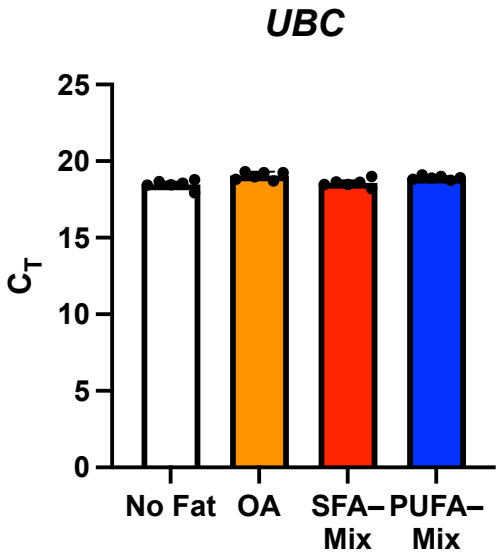

Supplemental Figure S3.1. Housekeeping Gene Expression. Absolute Ubiquitin C (*UBC*) expression, expressed as the cycle threshold (C_T) measured by quantitative-PCR in hiPSC-CMs treated with no fat, 76µM oleic acid (OA), or 400µM lipid-mix enriched with saturated (SFA) or polyunsaturated (PUFA) fatty acids for eight days with media changes every other day. Data: mean ± SEM, n=6 per group, * $p<0.05$.

3.1 Transcriptomic responses of hiPSC-CMs treated with OA compared with no-fat

Differential gene expression analysis between hiPSC-CMs treated with OA compared with no-fat helped characterise the transcriptomic response of the positive-control compared with negative-control treated hiPSC-CMs as a reference point for further comparisons. Differentially expressed genes were identified by an FDR <0.05 and FC >2 (OA) or <2 (no-fat) and visualised using a volcano plot (Fig. S3.2A). All five top upregulated genes in the OA compared with no-fat group are involved in FA metabolism (Fig. S3.2A, Table S3.2.), while the top five upregulated genes in the no-fat compared with OA-group appear unrelated (Fig. S3.2A, Table S3.2). In hiPSC-CMs treated with OA compared with no-fat, 1798 genes were significantly upregulated, 1501 genes were significantly downregulated, and 6757 genes were unchanged (Fig. S3.2B). Findings from this transcriptomic comparison were validated by qPCR confirming greater *PDK4* expression in hiPSC-CMs treated with OA compared with no-fat (Fig. S3.2C).

To determine which cellular pathways are differentially regulated in hiPSC-CMs treated with OA compared with no-fat, gene set enrichment analysis (GSEA) was performed using hallmark pathways. Three groups of pathways were significantly upregulated in OA compared with no-fat treated hiPSC-CMs: pathways involved in *i)* metabolism (hypoxia and glycolysis), *ii)* inflammatory signaling (hypoxia, TNFα signaling, IL2-STAT5 signaling, unfolded protein response), and *iii)* cell differentiation and development (mitotic spindle, estrogen response, UV response to DNA, hedgehog signaling and mTORC1 signaling) (Fig. S3.3). In hiPSC-CMs treated with no-fat compared with OA, four pathways with upregulated: epithelial-to-mesenchymal transition, coagulation, DNA repair, and IFNα response (Fig. S3.3).

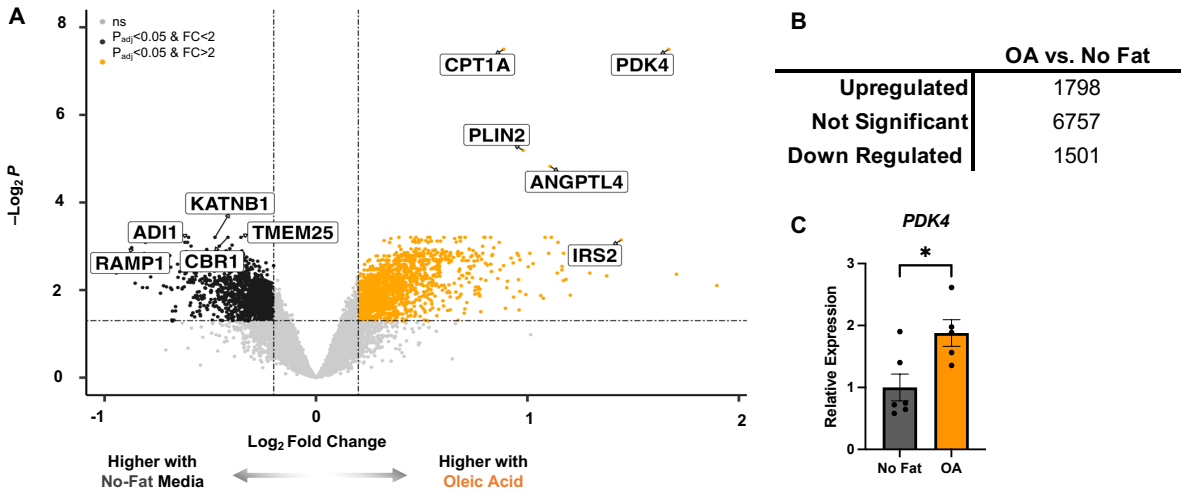

Figure S3.2. Transcriptional profile of hiPSC-CMs treated with oleic acid compared with no-fat. Transcriptomic analysis was performed on hiPSC-CMs treated with no fatty acids compared with 76µM oleic acid (OA) for eight days with media changes every other day. Data was visualised using a **(A)** volcano plot with individually differentially expressed genes (fold change (FC) > 2 and p_{adj} < 0.05) indicated by an orange dot if upregulated with OA or dark grey dot if upregulated with no-fat. **(B)** total number of differentially expressed genes in each condition. **(C)** *PDK4* expression measured by quantitative-PCR, data: mean ± SEM, n=6 per group, **p*<0.05.

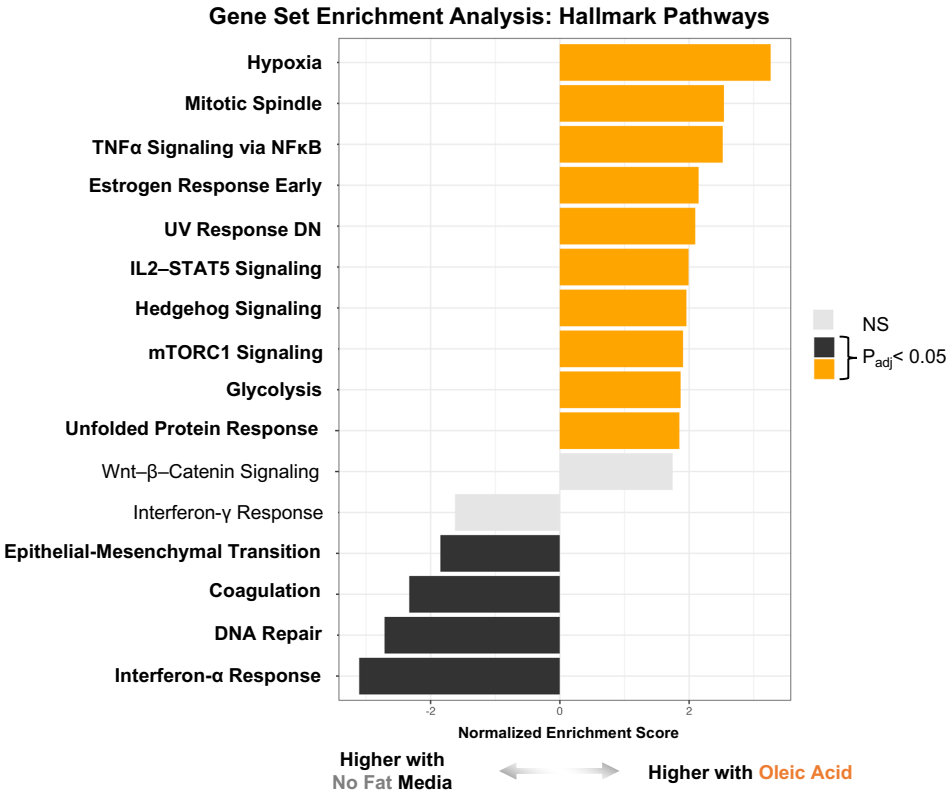

Figure S3.3. Pathway analysis of hiPSC-CMs treated with oleic acid compared with no fat. Gene set enrichment analysis was performed with hallmark pathways using the differentially expressed gene list generated by transcriptomic analysis of hiPSC-CMs treated with 76µM oleic acid compared with no fat. Significantly differentially regulated pathways (p_{adj}<0.05) between conditions are indicated by bold text and orange blocks if upregulated in response to oleic acid or dark grey blocks if upregulated in response to no fat, n=6 per group.

References

1. Rinella ME, Lazarus JV, Ratziu V, Francque SM, Sanyal AJ, Kanwal F, et al. A multisociety Delphi consensus statement on new fatty liver disease nomenclature. Hepatology. 2023;78(6):1966-86.
2. Schulze MB, Stefan N. Metabolically healthy obesity: from epidemiology and mechanisms to clinical implications. Nat Rev Endocrinol. 2024;20(11):633-46.
3. The Lancet Diabetes E. Redefining obesity: advancing care for better lives. Lancet Diabetes Endocrinol. 2025;13(2):75.
4. Emerging Risk Factors C, Wormser D, Kaptoge S, Di Angelantonio E, Wood AM, Pennells L, et al. Separate and combined associations of body-mass index and abdominal adiposity with cardiovascular disease: collaborative analysis of 58 prospective studies. Lancet. 2011;377(9771):1085-95.
5. Boutari C, Mantzoros CS. A 2022 update on the epidemiology of obesity and a call to action: as its twin COVID-19 pandemic appears to be receding, the obesity and dysmetabolism pandemic continues to rage on. Metabolism. 2022;133:155217.
6. Yki-Jarvinen H, Luukkonen PK, Hodson L, Moore JB. Dietary carbohydrates and fats in nonalcoholic fatty liver disease. Nat Rev Gastroenterol Hepatol. 2021;18(11):770-86.
7. Levelt E, Pavlides M, Banerjee R, Mahmod M, Kelly C, Sellwood J, et al. Ectopic and Visceral Fat Deposition in Lean and Obese Patients With Type 2 Diabetes. J Am Coll Cardiol. 2016;68(1):53-63.
8. Laine S, Sjoros T, Garthwaite T, Saarenhovi M, Kallio P, Loyttyniemi E, et al. Relationship between liver fat content and lifestyle factors in adults with metabolic syndrome. Sci Rep. 2022;12(1):17428.
9. Luukkonen PK, Sadevirta S, Zhou Y, Kayser B, Ali A, Ahonen L, et al. Saturated Fat Is More Metabolically Harmful for the Human Liver Than Unsaturated Fat or Simple Sugars. Diabetes Care. 2018;41(8):1732-9.
10. Rosqvist F, Iggman D, Kullberg J, Cedernaes J, Johansson HE, Larsson A, et al. Overfeeding polyunsaturated and saturated fat causes distinct effects on liver and visceral fat accumulation in humans. Diabetes. 2014;63(7):2356-68.
11. Rosqvist F, Kullberg J, Stahlman M, Cedernaes J, Heurling K, Johansson HE, et al. Overeating Saturated Fat Promotes Fatty Liver and Ceramides Compared With Polyunsaturated Fat: A Randomized Trial. J Clin Endocrinol Metab. 2019;104(12):6207-19.
12. Schonfeld P, Wojtczak L. Short- and medium-chain fatty acids in energy metabolism: the cellular perspective. J Lipid Res. 2016;57(6):943-54.
13. Hodson L, Skeaff CM, Fielding BA. Fatty acid composition of adipose tissue and blood in humans and its use as a biomarker of dietary intake. Prog Lipid Res. 2008;47(5):348-80.

14. Stremmel W, Lotz G, Strohmeyer G, Berk PD. Identification, isolation, and partial characterization of a fatty acid binding protein from rat jejunal microvillous membranes. J Clin Invest. 1985;75(3):1068-76.

15. Hamilton JA. New insights into the roles of proteins and lipids in membrane transport of fatty acids. Prostaglandins Leukot Essent Fatty Acids. 2007;77(5-6):355-61.

16. Luiken JJ, Willems J, van der Vusse GJ, Glatz JF. Electrostimulation enhances FAT/CD36-mediated long-chain fatty acid uptake by isolated rat cardiac myocytes. Am J Physiol Endocrinol Metab. 2001;281(4):E704-12.

17. Windler E, Greeve J, Robenek H, Rinninger F, Greten H, Jackle S. Differences in the mechanisms of uptake and endocytosis of small and large chylomicron remnants by rat liver. Hepatology. 1996;24(2):344-51.

18. Mashek DG, Coleman RA. Cellular fatty acid uptake: the contribution of metabolism. Curr Opin Lipidol. 2006;17(3):274-8.

19. Furler SM, Cooney GJ, Hegarty BD, Lim-Fraser MY, Kraegen EW, Oakes ND. Local factors modulate tissue-specific NEFA utilization: assessment in rats using 3H-(R)-2-bromopalmitate. Diabetes. 2000;49(9):1427-33.

20. Puchalska P, Crawford PA. Multi-dimensional Roles of Ketone Bodies in Fuel Metabolism, Signaling, and Therapeutics. Cell Metab. 2017;25(2):262-84.

21. Paulson DJ, Ward KM, Shug AL. Malonyl CoA inhibition of carnitine palmityltransferase in rat heart mitochondria. FEBS Lett. 1984;176(2):381-4.

22. Welte MA, Gould AP. Lipid droplet functions beyond energy storage. Biochim Biophys Acta Mol Cell Biol Lipids. 2017;1862(10 Pt B):1260-72.

23. Whyte M, Karmen A, Goodman DS. Fatty Acid Esterification and Chylomicron Formation during Fat Absorption. 2. Phospholipids. J Lipid Res. 1963;4:322-9.

24. Xie C, Woollett LA, Turley SD, Dietschy JM. Fatty acids differentially regulate hepatic cholesteryl ester formation and incorporation into lipoproteins in the liver of the mouse. J Lipid Res. 2002;43(9):1508-19.

25. Yen CE, Nelson DW, Yen MI. Intestinal triacylglycerol synthesis in fat absorption and systemic energy metabolism. J Lipid Res. 2015;56(3):489-501.

26. Kumar NS, Mansbach CM, 2nd. Prechylomicron transport vesicle: isolation and partial characterization. Am J Physiol. 1999;276(2):G378-86.

27. Hussain MM. A proposed model for the assembly of chylomicrons. Atherosclerosis. 2000;148(1):1-15.

28. Chen J, Fang Z, Luo Q, Wang X, Warda M, Das A, et al. Unlocking the mysteries of VLDL: exploring its production, intracellular trafficking, and metabolism as therapeutic targets. Lipids Health Dis. 2024;23(1):14.

29. Breyer ED, Le NA, Li X, Martinson D, Brown WV. Apolipoprotein C-III displacement of apolipoprotein E from VLDL: effect of particle size. J Lipid Res. 1999;40(10):1875-82.
30. Wu SA, Kersten S, Qi L. Lipoprotein Lipase and Its Regulators: An Unfolding Story. Trends Endocrinol Metab. 2021;32(1):48-61.
31. Goldstein JL, Brown MS. Binding and degradation of low density lipoproteins by cultured human fibroblasts. Comparison of cells from a normal subject and from a patient with homozygous familial hypercholesterolemia. J Biol Chem. 1974;249(16):5153-62.
32. Hodson L, Fielding BA. Stearoyl-CoA desaturase: rogue or innocent bystander? Prog Lipid Res. 2013;52(1):15-42.
33. Pramfalk C, Pavlides M, Banerjee R, McNeil CA, Neubauer S, Karpe F, et al. Fasting Plasma Insulin Concentrations Are Associated With Changes in Hepatic Fatty Acid Synthesis and Partitioning Prior to Changes in Liver Fat Content in Healthy Adults. Diabetes. 2016;65(7):1858-67.
34. Blouin A, Bolender RP, Weibel ER. Distribution of organelles and membranes between hepatocytes and nonhepatocytes in the rat liver parenchyma. A stereological study. J Cell Biol. 1977;72(2):441-55.
35. Hatting M, Tavares CDJ, Sharabi K, Rines AK, Puigserver P. Insulin regulation of gluconeogenesis. Ann N Y Acad Sci. 2018;1411(1):21-35.
36. Schwarz JM, Linfoot P, Dare D, Aghajanian K. Hepatic de novo lipogenesis in normoinsulinemic and hyperinsulinemic subjects consuming high-fat, low-carbohydrate and low-fat, high-carbohydrate isoenergetic diets. Am J Clin Nutr. 2003;77(1):43-50.
37. Kraegen EW, Sowden JA, Halstead MB, Clark PW, Rodnick KJ, Chisholm DJ, et al. Glucose transporters and in vivo glucose uptake in skeletal and cardiac muscle: fasting, insulin stimulation and immunoisolation studies of GLUT1 and GLUT4. Biochem J. 1993;295 (Pt 1)(Pt 1):287-93.
38. Fischer Y, Thomas J, Sevilla L, Munoz P, Becker C, Holman G, et al. Insulin-induced recruitment of glucose transporter 4 (GLUT4) and GLUT1 in isolated rat cardiac myocytes. Evidence of the existence of different intracellular GLUT4 vesicle populations. J Biol Chem. 1997;272(11):7085-92.
39. Kozka IJ, Clark AE, Reckless JP, Cushman SW, Gould GW, Holman GD. The effects of insulin on the level and activity of the GLUT4 present in human adipose cells. Diabetologia. 1995;38(6):661-6.
40. Abel ED. Insulin signaling in the heart. Am J Physiol Endocrinol Metab. 2021;321(1):E130-E45.
41. Carpentier AC. 100(th) anniversary of the discovery of insulin perspective: insulin and adipose tissue fatty acid metabolism. Am J Physiol Endocrinol Metab. 2021;320(4):E653-E70.
42. Frayn KN, Coppack SW, Humphreys SM, Clark ML, Evans RD. Periprandial regulation of lipid metabolism in insulin-treated diabetes mellitus. Metabolism. 1993;42(4):504-10.

43. Najjar SM, Perdomo G. Hepatic Insulin Clearance: Mechanism and Physiology. Physiology (Bethesda). 2019;34(3):198-215.

44. Janah L, Kjeldsen S, Galsgaard KD, Winther-Sorensen M, Stojanovska E, Pedersen J, et al. Glucagon Receptor Signaling and Glucagon Resistance. Int J Mol Sci. 2019;20(13).

45. Hodson L, Bickerton AS, McQuaid SE, Roberts R, Karpe F, Frayn KN, et al. The contribution of splanchnic fat to VLDL triglyceride is greater in insulin-resistant than insulin-sensitive men and women: studies in the postprandial state. Diabetes. 2007;56(10):2433-41.

46. Broedl UC, Maugeais C, Millar JS, Jin W, Moore RE, Fuki IV, et al. Endothelial lipase promotes the catabolism of ApoB-containing lipoproteins. Circ Res. 2004;94(12):1554-61.

47. Brown JD, Oligino E, Rader DJ, Saghatelian A, Plutzky J. VLDL hydrolysis by hepatic lipase regulates PPARdelta transcriptional responses. PLoS One. 2011;6(7):e21209.

48. Chan MP, Takenaka N, Abe Y, Satoh T. Insulin-stimulated translocation of the fatty acid transporter CD36 to the plasma membrane is mediated by the small GTPase Rac1 in adipocytes. Cell Signal. 2024;117:111102.

49. Miles JM, Park YS, Walewicz D, Russell-Lopez C, Windsor S, Isley WL, et al. Systemic and forearm triglyceride metabolism: fate of lipoprotein lipase-generated glycerol and free fatty acids. Diabetes. 2004;53(3):521-7.

50. Karpe F, Humphreys SM, Samra JS, Summers LK, Frayn KN. Clearance of lipoprotein remnant particles in adipose tissue and muscle in humans. J Lipid Res. 1997;38(11):2335-43.

51. Arbeeny CM, Rifici VA. The uptake of chylomicron remnants and very low density lipoprotein remnants by the perfused rat liver. J Biol Chem. 1984;259(15):9662-6.

52. Hodson L, Rosqvist F, Parry SA. The influence of dietary fatty acids on liver fat content and metabolism. Proc Nutr Soc. 2020;79(1):30-41.

53. Stralfors P, Bjorgell P, Belfrage P. Hormonal regulation of hormone-sensitive lipase in intact adipocytes: identification of phosphorylated sites and effects on the phosphorylation by lipolytic hormones and insulin. Proc Natl Acad Sci U S A. 1984;81(11):3317-21.

54. McGarry JD, Meier JM, Foster DW. The effects of starvation and refeeding on carbohydrate and lipid metabolism in vivo and in the perfused rat liver. The relationship between fatty acid oxidation and esterification in the regulation of ketogenesis. J Biol Chem. 1973;248(1):270-8.

55. Lewis GF, Carpentier A, Adeli K, Giacca A. Disordered fat storage and mobilization in the pathogenesis of insulin resistance and type 2 diabetes. Endocr Rev. 2002;23(2):201-29.

56. Chait A, Ginsberg HN, Vaisar T, Heinecke JW, Goldberg IJ, Bornfeldt KE. Remnants of the Triglyceride-Rich Lipoproteins, Diabetes, and Cardiovascular Disease. Diabetes. 2020;69(4):508-16.

57. Heeren J, Grewal T, Jackle S, Beisiegel U. Recycling of apolipoprotein E and lipoprotein lipase through endosomal compartments in vivo. J Biol Chem. 2001;276(45):42333-8.

58. Barrows BR, Parks EJ. Contributions of different fatty acid sources to very low-density lipoprotein-triacylglycerol in the fasted and fed states. J Clin Endocrinol Metab. 2006;91(4):1446-52.

59. Malmstrom R, Packard CJ, Caslake M, Bedford D, Stewart P, Yki-Jarvinen H, et al. Effects of insulin and acipimox on VLDL1 and VLDL2 apolipoprotein B production in normal subjects. Diabetes. 1998;47(5):779-87.

60. Donnelly KL, Smith CI, Schwarzenberg SJ, Jessurun J, Boldt MD, Parks EJ. Sources of fatty acids stored in liver and secreted via lipoproteins in patients with nonalcoholic fatty liver disease. J Clin Invest. 2005;115(5):1343-51.

61. Bjermo H, Iggman D, Kullberg J, Dahlman I, Johansson L, Persson L, et al. Effects of n-6 PUFAs compared with SFAs on liver fat, lipoproteins, and inflammation in abdominal obesity: a randomized controlled trial. Am J Clin Nutr. 2012;95(5):1003-12.

62. Magana MM, Lin SS, Dooley KA, Osborne TF. Sterol regulation of acetyl coenzyme A carboxylase promoter requires two interdependent binding sites for sterol regulatory element binding proteins. J Lipid Res. 1997;38(8):1630-8.

63. Magana MM, Osborne TF. Two tandem binding sites for sterol regulatory element binding proteins are required for sterol regulation of fatty-acid synthase promoter. J Biol Chem. 1996;271(51):32689-94.

64. Ericsson J, Jackson SM, Kim JB, Spiegelman BM, Edwards PA. Identification of glycerol-3-phosphate acyltransferase as an adipocyte determination and differentiation factor 1- and sterol regulatory element-binding protein-responsive gene. J Biol Chem. 1997;272(11):7298-305.

65. Chong MF, Hodson L, Bickerton AS, Roberts R, Neville M, Karpe F, et al. Parallel activation of de novo lipogenesis and stearoyl-CoA desaturase activity after 3 d of high-carbohydrate feeding. Am J Clin Nutr. 2008;87(4):817-23.

66. Ma L, Tsatsos NG, Towle HC. Direct role of ChREBP.Mlx in regulating hepatic glucose-responsive genes. J Biol Chem. 2005;280(12):12019-27.

67. Roberts R, Bickerton AS, Fielding BA, Blaak EE, Wagenmakers AJ, Chong MF, et al. Reduced oxidation of dietary fat after a short term high-carbohydrate diet. Am J Clin Nutr. 2008;87(4):824-31.

68. Hudgins LC, Hellerstein M, Seidman C, Neese R, Diakun J, Hirsch J. Human fatty acid synthesis is stimulated by a eucaloric low fat, high carbohydrate diet. J Clin Invest. 1996;97(9):2081-91.

69. Marques-Lopes I, Ansorena D, Astiasaran I, Forga L, Martinez JA. Postprandial de novo lipogenesis and metabolic changes induced by a high-carbohydrate, low-fat meal in lean and overweight men. Am J Clin Nutr. 2001;73(2):253-61.

70. Semple RK, Sleigh A, Murgatroyd PR, Adams CA, Bluck L, Jackson S, et al. Postreceptor insulin resistance contributes to human dyslipidemia and hepatic steatosis. J Clin Invest. 2009;119(2):315-22.

71. Randle PJ, Garland PB, Hales CN, Newsholme EA. The glucose fatty-acid cycle. Its role in insulin sensitivity and the metabolic disturbances of diabetes mellitus. Lancet. 1963;1(7285):785-9.

72. Hagenfeldt L, Wahren J, Pernow B, Raf L. Uptake of individual free fatty acids by skeletal muscle and liver in man. J Clin Invest. 1972;51(9):2324-30.

73. Rakhshandehroo M, Knoch B, Muller M, Kersten S. Peroxisome proliferator-activated receptor alpha target genes. PPAR Res. 2010;2010.

74. Rinella ME, Lazarus JV, Ratziu V, Francque SM, Sanyal AJ, Kanwal F, et al. A multisociety Delphi consensus statement on new fatty liver disease nomenclature. Hepatology. 2023;78(6):1966-86.

75. Westerbacka J, Lammi K, Hakkinen AM, Rissanen A, Salminen I, Aro A, et al. Dietary fat content modifies liver fat in overweight nondiabetic subjects. J Clin Endocrinol Metab. 2005;90(5):2804-9.

76. van Herpen NA, Schrauwen-Hinderling VB, Schaart G, Mensink RP, Schrauwen P. Three weeks on a high-fat diet increases intrahepatic lipid accumulation and decreases metabolic flexibility in healthy overweight men. J Clin Endocrinol Metab. 2011;96(4):E691-5.

77. Utzschneider KM, Bayer-Carter JL, Arbuckle MD, Tidwell JM, Richards TL, Craft S. Beneficial effect of a weight-stable, low-fat/low-saturated fat/low-glycaemic index diet to reduce liver fat in older subjects. Br J Nutr. 2013;109(6):1096-104.

78. Koopman KE, Caan MW, Nederveen AJ, Pels A, Ackermans MT, Fliers E, et al. Hypercaloric diets with increased meal frequency, but not meal size, increase intrahepatic triglycerides: a randomized controlled trial. Hepatology. 2014;60(2):545-53.

79. Luukkonen PK, Sadevirta S, Zhou Y, Kayser B, Ali A, Ahonen L, et al. Saturated Fat Is More Metabolically Harmful for the Human Liver Than Unsaturated Fat or Simple Sugars. Diabetes Care. 2018;41(8):1732-9.

80. McQuaid SE, Hodson L, Neville MJ, Dennis AL, Cheeseman J, Humphreys SM, et al. Downregulation of adipose tissue fatty acid trafficking in obesity: a driver for ectopic fat deposition? Diabetes. 2011;60(1):47-55.

81. Klein RJ, Viana Rodriguez GM, Rotman Y, Brown RJ. Divergent pathways of liver fat accumulation, oxidation, and secretion in lipodystrophy versus obesity-associated NAFLD. Liver Int. 2023;43(12):2692-700.

82. Sookoian S, Pirola CJ. Meta-analysis of the influence of I148M variant of patatin-like phospholipase domain containing 3 gene (PNPLA3) on the susceptibility and histological severity of nonalcoholic fatty liver disease. Hepatology. 2011;53(6):1883-94.

83. Mahdessian H, Taxiarchis A, Popov S, Silveira A, Franco-Cereceda A, Hamsten A, et al. TM6SF2 is a regulator of liver fat metabolism influencing triglyceride secretion and hepatic lipid droplet content. Proc Natl Acad Sci U S A. 2014;111(24):8913-8.

84. Boden G. Role of fatty acids in the pathogenesis of insulin resistance and NIDDM. Diabetes. 1997;46(1):3-10.

85. Karpe F, Dickmann JR, Frayn KN. Fatty acids, obesity, and insulin resistance: time for a reevaluation. Diabetes. 2011;60(10):2441-9.

86. Mittendorfer B, Magkos F, Fabbrini E, Mohammed BS, Klein S. Relationship between body fat mass and free fatty acid kinetics in men and women. Obesity (Silver Spring). 2009;17(10):1872-7.

87. Bugianesi E, Gastaldelli A, Vanni E, Gambino R, Cassader M, Baldi S, et al. Insulin resistance in non-diabetic patients with non-alcoholic fatty liver disease: sites and mechanisms. Diabetologia. 2005;48(4):634-42.

88. Kim MS, Krawczyk SA, Doridot L, Fowler AJ, Wang JX, Trauger SA, et al. ChREBP regulates fructose-induced glucose production independently of insulin signaling. J Clin Invest. 2016;126(11):4372-86.

89. Nakamuta M, Kohjima M, Higuchi N, Kato M, Kotoh K, Yoshimoto T, et al. The significance of differences in fatty acid metabolism between obese and non-obese patients with non-alcoholic fatty liver disease. Int J Mol Med. 2008;22(5):663-7.

90. Sunny NE, Parks EJ, Browning JD, Burgess SC. Excessive hepatic mitochondrial TCA cycle and gluconeogenesis in humans with nonalcoholic fatty liver disease. Cell Metab. 2011;14(6):804-10.

91. Ament Z, West JA, Stanley E, Ashmore T, Roberts LD, Wright J, et al. PPAR-pan activation induces hepatic oxidative stress and lipidomic remodelling. Free Radic Biol Med. 2016;95:357-68.

92. Parry SA, Rosqvist F, Cornfield T, Barrett A, Hodson L. Oxidation of dietary linoleate occurs to a greater extent than dietary palmitate in vivo in humans. Clin Nutr. 2021;40(3):1108-14.

93. Adiels M, Westerbacka J, Soro-Paavonen A, Hakkinen AM, Vehkavaara S, Caslake MJ, et al. Acute suppression of VLDL1 secretion rate by insulin is associated with hepatic fat content and insulin resistance. Diabetologia. 2007;50(11):2356-65.

94. Fabbrini E, Mohammed BS, Magkos F, Korenblat KM, Patterson BW, Klein S. Alterations in adipose tissue and hepatic lipid kinetics in obese men and women with nonalcoholic fatty liver disease. Gastroenterology. 2008;134(2):424-31.

95. Lytle KA, Bush NC, Triay JM, Kellogg TA, Kendrick ML, Swain JM, et al. Hepatic Fatty Acid Balance and Hepatic Fat Content in Humans With Severe Obesity. J Clin Endocrinol Metab. 2019;104(12):6171-81.

96. Lopaschuk GD, Ussher JR, Folmes CD, Jaswal JS, Stanley WC. Myocardial fatty acid metabolism in health and disease. Physiol Rev. 2010;90(1):207-58.

97. Belke DD, Larsen TS, Lopaschuk GD, Severson DL. Glucose and fatty acid metabolism in the isolated working mouse heart. Am J Physiol. 1999;277(4):R1210-7.

98. Bing RJ, Siegel A, Ungar I, Gilbert M. Metabolism of the human heart. II. Studies on fat, ketone and amino acid metabolism. Am J Med. 1954;16(4):504-15.

99. Shipp JC, Opie LH, Challoner D. Fatty Acid and Glucose Metabolism in the Perfused Heart. Nature. 1961;189(4769):1018-9.

100. Neely JR, Morgan HE. Relationship between carbohydrate and lipid metabolism and the energy balance of heart muscle. Annu Rev Physiol. 1974;36:413-59.

101. Saddik M, Lopaschuk GD. Myocardial triglyceride turnover and contribution to energy substrate utilization in isolated working rat hearts. J Biol Chem. 1991;266(13):8162-70.

102. Kessler G, Friedman J. Metabolism of fatty acids and glucose. Circulation. 1998;98(13):1351.

103. Goodwin GW, Arteaga JR, Taegtmeyer H. Glycogen turnover in the isolated working rat heart. J Biol Chem. 1995;270(16):9234-40.

104. Henning SL, Wambolt RB, Schonekess BO, Lopaschuk GD, Allard MF. Contribution of glycogen to aerobic myocardial glucose utilization. Circulation. 1996;93(8):1549-55.

105. Wisneski JA, Gertz EW, Neese RA, Mayr M. Myocardial metabolism of free fatty acids. Studies with 14C-labeled substrates in humans. J Clin Invest. 1987;79(2):359-66.

106. Honda H, Tanaka K, Akita N, Haneda T. Cyclical changes in high-energy phosphates during the cardiac cycle by pacing-Gated 31P nuclear magnetic resonance. Circ J. 2002;66(1):80-6.

107. Doenst T, Nguyen TD, Abel ED. Cardiac metabolism in heart failure: implications beyond ATP production. Circ Res. 2013;113(6):709-24.

108. Luiken JJ, Koonen DP, Willems J, Zorzano A, Becker C, Fischer Y, et al. Insulin stimulates long-chain fatty acid utilization by rat cardiac myocytes through cellular redistribution of FAT/CD36. Diabetes. 2002;51(10):3113-9.

109. Collins-Nakai RL, Noseworthy D, Lopaschuk GD. Epinephrine increases ATP production in hearts by preferentially increasing glucose metabolism. Am J Physiol. 1994;267(5 Pt 2):H1862-71.

110. Goodwin GW, Taylor CS, Taegtmeyer H. Regulation of energy metabolism of the heart during acute increase in heart work. J Biol Chem. 1998;273(45):29530-9.

111. Swanton EM, Saggerson ED. Effects of adrenaline on triacylglycerol synthesis and turnover in ventricular myocytes from adult rats. Biochem J. 1997;328 (Pt 3)(Pt 3):913-22.

112. Kreisberg RA. Effect of epinephrine on myocardial triglyceride and free fatty acid utilization. Am J Physiol. 1966;210(2):385-9.

113. Beer M, Seyfarth T, Sandstede J, Landschutz W, Lipke C, Kostler H, et al. Absolute concentrations of high-energy phosphate metabolites in normal, hypertrophied, and failing human myocardium measured noninvasively with (31)P-SLOOP magnetic resonance spectroscopy. J Am Coll Cardiol. 2002;40(7):1267-74.

114. Bottomley PA, Panjrath GS, Lai S, Hirsch GA, Wu K, Najjar SS, et al. Metabolic rates of ATP transfer through creatine kinase (CK Flux) predict clinical heart failure events and death. Sci Transl Med. 2013;5(215):215re3.

115. Diakos NA, Navankasattusas S, Abel ED, Rutter J, McCreath L, Ferrin P, et al. Evidence of Glycolysis Up-Regulation and Pyruvate Mitochondrial Oxidation Mismatch During Mechanical Unloading of the Failing Human Heart: Implications for Cardiac Reloading and Conditioning. JACC Basic Transl Sci. 2016;1(6):432-44.

116. Lei B, Lionetti V, Young ME, Chandler MP, d'Agostino C, Kang E, et al. Paradoxical downregulation of the glucose oxidation pathway despite enhanced flux in severe heart failure. J Mol Cell Cardiol. 2004;36(4):567-76.

117. Allard MF, Schonekess BO, Henning SL, English DR, Lopaschuk GD. Contribution of oxidative metabolism and glycolysis to ATP production in hypertrophied hearts. Am J Physiol. 1994;267(2 Pt 2):H742-50.

118. Neglia D, De Caterina A, Marraccini P, Natali A, Ciardetti M, Vecoli C, et al. Impaired myocardial metabolic reserve and substrate selection flexibility during stress in patients with idiopathic dilated cardiomyopathy. Am J Physiol Heart Circ Physiol. 2007;293(6):H3270-8.

119. Bing RJ, Siegel A, Vitale A, Balboni F, Sparks E, Taeschler M, et al. Metabolic studies on the human heart in vivo. I. Studies on carbohydrate metabolism of the human heart. Am J Med. 1953;15(3):284-96.

120. Davila-Roman VG, Vedala G, Herrero P, de las Fuentes L, Rogers JG, Kelly DP, et al. Altered myocardial fatty acid and glucose metabolism in idiopathic dilated cardiomyopathy. J Am Coll Cardiol. 2002;40(2):271-7.

121. Watson WD, Green PG, Lewis AJM, Arvidsson P, De Maria GL, Arheden H, et al. Retained Metabolic Flexibility of the Failing Human Heart. Circulation. 2023;148(2):109-23.

122. Paolisso G, Gambardella A, Galzerano D, D'Amore A, Rubino P, Verza M, et al. Total-body and myocardial substrate oxidation in congestive heart failure. Metabolism. 1994;43(2):174-9.

123. Pulinilkunnil T, Kienesberger PC, Nagendran J, Waller TJ, Young ME, Kershaw EE, et al. Myocardial adipose triglyceride lipase overexpression protects diabetic mice from the development of lipotoxic cardiomyopathy. Diabetes. 2013;62(5):1464-77.

124. Buchanan J, Mazumder PK, Hu P, Chakrabarti G, Roberts MW, Yun UJ, et al. Reduced cardiac efficiency and altered substrate metabolism precedes the onset of hyperglycemia and contractile dysfunction in two mouse models of insulin resistance and obesity. Endocrinology. 2005;146(12):5341-9.

125. Mather KJ, Hutchins GD, Perry K, Territo W, Chisholm R, Acton A, et al. Assessment of myocardial metabolic flexibility and work efficiency in human type 2 diabetes using 16-[18F]fluoro-4-thiapalmitate, a novel PET fatty acid tracer. Am J Physiol Endocrinol Metab. 2016;310(6):E452-60.

126. Rijzewijk LJ, van der Meer RW, Smit JW, Diamant M, Bax JJ, Hammer S, et al. Myocardial steatosis is an independent predictor of diastolic dysfunction in type 2 diabetes mellitus. J Am Coll Cardiol. 2008;52(22):1793-9.

127. Pillutla P, Hwang YC, Augustus A, Yokoyama M, Yagyu H, Johnston TP, et al. Perfusion of hearts with triglyceride-rich particles reproduces the metabolic abnormalities in lipotoxic cardiomyopathy. Am J Physiol Endocrinol Metab. 2005;288(6):E1229-35.

128. Gong H, Liu X, Cheng F. Relationship between non-alcoholic fatty liver disease and cardiac arrhythmia: a systematic review and meta-analysis. J Int Med Res. 2021;49(9):3000605211047074.

129. Salah HM, Pandey A, Van Spall HGC, Michos ED, McGarrah RW, Fudim M. Meta-Analysis of Nonalcoholic Fatty Liver Disease and Incident Heart Failure. Am J Cardiol. 2022;171:180-1.

130. Duell PB, Welty FK, Miller M, Chait A, Hammond G, Ahmad Z, et al. Nonalcoholic Fatty Liver Disease and Cardiovascular Risk: A Scientific Statement From the American Heart Association. Arterioscler Thromb Vasc Biol. 2022;42(6):e168-e85.

131. Alon L, Corica B, Raparelli V, Cangemi R, Basili S, Proietti M, et al. Risk of cardiovascular events in patients with non-alcoholic fatty liver disease: a systematic review and meta-analysis. Eur J Prev Cardiol. 2022;29(6):938-46.

132. Baratta F, Pastori D, Angelico F, Balla A, Paganini AM, Cocomello N, et al. Nonalcoholic Fatty Liver Disease and Fibrosis Associated With Increased Risk of Cardiovascular Events in a Prospective Study. Clin Gastroenterol Hepatol. 2020;18(10):2324-31 e4.

133. Yoshitaka H, Hamaguchi M, Kojima T, Fukuda T, Ohbora A, Fukui M. Nonoverweight nonalcoholic fatty liver disease and incident cardiovascular disease: A post hoc analysis of a cohort study. Medicine (Baltimore). 2017;96(18):e6712.

134. Shojaee-Moradie F, Cuthbertson DJ, Barrett M, Jackson NC, Herring R, Thomas EL, et al. Exercise Training Reduces Liver Fat and Increases Rates of VLDL Clearance But Not VLDL Production in NAFLD. J Clin Endocrinol Metab. 2016;101(11):4219-28.

135. Boren J, Watts GF, Adiels M, Soderlund S, Chan DC, Hakkarainen A, et al. Kinetic and Related Determinants of Plasma Triglyceride Concentration in Abdominal Obesity: Multicenter Tracer Kinetic Study. Arterioscler Thromb Vasc Biol. 2015;35(10):2218-24.

136. Joseph LC, Avula UMR, Wan EY, Reyes MV, Lakkadi KR, Subramanyam P, et al. Dietary Saturated Fat Promotes Arrhythmia by Activating NOX2 (NADPH Oxidase 2). Circ Arrhythm Electrophysiol. 2019;12(11):e007573.

137. Haim TE, Wang W, Flagg TP, Tones MA, Bahinski A, Numann RE, et al. Palmitate attenuates myocardial contractility through augmentation of repolarizing Kv currents. J Mol Cell Cardiol. 2010;48(2):395-405.

138. Pais R, Giral P, Khan JF, Rosenbaum D, Housset C, Poynard T, et al. Fatty liver is an independent predictor of early carotid atherosclerosis. J Hepatol. 2016;65(1):95-102.

139. Haas JT, Francque S, Staels B. Pathophysiology and Mechanisms of Nonalcoholic Fatty Liver Disease. Annu Rev Physiol. 2016;78:181-205.

140. Ionescu VA, Gheorghe G, Bacalbasa N, Diaconu CC. Metabolic Dysfunction-Associated Steatotic Liver Disease: Pathogenetic Links to Cardiovascular Risk. Biomolecules. 2025;15(2).

141. Seppala-Lindroos A, Vehkavaara S, Hakkinen AM, Goto T, Westerbacka J, Sovijarvi A, et al. Fat accumulation in the liver is associated with defects in insulin suppression of glucose production and serum free fatty acids independent of obesity in normal men. J Clin Endocrinol Metab. 2002;87(7):3023-8.

142. Gagnon E, Pelletier W, Gobeil E, Bourgault J, Manikpurage HD, Maltais-Payette I, et al. Mendelian randomization prioritizes abdominal adiposity as an independent causal factor for liver fat accumulation and cardiometabolic diseases. Commun Med (Lond). 2022;2:130.

143. Ference BA, Ginsberg HN, Graham I, Ray KK, Packard CJ, Bruckert E, et al. Low-density lipoproteins cause atherosclerotic cardiovascular disease. 1. Evidence from genetic, epidemiologic, and clinical studies. A consensus statement from the European Atherosclerosis Society Consensus Panel. Eur Heart J. 2017;38(32):2459-72.

144. Chen W, Wang S, Lv W, Pan Y. Causal associations of insulin resistance with coronary artery disease and ischemic stroke: a Mendelian randomization analysis. BMJ Open Diabetes Res Care. 2020;8(1).

145. Luukkonen PK, Zhou Y, Sadevirta S, Leivonen M, Arola J, Oresic M, et al. Hepatic ceramides dissociate steatosis and insulin resistance in patients with non-alcoholic fatty liver disease. J Hepatol. 2016;64(5):1167-75.

146. Akuta N, Kawamura Y, Arase Y, Saitoh S, Fujiyama S, Sezaki H, et al. PNPLA3 genotype and fibrosis-4 index predict cardiovascular diseases of Japanese patients with histopathologically-confirmed NAFLD. BMC Gastroenterol. 2021;21(1):434.

147. Simons N, Isaacs A, Koek GH, Kuc S, Schaper NC, Brouwers M. PNPLA3, TM6SF2, and MBOAT7 Genotypes and Coronary Artery Disease. Gastroenterology. 2017;152(4):912-3.

148. An J, Nichols GA, Qian L, Munis MA, Harrison TN, Li Z, et al. Prevalence and incidence of microvascular and macrovascular complications over 15 years among patients with incident type 2 diabetes. BMJ Open Diabetes Res Care. 2021;9(1).

149. Moon JH, Jeong S, Jang H, Koo BK, Kim W. Metabolic dysfunction-associated steatotic liver disease increases the risk of incident cardiovascular disease: a nationwide cohort study. EClinicalMedicine. 2023;65:102292.

150. Riley DR, Hydes T, Hernadez G, Zhao SS, Alam U, Cuthbertson DJ. The synergistic impact of type 2 diabetes and MASLD on cardiovascular, liver, diabetes-related and cancer outcomes. Liver Int. 2024;44(10):2538-50.

151. Keys A. Coronary heart disease in seven countries. Circulation. 1970;41(1):186-95.

152. Grundy SM, Stone NJ, Bailey AL, Beam C, Birtcher KK, Blumenthal RS, et al. 2018 AHA/ACC/AACVPR/AAPA/ABC/ACPM/ADA/AGS/APhA/ASPC/NLA/PCNA Guideline on the Management of Blood Cholesterol: Executive Summary: A Report of the American College of Cardiology/American Heart Association Task Force on Clinical Practice Guidelines. J Am Coll Cardiol. 2019;73(24):3168-209.

153. Griffin BA, Lovegrove JA. Saturated fat and CVD: importance of inter-individual variation in the response of serum low-density lipoprotein cholesterol. Proc Nutr Soc. 2024:1-11.

154. Trovato FM, Martines GF, Brischetto D, Trovato G, Catalano D. Neglected features of lifestyle: Their relevance in non-alcoholic fatty liver disease. World J Hepatol. 2016;8(33):1459-65.

155. Ferolla SM, Ferrari TC, Lima ML, Reis TO, Tavares WC, Jr., Couto OF, et al. Dietary patterns in Brazilian patients with nonalcoholic fatty liver disease: a cross-sectional study. Clinics (Sao Paulo). 2013;68(1):11-7.

156. Oddy WH, Herbison CE, Jacoby P, Ambrosini GL, O'Sullivan TA, Ayonrinde OT, et al. The Western dietary pattern is prospectively associated with nonalcoholic fatty liver disease in adolescence. Am J Gastroenterol. 2013;108(5):778-85.

157. Allard JP, Aghdassi E, Mohammed S, Raman M, Avand G, Arendt BM, et al. Nutritional assessment and hepatic fatty acid composition in non-alcoholic fatty liver disease (NAFLD): a cross-sectional study. J Hepatol. 2008;48(2):300-7.

158. Musso G, Gambino R, De Michieli F, Cassader M, Rizzetto M, Durazzo M, et al. Dietary habits and their relations to insulin resistance and postprandial lipemia in nonalcoholic steatohepatitis. Hepatology. 2003;37(4):909-16.

159. Aller R, Izaola O, de la Fuente B, De Luis Roman DA. Mediterranean Diet Is Associated with Liver Histology in Patients with Non Alcoholic Fatty Liver Disease. Nutr Hosp. 2015;32(6):2518-24.

160. Chan R, Wong VW, Chu WC, Wong GL, Li LS, Leung J, et al. Diet-Quality Scores and Prevalence of Nonalcoholic Fatty Liver Disease: A Population Study Using Proton-Magnetic Resonance Spectroscopy. PLoS One. 2015;10(9):e0139310.

161. Kontogianni MD, Tileli N, Margariti A, Georgoulis M, Deutsch M, Tiniakos D, et al. Adherence to the Mediterranean diet is associated with the severity of non-alcoholic fatty liver disease. Clin Nutr. 2014;33(4):678-83.

162. Hill RJ, Davies PS. The validity of self-reported energy intake as determined using the doubly labelled water technique. Br J Nutr. 2001;85(4):415-30.

163. Araya J, Rodrigo R, Videla LA, Thielemann L, Orellana M, Pettinelli P, et al. Increase in long-chain polyunsaturated fatty acid n - 6/n - 3 ratio in relation to hepatic steatosis in patients with non-alcoholic fatty liver disease. Clin Sci (Lond). 2004;106(6):635-43.

164. Erickson ML, Haus JM, Malin SK, Flask CA, McCullough AJ, Kirwan JP. Non-invasive assessment of hepatic lipid subspecies matched with non-alcoholic fatty liver disease phenotype. Nutr Metab Cardiovasc Dis. 2019;29(11):1197-204.

165. Puri P, Baillie RA, Wiest MM, Mirshahi F, Choudhury J, Cheung O, et al. A lipidomic analysis of nonalcoholic fatty liver disease. Hepatology. 2007;46(4):1081-90.

166. Puri P, Wiest MM, Cheung O, Mirshahi F, Sargeant C, Min HK, et al. The plasma lipidomic signature of nonalcoholic steatohepatitis. Hepatology. 2009;50(6):1827-38.

167. Sanders FWB, Acharjee A, Walker C, Marney L, Roberts LD, Imamura F, et al. Hepatic steatosis risk is partly driven by increased de novo lipogenesis following carbohydrate consumption. Genome Biol. 2018;19(1):79.

168. Chen H, Wang J, Li Z, Lam CWK, Xiao Y, Wu Q, et al. Consumption of Sugar-Sweetened Beverages Has a Dose-Dependent Effect on the Risk of Non-Alcoholic Fatty Liver Disease: An

Updated Systematic Review and Dose-Response Meta-Analysis. Int J Environ Res Public Health. 2019;16(12).

169. Ouyang X, Cirillo P, Sautin Y, McCall S, Bruchette JL, Diehl AM, et al. Fructose consumption as a risk factor for non-alcoholic fatty liver disease. J Hepatol. 2008;48(6):993-9.

170. Porto A, Pan Z, Zhou W, Sokol RJ, Klaczkiewicz K, Sundaram SS. Macronutrient and Micronutrient Intake in Adolescents With Non-alcoholic Fatty Liver Disease: The Association With Disease Severity. J Pediatr Gastroenterol Nutr. 2022;75(5):666-74.

171. Tseng TS, Lin WT, Ting PS, Huang CK, Chen PH, Gonzalez GV, et al. Sugar-Sweetened Beverages and Artificially Sweetened Beverages Consumption and the Risk of Nonalcoholic Fatty Liver (NAFLD) and Nonalcoholic Steatohepatitis (NASH). Nutrients. 2023;15(18).

172. Roumans KHM, Lindeboom L, Veeraiah P, Remie CME, Phielix E, Havekes B, et al. Hepatic saturated fatty acid fraction is associated with de novo lipogenesis and hepatic insulin resistance. Nat Commun. 2020;11(1):1891.

173. Noakes TD, Windt J. Evidence that supports the prescription of low-carbohydrate high-fat diets: a narrative review. Br J Sports Med. 2017;51(2):133-9.

174. Nordmann AJ, Nordmann A, Briel M, Keller U, Yancy WS, Jr., Brehm BJ, et al. Effects of low-carbohydrate vs low-fat diets on weight loss and cardiovascular risk factors: a meta-analysis of randomized controlled trials. Arch Intern Med. 2006;166(3):285-93.

175. Browning JD, Baker JA, Rogers T, Davis J, Satapati S, Burgess SC. Short-term weight loss and hepatic triglyceride reduction: evidence of a metabolic advantage with dietary carbohydrate restriction. Am J Clin Nutr. 2011;93(5):1048-52.

176. Kirk E, Reeds DN, Finck BN, Mayurranjan SM, Patterson BW, Klein S. Dietary fat and carbohydrates differentially alter insulin sensitivity during caloric restriction. Gastroenterology. 2009;136(5):1552-60.

177. Crabtree CD, Kackley ML, Buga A, Fell B, LaFountain RA, Hyde PN, et al. Comparison of Ketogenic Diets with and without Ketone Salts versus a Low-Fat Diet: Liver Fat Responses in Overweight Adults. Nutrients. 2021;13(3).

178. Lewis MC, Phillips ML, Slavotinek JP, Kow L, Thompson CH, Toouli J. Change in liver size and fat content after treatment with Optifast very low calorie diet. Obes Surg. 2006;16(6):697-701.

179. Otten J, Mellberg C, Ryberg M, Sandberg S, Kullberg J, Lindahl B, et al. Strong and persistent effect on liver fat with a Paleolithic diet during a two-year intervention. Int J Obes (Lond). 2016;40(5):747-53.

180. Steven S, Hollingsworth KG, Al-Mrabeh A, Avery L, Aribisala B, Caslake M, et al. Very Low-Calorie Diet and 6 Months of Weight Stability in Type 2 Diabetes: Pathophysiological Changes in Responders and Nonresponders. Diabetes Care. 2016;39(5):808-15.

181. Parry SA, Hodson L. Influence of dietary macronutrients on liver fat accumulation and metabolism. J Investig Med. 2017;65(8):1102-15.

182. Haufe S, Engeli S, Kast P, Bohnke J, Utz W, Haas V, et al. Randomized comparison of reduced fat and reduced carbohydrate hypocaloric diets on intrahepatic fat in overweight and obese human subjects. Hepatology. 2011;53(5):1504-14.

183. Bian H, Hakkarainen A, Lundbom N, Yki-Jarvinen H. Effects of dietary interventions on liver volume in humans. Obesity (Silver Spring). 2014;22(4):989-95.

184. Schutte S, Esser D, Siebelink E, Michielsen CJR, Daanje M, Matualatupauw JC, et al. Diverging metabolic effects of 2 energy-restricted diets differing in nutrient quality: a 12-week randomized controlled trial in subjects with abdominal obesity. Am J Clin Nutr. 2022;116(1):132-50.

185. van der Meer RW, Hammer S, Lamb HJ, Frolich M, Diamant M, Rijzewijk LJ, et al. Effects of short-term high-fat, high-energy diet on hepatic and myocardial triglyceride content in healthy men. J Clin Endocrinol Metab. 2008;93(7):2702-8.

186. Sobrecases H, Le KA, Bortolotti M, Schneiter P, Ith M, Kreis R, et al. Effects of short-term overfeeding with fructose, fat and fructose plus fat on plasma and hepatic lipids in healthy men. Diabetes Metab. 2010;36(3):244-6.

187. Basset-Sagarminaga J, Roumans KHM, Havekes B, Mensink RP, Peters HPF, Zock PL, et al. Replacing Foods with a High-Glycemic Index and High in Saturated Fat by Alternatives with a Low Glycemic Index and Low Saturated Fat Reduces Hepatic Fat, Even in Isocaloric and Macronutrient Matched Conditions. Nutrients. 2023;15(3).

188. Della Pepa G, Vetrani C, Brancato V, Vitale M, Monti S, Annuzzi G, et al. Effects of a multifactorial ecosustainable isocaloric diet on liver fat in patients with type 2 diabetes: randomized clinical trial. BMJ Open Diabetes Res Care. 2020;8(1).

189. Stonehouse W, Sergi D, Benassi-Evans B, James-Martin G, Johnson N, Thompson CH, et al. Eucaloric diets enriched in palm olein, cocoa butter, and soybean oil did not differentially affect liver fat concentration in healthy participants: a 16-week randomized controlled trial. Am J Clin Nutr. 2021;113(2):324-37.

190. Bozzetto L, Prinster A, Annuzzi G, Costagliola L, Mangione A, Vitelli A, et al. Liver fat is reduced by an isoenergetic MUFA diet in a controlled randomized study in type 2 diabetic patients. Diabetes Care. 2012;35(7):1429-35.

191. Errazuriz I, Dube S, Slama M, Visentin R, Nayar S, O'Connor H, et al. Randomized Controlled Trial of a MUFA or Fiber-Rich Diet on Hepatic Fat in Prediabetes. J Clin Endocrinol Metab. 2017;102(5):1765-74.

192. Parry SA, Rosqvist F, Mozes FE, Cornfield T, Hutchinson M, Piche ME, et al. Intrahepatic Fat and Postprandial Glycemia Increase After Consumption of a Diet Enriched in Saturated Fat Compared With Free Sugars. Diabetes Care. 2020;43(5):1134-41.

193. Marina A, von Frankenberg AD, Suvag S, Callahan HS, Kratz M, Richards TL, et al. Effects of dietary fat and saturated fat content on liver fat and markers of oxidative stress in overweight/obese men and women under weight-stable conditions. Nutrients. 2014;6(11):4678-90.

194. DeLany JP, Windhauser MM, Champagne CM, Bray GA. Differential oxidation of individual dietary fatty acids in humans. Am J Clin Nutr. 2000;72(4):905-11.

195. Kumashiro N, Erion DM, Zhang D, Kahn M, Beddow SA, Chu X, et al. Cellular mechanism of insulin resistance in nonalcoholic fatty liver disease. Proc Natl Acad Sci U S A. 2011;108(39):16381-5.

196. Teixeira FS, Pimentel LL, Vidigal S, Azevedo-Silva J, Pintado ME, Rodriguez-Alcala LM. Differential Lipid Accumulation on HepG2 Cells Triggered by Palmitic and Linoleic Fatty Acids Exposure. Molecules. 2023;28(5).

197. Nagarajan SR, Cross E, Johnson E, Sanna F, Daniels LJ, Ray DW, et al. Determining the temporal, dose, and composition effects of nutritional substrates in an in vitro model of intrahepatocellular triglyceride accumulation. Physiol Rep. 2022;10(20):e15463.

198. Gavino GR, Gavino VC. Rat liver outer mitochondrial carnitine palmitoyltransferase activity towards long-chain polyunsaturated fatty acids and their CoA esters. Lipids. 1991;26(4):266-70.

199. Magkos F, Su X, Bradley D, Fabbrini E, Conte C, Eagon JC, et al. Intrahepatic diacylglycerol content is associated with hepatic insulin resistance in obese subjects. Gastroenterology. 2012;142(7):1444-6 e2.

200. Petersen MC, Shulman GI. Roles of Diacylglycerols and Ceramides in Hepatic Insulin Resistance. Trends Pharmacol Sci. 2017;38(7):649-65.

201. Chabowski A, Zendzian-Piotrowska M, Konstantynowicz K, Pankiewicz W, Miklosz A, Lukaszuk B, et al. Fatty acid transporters involved in the palmitate and oleate induced insulin resistance in primary rat hepatocytes. Acta Physiol (Oxf). 2013;207(2):346-57.

202. Lee JY, Cho HK, Kwon YH. Palmitate induces insulin resistance without significant intracellular triglyceride accumulation in HepG2 cells. Metabolism. 2010;59(7):927-34.

203. de Sousa IF, Migliaccio V, Lepretti M, Paolella G, Di Gregorio I, Caputo I, et al. Dose- and Time-Dependent Effects of Oleate on Mitochondrial Fusion/Fission Proteins and Cell Viability in HepG2 Cells: Comparison with Palmitate Effects. Int J Mol Sci. 2021;22(18).

204. Eynaudi A, Diaz-Castro F, Borquez JC, Bravo-Sagua R, Parra V, Troncoso R. Differential Effects of Oleic and Palmitic Acids on Lipid Droplet-Mitochondria Interaction in the Hepatic Cell Line HepG2. Front Nutr. 2021;8:775382.

205. Gomez-Lechon MJ, Donato MT, Martinez-Romero A, Jimenez N, Castell JV, O'Connor JE. A human hepatocellular in vitro model to investigate steatosis. Chem Biol Interact. 2007;165(2):106-16.

206. Listenberger LL, Han X, Lewis SE, Cases S, Farese RV, Jr., Ory DS, et al. Triglyceride accumulation protects against fatty acid-induced lipotoxicity. Proc Natl Acad Sci U S A. 2003;100(6):3077-82.

207. Ricchi M, Odoardi MR, Carulli L, Anzivino C, Ballestri S, Pinetti A, et al. Differential effect of oleic and palmitic acid on lipid accumulation and apoptosis in cultured hepatocytes. J Gastroenterol Hepatol. 2009;24(5):830-40.

208. Moravcova A, Cervinkova Z, Kucera O, Mezera V, Rychtrmoc D, Lotkova H. The effect of oleic and palmitic acid on induction of steatosis and cytotoxicity on rat hepatocytes in primary culture. Physiol Res. 2015;64(Suppl 5):S627-36.

209. Keys A. Coronary heart disease in seven countries. Circulation. 1970;41:186-95.

210. Koutsos A, Griffin BA, Antoni R, Ozen E, Sellem L, Wong G, et al. Variation of LDL cholesterol in response to the replacement of saturated with unsaturated fatty acids: a nonrandomized, sequential dietary intervention; the Reading, Imperial, Surrey, Saturated fat Cholesterol Intervention ("RISSCI"-1) study. Am J Clin Nutr. 2024;120(4):854-63.

211. Cholesterol Treatment Trialists C, Baigent C, Blackwell L, Emberson J, Holland LE, Reith C, et al. Efficacy and safety of more intensive lowering of LDL cholesterol: a meta-analysis of data from 170,000 participants in 26 randomised trials. Lancet. 2010;376(9753):1670-81.

212. Mozaffarian D, Ascherio A, Hu FB, Stampfer MJ, Willett WC, Siscovick DS, et al. Interplay between different polyunsaturated fatty acids and risk of coronary heart disease in men. Circulation. 2005;111(2):157-64.

213. Ulven SM, Leder L, Elind E, Ottestad I, Christensen JJ, Telle-Hansen VH, et al. Exchanging a few commercial, regularly consumed food items with improved fat quality reduces total cholesterol and LDL-cholesterol: a double-blind, randomised controlled trial. Br J Nutr. 2016;116(8):1383-93.

214. Mensink RP, World Health O. Effects of saturated fatty acids on serum lipids and lipoproteins: a systematic review and regression analysis. Geneva: World Health Organization; 2016 2016.

215. Ruuth M, Lahelma M, Luukkonen PK, Lorey MB, Qadri S, Sadevirta S, et al. Overfeeding Saturated Fat Increases LDL (Low-Density Lipoprotein) Aggregation Susceptibility While Overfeeding Unsaturated Fat Decreases Proteoglycan-Binding of Lipoproteins. Arterioscler Thromb Vasc Biol. 2021;41(11):2823-36.

216. Wiese DM, Horst SN, Brown CT, Allaman MM, Hodges ME, Slaughter JC, et al. Serum Fatty Acids Are Correlated with Inflammatory Cytokines in Ulcerative Colitis. PLoS One. 2016;11(5):e0156387.

217. Schepp M, Freuer D, Peters A, Heier M, Teupser D, Meisinger C, et al. Is the Habitual Dietary Intake of Foods of Plant or Animal Origin Associated with Circulating Hemostatic Factors?-Results of the Population-Based KORA-Fit Study. Nutrients. 2024;16(3).

218. Delgado-Lista J, Lopez-Miranda J, Cortes B, Perez-Martinez P, Lozano A, Gomez-Luna R, et al. Chronic dietary fat intake modifies the postprandial response of hemostatic markers to a single fatty test meal. Am J Clin Nutr. 2008;87(2):317-22.

219. Ni S, Zhong Z, Wei J, Zhou J, Cai L, Yang M, et al. Association between dietary intake of polyunsaturated fatty acid and prevalence of hypertension in U.S. adults: A cross-sectional study using data from NHANES 2009-2016. Hypertens Res. 2022;45(3):516-26.

220. American Heart Association Nutrition C, Lichtenstein AH, Appel LJ, Brands M, Carnethon M, Daniels S, et al. Diet and lifestyle recommendations revision 2006: a scientific statement from the American Heart Association Nutrition Committee. Circulation. 2006;114(1):82-96.

221. Nakamura H, Tsujiguchi H, Kambayashi Y, Hara A, Miyagi S, Yamada Y, et al. Relationship between saturated fatty acid intake and hypertension and oxidative stress. Nutrition. 2019;61:8-15.

222. Abdelhamid AS, Brown TJ, Brainard JS, Biswas P, Thorpe GC, Moore HJ, et al. Omega-3 fatty acids for the primary and secondary prevention of cardiovascular disease. Cochrane Database Syst Rev. 2020;3(3):CD003177.

223. Griffin MD, Sanders TA, Davies IG, Morgan LM, Millward DJ, Lewis F, et al. Effects of altering the ratio of dietary n-6 to n-3 fatty acids on insulin sensitivity, lipoprotein size, and postprandial lipemia in men and postmenopausal women aged 45-70 y: the OPTILIP Study. Am J Clin Nutr. 2006;84(6):1290-8.

224. Mensink RP, Zock PL, Kester AD, Katan MB. Effects of dietary fatty acids and carbohydrates on the ratio of serum total to HDL cholesterol and on serum lipids and apolipoproteins: a meta-analysis of 60 controlled trials. Am J Clin Nutr. 2003;77(5):1146-55.

225. Harris WS, Mozaffarian D, Rimm E, Kris-Etherton P, Rudel LL, Appel LJ, et al. Omega-6 fatty acids and risk for cardiovascular disease: a science advisory from the American Heart Association Nutrition Subcommittee of the Council on Nutrition, Physical Activity, and Metabolism; Council on Cardiovascular Nursing; and Council on Epidemiology and Prevention. Circulation. 2009;119(6):902-7.

226. Jackson KH, Harris WS, Belury MA, Kris-Etherton PM, Calder PC. Beneficial effects of linoleic acid on cardiometabolic health: an update. Lipids Health Dis. 2024;23(1):296.

227. Green CJ, Pramfalk C, Charlton CA, Gunn PJ, Cornfield T, Pavlides M, et al. Hepatic de novo lipogenesis is suppressed and fat oxidation is increased by omega-3 fatty acids at the expense of glucose metabolism. BMJ Open Diabetes Res Care. 2020;8(1).

228. Ghio S, Scelsi L, Latini R, Masson S, Eleuteri E, Palvarini M, et al. Effects of n-3 polyunsaturated fatty acids and of rosuvastatin on left ventricular function in chronic heart failure: a substudy of GISSI-HF trial. Eur J Heart Fail. 2010;12(12):1345-53.

229. Albert CM, Hennekens CH, O'Donnell CJ, Ajani UA, Carey VJ, Willett WC, et al. Fish consumption and risk of sudden cardiac death. JAMA. 1998;279(1):23-8.

230. Liu L, Nettleton JA, Bertoni AG, Bluemke DA, Lima JA, Szklo M. Dietary pattern, the metabolic syndrome, and left ventricular mass and systolic function: the Multi-Ethnic Study of Atherosclerosis. Am J Clin Nutr. 2009;90(2):362-8.

231. Levitan EB, Ahmed A, Arnett DK, Polak JF, Hundley WG, Bluemke DA, et al. Mediterranean diet score and left ventricular structure and function: the Multi-Ethnic Study of Atherosclerosis. Am J Clin Nutr. 2016;104(3):595-602.

232. Lechner K, Scherr J, Lorenz E, Lechner B, Haller B, Krannich A, et al. Omega-3 fatty acid blood levels are inversely associated with cardiometabolic risk factors in HFpEF patients: the Aldo-DHF randomized controlled trial. Clin Res Cardiol. 2022;111(3):308-21.

233. Lechner K, von Schacky C, Scherr J, Lorenz E, Bock M, Lechner B, et al. Saturated Fatty Acid Blood Levels and Cardiometabolic Phenotype in Patients with HFpEF: A Secondary Analysis of the Aldo-DHF Trial. Biomedicines. 2022;10(9).

234. Arnlov J, Lind L, Sundstrom J, Andren B, Vessby B, Lithell H. Insulin resistance, dietary fat intake and blood pressure predict left ventricular diastolic function 20 years later. Nutr Metab Cardiovasc Dis. 2005;15(4):242-9.

235. Sundstrom J, Lind L, Vessby B, Andren B, Aro A, Lithell H. Dyslipidemia and an unfavorable fatty acid profile predict left ventricular hypertrophy 20 years later. Circulation. 2001;103(6):836-41.

236. Moertl D, Hammer A, Steiner S, Hutuleac R, Vonbank K, Berger R. Dose-dependent effects of omega-3-polyunsaturated fatty acids on systolic left ventricular function, endothelial function, and markers of inflammation in chronic heart failure of nonischemic origin: a double-blind, placebo-controlled, 3-arm study. Am Heart J. 2011;161(5):915 e1-9.

237. Nodari S, Triggiani M, Campia U, Manerba A, Milesi G, Cesana BM, et al. Effects of n-3 polyunsaturated fatty acids on left ventricular function and functional capacity in patients with dilated cardiomyopathy. J Am Coll Cardiol. 2011;57(7):870-9.

238. Carbone S, Billingsley HE, Canada JM, Kadariya D, Medina de Chazal H, Rotelli B, et al. Unsaturated Fatty Acids to Improve Cardiorespiratory Fitness in Patients With Obesity and HFpEF: The UFA-Preserved Pilot Study. JACC Basic Transl Sci. 2019;4(4):563-5.

239. Broussard JL, Nelson MD, Kolka CM, Bediako IA, Paszkiewicz RL, Smith L, et al. Rapid development of cardiac dysfunction in a canine model of insulin resistance and moderate obesity. Diabetologia. 2016;59(1):197-207.

240. Rivet DR, Nelson OL, Vella CA, Jansen HT, Robbins CT. Systemic effects of a high saturated fat diet in grizzly bears (Ursus arctos horribilis). Canadian Journal of Zoology. 2017;95(11):797-807.

241. Arinell K, Sahdo B, Evans AL, Arnemo JM, Baandrup U, Frobert O. Brown bears (Ursus arctos) seem resistant to atherosclerosis despite highly elevated plasma lipids during hibernation and active state. Clin Transl Sci. 2012;5(3):269-72.

242. Ritterhoff J, Young S, Villet O, Shao D, Neto FC, Bettcher LF, et al. Metabolic Remodeling Promotes Cardiac Hypertrophy by Directing Glucose to Aspartate Biosynthesis. Circ Res. 2020;126(2):182-96.

243. Mulligan CM, Sparagna GC, Le CH, De Mooy AB, Routh MA, Holmes MG, et al. Dietary linoleate preserves cardiolipin and attenuates mitochondrial dysfunction in the failing rat heart. Cardiovasc Res. 2012;94(3):460-8.

244. Yamamoto T, Endo J, Kataoka M, Matsuhashi T, Katsumata Y, Shirakawa K, et al. Decrease in membrane phospholipids unsaturation correlates with myocardial diastolic dysfunction. PLoS One. 2018;13(12):e0208396.

245. Yamamoto T, Endo J, Kataoka M, Matsuhashi T, Katsumata Y, Shirakawa K, et al. Sirt1 counteracts decrease in membrane phospholipid unsaturation and diastolic dysfunction during saturated fatty acid overload. J Mol Cell Cardiol. 2019;133:1-11.

246. Xiao YF, Sigg DC, Leaf A. The antiarrhythmic effect of n-3 polyunsaturated fatty acids: modulation of cardiac ion channels as a potential mechanism. J Membr Biol. 2005;206(2):141-54.

247. Elinder F, Liin SI. Actions and Mechanisms of Polyunsaturated Fatty Acids on Voltage-Gated Ion Channels. Front Physiol. 2017;8:43.

248. Dietary supplementation with n-3 polyunsaturated fatty acids and vitamin E after myocardial infarction: results of the GISSI-Prevenzione trial. Gruppo Italiano per lo Studio della Sopravvivenza nell'Infarto miocardico. Lancet. 1999;354(9177):447-55.

249. Zhang L, Ussher JR, Oka T, Cadete VJ, Wagg C, Lopaschuk GD. Cardiac diacylglycerol accumulation in high fat-fed mice is associated with impaired insulin-stimulated glucose oxidation. Cardiovasc Res. 2011;89(1):148-56.

250. Zhou H, Summers SA, Birnbaum MJ, Pittman RN. Inhibition of Akt kinase by cell-permeable ceramide and its implications for ceramide-induced apoptosis. J Biol Chem. 1998;273(26):16568-75.

251. Gudz TI, Tserng KY, Hoppel CL. Direct inhibition of mitochondrial respiratory chain complex III by cell-permeable ceramide. J Biol Chem. 1997;272(39):24154-8.

252. Law BA, Liao X, Moore KS, Southard A, Roddy P, Ji R, et al. Lipotoxic very-long-chain ceramides cause mitochondrial dysfunction, oxidative stress, and cell death in cardiomyocytes. FASEB J. 2018;32(3):1403-16.

253. Akoumi A, Haffar T, Mousterji M, Kiss RS, Bousette N. Palmitate mediated diacylglycerol accumulation causes endoplasmic reticulum stress, Plin2 degradation, and cell death in H9C2 cardiomyoblasts. Exp Cell Res. 2017;354(2):85-94.

254. Karpe F, Vasan SK, Humphreys SM, Miller J, Cheeseman J, Dennis AL, et al. Cohort Profile: The Oxford Biobank. Int J Epidemiol. 2018;47(1):21-g.

255. Morrison DJ, Dodson B, Slater C, Preston T. (13)C natural abundance in the British diet: implications for (13)C breath tests. Rapid Commun Mass Spectrom. 2000;14(15):1321-4.

256. Ritz P, Vol S, Berrut G, Tack I, Arnaud MJ, Tichet J. Influence of gender and body composition on hydration and body water spaces. Clin Nutr. 2008;27(5):740-6.

257. Pinnick KE, Gunn PJ, Hodson L. Measuring Human Lipid Metabolism Using Deuterium Labeling: In Vivo and In Vitro Protocols. Methods Mol Biol. 2019;1862:83-96.

258. Folch J, Lees M, Sloane Stanley GH. A simple method for the isolation and purification of total lipides from animal tissues. J Biol Chem. 1957;226(1):497-509.

259. Heath RB, Karpe F, Milne RW, Burdge GC, Wootton SA, Frayn KN. Selective partitioning of dietary fatty acids into the VLDL TG pool in the early postprandial period. J Lipid Res. 2003;44(11):2065-72.

260. Burdge GC, Wright P, Jones AE, Wootton SA. A method for separation of phosphatidylcholine, triacylglycerol, non-esterified fatty acids and cholesterol esters from plasma by solid-phase extraction. Br J Nutr. 2000;84(5):781-7.

261. Kim IY, Suh SH, Lee IK, Wolfe RR. Applications of stable, nonradioactive isotope tracers in in vivo human metabolic research. Exp Mol Med. 2016;48(1):e203.

262. Chong MF, Fielding BA, Frayn KN. Mechanisms for the acute effect of fructose on postprandial lipemia. Am J Clin Nutr. 2007;85(6):1511-20.

263. Wolfe RR. Isotope Tracers in Metabolic Research. 2nd Edition ed: Wiley & Sons Ltd; 2005.

264. Bickerton AS, Roberts R, Fielding BA, Hodson L, Blaak EE, Wagenmakers AJ, et al. Preferential uptake of dietary Fatty acids in adipose tissue and muscle in the postprandial period. Diabetes. 2007;56(1):168-76.

265. Diraison F, Pachiaudi C, Beylot M. Measuring lipogenesis and cholesterol synthesis in humans with deuterated water: use of simple gas chromatographic/mass spectrometric techniques. J Mass Spectrom. 1997;32(1):81-6.

266. Reference and Intercomparison Materials for Stable Isotopes of Light Elements. Vienna: INTERNATIONAL ATOMIC ENERGY AGENCY; 1995.

267. Sessions AL, Burgoyne TW, Hayes JM. Determination of the the H3 factor in hydrogen isotope ratio monitoring mass spectrometry. Anal Chem. 2001;73(2):200-7.

268. Matthews DR, Hosker JP, Rudenski AS, Naylor BA, Treacher DF, Turner RC. Homeostasis model assessment: insulin resistance and beta-cell function from fasting plasma glucose and insulin concentrations in man. Diabetologia. 1985;28(7):412-9.

269. Hodson L, McQuaid SE, Humphreys SM, Milne R, Fielding BA, Frayn KN, et al. Greater dietary fat oxidation in obese compared with lean men: an adaptive mechanism to prevent liver fat accumulation? Am J Physiol Endocrinol Metab. 2010;299(4):E584-92.

270. Frayn KN. Calculation of substrate oxidation rates in vivo from gaseous exchange. J Appl Physiol Respir Environ Exerc Physiol. 1983;55(2):628-34.

271. Rinella ME, Lazarus JV, Ratziu V, Francque SM, Sanyal AJ, Kanwal F, et al. A multi-society Delphi consensus statement on new fatty liver disease nomenclature. J Hepatol. 2023.

272. Lee JJ, Lambert JE, Hovhannisyan Y, Ramos-Roman MA, Trombold JR, Wagner DA, et al. Palmitoleic acid is elevated in fatty liver disease and reflects hepatic lipogenesis. Am J Clin Nutr. 2015;101(1):34-43.

273. Mifflin MD, St Jeor ST, Hill LA, Scott BJ, Daugherty SA, Koh YO. A new predictive equation for resting energy expenditure in healthy individuals. Am J Clin Nutr. 1990;51(2):241-7.

274. Hems R, Saez GT. Equilibration of metabolic CO2 with preformed CO2 and bicarbonate. An unexpected finding. FEBS Lett. 1983;153(2):438-40.

275. Kloppenburg WD, Wolthers BG, Stellaard F, Elzinga H, Tepper T, de Jong PE, et al. Determination of urea kinetics by isotope dilution with [13C]urea and gas chromatography-isotope ratio mass spectrometry (GC-IRMS) analysis. Clin Sci (Lond). 1997;93(1):73-80.

276. Muller MJ. Hepatic fuel selection. Proc Nutr Soc. 1995;54(1):139-50.

277. Hodson L, Karpe F. Is there something special about palmitoleate? Curr Opin Clin Nutr Metab Care. 2013;16(2):225-31.

278. Jones PJ, Pencharz PB, Clandinin MT. Whole body oxidation of dietary fatty acids: implications for energy utilization. Am J Clin Nutr. 1985;42(5):769-77.

279. Schmidt DE, Allred JB, Kien CL. Fractional oxidation of chylomicron-derived oleate is greater than that of palmitate in healthy adults fed frequent small meals. J Lipid Res. 1999;40(12):2322-32.

280. Koutsari C, Sidossis LS. Effect of isoenergetic low- and high-carbohydrate diets on substrate kinetics and oxidation in healthy men. Br J Nutr. 2003;90(2):413-8.

281. Bonen A, Benton CR, Campbell SE, Chabowski A, Clarke DC, Han XX, et al. Plasmalemmal fatty acid transport is regulated in heart and skeletal muscle by contraction, insulin and leptin, and in obesity and diabetes. Acta Physiol Scand. 2003;178(4):347-56.

282. Jeppesen PB, Christensen MS, Hoy CE, Mortensen PB. Essential fatty acid deficiency in patients with severe fat malabsorption. Am J Clin Nutr. 1997;65(3):837-43.

283. Nelson RH, Mundi MS, Vlazny DT, Smailovic A, Muthusamy K, Almandoz JP, et al. Kinetics of saturated, monounsaturated, and polyunsaturated fatty acids in humans. Diabetes. 2013;62(3):783-8.

284. Piche ME, Parry SA, Karpe F, Hodson L. Chylomicron-Derived Fatty Acid Spillover in Adipose Tissue: A Signature of Metabolic Health? J Clin Endocrinol Metab. 2018;103(1):25-34.

285. Brennan IM, Feltrin KL, Nair NS, Hausken T, Little TJ, Gentilcore D, et al. Effects of the phases of the menstrual cycle on gastric emptying, glycemia, plasma GLP-1 and insulin, and energy intake in healthy lean women. Am J Physiol Gastrointest Liver Physiol. 2009;297(3):G602-10.

286. Popeijus HE, van Otterdijk SD, van der Krieken SE, Konings M, Serbonij K, Plat J, et al. Fatty acid chain length and saturation influences PPARalpha transcriptional activation and repression in HepG2 cells. Mol Nutr Food Res. 2014;58(12):2342-9.

287. Kien CL, Bunn JY, Ugrasbul F. Increasing dietary palmitic acid decreases fat oxidation and daily energy expenditure. Am J Clin Nutr. 2005;82(2):320-6.

288. Browning JD, Szczepaniak LS, Dobbins R, Nuremberg P, Horton JD, Cohen JC, et al. Prevalence of hepatic steatosis in an urban population in the United States: impact of ethnicity. Hepatology. 2004;40(6):1387-95.

289. Srnic N, Dearlove D, Johnson E, MacLeod C, Krupa A, McGonnell A, et al. Greater oxidation of dietary linoleate compared to palmitate in humans following an acute high-carbohydrate diet. Clin Nutr. 2024;43(10):2305-15.

290. Hodson L, Skeaff CM, McKenzie JE. Maximal response to a plasma cholesterol-lowering diet is achieved within two weeks. Nutr Metab Cardiovasc Dis. 2002;12(5):291-5.

291. Hodson L, Skeaff CM, Chisholm WA. The effect of replacing dietary saturated fat with polyunsaturated or monounsaturated fat on plasma lipids in free-living young adults. Eur J Clin Nutr. 2001;55(10):908-15.

292. Bruhn H, Frahm J, Gyngell ML, Merboldt KD, Hanicke W, Sauter R. Localized proton NMR spectroscopy using stimulated echoes: applications to human skeletal muscle in vivo. Magn Reson Med. 1991;17(1):82-94.

293. Purvis LAB, Clarke WT, Biasiolli L, Valkovic L, Robson MD, Rodgers CT. OXSA: An open-source magnetic resonance spectroscopy analysis toolbox in MATLAB. PLoS One. 2017;12(9):e0185356.

294. Rodgers CT, Clarke WT, Snyder C, Vaughan JT, Neubauer S, Robson MD. Human cardiac 31P magnetic resonance spectroscopy at 7 Tesla. Magn Reson Med. 2014;72(2):304-15.

295. Hundertmark MJ, Agbaje OF, Coleman R, George JT, Grempler R, Holman RR, et al. Design and rationale of the EMPA-VISION trial: investigating the metabolic effects of empagliflozin in patients with heart failure. ESC Heart Fail. 2021;8(4):2580-90.

296. Rider OJ, Francis JM, Tyler D, Byrne J, Clarke K, Neubauer S. Effects of weight loss on myocardial energetics and diastolic function in obesity. Int J Cardiovasc Imaging. 2013;29(5):1043-50.

297. Rider OJ, Holloway CJ, Emmanuel Y, Bloch E, Clarke K, Neubauer S. Increasing plasma free fatty acids in healthy subjects induces aortic distensibility changes seen in obesity. Circ Cardiovasc Imaging. 2012;5(3):367-75.

298. Cecelja M, Ruijsink B, Puyol-Anton E, Li Y, Godwin H, King AP, et al. Aortic Distensibility Measured by Automated Analysis of Magnetic Resonance Imaging Predicts Adverse Cardiovascular Events in UK Biobank. J Am Heart Assoc. 2022;11(23):e026361.

299. Shojaee-Moradie F, Jackson NC, Jones RH, Mallet AI, Hovorka R, Umpleby AM. Quantitative measurement of 3-O-methyl-D-glucose by gas chromatography-mass spectrometry as a measure of glucose transport in vivo. J Mass Spectrom. 1996;31(9):961-6.

300. Chacko SK, Sunehag AL, Sharma S, Sauer PJ, Haymond MW. Measurement of gluconeogenesis using glucose fragments and mass spectrometry after ingestion of deuterium oxide. J Appl Physiol (1985). 2008;104(4):944-51.

301. Van Cauter E, Mestrez F, Sturis J, Polonsky KS. Estimation of insulin secretion rates from C-peptide levels. Comparison of individual and standard kinetic parameters for C-peptide clearance. Diabetes. 1992;41(3):368-77.

302. Gastaldelli A, Abdul Ghani M, DeFronzo RA. Adaptation of Insulin Clearance to Metabolic Demand Is a Key Determinant of Glucose Tolerance. Diabetes. 2021;70(2):377-85.

303. Polidori DC, Bergman RN, Chung ST, Sumner AE. Hepatic and Extrahepatic Insulin Clearance Are Differentially Regulated: Results From a Novel Model-Based Analysis of Intravenous Glucose Tolerance Data. Diabetes. 2016;65(6):1556-64.

304. Ruge T, Hodson L, Cheeseman J, Dennis AL, Fielding BA, Humphreys SM, et al. Fasted to fed trafficking of Fatty acids in human adipose tissue reveals a novel regulatory step for enhanced fat storage. J Clin Endocrinol Metab. 2009;94(5):1781-8.

305. Mancina RM, Dongiovanni P, Petta S, Pingitore P, Meroni M, Rametta R, et al. The MBOAT7-TMC4 Variant rs641738 Increases Risk of Nonalcoholic Fatty Liver Disease in Individuals of European Descent. Gastroenterology. 2016;150(5):1219-30 e6.

306. Santoro N, Zhang CK, Zhao H, Pakstis AJ, Kim G, Kursawe R, et al. Variant in the glucokinase regulatory protein (GCKR) gene is associated with fatty liver in obese children and adolescents. Hepatology. 2012;55(3):781-9.

307. Pramfalk C, Pavlides M, Banerjee R, McNeil CA, Neubauer S, Karpe F, et al. Sex-Specific Differences in Hepatic Fat Oxidation and Synthesis May Explain the Higher Propensity for NAFLD in Men. J Clin Endocrinol Metab. 2015;100(12):4425-33.

308. Kliewer SA, Sundseth SS, Jones SA, Brown PJ, Wisely GB, Koble CS, et al. Fatty acids and eicosanoids regulate gene expression through direct interactions with peroxisome proliferator-activated receptors alpha and gamma. Proc Natl Acad Sci U S A. 1997;94(9):4318-23.

309. Jans A, Konings E, Goossens GH, Bouwman FG, Moors CC, Boekschoten MV, et al. PUFAs acutely affect triacylglycerol-derived skeletal muscle fatty acid uptake and increase postprandial insulin sensitivity. Am J Clin Nutr. 2012;95(4):825-36.

310. Neubauer S, Horn M, Cramer M, Harre K, Newell JB, Peters W, et al. Myocardial phosphocreatine-to-ATP ratio is a predictor of mortality in patients with dilated cardiomyopathy. Circulation. 1997;96(7):2190-6.

311. Heran BS, Wong MM, Heran IK, Wright JM. Blood pressure lowering efficacy of angiotensin converting enzyme (ACE) inhibitors for primary hypertension. Cochrane Database Syst Rev. 2008;2008(4):CD003823.

312. Park LK, Garr Barry V, Hong J, Heebink J, Sah R, Peterson LR. Links between ceramides and cardiac function. Curr Opin Lipidol. 2022;33(1):47-56.

313. Lundsgaard AM, Holm JB, Sjoberg KA, Bojsen-Moller KN, Myrmel LS, Fjaere E, et al. Mechanisms Preserving Insulin Action during High Dietary Fat Intake. Cell Metab. 2019;29(1):50-63 e4.

314. Koska J, Ozias MK, Deer J, Kurtz J, Salbe AD, Harman SM, et al. A human model of dietary saturated fatty acid induced insulin resistance. Metabolism. 2016;65(11):1621-8.

315. Tierney AC, McMonagle J, Shaw DI, Gulseth HL, Helal O, Saris WH, et al. Effects of dietary fat modification on insulin sensitivity and on other risk factors of the metabolic syndrome--LIPGENE: a European randomized dietary intervention study. Int J Obes (Lond). 2011;35(6):800-9.

316. von Frankenberg AD, Marina A, Song X, Callahan HS, Kratz M, Utzschneider KM. A high-fat, high-saturated fat diet decreases insulin sensitivity without changing intra-abdominal fat in weight-stable overweight and obese adults. Eur J Nutr. 2017;56(1):431-43.

317. Xiao C, Giacca A, Carpentier A, Lewis GF. Differential effects of monounsaturated, polyunsaturated and saturated fat ingestion on glucose-stimulated insulin secretion, sensitivity and clearance in overweight and obese, non-diabetic humans. Diabetologia. 2006;49(6):1371-9.

318. Smith K, Taylor GS, Allerton DM, Brunsgaard LH, Bowden Davies KA, Stevenson EJ, et al. The Postprandial Glycaemic and Hormonal Responses Following the Ingestion of a Novel, Ready-to-Drink Shot Containing a Low Dose of Whey Protein in Centrally Obese and Lean Adult Males: A Randomised Controlled Trial. Front Endocrinol (Lausanne). 2021;12:696977.

319. Beysen C, Karpe F, Fielding BA, Clark A, Levy JC, Frayn KN. Interaction between specific fatty acids, GLP-1 and insulin secretion in humans. Diabetologia. 2002;45(11):1533-41.

320. Feng DD, Luo Z, Roh SG, Hernandez M, Tawadros N, Keating DJ, et al. Reduction in voltage-gated K+ currents in primary cultured rat pancreatic beta-cells by linoleic acids. Endocrinology. 2006;147(2):674-82.

321. Feng DD, Zhao YF, Luo ZQ, Keating DJ, Chen C. Linoleic acid induces Ca2+-induced inactivation of voltage-dependent Ca2+ currents in rat pancreatic beta-cells. J Endocrinol. 2008;196(2):377-84.

322. Jacobson DA, Weber CR, Bao S, Turk J, Philipson LH. Modulation of the pancreatic islet beta-cell-delayed rectifier potassium channel Kv2.1 by the polyunsaturated fatty acid arachidonate. J Biol Chem. 2007;282(10):7442-9.

323. Lambert JE, Ramos-Roman MA, Browning JD, Parks EJ. Increased de novo lipogenesis is a distinct characteristic of individuals with nonalcoholic fatty liver disease. Gastroenterology. 2014;146(3):726-35.

324. Umpleby AM, Shojaee-Moradie F, Fielding B, Li X, Marino A, Alsini N, et al. Impact of liver fat on the differential partitioning of hepatic triacylglycerol into VLDL subclasses on high and low sugar diets. Clin Sci (Lond). 2017;131(21):2561-73.

325. Heather LC, Gopal K, Srnic N, Ussher JR. Redefining Diabetic Cardiomyopathy: Perturbations in Substrate Metabolism at the Heart of Its Pathology. Diabetes. 2024;73(5):659-70.

326. Spallotta F, Cencioni C, Atlante S, Garella D, Cocco M, Mori M, et al. Stable Oxidative Cytosine Modifications Accumulate in Cardiac Mesenchymal Cells From Type2 Diabetes Patients: Rescue by alpha-Ketoglutarate and TET-TDG Functional Reactivation. Circ Res. 2018;122(1):31-46.

327. Kronlage M, Dewenter M, Grosso J, Fleming T, Oehl U, Lehmann LH, et al. O-GlcNAcylation of Histone Deacetylase 4 Protects the Diabetic Heart From Failure. Circulation. 2019;140(7):580-94.

328. De Loof M, Renguet E, Ginion A, Bouzin C, Horman S, Beauloye C, et al. Enhanced protein acetylation initiates fatty acid-mediated inhibition of cardiac glucose transport. Am J Physiol Heart Circ Physiol. 2023;324(3):H305-H17.

329. Alrob OA, Sankaralingam S, Ma C, Wagg CS, Fillmore N, Jaswal JS, et al. Obesity-induced lysine acetylation increases cardiac fatty acid oxidation and impairs insulin signalling. Cardiovasc Res. 2014;103(4):485-97.

330. Dodd MS, Sousa Fialho MDL, Montes Aparicio CN, Kerr M, Timm KN, Griffin JL, et al. Fatty Acids Prevent Hypoxia-Inducible Factor-1alpha Signaling Through Decreased Succinate in Diabetes. JACC Basic Transl Sci. 2018;3(4):485-98.

331. Yu J, Vodyanik MA, Smuga-Otto K, Antosiewicz-Bourget J, Frane JL, Tian S, et al. Induced pluripotent stem cell lines derived from human somatic cells. Science. 2007;318(5858):1917-20.

332. Lian X, Zhang J, Azarin SM, Zhu K, Hazeltine LB, Bao X, et al. Directed cardiomyocyte differentiation from human pluripotent stem cells by modulating Wnt/beta-catenin signaling under fully defined conditions. Nat Protoc. 2013;8(1):162-75.

333. Lopez CA, Al-Siddiqi H, Purnama U, Iftekhar S, Bruyneel AAN, Kerr M, et al. Physiological and pharmacological stimulation for in vitro maturation of substrate metabolism in human induced pluripotent stem cell-derived cardiomyocytes. Sci Rep. 2021;11(1):7802.

334. Livak KJ, Schmittgen TD. Analysis of relative gene expression data using real-time quantitative PCR and the 2(-Delta Delta C(T)) Method. Methods. 2001;25(4):402-8.

335. Robinson MD, McCarthy DJ, Smyth GK. edgeR: a Bioconductor package for differential expression analysis of digital gene expression data. Bioinformatics. 2010;26(1):139-40.

336. Robinson MD, Oshlack A. A scaling normalization method for differential expression analysis of RNA-seq data. Genome Biol. 2010;11(3):R25.

337. Ritchie ME, Phipson B, Wu D, Hu Y, Law CW, Shi W, et al. limma powers differential expression analyses for RNA-sequencing and microarray studies. Nucleic Acids Res. 2015;43(7):e47.

338. Liberzon A, Birger C, Thorvaldsdottir H, Ghandi M, Mesirov JP, Tamayo P. The Molecular Signatures Database (MSigDB) hallmark gene set collection. Cell Syst. 2015;1(6):417-25.

339. Ashburner M, Ball CA, Blake JA, Botstein D, Butler H, Cherry JM, et al. Gene ontology: tool for the unification of biology. The Gene Ontology Consortium. Nat Genet. 2000;25(1):25-9.

340. Gene Ontology C, Aleksander SA, Balhoff J, Carbon S, Cherry JM, Drabkin HJ, et al. The Gene Ontology knowledgebase in 2023. Genetics. 2023;224(1).

341. Xie Z, Bailey A, Kuleshov MV, Clarke DJB, Evangelista JE, Jenkins SL, et al. Gene Set Knowledge Discovery with Enrichr. Curr Protoc. 2021;1(3):e90.

342. Han H, Cho JW, Lee S, Yun A, Kim H, Bae D, et al. TRRUST v2: an expanded reference database of human and mouse transcriptional regulatory interactions. Nucleic Acids Res. 2018;46(D1):D380-D6.

343. Chen EY, Tan CM, Kou Y, Duan Q, Wang Z, Meirelles GV, et al. Enrichr: interactive and collaborative HTML5 gene list enrichment analysis tool. BMC Bioinformatics. 2013;14:128.

344. Grundy SM, Stone NJ, Bailey AL, Beam C, Birtcher KK, Blumenthal RS, et al. 2018 AHA/ACC/AACVPR/AAPA/ABC/ACPM/ADA/AGS/APhA/ASPC/NLA/PCNA Guideline on the

Management of Blood Cholesterol: Executive Summary: A Report of the American College of Cardiology/American Heart Association Task Force on Clinical Practice Guidelines. Circulation. 2019;139(25):e1046-e81.

345. Lockridge JB, Sailors ML, Durgan DJ, Egbejimi O, Jeong WJ, Bray MS, et al. Bioinformatic profiling of the transcriptional response of adult rat cardiomyocytes to distinct fatty acids. J Lipid Res. 2008;49(7):1395-408.

346. Okere IC, Chandler MP, McElfresh TA, Rennison JH, Sharov V, Sabbah HN, et al. Differential effects of saturated and unsaturated fatty acid diets on cardiomyocyte apoptosis, adipose distribution, and serum leptin. Am J Physiol Heart Circ Physiol. 2006;291(1):H38-44.

347. Cetrullo S, D'Adamo S, Panichi V, Borzi RM, Pignatti C, Flamigni F. Modulation of Fatty Acid-Related Genes in the Response of H9c2 Cardiac Cells to Palmitate and n-3 Polyunsaturated Fatty Acids. Cells. 2020;9(3).

348. Capel F, Cheraiti N, Acquaviva C, Henique C, Bertrand-Michel J, Vianey-Saban C, et al. Oleate dose-dependently regulates palmitate metabolism and insulin signaling in C2C12 myotubes. Biochim Biophys Acta. 2016;1861(12 Pt A):2000-10.

349. Hickson-Bick DL, Buja LM, McMillin JB. Palmitate-mediated alterations in the fatty acid metabolism of rat neonatal cardiac myocytes. J Mol Cell Cardiol. 2000;32(3):511-9.

350. Chabowski A, Momken I, Coort SL, Calles-Escandon J, Tandon NN, Glatz JF, et al. Prolonged AMPK activation increases the expression of fatty acid transporters in cardiac myocytes and perfused hearts. Mol Cell Biochem. 2006;288(1-2):201-12.

351. Smith J, Su X, El-Maghrabi R, Stahl PD, Abumrad NA. Opposite regulation of CD36 ubiquitination by fatty acids and insulin: effects on fatty acid uptake. J Biol Chem. 2008;283(20):13578-85.

352. Miller TA, LeBrasseur NK, Cote GM, Trucillo MP, Pimentel DR, Ido Y, et al. Oleate prevents palmitate-induced cytotoxic stress in cardiac myocytes. Biochem Biophys Res Commun. 2005;336(1):309-15.

353. Cetrullo S, Tantini B, Flamigni F, Pazzini C, Facchini A, Stefanelli C, et al. Antiapoptotic and antiautophagic effects of eicosapentaenoic acid in cardiac myoblasts exposed to palmitic acid. Nutrients. 2012;4(2):78-90.

354. Sousa Fialho MDL, Purnama U, Dennis K, Montes Aparicio CN, Castro-Guarda M, Massourides E, et al. Activation of HIF1alpha Rescues the Hypoxic Response and Reverses Metabolic Dysfunction in the Diabetic Heart. Diabetes. 2021;70(11):2518-31.

355. Crozier SJ, Bolster DR, Reiter AK, Kimball SR, Jefferson LS. Beta -oxidation of free fatty acids is required to maintain translational control of protein synthesis in heart. Am J Physiol Endocrinol Metab. 2002;283(6):E1144-50.

356. Rannels DE, Hjalmarson AC, Morgan HE. Effects of noncarbohydrate substrates on protein synthesis in muscle. Am J Physiol. 1974;226(3):528-39.

357. Hass DT, Zhang Q, Autterson GA, Bryan RA, Hurley JB, Miller JML. Medium Depth Influences O2 Availability and Metabolism in Human RPE Cultures. Invest Ophthalmol Vis Sci. 2023;64(14):4.

358. Miyagawa Y, Mori T, Goto K, Kawahara I, Fujiwara-Tani R, Kishi S, et al. Intake of medium-chain fatty acids induces myocardial oxidative stress and atrophy. Lipids Health Dis. 2018;17(1):258.

359. Jackson KG, Zampelas A, Knapper JM, Roche HM, Gibney MJ, Kafatos A, et al. Differences in glucose-dependent insulinotrophic polypeptide hormone and hepatic lipase in subjects of southern and northern Europe: implications for postprandial lipemia. Am J Clin Nutr. 2000;71(1):13-20.

360. Ma Y, Tucker KL, Smith CE, Lee YC, Huang T, Richardson K, et al. Lipoprotein lipase variants interact with polyunsaturated fatty acids for obesity traits in women: replication in two populations. Nutr Metab Cardiovasc Dis. 2014;24(12):1323-9.

361. Akagiri S, Naito Y, Ichikawa H, Mizushima K, Takagi T, Handa O, et al. A Mouse Model of Metabolic Syndrome; Increase in Visceral Adipose Tissue Precedes the Development of Fatty Liver and Insulin Resistance in High-Fat Diet-Fed Male KK/Ta Mice. J Clin Biochem Nutr. 2008;42(2):150-7.

362. Jornayvaz FR, Samuel VT, Shulman GI. The role of muscle insulin resistance in the pathogenesis of atherogenic dyslipidemia and nonalcoholic fatty liver disease associated with the metabolic syndrome. Annu Rev Nutr. 2010;30:273-90.

363. Clegg DJ, Mauvais-Jarvis F. An integrated view of sex differences in metabolic physiology and disease. Mol Metab. 2018;15:1-2.

364. Maher AC, Akhtar M, Vockley J, Tarnopolsky MA. Women have higher protein content of beta-oxidation enzymes in skeletal muscle than men. PLoS One. 2010;5(8):e12025.

365. Devries MC, Lowther SA, Glover AW, Hamadeh MJ, Tarnopolsky MA. IMCL area density, but not IMCL utilization, is higher in women during moderate-intensity endurance exercise, compared with men. Am J Physiol Regul Integr Comp Physiol. 2007;293(6):R2336-42.

366. Tarnopolsky MA, Rennie CD, Robertshaw HA, Fedak-Tarnopolsky SN, Devries MC, Hamadeh MJ. Influence of endurance exercise training and sex on intramyocellular lipid and mitochondrial ultrastructure, substrate use, and mitochondrial enzyme activity. Am J Physiol Regul Integr Comp Physiol. 2007;292(3):R1271-8.

367. Hewitt KN, Pratis K, Jones ME, Simpson ER. Estrogen replacement reverses the hepatic steatosis phenotype in the male aromatase knockout mouse. Endocrinology. 2004;145(4):1842-8.

368. Paquette A, Wang D, Jankowski M, Gutkowska J, Lavoie JM. Effects of ovariectomy on PPAR alpha, SREBP-1c, and SCD-1 gene expression in the rat liver. Menopause. 2008;15(6):1169-75.

369. Harrison SA, Browne SK, Suschak JJ, Tomah S, Gutierrez JA, Yang J, et al. Effect of pemvidutide, a GLP-1/glucagon dual receptor agonist, on MASLD: A randomized, double-blind, placebo-controlled study. J Hepatol. 2025;82(1):7-17.

370. Duerden M, O'Flynn N, Qureshi N. Cardiovascular risk assessment and lipid modification: NICE guideline. Br J Gen Pract. 2015;65(636):378-80.